

Digital quality assurance system for additive manufacturing
based on machine learning methods and blockchain
technology

Kumulative Dissertation

zur Erlangung des akademischen Grades

Doktor-Ingenieur (Dr.-Ing.)

der Fakultät für Maschinenbau und Schiffstechnik

der Universität Rostock

vorgelegt von

Dipl.-Ing. Erik Westphal

aus Waren (Müritz)

Waren (Müritz), 2023



Dieses Werk ist lizenziert unter einer
Creative Commons Namensnennung 4.0 International Lizenz.

Gutachter:

Prof. Dr.-Ing. Hermann Seitz

Universität Rostock, Fakultät für Maschinenbau und Schiffstechnik

Prof. Dr.-Ing. habil Knuth-Michael Henkel

Universität Rostock, Fakultät für Maschinenbau und Schiffstechnik

Prof. Dr. Benjamin Leiding

Technische Universität Clausthal, Institute for Software and Systems Engineering

Jahr der Einreichung: 2023

Jahr der Verteidigung: 2024

Abstract

The number of additively manufactured functional parts is increasing, making special quality aspects, such as a predictable and reproducible manufacturing process that leads to high-quality results, are becoming more and more important. In this context, traceable and digital quality management (QM), process-integrated and fast quality assurance (QA), and suitable process monitoring are key elements for additive manufacturing (AM). However, the effective implementation of corresponding quality-relevant aspects is hindered by a lack of process understanding and immature networking of the additive process chain, so that innovative technological potential in these areas is not recognized. Instead, conventional processes that have been established for years and which are generally complex, slow and expensive, are used without restriction as the standard without regard to technological innovations.

Therefore, the aim of this work is to investigate technological innovations in the context of process digitization and to develop a digital quality assurance system for additive manufacturing based on specific artificial intelligence (AI) methods and blockchain technology to enable more reproducible as well as predictable AM processes and parts. To this end, this cumulative work considers the implementation of special quality assurance methods based on AI algorithms, the development of a digitalized quality management system based on blockchain, and the conceptual combination of these aspects into a real-time capable digital quality assurance system for AM as three main areas of investigation.

The research investigations show that complex machine learning (ML) algorithms are capable of automatically detecting and classifying defects and irregularities based on image and sensor data from selected AM processes. Detailed analyses and comparisons of different algorithms have also demonstrated the effectiveness of the data-based methods and their suitability as fast, non-destructive and process-integrated alternative to conventional QA methods. Further investigations show that a blockchain-based QM can digitally map the value chain of a complex AM process. This also enables a cross-company digital QM of data along the entire supply chain, including data from conventional and data-based QA methods. Analyses based on specific evaluation criteria have shown that a corresponding digital quality assurance system can fundamentally improve quality in AM.

Acknowledgements

This dissertation is a matter of the heart and gives me the certainty of having extracted what is in me from my academic career with hard work. After several years in industry, returning to the university was not always easy. The meticulous research with the academic writing was in strong contrast to the fast-paced, solution-oriented daily business in industry. However, I am very happy that I ventured this return and found new enthusiasm for additive manufacturing as well as for the development of intelligent algorithms. I will continue to retain this enthusiasm.

This dissertation was written during my employment as research assistant at the Chair of Microfluidics (LFM) at the University of Rostock. My special thanks go to the chair holder, Prof. Dr.-Ing. Hermann Seitz, who supported, motivated and encouraged me from the first idea to the employment as a research assistant to the finished dissertation. I have always appreciated your advice and support in conducting research.

I would like to thank Prof. Dr.-Ing. Benjamin Leiding very much for sharing his expertise and our discussions about Blockchain and smart contracts, which were very insightful and a great support for me.

A big thank you also goes to my colleagues at the chair: it is always a pleasure to work with all of you, to learn from you and to celebrate successes with you. Special thanks go to our secretariat, which often took a lot of bureaucracy from me and supported me effectively in my research tasks. I would also like to thank all the unknown researchers who took the time to review my research.

Finally, I thank my family for their support and encouragement. I would especially like to thank my wife Laura, who has often given me patience and space as well as support.

Für Laura und meine Kinder.

Erik Westphal

Waren (Müritz), August 2023

Table of Contents

1	Introduction	1
1.1	Classification and motivation	1
1.2	Objectives and focus of investigation	2
1.3	Methodology and structure of the work	3
2	State of the art	5
2.1	Fundamentals of additive manufacturing	5
2.1.1	Technology and process chain	5
2.1.2	Process categories	7
2.1.3	Applications, challenges and trends	8
2.2	Quality in the context of additive manufacturing	10
2.2.1	Quality management	10
2.2.2	Quality assurance and quality control	11
2.2.3	Qualification, certification and standardization	12
2.3	Blockchain for quality improvement in additive manufacturing	14
2.3.1	Fundamentals of distributed ledgers, blockchain and smart contracts	14
2.3.2	Blockchain-based part record for the additive manufacturing value chain	18
2.3.3	Connecting blockchain, digital twin and data for real-time quality analytics	19
2.4	Quality assurance through data analytics and machine learning	20
2.4.1	Distinction of data analytics, machine learning and artificial intelligence	20
2.4.2	Machine learning methods for quality assurance in additive manufacturing	28
2.4.3	Closed-loop quality and process control for additive manufacturing through machine learning	30
3	Conception and implementation	32
4	Results	35
4.1	Development and implementation of data-based quality assurance methods for additive manufacturing (from [I] and [II])	35
4.1.1	Machine learning architectures for image-based defect detection in selective laser sintering (from [I])	35

4.1.2	Performance evaluation of an automatic classification method of powder bed defects (from [I])	36
4.1.3	Machine learning algorithms for sensor-based data classification in fused deposition modelling (from [II])	38
4.1.4	Evaluation of a proof of concept data analysis method for classifying 3D printing conditions (from [II])	41
4.2	Blockchain-based additive manufacturing quality management (from [III]).....	42
4.2.1	Development and implementation of a basic digital quality assurance concept as a blockchain-based additive manufacturing part record (from [III])	43
4.2.2	Integration of machine learning methods and blockchain technology into a digital quality assurance system for additive manufacturing (from [I] - [III]).....	46
5	Discussion	47
5.1	Development of non-destructive quality assurance methods for additive manufacturing processes based on machine learning (from [I] and [II])	47
5.1.1	Machine learning for defect detection in selective laser sintering	47
5.1.2	Machine learning for intelligent data analysis in fused deposition modelling	49
5.2	Development of digital quality management for additive manufacturing based on blockchain technology (from [III])	51
5.3	Digital quality assurance system consisting of data-based quality assurance and digitalized quality management (from [I] - [III]).....	54
5.4	Summary and delimitation	55
6	Conclusions	56
	References.....	58
	Annotations	75
	Appendix A - Test methods in additive manufacturing	76
	Appendix B - Functionality of neural networks	78
	Statutory declaration.....	83
	Scientific publications	84
	List of Appended Publications	86
	Publications.....	89

Table of Figures

Figure 1:	Process chain in additive manufacturing with eight general process steps (based on [1]).	7
Figure 2:	Areas of quality management.	11
Figure 3:	Results of various test methods on additively manufactured parts. (a) CT scan for analysis of internal part defects.; (b) Laser scan to investigate surface roughness; (c) 3D scan for analysis of part dimensional deviations; (d) Camera-based imaging with supporting ML analysis for fault detection.	12
Figure 4:	Concatenation of information blocks of a blockchain via cryptographic hash functions.	16
Figure 5:	Schematic representation of a digital signature with asymmetric encryption.	17
Figure 6:	Components of QM along the AM value chain (simplified representation).	19
Figure 7:	Data analytics development stages.	21
Figure 8:	Information processing in ML with human assistance by feature extraction of relevant image regions in powder bed images of the SLS process.	22
Figure 9:	Basic performance evaluations of ML models. left: CM with commonly used metrics, right: Visualization of two typical ROC curves and the performance of random guessing.	25
Figure 10:	Information processing in Deep Learning exemplified by a pattern recognition algorithm for defect detection in powder bed images of the SLS process (adapted from [125] and the design of Lucy Reading-Ikkanda).	27
Figure 11:	Schematic representation of a closed-loop feedback system.	30
Figure 12:	Schematic representation of an AI- or ML-based closed-loop feedback system.	30
Figure 13:	Overview of the conceptual design as well as the developed implementations of the digital quality assurance system.	32
Figure 14:	Image examples from the dataset of a SLS print job with: (a) a powder bed without sintered elements and irregularities; (b) a powder bed without sintered elements with irregularities; (c) a powder bed with a sintered element without irregularities and (d) a powder bed with a sintered element and irregularities (according to [I], CC BY 4.0 (https://creativecommons.org/licenses/by/4.0/)).	35

Figure 15: ML architecture of the transfer learning process with the powder bed data (according to [I], CC BY 4.0 (https://creativecommons.org/licenses/by/4.0/)).	36
Figure 16: ROC curves and AUC metrics of the implemented models. The dashed lines represent the ROC curve of a completely random classifier and that of a perfect classifier. Plot of the ROC curves of the implemented models (left) and zoomed in version of the top part plots (right) (according to [I], CC BY 4.0 (https://creativecommons.org/licenses/by/4.0/)).	37
Figure 17: Activation maps for powder bed recordings during the SLS process with visible powder bed defects (according to [I], CC BY 4.0 (https://creativecommons.org/licenses/by/4.0/)). Defects were detected and localized by the CNN architectures. With the VGG16 model, a more precise localization of the effects could be achieved than with the Xception model.	38
Figure 18: Data preprocessing steps carried out for the ML investigations with the environmental sensor data (according to [II], Copyright Elsevier).	39
Figure 19: Training and validation loss plots of the used ML algorithms with the main dataset (according to [II], Copyright Elsevier).	40
Figure 20: Training and validation loss plots of the RNN LSTM (left) and XceptionTime (right) algorithms with the ablation dataset (according to [II], Copyright Elsevier).	41
Figure 21: Dimensional control with an optical 3D light scanner to compare the quality of the printed parts with the different printing conditions (according to [II], CC BY 4.0 (https://creativecommons.org/licenses/by/4.0/)).	42
Figure 22: Manufacturing processes of a digital, secure and trustworthy AM part record with important parameters to be stored on a blockchain (according to [III], CC BY 4.0 (https://creativecommons.org/licenses/by/4.0/)).	44
Figure 23: Architecture and process flow for the proposed blockchain-based digital AM part record.	44
Figure B-1: Multiple interconnected neurons (left) and representation of an artificial neural network (right) according to [126].	78
Figure B-2: Weighted neural network related to [126]. The small numbers illustrate the signal progression, e.g. $W_{2,3}$ means the signal goes from node two in one layer to node three in the next layer.	78

Figure B-3: Basic input, weight and output values of a neural network (left) and a calculation example with randomly selected input values, weights and the calculated outputs (right). 79

Figure B-4: Backpropagation with output error (left) and continuation of the calculation example with concrete calculation values (right). 80

Figure B-5: Backpropagation with error calculation based on the calculation example. 81

Figure B-6: Back propagation with calculation of error increase and weight adjustment based on the calculation example. 82

List of Tables

Table 1:	AM main process categories according to ISO/ASTM 52900 [16].	7
Table 2:	Standards for the AM process chain according to ISO/ASTM 52920 [45] (^a in progress).	13
Table 3:	Learning methods, algorithms and tasks in ML according to [102].	23
Table 4:	ML Methods for better QA and QC in AM.	29
Table 5:	Confusion matrices and performance parameters for the examined CNN architectures for the classification of powder bed defects at the SLS process for all experiments carried out (according to [I], CC BY 4.0 (https://creativecommons.org/licenses/by/4.0/)).	37
Table 6:	FDM process characteristics for different 3D printing conditions (see full table in publication [II], Copyright Elsevier).	39
Table 7:	Performance metrics for ML algorithms for the classification of sensor data at the FDM process for all investigations with the main dataset (the full table can be found in publication [II], Copyright Elsevier).	39
Table 8:	Performance metrics for the RNN LSTM and XceptionTime algorithm for the classification of sensor data at the FDM process for all investigations with the ablation dataset (see full table in publication [II], Copyright Elsevier).	41
Table A-1 :	Test methods of additive manufacturing processes and parts.	76

List of Abbreviations

AI	Artificial intelligence
AM	Additive manufacturing
ANN	Artificial neural network
AUC	Area under the curve
CAD	Computer-aided design
CAM	Computer-aided manufacturing
CNC	Computer numerical control
CNN	Convolutional neural network
CT	Computed tomography
DL	Deep learning
DLT	Distributed ledger technology
FDM	Fused deposition modeling
GAN	Generative adversarial networks
Grad-CAM	Gradient-weighted class activation mapping
IPFS	Interplanetary file system
LSTM	Long short-term memory
MEX	Material extrusion
ML	Machine learning
MLP	Multilayer perceptron
NDT	Non-destructive test
PBF	Powder bed fusion
PoS	Proof-of-Stake
PoW	Proof-of-Work
QA	Quality assurance
QC	Quality control
QM	Quality management
RNN	Recurrent neural network
ROC	Receiver operator characteristic
SLS	Selective laser sintering
STL	Standard tessellation language

1 Introduction

1.1 Classification and motivation

Additive manufacturing (AM) is a modern manufacturing technology that has become increasingly important in recent years. According to Gibson et al [1], the term AM stands for the layer-by-layer manufacturing process of components from three-dimensional computer-aided design (CAD) files. The technology is now widely used in research and industry, as well as by non-industrial home users, and is often referred to as 3D printing [2]. In the future, AM will make a significant contribution to digitalization in manufacturing and thus further increase its acceptance in the industry, among other things [3].

Digitization in itself is changing the business environment of entire corporate divisions at a rapid pace, and digital transformation in companies is creating new opportunities to increase productivity and value creation through the use of disruptive technologies [4]. The industry is even moving to holistically adapt entirely new, digital business models and completely redesign products and services [4]. The digital transformation in manufacturing, where processes are increasingly automated, connected and facilitated with the help of sensors, data analytics, cloud services, blockchain, machine learning (ML) and artificial intelligence (AI), is also changing the AM industry [5]. Additive manufacturing, as a versatile, flexible and highly customizable manufacturing process that can be used in many areas of industrial production, can benefit greatly from this development [3].

Despite all the possibilities offered by digitization, the predictable and reproducible production of functional parts remains a major challenge. Due to the increasing number of additively manufactured functional parts, special quality aspects are becoming more and more important. Traceable and digital quality management (QM), process-integrated and fast quality assurance (QA), and suitable process monitoring are important elements in this context. According to Tofail et al. [3], the following topics still have great potential for development in this respect:

- a real-time quality assurance in manufacturing,
- process monitoring for quality optimization,
- adaptable in-situ measurement methods,
- high measurement accuracy and speed as well as
- an effective data communication with increasing networking.

With regard to predictable and reproducible production of additively manufactured parts, however, the situation is currently such that the parts are largely only evaluated after the printing process, the processes are also only optimized downstream, measurement accuracies and speeds

are severely limited, and in-situ measurements are usually impractical [6–8]. Furthermore, the system requirements for effective networking of production plants and processes are often immature, so that, for example, data acquisition, communication and evaluation are inconsistent and their potential, especially for quality-relevant aspects, is not recognized. Data-based conclusions about the manufacturing process cannot be implemented efficiently in this way, and information about the value chain cannot be distributed effectively. Instead, conventional processes that have been established for years are used as standard without restriction, regardless of technological innovations [9,10]. However, increasing process digitization can, among other things, enable digital, traceable and secure standardization, qualification and documentation processes. Correct implementation and complete documentation of QM and conventional as well as innovative QA procedures across the entire AM value chain can also form the basis for digital process and part certification.

Conventional QA procedures in additive manufacturing processes include visual inspections, mechanical tests and CT examinations, as well as many other procedures, which, as already explained, are mostly not performed in real time but only after the printing process has been completed [11]. These methods are also usually complex, slow, expensive and difficult to integrate into a digitized process chain. However, they are necessary to detect part defects, to enable conclusions to be drawn about process irregularities and to improve process understanding. The need for innovative, real-time process monitoring solutions with information feedback to the production plants exists and is increasingly being met by plant manufacturers, but the data collected is often not further analyzed for errors and irregularities [3]. Often, production data is only monitored, possibly stored, but not processed in real time as part of a closed-loop feedback system [12]. In addition, there is a lack of understanding of the relevance and meaningfulness of the data collected, or of what data is really important, how it should be collected and processed, and in what form [13].

1.2 Objectives and focus of investigation

The goal of this dissertation is to develop a digital quality assurance system for additive manufacturing based on specific AI methods and blockchain technology to enable better reproducibility and predictability of AM processes and part qualities. To achieve this goal, three main areas of investigation are planned.

- **First:** the development and implementation of data-based quality assurance procedures based on specialized AI methods such as machine learning and artificial neural networks for non-destructive quality evaluation of selected additive manufacturing processes.

- **Second:** the development and exemplary implementation of a blockchain-based, cross-company solution for the digital management of quality-relevant data of the entire AM value chain.
- **Third:** the conceptually linking of blockchain-based quality management and data-based quality assurance to a real-time digital quality assurance system that also addresses the aspects of effective data storage and documentation.

1.3 Methodology and structure of the work

All main areas of investigation have an explorative and experimental focus. Thus, for each research focus, relevant fundamentals are first elaborated and, based on this, exemplary implementation ideas are designed, implemented and analyzed. The scientific publications produced in the context of this cumulative dissertation thereby highlight essential aspects for the development of a digital quality assurance system for AM:

*Publication [I]*¹

First, an ML-based method for automatic classification of defects and irregularities in powder bed images of the selective laser sintering (SLS) process was developed. This method enables the quality assessment of individual additively manufactured part layers based on in-situ acquired image data, which ultimately enables non-destructive quality assurance as well as digital manufacturing documentation of AM parts. The creation and pre-processing of an SLS image dataset as well as the design, implementation, and evaluation of the effectiveness of two different ML architectures are also considered in this paper.

*Publication [III]*²

This is followed by the development of a data analysis for environmental sensor data in the fused deposition modeling (FDM) process based on a supervised learning classification approach. Within the scope of the investigations, datasets were acquired during differently parameterized printing processes of an AM part, processed according to a new data pre-processing methodology for analysis by various state-of-the-art ML algorithms, and the results were evaluated. The prediction results of the data-based ML investigations were then compared in a

¹ This article was published in Additive Manufacturing, 41, Westphal & Seitz, A machine learning method for defect detection and visualization in selective laser sintering based on convolutional neural networks, 101965, Open access article under the CC BY 4.0 (<https://creativecommons.org/licenses/by/4.0/>) license (2021).

² This article was published in Additive Manufacturing, 50, Westphal & Seitz, Machine learning for the intelligent analysis of 3D printing conditions using environmental sensor data to support quality assurance, 102535, Copyright Elsevier (2022).

proof-of-concept with 3D scanning inspections of the real parts to point out the effectiveness and speed of analyzing environmental sensor data in the context of QA processes.

Publication [III]³

The digital quality assurance system for AM was conceptualized and experimentally implemented in this paper using an exemplary implementation for the value chain of a metal-based FDM process. For this purpose, a digital quality management solution consisting of a web application for data collection, a decentralized data storage, a smart contract for automated processing of manufacturing events, and an Ethereum blockchain for data documentation was developed. The solution enables a digital QM with transparent, tamper-proof and traceable documentation of all quality information across company boundaries along the AM value chain. Aspects of data storage and data management of conventional as well as the in [I] and [II] developed ML-based QA methods were also considered in the context of an AM part record and conceptually extended with respect to future implementations.

³ This article was published in Industrial Information Integration, 35, Westphal et al., Blockchain-based quality management for a digital additive manufacturing part record, 100517, Open access article under the CC BY 4.0 (<https://creativecommons.org/licenses/by/4.0/>) license (2023).

2 State of the art

In this chapter, the necessary basics as well as the state of the art on the relevant topics of this thesis are presented in a structured way. This includes fundamental aspects of additive manufacturing as well as methods of quality assurance and process monitoring. Furthermore, the basics of blockchain technology and artificial intelligence are considered, which form the central approaches for the digital quality assurance system developed in this work.

2.1 Fundamentals of additive manufacturing

Basic knowledge of additive manufacturing, considering international terminology, is necessary in order to be able to place the scientific findings of this thesis in the context of AM. All research aspects discussed in this thesis refer to or result from the basic principles listed below.

2.1.1 Technology and process chain

Additive manufacturing is the generic term for various layer-by-layer manufacturing processes for producing geometrically complex parts from digital, three-dimensional (3D) files [1]. The technology is becoming increasingly important both in research and in the industrial environment, transforming itself from a rapid prototyping method to an established manufacturing process in industrial production [14].

According to Gibson et al. [1], AM technology is based on a variety of developments in different technology areas. In particular, advanced computer-aided design for creating 3D part designs, as well as computer-aided manufacturing (CAM) and computer numerical control (CNC), are fundamental to the additive manufacturing of complex shapes and structures [15]. Modern CAD systems offer comprehensive and efficient solutions for AM designs and also have the functionality to generate a generic output format for 3D printing processes. The data format is called Standard Tessellation Language (STL) and is currently the standard output format for 3D printing used by many AM system vendors [1,15].

New developments in the relevant technology areas have already led to countless different AM processes, but all of them have a relatively similar process chain. The generic AM process chain is shown in Figure 1 and, according to Gibson et al. [1], comprises eight process steps from CAD design to use of the printed component:

- **CAD design:** Visualization or design of the part idea with a CAD program on the computer and creation of a 3D model. Existing designs can also be digitized as a 3D model by reverse engineering with laser or optical scanners.
- **STL conversion and export:** Conversion of CAD data into an STL format from which AM processes obtain their geometry information. The STL format is a de facto standard for processing AM data. During conversion, the 3D digital models are approximated by triangles that describe the outer surfaces of the model.
- **Data preparation and slicing:** Special print preparation software (slicer) is then used to convert the STL data into a format that can be read by the 3D printer. In the process, the STL files are divided into layers, positioned and aligned in the build space, and the material consumption, the travel paths of the 3D printer and any necessary support structures are calculated. The print file is then transferred to the production system.
- **Machine preparation and print setup:** Before printing, the 3D printer must be set up on the hardware side (and possibly also on the software side). This usually includes, for example, leveling and preparing the print bed, loading the material, and possibly configuring additional monitoring solutions.
- **3D printing:** Start of the printing process, which is largely automated and can usually be carried out unattended by the system. To ensure a successful printing process, the printer and the printing process should still be monitored to ensure that no errors occur, such as lack of materials, software problems, print aborts, etc. The printing process can also be monitored by the operator of the printer.
- **Part removal:** Removal of the parts from the build chamber after completion of the printing process. This requires plant-specific defined processes in which, for example, safety mechanisms have to be unlocked, moving components secured or operating temperatures cooled down.
- **Post-processing and finishing of the parts:** Post-processing of the printed parts by mostly manual work steps such as the removal of support structures or the reworking of holes. Furthermore, machining of the part surface and additional finishing may be necessary to achieve the desired part quality.
- **Application or use of the printed part:** Use of the AM parts. However, there may also be other requirements, especially with regard to the quality of the parts. These are, for example, mechanical as well as statistical quality control methods, special certifications and documentation on production.

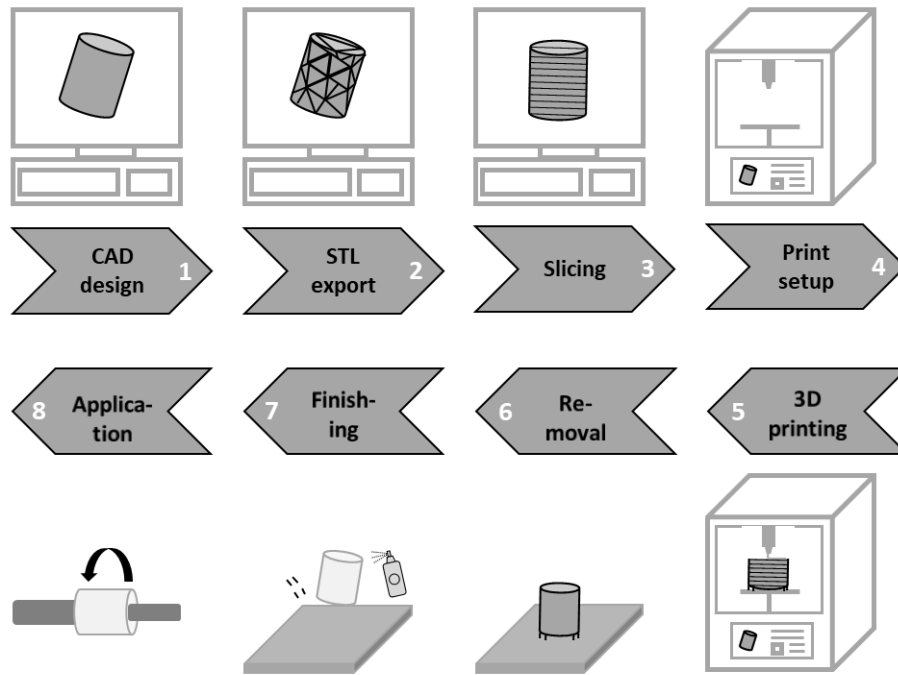






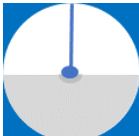


Figure 1: Process chain in additive manufacturing with eight general process steps (based on [1]).

2.1.2 Process categories

Process categories of additive manufacturing are defined in ISO/ASTM 52900 [16]. The definitions and terms listed in this document represent the internationally recognized standard and provide an overview of the main processes into which most AM systems can be divided. The ISO/ASTM 52900 terminology also serves as a standard for this work to enable clear and unambiguous communication. In the industrial environment other process designations are also listed, which are often used by machine manufacturers as registered trademarks for their respective manufacturing principle. Table 1 lists the seven main AM process categories according to ISO/ASTM 52900 and explains them in detail.

Table 1: AM main process categories according to ISO/ASTM 52900 [16].

Process category	Definition	Material type	Related technology	
Binder jetting (BJT)	AM process in which a liquid binder is selectively applied to powder materials to cause them to bond.	Polymer, Metals, Glass, Sand	Binder jetting	
Directed energy deposition (DED)	AM process that uses focused thermal energy to fuse materials together during deposition.	Metals, Polymers, Ceramics	Electron beam AM (EBAM), Wire arc AM (WAAM)	

Process category	Definition	Material type	Related technology	
Material extrusion (MEX)	AM process in which materials are selectively applied through a nozzle or orifice.	Polymers, concrete	Fused deposition modeling (FDM)	
Material jetting (MJT)	AM process in which drops of the starting material are applied in a targeted manner.	Polymers, metals, biomaterial	Multi jet modeling (MJM), drop-on-demand (DOD)	
Powder bed fusion (PBF)	AM process in which thermal energy selectively melts areas of a powder bed.	Polymers, metals, ceramics	Electron beam melting (EBM), selective laser sintering (SLS) and melting (SLM)	
Sheet lamination (SHL)	AM process in which sheets of material are joined to form a component.	Polymers, metals	Laminated object manufacturing (LOM)	
VAT photopolymerization (VPP)	AM process in which liquid photopolymer is selectively cured in a bath by light-activated polymerization.	Polymers, ceramics	Stereolithography (SLA), digital light processing (DLP)	

2.1.3 Applications, challenges and trends

Additive manufacturing processes are increasingly used in various industries for technical and non-technical applications [17]. In aerospace, AM enables the production of complex parts with lightweight yet strong and robust structures to improve fuel efficiency and reduce pollutant emissions [17,18]. In medical technology, AM processes contribute to the production of individualized, osseointegrative structures with complicated and complex geometries, among other things, due to their manufacturing design freedom [19]. AM can also be used to create artificial tissues, organs and implants, to produce anatomical models and to reconstruct 3D anatomical patient models using medical imaging [19–21]. Additive manufacturing processes can also be an important element of part development in the automotive sector. They can shorten the product development cycle, lower manufacturing and production costs, and reduce lead times, labor and logistics costs [22]. Corresponding processes are used here to produce small batches of structural, functional and auxiliary parts such as drive shafts, transmission components and tools [22,23]. Specially adapted AM processes can also be used in the construction industry to automate manual processes, reduce labor and cut material consumption, among others [24–26].

Industrial applications of AM technology always attempt to exploit its fundamental strengths over conventional, subtractive and formative manufacturing processes. A variety of corresponding advantages and disadvantages of AM technology are described in the literature [3,9,27,28]. Core aspects that speak for the use of AM can be summarized as follows:

- **Individualization:** Individualization or personalization and economical production of small batches from batch size 1.
- **Efficient production:** Sustainable use of resources (material, time, energy). Reduction of waste, assembly and tooling costs through substitution of parts as a result of additive design.
- **Production on demand:** Fast, on-demand manufacturing. Reduction of development times and part costs through rapid prototyping.
- **Optimized part designs:** Design freedom and topology optimization. Complex designs integrate special functions, reduce weight and improve mechanical part properties.
- **Shorter supply chains:** Local, decentralized manufacturing. Shortening of supply chains, savings in shipping costs and CO₂ emissions due to shorter transport routes.

Despite the aforementioned aspects, a broad acceptance and application of AM in industry is currently not given, since many AM processes are not able to guarantee certain manufacturing properties (e.g. production speed, accuracy and costs) for certain processes in a predictable and reproducible way [22,29]. This means that companies cannot be confident that printed parts will have the mechanical properties required for their intended applications. To enable predictable and reproducible AM processes, the process variability as well as the sensitivity to process variations must be reduced, among other things [22]. In addition, special requirements for QM and QA must be met, process understanding and automation must be improved, and uniform standards and certifications must be developed [27,29].

In the future, new AM processes and materials as well as improved simulation, standardization and testing methods will lead to better additive part manufacturing [1,22,27]. However, especially in the course of Industry 4.0 and the increasing digitalization of the manufacturing industry, transformation opportunities will arise for AM to solve special process-specific challenges [11,30]. Digitization creates completely new, data-based opportunities to optimize AM processes, products and services [3]. Continuous data collection enables, for example, the integration of customer and experience data into production to create personalized offers [31]. The integration of sensors into the AM process enables the early detection of defective or wearing production equipment based on data analysis as part of predictive maintenance [32]. In addition,

digital technologies based on ML and AI can be used in AM processes to improve the design process [33], optimize the manufacturing process, or support aspects of QA. [34]. Digital part records based on cryptographic processes can in principle also map documentation, standardization and certification processes on a blockchain in a tamper-proof, transparent and trustworthy manner, thus enabling digital AM QM [30,35].

2.2 Quality in the context of additive manufacturing

The immature quality of AM processes and products is currently an obstacle to the widespread adoption of the technology, but this can be fundamentally countered with effective management of AM quality [3,11]. Comprehensive QM is one aspect, as is efficient QA with associated quality control (QC). Further aspects are the qualification and certification of AM processes and additively manufactured parts as well as the current standardization. In the following, a characterization of the individual quality-relevant terms is given.

2.2.1 Quality management

All organizational measures for improving process and product quality in a company are summarized under the generic term quality management according to DIN EN ISO 9000. Effective QM, especially in AM, requires a range of quality-oriented activities, from quality planning to QA and QC to continuous quality improvement [11]. Quality planning establishes product requirements prior to manufacturing, while quality assurance focuses on establishing and validating control procedures and standards during manufacturing, and quality control verifies compliance with requirements and standards mostly after manufacturing (see Figure 2). Quality improvement can then be achieved by using the results and findings of QA and QC to optimize future manufacturing processes. QM is not limited to the manufacturing process, but encompasses the entire AM value chain from the customer's initial manufacturing request through the development, manufacturing and testing processes and the use of the part to recycling (see also Figure 6 in chapter 2.3.2). In the process, technical, operational and management activities are recorded to ensure that AM production complies with standards and works continuously to improve quality [11]. This is supported by specific QM methods such as Six-Sigma [11], 8D reports [36], Ishikawa diagrams [37], Quality Function Deployment (QFD) [38], Design of Experiments (DOE) [39], etc.



Figure 2: Areas of quality management.

2.2.2 Quality assurance and quality control

QA is a component of QM and, according to DIN EN ISO 9000, comprises all activities aimed at creating confidence in order to ensure specified quality requirements. QC, in turn, is a subtask of QA and includes observation and inspection activities to fulfil product-oriented quality requirements or quality-relevant characteristics such as geometry, surface, appearance, etc. [34] Today, special test methods are used in all phases of AM production as part of QA and QC, which can basically be divided into destructive and non-destructive test (NDT) methods [6]. NDT methods do not affect the future usability of the part to be tested (e.g. 3D and CT scans, ML image analysis), but destructive testing methods do, so that only a limited number of test samples are ever tested there and not the final part. Destructive testing (e.g. tensile and compression tests, micrograph analysis) is therefore mostly used to evaluate the mechanical properties of AM parts, and non-destructive testing is used to examine the finished parts before delivery to the customer [6]. Another method of QC for AM is in-situ monitoring (visual, sensory and acoustic process detection) for efficient tracking and control of the printing process and print quality [40]. However, the possibility of directly monitoring the printing process in-situ is not yet very well developed at AM and is therefore the subject of numerous research activities [12].

Appendix A provides an overview of destructive test and NDT methods currently used in AM and their potential suitability as in-situ or ex-situ monitoring solutions (see Table A-1). Moreover, Wu et al. [41] comprehensively summarize current ML techniques for predicting mechanical, physical and geometrical properties of AM parts as well as ML-based in-situ monitoring

solutions for AM processes. Figure 3 illustrates some results of conventional as well as data- and ML-based testing methods for additively manufactured parts.

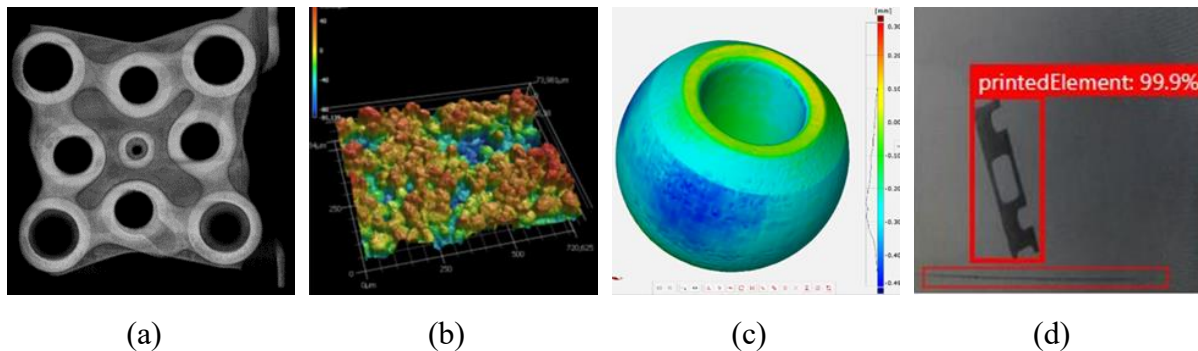


Figure 3: Results of various test methods on additively manufactured parts. (a) CT scan for analysis of internal part defects.; (b) Laser scan to investigate surface roughness; (c) 3D scan for analysis of part dimensional deviations; (d) Camera-based imaging with supporting ML analysis for fault detection.

2.2.3 Qualification, certification and standardization

According to DebRoy et al. [42], in addition to detailed QM, efficient QA and comprehensive QC, special qualifications and certifications of AM processes and parts are crucial aspects for a successful manufacturing process and increased popularity of the manufacturing technology. Qualifications and certifications are ultimately used to demonstrate that a product has passed certain performance and quality assurance tests and meets criteria set forth in regulations, specifications or contracts [43].

In this context, qualification is an evaluation process that focuses on the conformity of products and their industrial requirements, while certification rather verifies the compliance of the products with the legal requirements [44]. For conventionally manufactured products, qualification is often accomplished through the application of recognized norms and standards, as the resulting data can then be compared to known data ranges and specifications to ensure that the products meet the manufacturer's and end user's requirements [43]. According to Bae et al. [43], successful qualification and certification therefore depends heavily on quality in terms of part reliability and process repeatability. However, as mentioned above, this cannot be guaranteed for many AM processes, also because many standards and specifications of conventional processes are not directly transferable to additive manufacturing processes and thus the path to successful qualification and certification of AM products is often still unclear [43,44]. For this reason, standardization is taking on an increasingly important role in AM by providing a basis for consistency in part validation and processing, establishing repeatability, providing guidelines for maintenance and repair, and defining uniform terminologies [43,44].

A detailed look at the current standardization situation in additive manufacturing shows that various AM-specific standards have already been published. However, these always represent only sub-areas of AM. The ISO/ASTM 52900 series and in particular ISO/ASTM 52920 [45], which describes the QA requirements for AM, are fundamental in this respect. DIN SPEC 17071 is also the first fundamental guideline for establishing quality-assured processes in AM [46]. Relevant standards or standards in progress have been defined in ISO/ASTM 52920 for essential AM aspects, classified according to important sub-areas of the process chain. An overview can be found in Table 2.

Table 2: Standards for the AM process chain according to ISO/ASTM 52920 [45] (^a in progress).

AM aspect	Sub-area	Standards
Production management	Quality management	ISO 9001, ISO 9100, ISO 13485
	Health & safety environment	ISO 45001, IEC 60079-10-2, HSG103
	Quality assurance	ASTM F3091/F3091M, VDI 3405 Sheet 1
	Personnel	DIN 35225, ISO 9712 ISO/ASTM 52926-1 ^a , ISO/ASTM 52935 ^a
Customer management	Terminology	ISO/ASTM 52900, ISO 18739, ISO/ASTM 52921
	Risk assessment	ISO 31000, ISO/IEC 31010, ISO 14971
	Design guidelines	ISO/ASTM 52910, VDI 3405 Sheet 3, ISO/ASTM 52911-1, ISO/ASTM 52911-3 ^a , VDI 3405 Sheet 3.5
	Order requirements	ISO/ASTM 52901, ISO 17296-3, ISO 129-1, ISO 286-1, ISO 2768-1, ISO 1302, ISO 1101, ISO 14405-1
Data management	IT security	ISO/IEC 27001
	Data processing	ISO/ASTM 52950, ISO/ASTM 52915
Feedstock management	Material data sheet	ASTM F2924, ASTM F3184, VDI 3405 Sheet 2.1, Sheet 2.2, Sheet 2.4
	Characterization	ISO/ASTM 52907, DIN 65122, VDI 3405 Sheet 2.3
	Analysis, Viscosity, Flowability, Density, Particle size distribution, Sampling, Welding gas	ISO 11357-1, ISO 11358-1, ISO 1628-1, ISO 4324, ISO 1133, ISO 4490, ASTM B213, ASTM B964, ISO 1068, ISO 3923-1, -2, ASTM B212, ASTM B329, ISO 2591-1, ISO 13320, ISO 4497, ASTM B214, ISO 3954, ASTM B215, ISO 14175
AM process qualification		ISO/ASTM 52902, ASTM F2971, ISO/ASTM 52904, DIN 35224, ISO/ASTM TR 52906 ^a , ISO/ASTM TR 52929 ^a , ISO/ASTM TS 52930
Thermal post-processing		ASTM F3301 ^a
Test methodology	Guide	ASTM F 3122, DIN 65123
	Tolerances	ISO 2768-1, ISO 2768-2, ISO 1938-1, DIN 16742
	Hardness, Tensile tests, Compression, Impact, Analysis, Density	ISO 868, ISO 2039-1, -2, ISO 527-1, -2, ISO 527-4, ASTM D638, ISO 6892-1, ASTM E8/E8M, ISO 604, ISO 4506, ISO 179-1, -2, ISO 180, ISO 148-1, -2, ISO 7625, ISO 3651-1, ASTM G28B, ISO 3369

The list shows that standards specifically for data analysis and data storage in AM have not yet been explicitly published. However, these areas in particular are relevant for future technologies. Chen et al. [44], for example, propose a digital methodology for qualification, certification and standardization in AM. Of particular importance there are data-based digital process monitoring, e.g., through data-driven in-situ inspections or data-based process configurations, and digital transformation of AM processes, e.g., through machine learning optimized QC and blockchain-based decentralized AM supply chain documentation. Accordingly, the digital transformation of AM will proactively minimize errors, reduce human intervention, and improve transparency in documentation, ultimately leading to optimization of all quality-related aspects [44]. In order to do this efficiently, uniformly, and comparably, further standardization activities are needed in areas such as AI, blockchain, and data processing.

2.3 Blockchain for quality improvement in additive manufacturing

The combination of additive manufacturing and blockchain technology can enable a solution that maps the entire AM value chain in a digital, transparent, traceable and tamper-proof way, contributing to the digital transformation of AM QM [47]. One added value of blockchain technology is to improve the existing QM in AM in such a way that quality is more in focus, every actor in the value creation process is involved in the QM process and quality issues are documented transparently and effectively [11].

In addition to basic knowledge of distributed ledgers, blockchain technology and smart contracts, knowledge of the value and supply chains of additively manufactured parts is also necessary to implement an appropriate solution. Linking these aspects can then lead to a digital part record for AM parts. Based on this, a QM architecture can be designed that can also incorporate QA and QC data. By integrating modern data analysis methods and ML algorithms, a correspondingly transparent real-time evaluation of AM manufacturing data for in-situ NDT methods can also be performed. The basic methods and concepts for this are explained in the next sections.

2.3.1 Fundamentals of distributed ledgers, blockchain and smart contracts

Distributed ledger technology

Distributed ledger technology (DLT) is generally understood as a decentralized data architecture that enables the storage and distribution of data in a synchronized manner while ensuring its integrity through the use of consensus-based validation protocols and cryptographic signatures [48]. In other words, distributed ledgers are basically identical copies of file stores that

record transactions, are stored in multiple locations and are verified by a consensus algorithm [49].

Blockchain

The best-known form of DLT is blockchain, which is essentially a distributed database architecture based on cryptographically linked blocks of information, which in turn contain consensus-validated datasets [48,50]. The first known blockchain was released in 2008 as Bitcoin blockchain [51]. Another popular variant is the Ethereum blockchain, which was conceived by Buterin [49] and Wood [52] in 2014. Ethereum can be seen as an extension of the Bitcoin blockchain, which additionally enables, for example, the creation of digital contracts using cryptographic methods [49]. For the testing of corresponding smart contracts as well as other applications, Ethereum has special test networks. One test network is, for example, the Ethereum Ropsten Testnet.

Cryptographic Hashing

Individual blocks of a blockchain are linked to each other via cryptographic signatures, so-called hashes. (see Figure 4). Hash functions generate for each block from the records of arbitrary length a characteristic string with a specific length and structure [53]. The character string is referred to as a cryptographic checksum or hash value and represents a unique fingerprint for each block, which in turn is stored in the subsequent block. In this way, the blocks are chained together and unnoticed manipulation of individual blocks is virtually impossible [54,55]. However, hash functions cannot be equated with encryption in this context because, according to Rogaway and Shrimpton [54] as well as Yaga et al. [53], they have the following properties:

- they are preimage resistant or one-way, i.e. messages can be converted into a hash value, but the reverse is no longer computationally possible,
- they are second preimage resistant or deterministic, which ensures that the same input always generates the same output hash, and
- they are collision resistant, whereby it is not possible to find two different inputs that produce the same output hash.

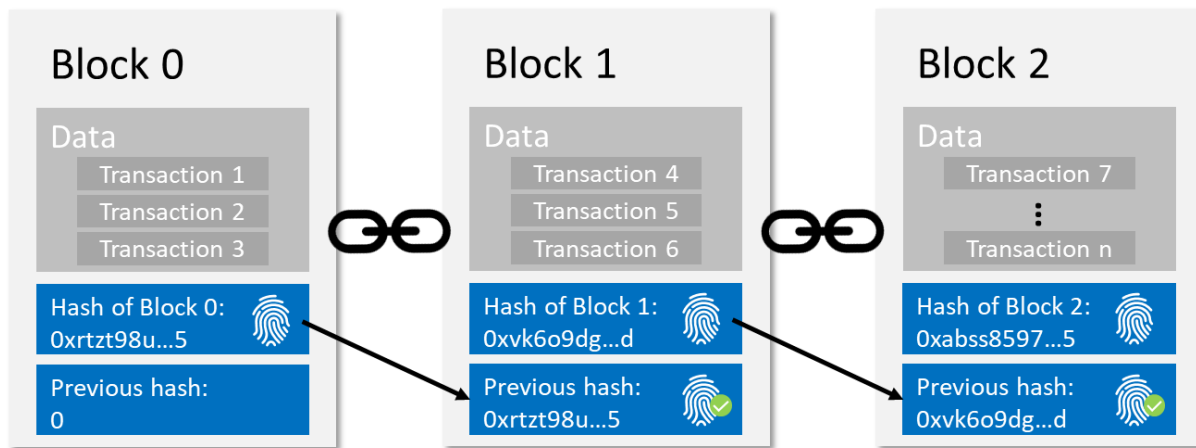


Figure 4: Concatenation of information blocks of a blockchain via cryptographic hash functions.

Digital signature

Due to the special properties of a hash, even the smallest changes in the data of a block lead to a significantly different hash. This principle is also used for digital signatures to ensure that a data record has not been changed after transmission. However, it must be ensured that the signature cannot be copied and cannot be executed by anyone other than the signature creator [56]. For this problem, public key cryptography or asymmetric encryption is used. With this method, a public and a private key are created for each network participant. Both keys consist of mathematically generated alphanumeric characters of a certain length and are not identical, but dependent on each other [56]. The public key is a publicly accessible information, while the private key is an information that is kept secret.

In a blockchain, transactions are authenticated by digital signatures by first creating a signature from the sender and then verifying that the signature is valid in a second step [57]. First, the hash value of a data record is calculated. Using the sender's private key, an encrypted digital signature is then generated by an algorithm and appended to the end of the data record. To verify the signature, the sender's publicly available public key is then used to decrypt the encrypted signature back into a readable hash at the end of the record. In addition, the receiver also calculates the hash value of the original data record. If the hash values of the decrypted signature and the original data record are identical, nothing has been changed after the data transmission. The digital signature process is shown again in detail in the following Figure 5.

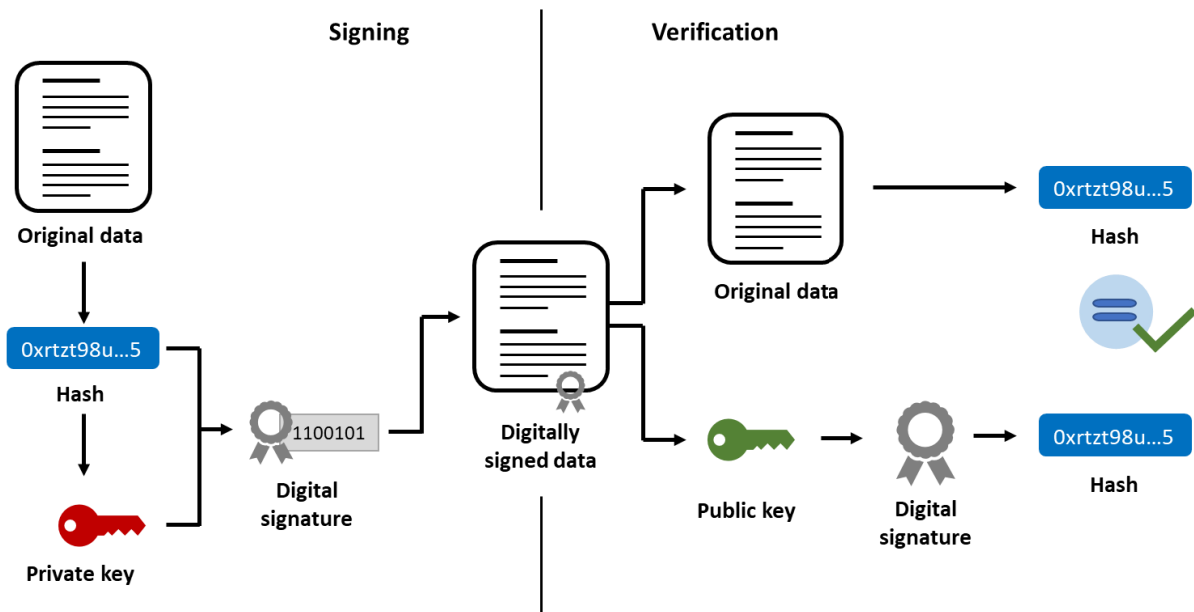


Figure 5: Schematic representation of a digital signature with asymmetric encryption.

Consensus protocol

Signed records or transactions on a blockchain are checked for validity before they are stored. This is done by special network participants (also called “miner”). To ensure that transactions are verified by network participants in the first place and to determine the order in which transactions are recorded and stored in the blockchain, the existence of a consensus mechanism is an essential requirement [58,59]. Special consensus mechanisms or consensus protocols thus ensure compliance with certain rules in the blockchain network and set the conditions for user participation in the network, which enforces consistency and integrity and ultimately leads to tamper resistance and immutability of the stored information [59]. Blockchain consensus protocols are divided into two distinct classes according to Oyinloye et al. [59]:

- evidence-based consensus protocols such as Proof-of-Work (PoW) [50,55], which require proof of computational effort by network participants to verify transactions, and
- voting-based consensus protocols such as Proof-of-Stake (PoS) [50,55], which require participating entities to first share their individual verification results in the network before a final decision is made to verify transactions.

In addition to these main classes, other consensus mechanisms have been established, but there is no perfect consensus protocol in distributed systems, since a compromise between consistency, availability, and fault tolerance must always be found [60]. Furthermore, the problem of malicious network participants who intentionally undermine the consensus process must also be considered [61].

Smart contracts

Due to its properties and the implemented basic cryptographic principles, blockchain technology offers for the first time a suitable infrastructure for the implementation of smart contracts [62]. The concept of smart contracts was published as early as 1994 by Szabo [63] and describes them as computer programs with self-checking, self-executing, and tamper-proof properties. Appropriate consensus-based programs can then be used to define user-defined rules for ownership, transactions, and state transitions so that the entire transaction process can be mapped through automated contract execution in a cost-effective, transparent, and secure manner [64]. Smart contracts leverage and extend the blockchain technology [53]. According to Yaga et al. [53], they are program codes stored on the blockchain that consist of functions and states provided by cryptographically signed transactions on the blockchain network. Accordingly, users of a blockchain network can interact with smart contracts and use them to perform calculations, store information, publicly reflect states, and automatically send funds to other network participants [53]. The smart contract code can also be used to map transactions with multiple parties and to map entire business processes, e.g. for documentation and traceability of supply chains. This has the advantage of promoting transparency and trust, saving costs and time, and enabling better as well as faster business decisions [53].

Smart contracts are often used in so-called decentralized applications (dApps), which provide a user-friendly interface for smart contracts. The development of dApps, where certain data and processes are stored on a blockchain, is growing more and more [65]. A typical example of a dApp is an exchange for cryptocurrencies running on a blockchain network. In the process, the usual structure of the decentralized application consists of a frontend (web application) and a backend (database or decentralized storage system). It is also possible to interact directly with the smart contract via a so-called blockchain explorer (e.g. the web application Etherscan [66]). A decentralized storage system is the counterpart to a centralized data storage server and consists of a network of users who all provide cryptographically protected storage for data, creating a robust data storage and exchange system for larger amounts of data. An appropriately merged, decentralized, and cost-effective storage solution for larger amounts of data is, for example, the Interplanetary File System (IPFS) [67].

2.3.2 Blockchain-based part record for the additive manufacturing value chain

For additive manufacturing, blockchain technology with its cryptographic encryption principles and automated smart contracts offers new opportunities. These include, for example, data and intellectual property protection in 3D printing supply chains [68] and data [69], traceability, tamper resistance, and certification of parts and quality-related documents [30,70], as well as

increasing process automation and decentralization of manufacturing through direct machine-to-machine communication [70–72].

Connecting the digitized AM process chain with a blockchain-based infrastructure can, for example, enable digital, secure, immutable and transparent AM part documentation and, if necessary, certification, which in turn helps to improve QM, also between different companies [30]. A corresponding solution can enable the digital mapping of the entire value chain of an AM process, from the initial customer inquiry through development, production, quality inspection and use of the part to its recycling (see Figure 6). Basic concept ideas [35,73], partial solutions and implementations [30,74] have already been created for this purpose. However, a holistic solution or demonstration study for digitally mapping the entire value chain of an AM process has not yet been documented. In addition, the increasingly important and very extensive aspect of production data acquisition, documentation and real-time evaluation has also been insufficiently considered in this context. However, in Germany, for example, there are publicly funded initiatives that are increasingly addressing the issue [75–77].

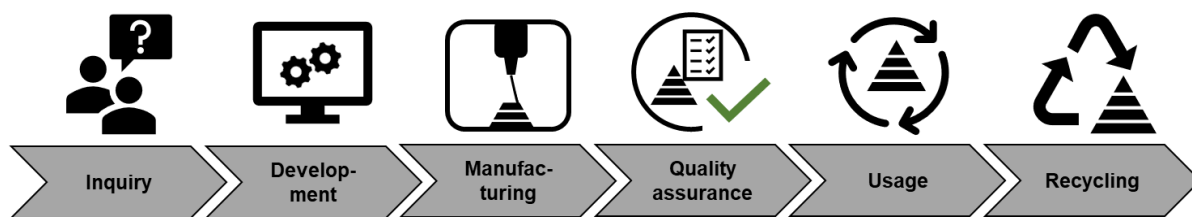


Figure 6: Components of QM along the AM value chain (simplified representation).

2.3.3 Connecting blockchain, digital twin and data for real-time quality analytics

Concepts for manufacturing data acquisition and documentation are currently often developed in conjunction with a digital twin to derive a form of digital intelligence from digitally accessible data [78]. In doing so, digital twins provide an accurate digital representation of physical elements and help to better understand, analyze and improve a product, service or manufacturing process [78,79]. In AM, digital twins are primarily used to collect data for process simulation, monitoring and control, and to present this data in a form suitable for information retrieval [79,80].

The connection of digital twin and blockchain technology for secure, traceable recording and documentation of manufacturing data has only been considered in isolated cases to date. In this regard, Guo et al. [81] developed a framework that enables personalized part production with AM based on blockchain and digital twin. Data on the product lifecycle is stored there as a digital twin on a blockchain and transmitted authentically to customers and part manufacturers. Mandolla et al. [82] have developed a digital twin of the entire AM manufacturing chain and

stored relevant manufacturing information in it. At the same time, a secure transaction layer for the information was created via a blockchain, which secures all data in the digital twin against changes by cryptographic hashing. As an extension of the existing solutions, research is increasingly being conducted not only on data acquisition and storage, but also on data processing and analysis, e.g., through artificial intelligence and machine learning [79]. In addition, the integration of sensor technology for real-time data acquisition is also being investigated [83]. Only in this way it is possible to process manufacturing data efficiently and securely, to create traceable datasets, and to develop generally accepted AI solutions that can then be used in QA and in-situ QC, for example.

2.4 Quality assurance through data analytics and machine learning

The analysis of manufacturing data and the use of AI or ML extend the mere collection, storage and distribution of information of a digital twin with additional methods for generating intelligence based on data [78]. As digital QA or QC solutions, data analytics and ML algorithms can be directly integrated into a digital QM strategy, enabling e.g. automated in-situ monitoring applications through appropriate implementations [84,85] and intelligent real-time analyses [86,87], that constantly control and optimize themselves by evaluating and integrating ever new data.

Corresponding solutions are based in principle on the extraction of knowledge from data [88]. Various methods and technologies are used for this purpose, such as data, text and statistical analyses, data visualizations, signal processing and ML. In this context, ML methods in particular are considered as a form of artificial intelligence because, unlike model-based control, for example, they are capable of making own assumptions, re-evaluating and testing themselves, and automatically making predictions for future events without reprogramming. This is done via computer so quickly that real-time process analyses, data evaluations and reactions are possible, which then contribute as a supplement or alternative to conventional QA and NDT methods. The basics for this are described in the following sections.

2.4.1 Distinction of data analytics, machine learning and artificial intelligence

Data analytics

Data analytics is the use of computer systems to analyze large amounts of data to support decision-making processes [89]. A corresponding data analysis system collects data, analyzes as well as extracts information from the data and displays the found knowledge to the user [90]. Nowadays, data volumes are very large, composed of different data types and also include streaming data [91]. Corresponding amounts of data, referred to as “Big Data”, are usually high-

dimensional, complex, unstructured, incomplete, noisy or erroneous, and therefore require new data analysis concepts, also referred to as “Big Data Analytics”. [90,92]. In big data analytics, there are different stages of development from descriptive analytics to predictive analytics to prescriptive analytics (see also Figure 7) [93–97]. The individual developmental stages show an increasingly higher degree of intelligence and can be described as follows:

- **Descriptive Analytics:** Summarize data in an appropriate way and report on the past. They answer the question “What happened?” and extract information from raw data. As an extension of this stage of development, diagnostic analytics are often listed as also reporting on the past, but more likely answering the question of why something happened and helping to understand relationships between data. Examples are business and sales reports.
- **Predictive Analytics:** Use the results of descriptive analysis as well as special ML algorithms and detection techniques to build models to predict the future. They answer the question “What will happen in the future and why?”. Predictive analytics help identify patterns in historical data and are more accurate the more data there is. Examples are predictions for process trajectories and error probabilities.
- **Prescriptive Analytics:** Generate adaptive, automated, and optimal decisions to create defined value. They answer the question “What should I do and why?”. Prescriptive analytics provide recommendations based on predictions from predictive analytics as well as specific constraints and support feedback mechanisms to intelligently link data, predictions, recommended actions and results. Examples are recommendations for process settings and closed-loop systems.

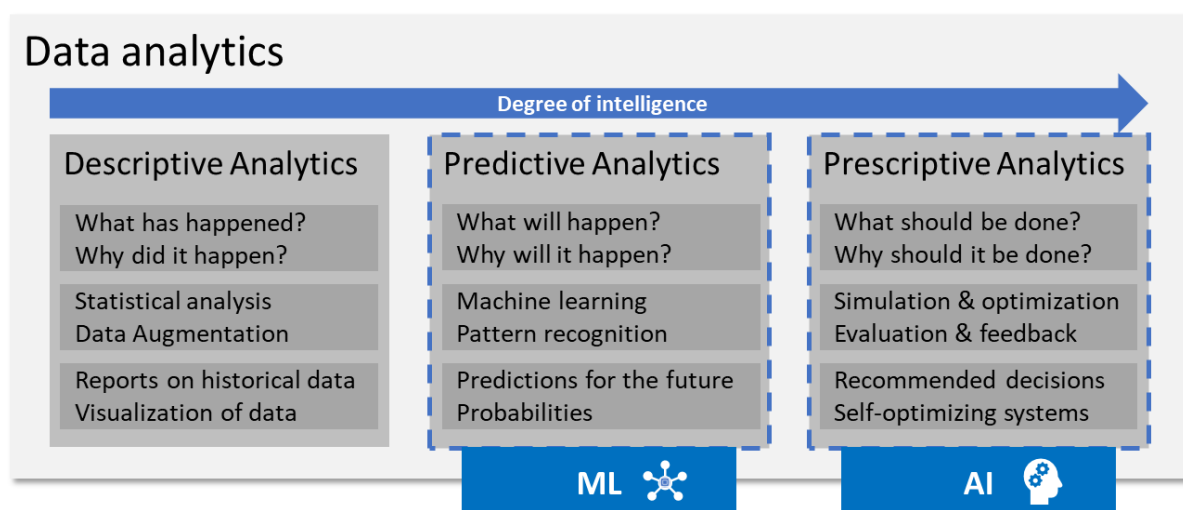


Figure 7: Data analytics development stages.

Machine learning

ML techniques provide a way to evaluate large amounts of data in near real-time and identify complex, non-linear relationships in the data [98]. These correlations can subsequently reveal hidden patterns in the data and enable predictions or decisions for future events [99]. For corresponding ML methods, the acquisition of large amounts of data is fundamental, since an ML algorithm is not explicitly programmed but trained with the acquired data [100]. Human programming effort decreases because after a certain point, an ML algorithm learns independently of the underlying data and automatically improves its performance through experience and the detected correlations in the data [99,101]. Up to this point, however, humans must assist in the learning process, e.g., through data analysis and data preparation (feature extraction) [99]. Figure 8 illustrates the initial ML process using the example of image data.

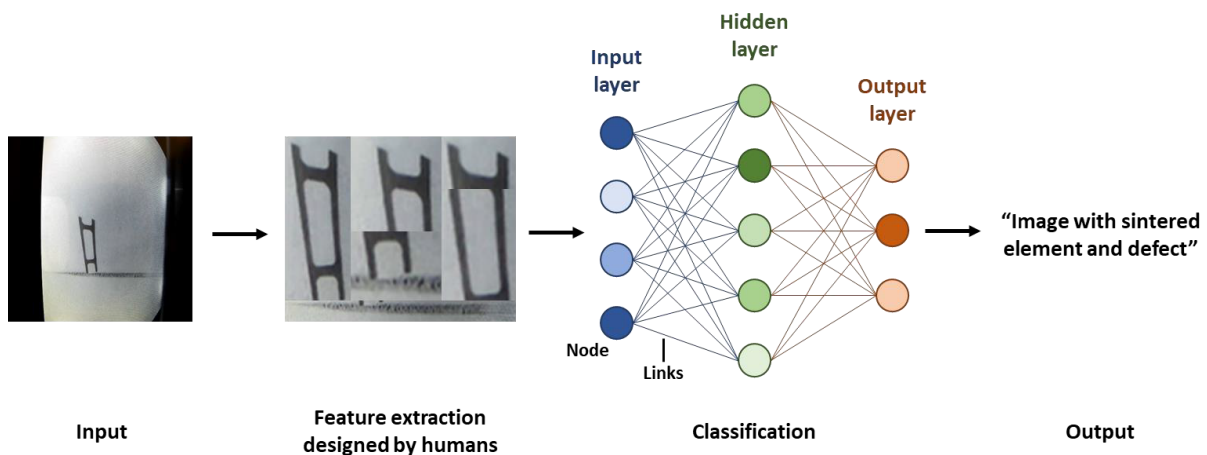


Figure 8: Information processing in ML with human assistance by feature extraction of relevant image regions in powder bed images of the SLS process.

In the application of ML, the focus is on the learning methods that are used to learn from data: supervised, unsupervised and reinforcement learning [100,102]. Supervised learning requires training with labeled, structured data that has inputs and outputs (e.g., database tables, CSV files). Unsupervised learning, on the other hand, does not require labeled data and can also use unstructured data with inputs without direct outputs (e.g., images, videos, speech), where the goal is to find hidden structures in the inputs. Reinforcement learning enables learning by evaluating feedback in the form of reward or punishment to determine the optimal behavior to improve efficiency in a given environment [103]. This involves trying an action in a particular state, evaluating the consequences based on rewards or punishments, and determining a new state. By repeatedly trying all actions in all states then teaches which actions, as measured by reward, are best in the long run [104]. For all learning methods there are different ML algorithms suitable for different problems (see Table 3).

In ML, the ultimate goal is always to develop models that generalize, i.e., produce good results even with unknown data [100]. There are several methods and performance metrics to assess and reliably measure the generalization capability of corresponding models.

Table 3: Learning methods, algorithms and tasks in ML according to [102].

Learning method	Model building	Tasks	Algorithms	Reference
Supervised learning	Algorithms learn from labelled data (task-driven)	Classification/ Regression	Regression analysis	[105]
			Support vector machine	[105]
			Decision tree	[105]
			Naive Bayes	[101]
			Neural networks	[100]
Unsupervised learning	Algorithms learn from unlabeled data (data-driven)	Clustering/ Prediction	K-means	[105]
			Principal component analysis	[105]
Reinforcement learning	Models are based on reward or penalty for actions (environment-driven)	Decision-making	Q-learning	[104]
			R-learning	[106]
			TD-learning	[107]

Performance evaluation methods and metrics

To evaluate the performance of an ML algorithm, two aspects are considered below. First, methods to mitigate overfitting and maximize generalization, and the evaluation or measurement of model performance by specific metrics.

According to Chollet [100], the evaluation of a model always boils down to the splitting of the underlying dataset into training, validation and test data. The goal is then first to minimize the prediction error of the model on the training data (training loss) [108]. The actual prediction accuracy of the model is the prediction error on new (test) data unknown to the model (test loss). In order to achieve good model performance, efforts are usually made to minimize training loss and keep the gap between training and test loss small [108]. If a low training loss is not achieved, the model is underfitted, if the distance between training and test loss is too large, the model is overfitted [100]. According to Chollet [100], overfitting always occurs in ML models, and usually occurs both with new data and with too little data, although advanced methods (such as hold-out, K-fold, and iterated K-fold validation) can be used to mitigate overfitting, especially with too little data. In addition, especially for more complex ML algorithms such as neural networks, special regularization methods are used to prevent overfitting:

- **Data augmentation:** Artificial expansion of the dataset by applying transformations to individual data samples in real time [100,109].
- **Hyperparameter tuning:** Iterative optimization of the default settings of an ML algorithm defined by common ML libraries to improve model performance [100,110].
- **Weight regularization:** Reduction of the complexity of the algorithm by specifying special boundary conditions with the goal of achieving a more uniform distribution of weighting values [100].
- **Dropout:** Random removal (set to zero) of output signals and their connections from a neural network during training to prevent overfitting of directly connected neurons [100,111].

Another very effective method for avoiding overfitting in complex neural networks, especially for very small or highly imbalanced datasets, is transfer learning [112]. Transfer learning reduces the effort required to create a new classification task by transferring knowledge between neural networks of different feature domains [112,113]. Practically, this means that the already learned information of a trained neural network with dataset X is used as initial values for training another neural network with a completely different dataset Y. This method is often used when the dataset under investigation does not contain enough training data or when the distribution of the data among the individual classes of the dataset is too unbalanced [113]. Then, a neural network is first trained with a large, preferably balanced dataset of relatively easy-to-obtain data, and the knowledge gained is then transferred to the neural network for the actual classification task. For example, a very well-known dataset for transfer learning is the open-source ImageNet dataset, which consists of more than 15 million images divided into more than 22000 categories [114].

A success evaluation of ML models, or the measurement of model performance, is done using a variety of metrics that provide different information about the particular model, e.g., its ability to predict mean values, its robustness to outliers, the uncertainty of predictions, etc. [115]. By Naser and Alavi [116], performance metrics for the evaluation of regression and classification algorithms are subdivided and comprehensively presented with their foundations, recommendations, and limitations in the context of ML model evaluation.

Selecting an appropriate metric to examine and distinguish the performance of different algorithms is an important aspect of ML, as the proper selection of the metric ensures that the training of algorithms is consistently evaluated against appropriate criteria [117,118]. The results of this evaluation are often presented in classification tasks in the form of a special confusion matrix (CM) [109]. This matrix contains statistics on actual and predicted classifications and

forms the basis on which further metrics for performance evaluation are subsequently derived (see Figure 9, left) [116]. One way to visually evaluate classification algorithms is to use the receiver operator characteristic (ROC) curve [119]. It is widely used to illustrate and compare binary classification problems based on complex neural networks (see Figure 9, right) [115,119,120]. However, ROC curves are not per se a comparable performance indicator [121]. This one is only determined by the value of the area under the curve (AUC), which is often used to compare the performance of different ML models [121]. The larger the area under the ROC curve, the better the algorithm performs. Another visual evaluation method for the performance of special convolutional neural network models is the gradient-weighted class activation mapping (Grad-CAM) of Selvaraju et al. [122], which provides a heat map for locating and predicting regions of interest in images.

		Predicted class		
		Positive	Negative	
True class	Positive	True Positive (TP)	False Negative (FN)	Sensitivity $\frac{TP}{(TP + FN)}$
	Negative	False Positive (FP)	True Negative (TN)	Specificity $\frac{TN}{(TN + FP)}$
		Precision $\frac{TP}{(TP + FP)}$	Negative predictive value $\frac{TN}{(TN + FN)}$	Accuracy $\frac{TP + TN}{(TP + TN + FP + FN)}$

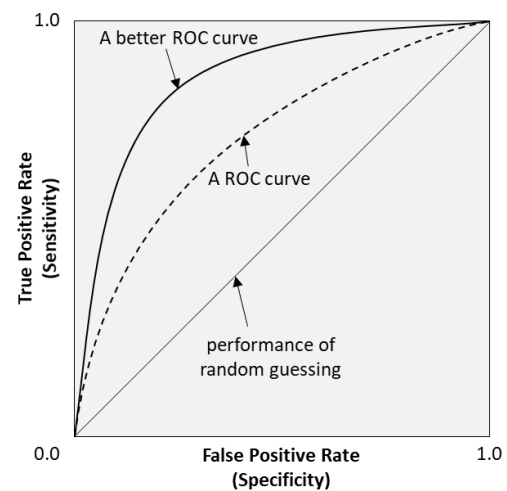


Figure 9: Basic performance evaluations of ML models. left: CM with commonly used metrics, right: Visualization of two typical ROC curves and the performance of random guessing.

Artificial neural networks

Artificial neural networks (ANN) are powerful ML algorithms that are ideal for processing large amounts of data [123]. They are relatively easy-to-implement computer-based computational models used for problems such as pattern classification and pattern recognition [124].

The principle of an ANN is to process signals by sending them through a network of artificial nodes or neurons that mimic the human brain [125]. Analogous to the synapses of the brain, the signals are also transmitted between the artificial neurons via connections and thereby weighted [125]. This process represents “learning”, whereby weights are amplified or attenuated with each signal transmission [126]. In most ANNs, neurons are arranged in a series of layers. For example, a network specialized for images has a layer of input nodes that respond to individual pixels (e.g., their brightness) [125]. Once activated, these nodes pass on their activation level

via the weighted links to other nodes at the next layer, which combine the incoming signals and thus may or may not also be activated [125]. This process continues until the signals reach an output layer, where the activation pattern gives a concrete answer to what is seen in the image. If this response is reported to the network as incorrect, a so-called backpropagation algorithm performs a backward adjustment of the weighting of the connections through the layers to improve the result next time [125,126]. In order to use the backpropagation algorithm, the ANN must always have some form of supervised learning in addition to unsupervised, since for each image there must be a correct answer that can be transmitted to the network in case of incorrect statements. The signal processing with weighting and backpropagation is explained again in detail for better understanding in appendix B.

Deep learning

Conventional ML algorithms have limited ability to process unstructured data in its raw form (e.g., images, videos, natural language) [127]. According to LeCun et al. [127], such raw data are increasingly processed using advanced state of the art algorithms based on Deep Learning (DL). DL here is a new way of looking at learning information from data, focusing on learning from successive layers of increasingly complex data representations (see Figure 10) [100]. A key aspect of DL, according to LeCun et al. [127], is that a function extractor is no longer designed by human developers, but is learned by a learning process from data only. Learning with the layer representations is then done as in conventional ML, again with artificial neural networks, but with many more layers and thus complexity (the networks are “deeper”) [100]. Figure 10 illustrates the information processing in DL using an example of pattern recognition in images, where the features in the individual network layers are searched for independently from the data.

Over time, DL architectures of varying complexity have been developed [128]. In principle, any architecture can be used for any task, but some variants are better suited for specific data such as time series or images [129]. A multilayer perceptron (MLP) is the simplest and most original form of DL architectures [130]. One of the most popular DL implementations for modeling spatial and temporal correlations are convolutional neural networks (CNN) [131]. CNN implementations are state of the art in image and speech processing [114]. Another commonly used DL implementation for Big Data analytics are recurrent neural networks (RNN) such as the long short-term memory (LSTM) architectures, which are capable of learning long term dependencies in sequential data [132]. Other well-known DL architectures are autoencoders and generative adversarial networks (GAN) [128,129].

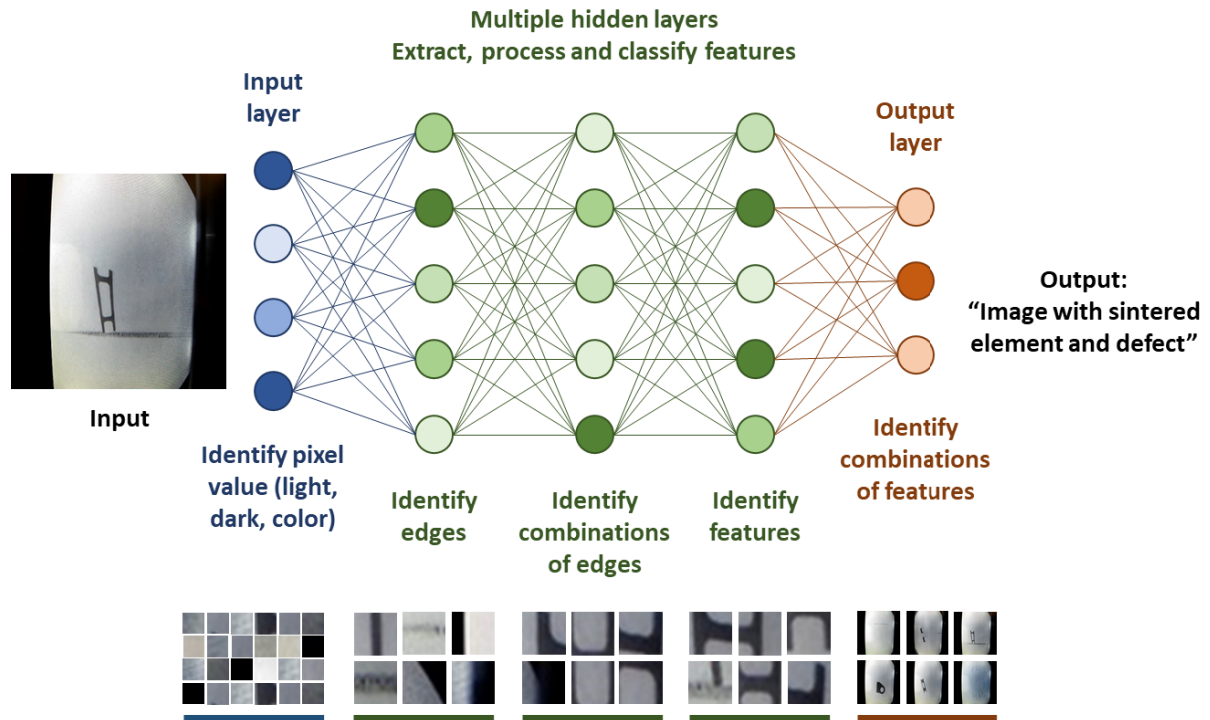


Figure 10: Information processing in Deep Learning exemplified by a pattern recognition algorithm for defect detection in powder bed images of the SLS process (adapted from [125] and the design of Lucy Reading-Ikkanda).

Artificial intelligence

ML and DL algorithms have proven to be extremely powerful predictive systems and are also referred to as artificial intelligence by many institutions, developers, and companies, but this does not correspond to the original core idea of AI [133]. Rather, according to McCarty et al. [134], the core idea of artificial intelligence is that intelligent human behavior consists of processes that can be formalized and reproduced by a machine. Human intelligence is the central element on which automation efforts should be based. But today, most researchers want to develop automated systems that perform well in complex problem domains, using all kinds of means, not just human-like means [135]. Thus, even today's ML systems, currently the most powerful and profitable forms of artificial intelligence, exhibit a rather limited range of intelligent behavior [133].

For this reason, ML is also considered more of a subfield of AI, based on the concept that machines learn even from large amounts of data [96,99,100]. According to Kibria et al. [96], ML is more suitable for predictive analysis, while AI goes beyond corresponding predictions and offers suggestions with implications for the realization of added value in the context of prescriptive analysis, which has already been indicated in Figure 7.

2.4.2 Machine learning methods for quality assurance in additive manufacturing

As in many other fields, ML has gradually gained importance in AM too, especially due to the high performance of data processing algorithms in tasks such as classification, regression, and clustering [136]. ML is increasingly playing a critical role in addressing AM-specific challenges such as ensuring predictable, reproducible and high part quality, developing optimized design principles, standardization and quality control [137]. ML is therefore already used intensively in many AM areas, e.g. to generate high-performance materials and topological designs, to optimize process parameters, or to be able to perform error monitoring during the process [136]. Accordingly, several scientific reports have already been published on the general use of ML in AM [115,136–139].

Specific methods for optimizing QA and QC through the use of ML are also being intensively investigated, with core aspects increasingly (but not exclusively) divided into manufacturing support (defect detection, surface prediction), process improvement (process monitoring, process control), and design optimization (design recommendation) [140]. Table 4 clearly summarizes these ML core aspects, the ML-based solution principles behind them, the achievable benefits in terms of QA and QC, and the relevant sources.

Finally, the listed ML applications alone or in combination do not yet represent fully reliable QA and QC methods. They can currently be useful as complementary methods alongside conventional methods such as CT scans, micrograph analyses or mechanical testing to provide information on print and part quality already during the printing process, although their efficiency and suitability for industrial AM series production still needs to be evaluated in most cases [137,140–142]. Although corresponding ML solutions can in principle enable closed-loop strategies for predictable and reproducible quality optimization [143,144], they do not include certain quality-relevant aspects such as data management, documentation, or conformity to standards and can therefore only be part of a comprehensive quality assurance system for AM.

Table 4: ML Methods for better QA and QC in AM.

ML-aspect and solution principles	Advantages for QA and QC	Source
<p>Defect detection: Mostly in the form of DL image analyses of process images captured with cameras during printing. ML analyses of sensor process or geometry data to detect process irregularities are also used. Some form of supervised learning is usually implemented.</p>	<p>Solutions are usually easy to integrate into the AM process and are non-destructive. In-situ analyses are also possible and the achievable prediction accuracies are very high.</p>	<p>[145–149]</p>
<p>Surface prediction: ML algorithms are trained using process parameters recorded or specified by sensors, and the prediction results are correlated with the resulting print results. With the print parameters set, a prediction can then be made about the surface quality even before the printing process. In principle, supervised or unsupervised learning strategies are used for this purpose.</p>	<p>Better surfaces are possible during printing and the selection of good process parameters is much faster. The predictions are very precise and fast. Automated adjustment of process parameters is also possible.</p>	<p>[150–154]</p>
<p>Process monitoring and control: For process control, certain parameters are monitored and recorded via sensors throughout the manufacturing process and analyzed for irregularities in the data sequences by pre-trained ML algorithms. The immediate feedback of product quality resulting or predicted from these parameters is then directly used to optimize the process parameters inline as automatically as possible (via reinforcement learning). Currently, the parameters are often first adjusted offline and the settings optimized for the next print.</p>	<p>The entire process is monitored and recorded by sensors. This enables real-time data analyses that directly detect changes in the printing process. In the future, increasing automation in information processing will also enable closed control loops that can react directly to irregularities and optimize printing parameters independently.</p>	<p>[155–159]</p>
<p>Design recommendation: AM machine and material settings are analyzed by ML algorithms to verify the manufacturability of a given AM design with the selected parameters. Based on historical manufacturing and part data, the algorithms also automatically enable recommendations for design changes to optimize parts, processes, or costs without the need for specific instructions. Supervised and unsupervised learning strategies are mostly used in the training phases, which are then increasingly complemented by reinforcement learning for decision-making tasks.</p>	<p>Automated design recommendations based on historical data can enable AM-compliant designs even for inexperienced users. In addition, time and cost savings are possible. A growing database also enables increasingly detailed recommendations and better parts. Thus, design recommendations can be made without human guidance in the future.</p>	<p>[141,160–163]</p>

2.4.3 Closed-loop quality and process control for additive manufacturing through machine learning

Closed-loop control systems, also known as feedback control systems, are a form of automation system that have one or more feedback loops and attempt to compensate for deviations that arise in the system [164]. According to Khosravanian and Aadnøy [165], system design uses a controller or algorithm that calculates setpoint deviations via real-time measurements and then activates a process to return the system to the fixed setpoint (see Figure 11). However, this requires a large amount of data for the decision making [165].

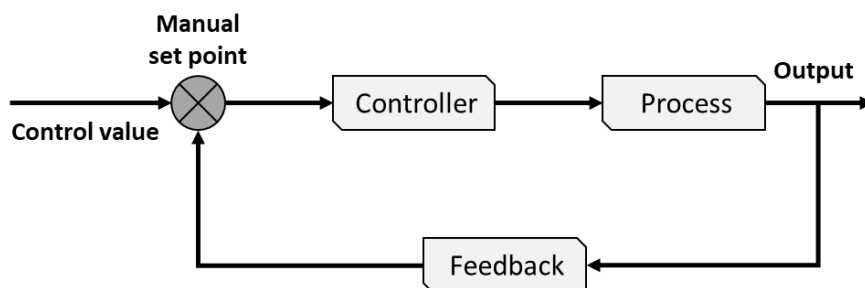


Figure 11: Schematic representation of a closed-loop feedback system.

The integration of ML-based data analytics into AM QA structures can increasingly help implement closed-loop quality and process control systems that combine process knowledge and process information in the form of recorded data [144,158]. This is mostly automated within the manufacturing process of a company [158]. The use of an ML algorithm then reduces the system design effort in principle by replacing the human description of a physical model and controller design with the automatic generation of an empirical model by AI and ML, respectively [144]. Nevertheless, training of the ML algorithm with respect to the setpoints and with result feedback is necessary to determine a continuously self-optimizing setpoint. Figure 12 schematically shows a corresponding ML-based process control loop.

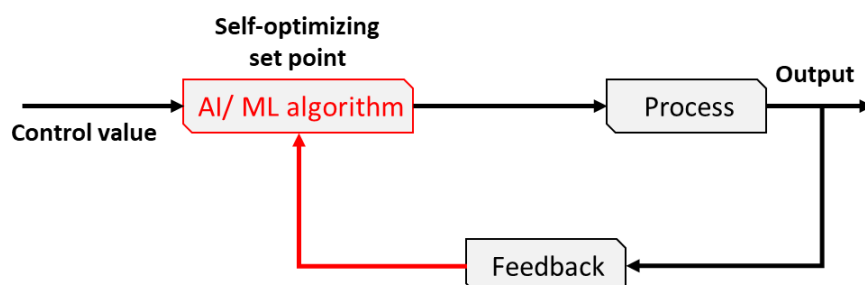


Figure 12: Schematic representation of an AI- or ML-based closed-loop feedback system.

Various process feedback systems have already been implemented in different AM processes, e.g., to detect defects during the FDM manufacturing process [143], to perform corrections

during printing [166], or to avoid time and material losses [167]. Rahman et al. [168] have also developed a holistic process and data framework for AM that enables knowledge management and information feedback in a closed loop system. Within this framework, all AM sub-processes are connected to an information system that captures, stores and analyzes the flow of data along the process chain and feeds the knowledge gained back to the respective sub-process in a feedback loop for process improvement. Liu et al. [158] have developed a similar system consisting of four individual feedback loops for specific subprocesses. Razaviarab et al. [143] have implemented a special process control by DL image analyses of process images during part fabrication. The results of the analyses are used by an intelligent 3D printer to automatically change the manufacturing parameters. A general summary of design and implementation methods for control systems for AM was presented by Fang et al. [169]. Thereby, it was found that the integration of feedback loops significantly improves the reliability and repeatability of an AM process as well as the mechanical-physical quality of AM parts [169].

3 Conception and implementation

This chapter describes the conceptual structure of the digital quality assurance system. In addition, this chapter also shows exemplary implementations of solution ideas that go beyond the theoretical concept ideas and demonstrate the functionality of the digital quality assurance system. Within the framework of a cumulative work, an added value for quality management as well as quality assurance in additive manufacturing is created via individual scientific publications, which offers the users of the technology new possibilities for a qualitatively better, faster and more efficient part production. Figure 13 provides an overview of the developed concept with current structures (gray-black areas) and digital extensions in the form of exemplary implementation solutions (blue-white areas).

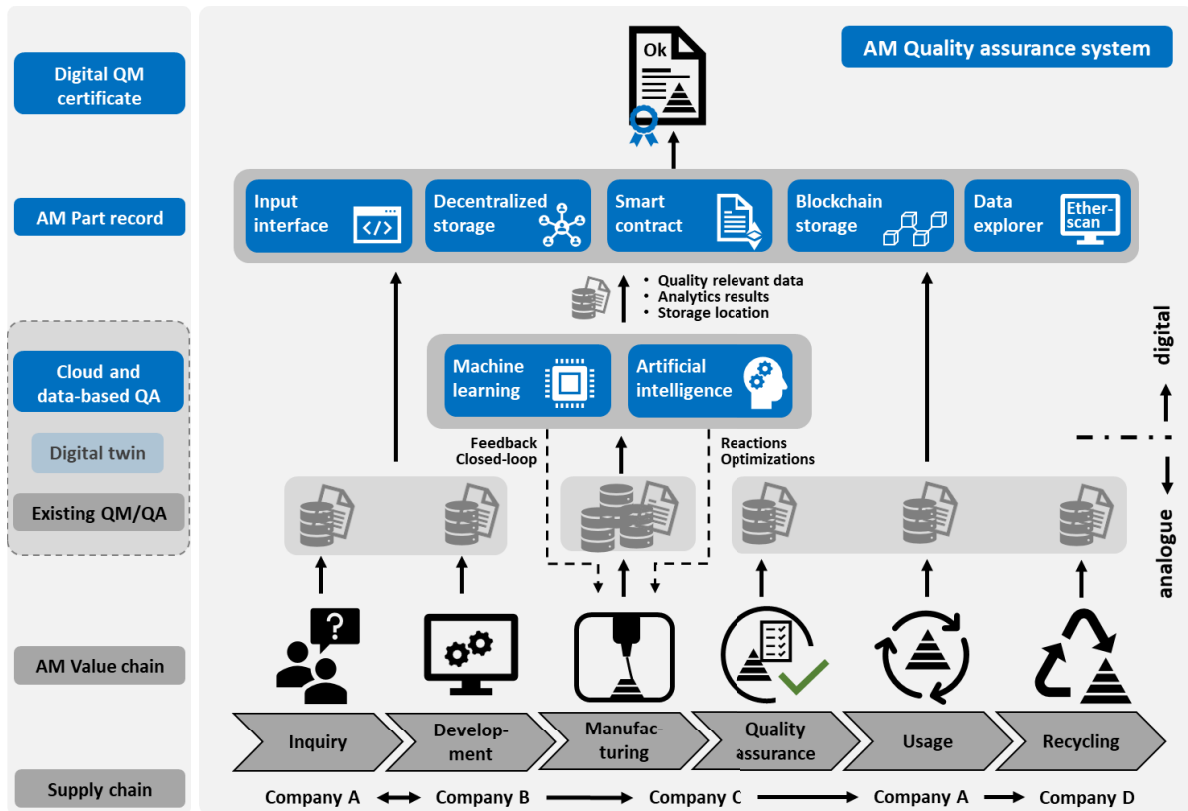


Figure 13: Overview of the conceptual design as well as the developed implementations of the digital quality assurance system.

Current AM QM increasingly relies on analog processes (e.g., paper-based documentation) and conventional QA with complex and expensive methods. This means that QM and QA are not carried out efficiently and with the necessary level of detail, which ultimately leads to partially suboptimal printing processes and part qualities. In addition, corresponding quality-relevant documentation is usually limited to the processes carried out within a single company. However, since several companies are usually involved in the AM value and supply chain, quality

documentation must be consistent across companies and transparent, tamper-proof and traceable for all participants.

The aim was therefore to improve this situation through research in order to achieve a more predictable and reproducible quality of AM processes and parts. Based on the existing QM and QA processes, a concept was developed that incorporates these areas and expands, links and, of necessary, optimizes them with digital solutions. In principle, the investigations carried out can be divided into two areas with three objectives. On the one hand, in an overarching blockchain area with a focus on digital QM and the development of a cross-company blockchain-based AM part record. The specific aim is to create a transparent, tamper-proof and traceable decentralized structure that can be mapped digitally, is cross-company, resource-efficient (in terms of cost, effort, time) and expandable. On the other hand, into an AI and ML area with the analysis of manufacturing data as well as the development and implementation of intelligent algorithms to support conventional QA processes in 3D printing. This is intended to enable fast, efficient, cloud and data-based alternatives for QA in AM that allow real-time process analyses and can be integrated into the higher-level digital QM. Both together then form the basis for a coherent, digital AM quality assurance system that builds on existing QM and QA solutions and contains all relevant information and data from the AM value chain and the respective transaction processes. The digital mapping of all quality-relevant data of a printed part across company boundaries in the digital quality assurance system to be developed should ultimately enable fast, automated information distribution of the production data analyzed in real time, which in turn allows immediate reactions to the printing process to be derived. This will form the basis for future closed-loop feedback systems that can achieve better predictability and reproducibility in AM processes through automated system parameterization. In addition, existing concepts such as digital twins as well as centralized, cloud-based data analyses can be integrated into the digital quality assurance system and provide solutions specifically for the rapid information feedback of the analyzed data to the 3D printers. Ultimately, this will also enable users of the technology to significantly improve part quality and reduce scrap and manufacturing costs in 3D printing. For authorities and certification bodies, the quality assurance system will also provide the opportunity to offer accelerated digital certification and qualification processes.

Accordingly, the individual scientific publications present exemplary implementation solutions that demonstrate the functionality of the individual aspects of the digital quality assurance system. Thus, with a smart contract, the concrete value chain of an AM sample process is linked via a web application with a decentralized data storage, a blockchain and interfaces for data

input and output. This forms the basic framework of the digital, cross-company QM in the form of an AM part record. Using special ML algorithms, two effective data-based QA methods are also implemented, each in its own publication, which represent digital alternatives or supplements to conventional QA solutions and also enable real-time analysis of large manufacturing datasets. The solutions developed also differ in terms of the type of data analyzed (images and sensor data), which illustrates the great potential of data-based quality assurance. Complex neural networks are used to create a comparable analysis basis for image and sensor data. Specially adapted algorithms developed for the AM data at hand are first trained with specially created datasets and, after the training phase, independently generate compact quality statements about the printing process. Only these extracted analysis results, as well as other quality-relevant data and a reference to the storage location of the entire datasets, are then transferred to the digital part record, saving time, costs and labor. The analysis results are also reported back to the production systems as feedback as part of a closed-loop system in order to be able to react to any irregularities detected on site and to be able to optimize the printing process.

Finally, the AM part record can also be used to create a digital certificate for documentation and compliance with special boundary conditions and specifications, which is handed over to the part users with the physical AM part. Via this certificate, the user can obtain information about the quality and production history of his part at any time. In addition, the part user and other parties involved can add further data to the AM part record during the use phase of the part up to recycling. All parties involved in the manufacturing process have tamper-proof access to the value-added data of the part at all times and can in turn use this data to optimize their manufacturing processes. The digital quality assurance system thus offers AM a digitized QM process with an integration and holistic view of QA, QC and quality documentation across the entire value chain of the part and thus new, previously unavailable possibilities.

4 Results

4.1 Development and implementation of data-based quality assurance methods for additive manufacturing (from [I] and [II])

The publications [I] and [II] contribute significantly to the first research focus of the dissertation with the development and implementation of ML algorithms for data-based and non-destructive QA processes in AM. In addition, aspects of data collection, data processing, and data analysis of both publications can also be partially attributed to the third focus of the thesis, which is the conceptual linking of blockchain-based QM and data-based QA to a real-time digital quality assurance system.

4.1.1 Machine learning architectures for image-based defect detection in selective laser sintering (from [I])

For the development of ML architectures for image analysis, a small dataset of images of the powder bed surface of an SLS printing process (see Figure 14) was first created. A uniformly distributed powder bed, without irregularities, is desirable for good quality of the printed parts, see e. g. Figure 14 (a) and (c). However, various irregularities can occur in the powder bed, such as foreign bodies, part edges, powder accumulations and powder trenches, which are collectively referred to as powder bed defects and are shown in Figure 14 (b) and (d). These powder bed defects can lead to deficiencies in part quality and part properties, and even up to quality-related rejects of parts, but this is to be avoided or reduced by ML.

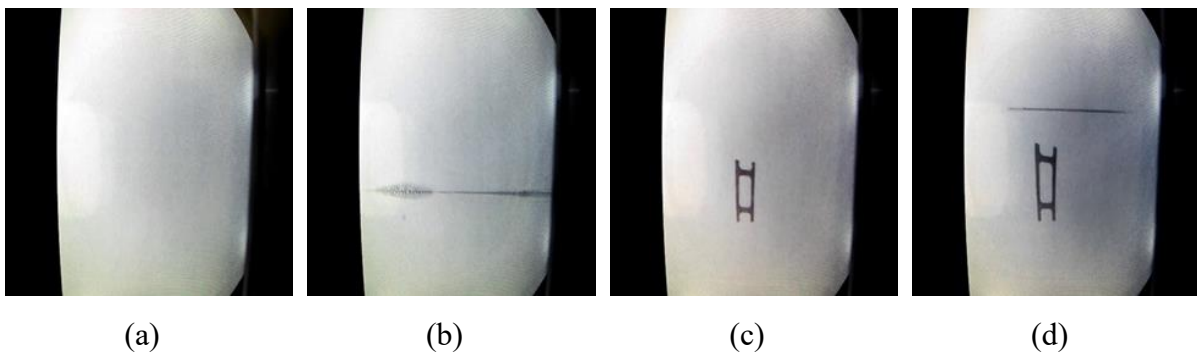


Figure 14: Image examples from the dataset of a SLS print job with: (a) a powder bed without sintered elements and irregularities; (b) a powder bed without sintered elements with irregularities; (c) a powder bed with a sintered element without irregularities and (d) a powder bed with a sintered element and irregularities (according to [I], CC BY 4.0 (<https://creativecommons.org/licenses/by/4.0/>)).

After the dataset was created, the SLS powder bed images were preprocessed for analysis with the VGG16 CNN as well as the Xception CNN and enhanced by special data augmentation. Subsequently, the selected CNN models were integrated into an ML architecture suitable for

the dataset and for defect detection with pre-trained weights of the ImageNet dataset and a transfer learning process. (see Figure 15). In three experiments, a performance analysis of the VGG16 and Xception architectures was performed with and without neural network pretraining and with and without data augmentation of the dataset to find the most effective ML architecture configuration with the best results. The results were then presented and summarized in the form of confusion matrices. Additional metrics were derived from the CM to evaluate the performance of the CNN models, such as accuracy, precision, and recall. ROC curves and associated AUC measures are also useful metrics and were obtained, too.

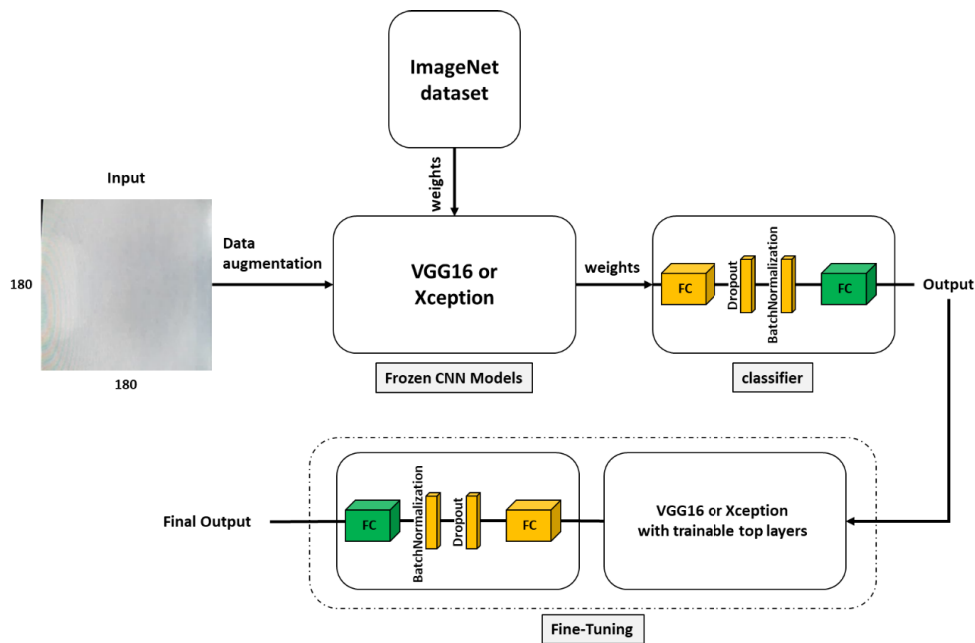


Figure 15: ML architecture of the transfer learning process with the powder bed data (according to [I], CC BY 4.0 (<https://creativecommons.org/licenses/by/4.0/>)).

4.1.2 Performance evaluation of an automatic classification method of powder bed defects (from [I])

The best performance was achieved with a test accuracy of 97.7% and a ROC AUC value of 0.993 with the pre-trained VGG16 architecture without data augmentation (see Table 5, 2nd experiment). With 95.8% test accuracy and a ROC AUC value of 0.982, the pre-trained VGG16 architecture with data augmentation achieves only a slightly worse value (Table 5, 1st experiment). However, this is the only configuration in which the Xception architecture also provides comparatively good classification, with 89.4% test accuracy and a ROC AUC value of 0.934. The ROC curves of all model architectures and configurations correlate with these results and are shown in Figure 16. The VGG16 architecture shows higher AUC values in the 1st as well as in the 2nd experiment. The AUC values of the Xception architecture are lower, which is

reflected in flatter ROC curves. This diagram also clearly shows that no classification took place in the 3rd experiment and that the ROC curves basically correspond to a random guessing.

Table 5: Confusion matrices and performance parameters for the examined CNN architectures for the classification of powder bed defects at the SLS process for all experiments carried out (according to [I], CC BY 4.0 (<https://creativecommons.org/licenses/by/4.0/>)).

Experiment	Model	Confusion Matrix		Accuracy	Precision	Recall (TPR)	FPR	F1-Score	ROC-AUC
1 st	VGG16	490	10	0.958	0.980	0.939	0.021	0.959	0.982
		32	468						
1 st	Xception	459	41	0.894	0.918	0.876	0.086	0.897	0.934
		65	435						
2 nd	VGG16	496	4	0.977	0.992	0.963	0.008	0.977	0.993
		19	481						
2 nd	Xception	500	0	0.500	1.000	0.500	0.500	0.667	0.514
		500	0						
3 rd	VGG16	180	320	0.515	0.360	0.522	0.489	0.426	0.525
		165	335						
3 rd	Xception	500	0	0.500	1.000	0.500	0.500	0.667	0.526
		500	0						

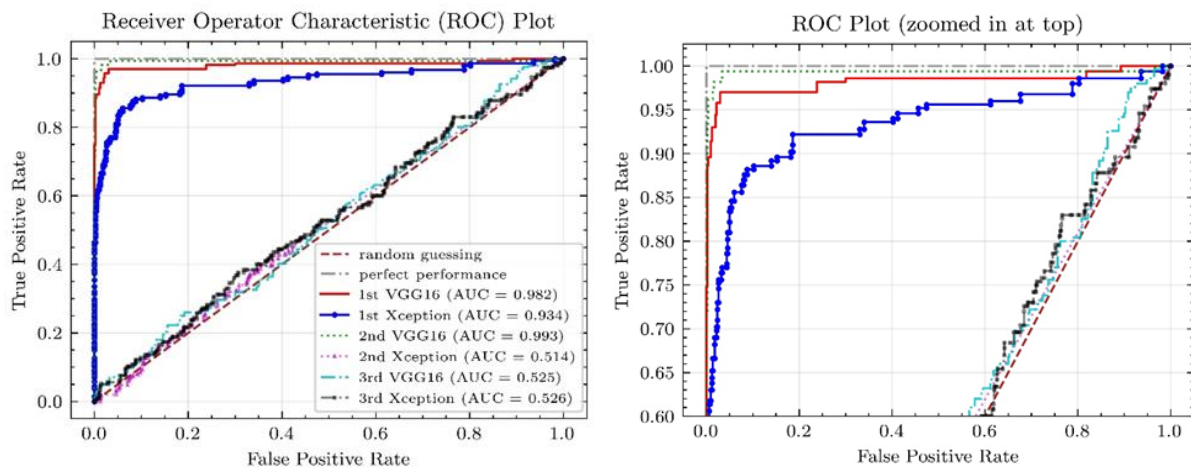


Figure 16: ROC curves and AUC metrics of the implemented models. The dashed lines represent the ROC curve of a completely random classifier and that of a perfect classifier. Plot of the ROC curves of the implemented models (left) and zoomed in version of the top part plots (right) (according to [I], CC BY 4.0 (<https://creativecommons.org/licenses/by/4.0/>)).

Finally, for a better visual explanation of the results, a Grad-CAM representation was created for selected test images. For this purpose, the activation maps of the pre-trained VGG16 and Xception models are presented and highlighted based on the gradients of the last convolutional layer. Here, the areas of the image that are most interesting for the algorithms' decision making are highlighted in red and the fewer interesting areas are highlighted in blue (see Figure 17). Thus, under certain conditions (pre-training and data augmentation), both ML architectures

investigated are in principle capable of detecting and localizing irregularities in the powder bed, with the VGG16 model architecture performing better overall than the Xception architecture.

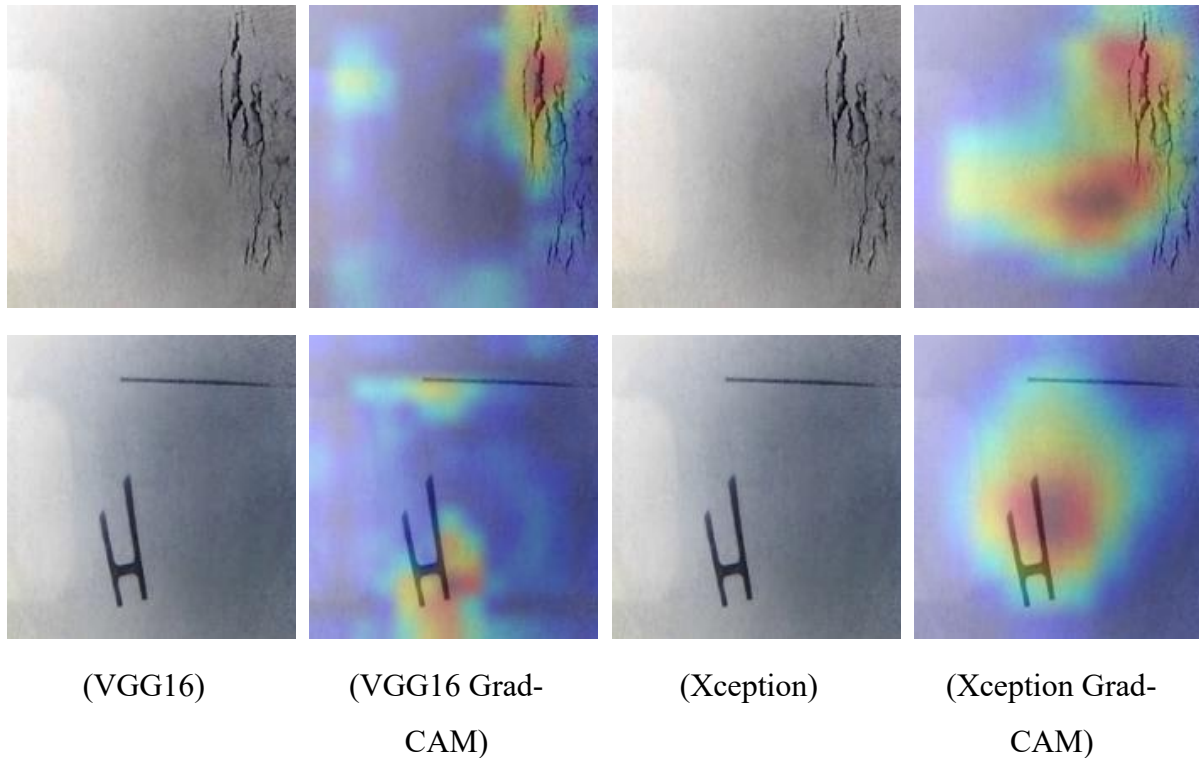


Figure 17: Activation maps for powder bed recordings during the SLS process with visible powder bed defects (according to [I], CC BY 4.0 (<https://creativecommons.org/licenses/by/4.0/>)). Defects were detected and localized by the CNN architectures. With the VGG16 model, a more precise localization of the effects could be achieved than with the Xception model.

4.1.3 Machine learning algorithms for sensor-based data classification in fused deposition modelling (from [II])

Complementing the image-based ML defect analysis, a completely different type of data was also investigated and thus an intelligent classification of sensor data by ML algorithms was developed. For this, the environmental process parameters temperature, humidity, air pressure and gas particles, which were recorded via an environmental sensor during several, differently parameterized FDM prints, were sequenced according to a newly developed data pre-processing strategy (see Figure 18) and pre-classified into different 3D printing conditions. A sensitivity analysis was then performed to determine the relevance of each recorded sensor parameter to the ML analyses, with atmospheric pressure having the greatest impact on classification.

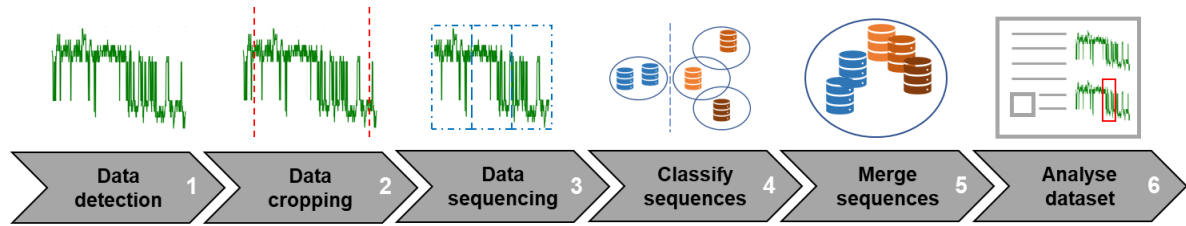


Figure 18: Data preprocessing steps carried out for the ML investigations with the environmental sensor data (according to [II], Copyright Elsevier).

The sequenced data from the datasets of each FDM print job were then stored in a larger, unbalanced dataset (main dataset) and a smaller, balanced dataset (ablation dataset). An unbalanced dataset is more likely to reflect the reality of printing, as the printing process is always optimized for a good print result and thus more good data sequences are available. A balanced dataset provides more detailed insights into the effectiveness of ML analyses. Both datasets then served as the basis for data analyses based on a supervised learning classification approach, in which individual 3D printing states were classified based on specific features resulting from the partially different process parameterization (see Table 6) in the sequenced data runs by various state-of-the-art ML algorithms.

Table 6: FDM process characteristics for different 3D printing conditions (see full table in publication [II], Copyright Elsevier).

3D printing condition	normal_01	defect_01	defect_02	defect_03	defect_04	defect_05
FDM process characteristic	optimal settings	old filament	new nozzle	higher temperature	higher speed	blocked nozzle

In the studies, ML models of different complexity were then implemented in a comparable and reproducible manner with a uniform process flow and trained with (1st experiment) or without (2nd experiment) the weighty air pressure parameters. Purely in terms of classification results, all the ML algorithms studied perform very well on the larger main dataset, with accuracies ranging from 94.7% to 99.9% (see Table 7).

Table 7: Performance metrics for ML algorithms for the classification of sensor data at the FDM process for all investigations with the main dataset (the full table can be found in publication [II], Copyright Elsevier).

Experiment	Model	Accuracy	Macro Avg Precision	Macro Avg Recall	Macro F1-Score	Time [mm:ss]
1 st	MLP	0.999	0.999	0.998	0.999	00:20
	1D CNN	0.999	0.999	0.999	0.999	09:01
	RNN LSTM	0.991	0.986	0.989	0.988	17:23
	InceptionTime	0.999	0.999	0.999	0.999	39:16
	XceptionTime	0.997	0.997	0.996	0.997	38:03
	XCM	0.999	0.999	0.999	0.999	19:15

2 nd	MLP	0.947	0.968	0.938	0.952	00:20
	1D CNN	0.952	0.976	0.941	0.958	08:47
	RNN LSTM	0.989	0.985	0.987	0.986	16:39
	InceptionTime	0.953	0.976	0.942	0.959	37:21
	XceptionTime	0.952	0.977	0.941	0.959	37:41
	XCM	0.951	0.975	0.941	0.957	15:01

However, this is not confirmed in the accuracy and loss curves of the training and validation data, especially for the second experiment without the air pressure values (see Figure 19). With the exception of the XceptionTime algorithm, the validation loss curves are very noisy and no longer decrease steadily, but increase again after some time. This is characteristic for overfitting and indicates that the algorithms cannot apply the learned information to new, unknown validation data. Exceptions are the XceptionTime and the RNN algorithm. Both algorithms achieved the best results overall with high performance metrics and good robustness against overfitting.

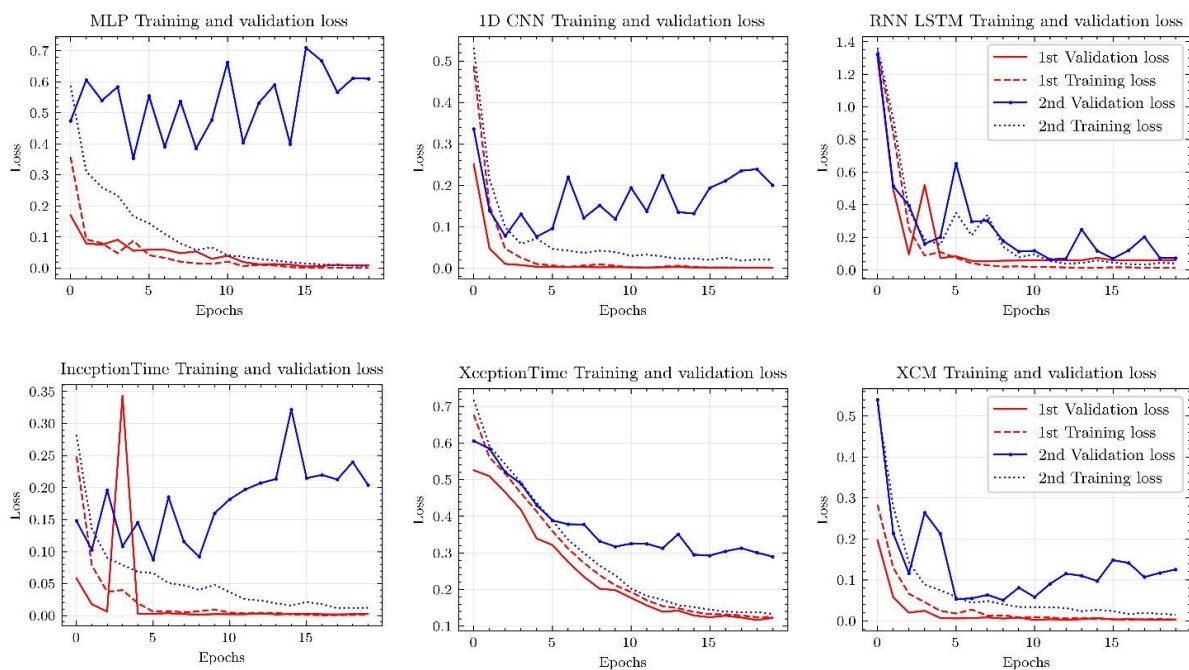


Figure 19: Training and validation loss plots of the used ML algorithms with the main dataset (according to [II], Copyright Elsevier).

The effectiveness of the XceptionTime as well as the RNN algorithm was then validated again with the ablation dataset in two experiments, with and without air pressure values, but only the XceptionTime algorithm achieved very good classification results with about 97.0% accuracy as well as excellent training and validation loss results (see Table 8 and Figure 20). In this way, an effective classification of 3D printing condition classes could be enabled. As a further result of the investigations, however, it was also found that the computing times of the individual

algorithms increase with increasing complexity and that XceptionTime in particular required the most computing time.

Table 8: Performance metrics for the RNN LSTM and XceptionTime algorithm for the classification of sensor data at the FDM process for all investigations with the ablation dataset (see full table in publication [II], Copyright Elsevier).

Experiment	Model	Accuracy	Macro Avg Precision	Macro Avg Recall	Macro F1-Score	Time [mm:ss]
1 st	RNN LSTM	0.741	0.750	0.632	0.686	03:41
	XceptionTime	0.972	0.973	0.827	0.894	07:17
2 nd	RNN LSTM	0.676	0.683	0.670	0.676	03:16
	XceptionTime	0.969	0.970	0.830	0.895	07:09

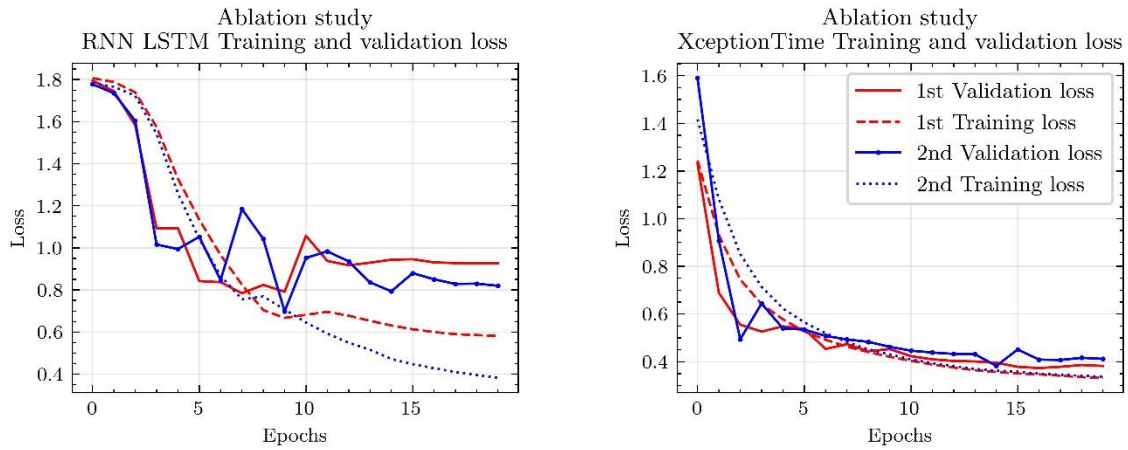


Figure 20: Training and validation loss plots of the RNN LSTM (left) and XceptionTime (right) algorithms with the ablation dataset (according to [II], Copyright Elsevier).

4.1.4 Evaluation of a proof of concept data analysis method for classifying 3D printing conditions (from [II])

In a first proof of concept, the results of the promising XceptionTime data analyses were compared with optical 3D scan part quality investigations. For this purpose, the FDM components printed during the individual print jobs were first optically scanned and compared with their CAD reference geometry in order to subsequently determine the dimensional deviations resulting from the printing process and also to be able to derive the 3D printing condition classes (see Figure 21). However, the dimensional deviations in the 3D printing conditions studied are usually relatively small and difficult to detect visually.

Yellow and green areas in the 3D scans represent very small to small negative deviations, blue areas visualize larger negative deviations compared to the CAD reference and red areas maximum positive deviations. Gray areas could not be detected by the scanner. The set 3D printing

conditions with the associated FDM process properties can be found in Table 6. All 3D scans, with the exception of defect_05, look very similar at first glance. Only a closer look reveals minor deviations. The "normal_01" print condition forms the reference with optimum print settings and a maximum deviation of +0.10 mm to -0.32 mm. In comparison, the "defect_01" print condition has a slightly higher negative deviation of -0.34 mm. The 3D printing conditions "defective_02" and "defective_03" again show slightly higher positive deviations of +0.11 mm to "normal_01", but are visually indistinguishable from each other. The "defect_04" condition deviates slightly more from the optimal conditions, both positively with +0.15 mm and negatively with -0.35 mm. Overall, the differentiation of 3D printed conditions based on the 3D optical scans is difficult. The results of ML data analysis of environmental sensor data show a more effective alternative in this respect.

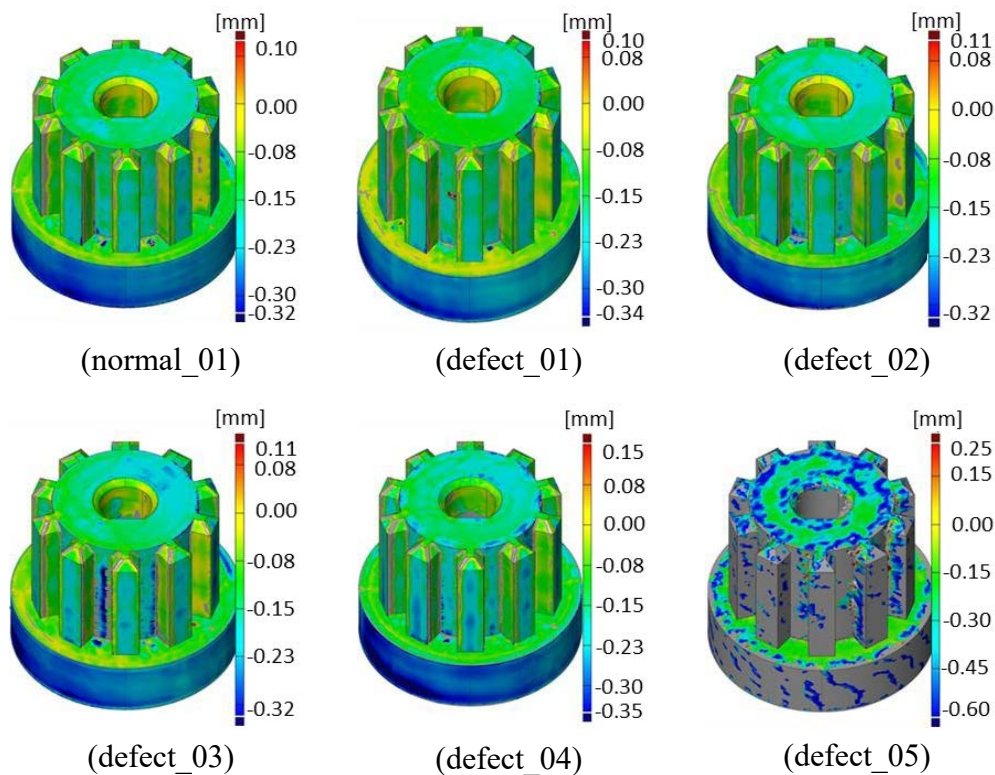


Figure 21: Dimensional control with an optical 3D light scanner to compare the quality of the printed parts with the different printing conditions (according to [II], CC BY 4.0 (<https://creativecommons.org/licenses/by/4.0/>)).

4.2 Blockchain-based additive manufacturing quality management (from [III])

The publication [III] addresses the second research focus of this dissertation, the development and exemplary implementation of a blockchain-based, cross-company digital QM for all quality-relevant data in the AM value chain. In addition, the third research focus of this thesis, the conceptual linking of blockchain-based QM and data-based QA to a digital quality assurance system, is again addressed in detail.

4.2.1 Development and implementation of a basic digital quality assurance concept as a blockchain-based additive manufacturing part record (from [III])

ML analyses of image and sensor data leads to large volumes of data, analysis results and quality insights that need to be managed securely, traceably and increasingly digitally inside and outside of a single company as part of QM and QA. For this purpose, this data must also be set in relation to the existing QM as well as the conventional QA in AM and merged with the present structure. To this end, a concept was developed (refer also section 3) that digitally maps the value chain of the metal FDM process via a dApp based on a smart contract and blockchain-based as well as decentralized data processing and data storage solutions. The objective here is to digitally record the data of all physical and digital manufacturing process steps as part of an overarching digital quality assurance system. This quality assurance system was implemented as a prototype in the form of a digital AM part record in which all quality-relevant data of an additively manufactured part are summarized in a tamper-proof, traceable and transparently accessible manner. The manufacturing documentation of the digital AM part record for a metallic FDM part was thereby divided into four processes with the associated data (see Figure 22). In a development, manufacturing, sintering and control process, quality-relevant data is recorded, collected in special documents and stored cryptographically in the decentralized off-chain storage system IPFS. References to the file storage location, as well as specific manufacturing data and events of all participants, are also captured via a smart contract and then stored separately as well as automatically on the Ropsten Ethereum testnet blockchain on-chain. Via the blockchain explorer Ropsten Etherscan, the current on-chain part data is available to the customer or downstream service providers after each manufacturing process.

The general architecture of the AM part record is based on the value chain of the metal FDM process and consists, on the manufacturing side, of the QM and QA of the parties involved in the value creation, of a dApp composed of web application, decentralized storage, blockchain and smart contract, of the transport transactions as well as, on the customer side, of the manufactured AM part, the transparent access to the quality documentation data via the blockchain explorer Ropsten Etherscan as well as the final acceptance decision of the customer (Figure 23). Within this architecture, all involved actors, applications and processes of the digital AM part record, as well as their respective interactions with each other, are digitally linked.

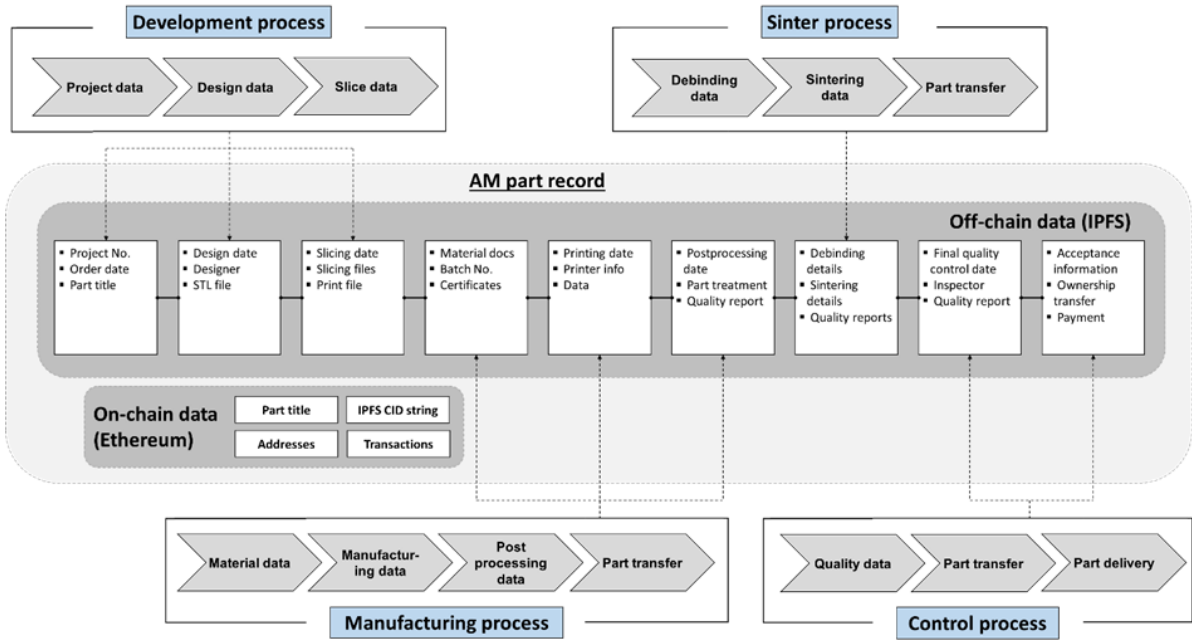


Figure 22: Manufacturing processes of a digital, secure and trustworthy AM part record with important parameters to be stored on a blockchain (according to [III], CC BY 4.0 (<https://creativecommons.org/licenses/by/4.0/>)).

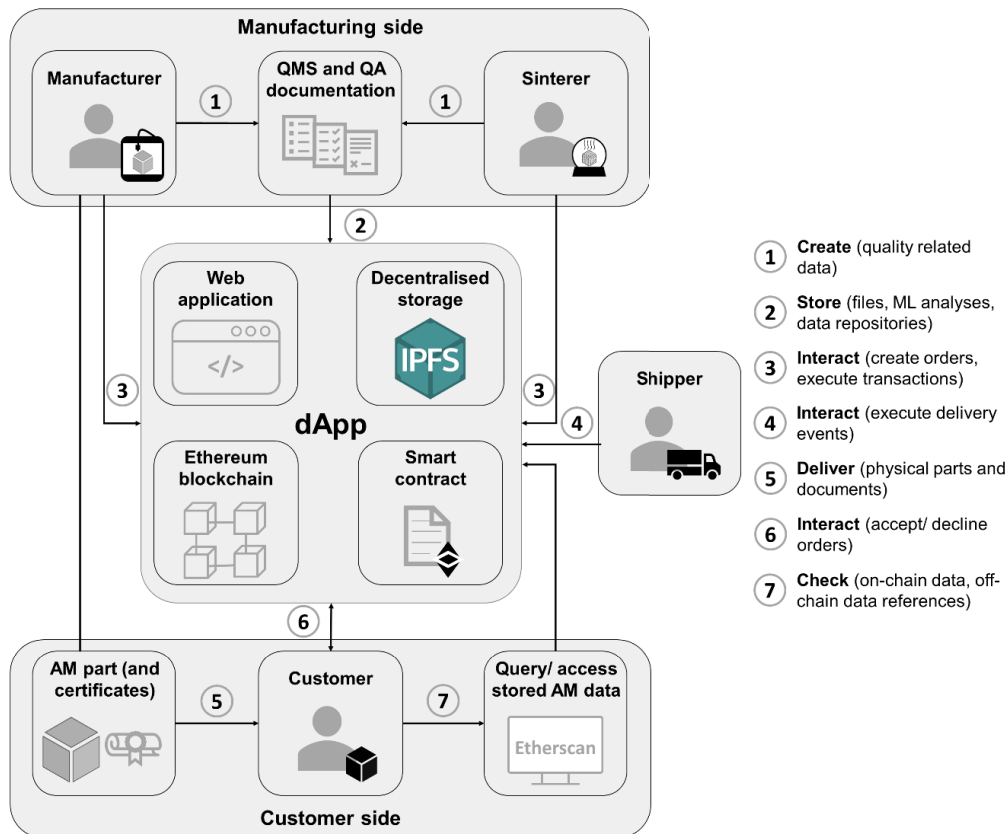


Figure 23: Architecture and process flow for the proposed blockchain-based digital AM part record.

The digital implementation of the developed quality assurance system as an AM part record was usefully shown in a demonstration study on a metal FDM process. All system components

and processes were successfully tested and evaluated using three sample parts. Ultimately, all quality-relevant data of the AM value chain of the parts under consideration were digitally recorded and stored decentrally in individual part records. The references to the decentralized storage locations as well as specific process events were successfully captured via a smart contract and automatically stored on the Ropsten Ethereum Blockchain. Via Ropsten Etherscan, this on-chain information can be retrieved at any time in a transparent, traceable and tamper-proof manner by specifying the address of the smart contract.

In addition, concrete objectives were defined, which could also be almost completely implemented with the digital quality assurance system, to enable an evaluation of the AM part record with regard to digital integrity, costs, efficiency, traceability, availability and expandability. It was shown that the AM part record enables both digitized part and FDM process documentation as well as decentralized storage of conventional quality documentation processes (e.g. paper-based logs and certificates, etc.) across multiple companies. The costs incurred in the process were evaluated and documented in the demonstration study using an example part. Depending on the blockchain used as well as the data traffic available there at the time of data storage, transaction costs of approximately €17.72 were incurred. The AM part record thus offers an economical alternative or relatively low-cost supplement to existing solutions, such as time-consuming paper-based documentation processes or expensive process management software. However, the solution is not yet effective enough, especially for decentralized storage of large amounts of data. For this aspect, the AM part record must still be conceptually expanded and implemented accordingly in the future. In this context, a concept was first developed that represents an intelligent evaluation of manufacturing data by means of ML algorithms and only stores the results of the analyses decentrally. The actual manufacturing datasets are stored centrally. With regard to traceability, it could be shown once again that a detailed, traceable and tamper-proof documentation of the entire value chain and the information flow is possible through the AM part record. In addition, this form of quality assurance offers constant and location-independent availability of data as well as relatively fast updating of production and quality information for all parties involved. Finally, the AM part record also has good expansion possibilities. By integrating certification facilities and regulatory authorities into the digital process flow, certification processes for AM parts could be simplified or accelerated, for example, by providing these parties with digital access to the QA data immediately after decentralized storage.

4.2.2 Integration of machine learning methods and blockchain technology into a digital quality assurance system for additive manufacturing (from [I] - [III])

Conventional QA methods (e.g., checklists and reports) have already been considered in the development of the AM part record as well as in the printing of sample parts as part of the demonstration study. In data-driven QA, e.g. through ML analyses, key elements such as data acquisition and data storage have also already been considered. Analogous to the image analysis in the SLS process, here images of each individual FDM print layer were captured via a camera, and also analogous to the FDM environmental data analysis, in-situ process data were captured via an environmental sensor. The data generated in the process very quickly comprises several gigabytes of storage capacity, which rules out storage on the blockchain from the outset due to storage limits and costs. Decentralized storage of large amounts of data has also been shown in the studies to be inefficient and unsustainable due to cryptographic security principles involved in frequent digital transmission and duplication of data. Instead, the FDM manufacturing data was stored on a central server and only the online address of the records was noted in the AM part record.

Based on this, a more efficient solution was conceptually discussed, which also considers the data analysis and the storage of the ML-based analysis results in the AM part record. Here, manufacturing data is captured outside the AM part record by the manufacturing company (e.g., in a digital twin), stored locally and analyzed by ML algorithms, and only the analysis results extracted from the data are then stored decentrally in the part record and shared with other stakeholders. This eliminates the need for decentralized storage of large amounts of manufacturing data, which significantly improves the efficiency and sustainability of the part record.

With an adapted data processing structure, corresponding ML analyses can thus also be carried out in real time and process irregularities and quality defects can be quickly detected. As part of a closed-loop quality control system, the printing process can then be automatically optimized via direct process feedback. To do this, trusted sensors that are constantly connected to the Internet must send sensor data in a traceable and near real-time manner to a cloud-based database, where it is evaluated directly via automated analysis scripts and pre-trained AI algorithms. The results can then be retrieved in real time and alarms triggered directly when thresholds are exceeded or sensor signals are absent. In turn, these messages must be automatically captured via an extended smart contract and stored on-chain on a blockchain. Ultimately, the data remains local in the cloud and only the analysis results are stored in the AM component file.

5 Discussion

In this chapter, the three main research areas of the thesis are discussed. For this purpose, the results from the attached publications are considered and related to the overall objective of the dissertation.

5.1 Development of non-destructive quality assurance methods for additive manufacturing processes based on machine learning (from [I] and [II])

During the investigations on non-destructive quality assurance with methods of artificial intelligence, findings were obtained in the publications [I] and [II], which on the one hand can be assigned to AM as well as especially to the QA of AM processes, but on the other hand also provide information on the development of ML algorithms. In section 5.1.1, these aspects are subsequently considered based on the findings from [I]. Section 5.1.2 discusses the individual findings based on the results from [II].

5.1.1 Machine learning for defect detection in selective laser sintering

The ML-based method for defect detection of powder bed images during selective laser sintering delivers excellent results, so that it enables in principle a very well-functioning non-destructive quality assurance of AM parts. From the results of the 1st experiment in Table 5 with algorithm pre-training and data augmentation, it can be concluded that the VGG16 model architecture has better performance than the Xception architecture. Thus, the developed VGG16 CNN architecture is more suitable for making predictions about the quality of unseen powder bed images.

The results of each experiment from Table 5 show the influence of pre-training and data augmentation on model performance. The results of the 2nd experiment show that the pre-trained VGG16 model without data augmentation even achieves slightly better performance metrics than the 1st experiment with data augmentation. This is basically understandable, since the data augmentation extends the relatively small image dataset in the 1st experiment by special operations (image rotation, image mirroring, etc.) and thus has a larger training base with increased complexity and lower similarity of the individual images compared to the 2nd experiment, which ultimately complicates the image classification for the ML models. According to Chollet [100], this is also a desired effect to allow better generalization of the models and to avoid overfitting. For the Xception model, it is obvious in the 2nd experiment that no learning effect has occurred and the model cannot classify the data without data augmentation. This is due to overfitting, which may have occurred because the model learned misleading or irrelevant information for classification during training, or because it has a too complex structure to learn from a smaller

database. A similar behavior is seen for both ML models in the 3rd experiment, where there was no pre-training but again data augmentation. With both model architectures, no learning successes could be achieved, which can also be attributed to overfitting, which probably also occurred here due to the too small data basis as well as a too short training time.

So, in summary, the presented method with data augmentation and a pre-training with the ImageNet dataset is beneficial to achieve better classification results and to implement more robust models. Data augmentation effectively avoids overfitting by increasing the size of the database and the complexity of the data. Pre-training with the weights from the ImageNet dataset also saves significant computational effort, since it has already been done there and the models can build on it. Furthermore, it could be shown that both investigated CNN model architectures can learn features from the image data as described in the literature (see also Figure 10 as an example) in order to be able to automatically evaluate the quality of the powder bed images afterwards. This can provide data-based support for conventional QA of additively manufactured parts, e.g. as a supplement to downstream, non-destructive evaluation of part quality or also as in-situ monitoring of the AM process.

The activation maps created were also used to show how the algorithms identify and locate the defects in the powder bed. Figure 17 again shows that the VGG16 model architecture was able to identify the defects more accurately than the Xception architecture and is therefore more suitable for image analysis for QA in SLS. One reason for the better performance could ultimately be the complexity of the model. The VGG16 model used has a large number of model parameters (about 138 million) distributed over relatively few model layers (23), which allows a very detailed analysis of the image data [170]. The Xception model comprises significantly fewer parameters (approx. 23 million), which are distributed over much more layers (126) [171]. Because of this deeper model structure, the Xception model also requires a larger amount of data to learn sufficiently.

Accordingly, the lack of available data was a major problem in the developed ML classification of powder bed defects. Usually DL models are trained with several 10000 image data [114]. Training CNN with a small dataset of a few 1000 images can easily lead to inaccurate classifications and affect the generalization ability of the models. The imbalance of the dataset with a lack of defect images is also seen as limiting in the studies. The performance of the presented models could be increased if more images with visible powder bed defects were available. However, to evaluate whether more data actually lead to better and more resource-efficient results, further studies should first perform a so-called ablation study [172].

In addition to the lack of data, another difficulty with these studies was the interpretation of the visualization results of the CNN models. A deeper understanding of the visual properties of a digital image and the individual convolutional operations within the neural networks is required to explain the predictions and visualization results in detail. The resulting activation maps were included in this context and analyzed in a basic way, but further explanation is needed to understand why the model emphasizes certain areas of the picture. These interpretation issues should be further investigated in the future, especially with larger datasets.

5.1.2 Machine learning for intelligent data analysis in fused deposition modelling

In addition to image analysis of SLS powder bed images, a second data-based ML method was developed to also use sensor data to support conventional QA processes and to classify them intelligently and automatically into special printing condition classes using FDM printing as an example. Based on the results of the SLS image analyses, extensive datasets were directly created here and an ablation study was performed.

With the experimental setup for data acquisition, various environmental sensor data such as air pressure, humidity, temperature and special gas particles can be recorded directly at the extruder during the FDM process and further processed in a simple way. Analysis of the acquired and pre-processed data is then possible through a supervised learning classification approach using state of the art ML algorithms. Thus, different 3D printing conditions can be characterized and used for effective training of ML algorithms. Finally, the trained ML algorithms enable automatic classification of the environmental sensor data into appropriate 3D printing condition classes.

Not all environmental sensor data are equally important for ML analyses in this context. A sensitivity analysis carried out showed that AM-relevant process parameters can have different significance in the ML context. In particular, barometric air pressure is usually not of great importance for the printing process, but it is for the ML analyses. In the studies conducted here, it was the most relevant, followed by humidity, temperature, and gas particles. It should be noted that the use of an open 3D printing system means that the external environmental influence on the data is more pronounced and thus changes in environmental conditions can be more strongly reflected in the ML analyses than in a closed system. However, the strong relevance of barometric air pressure to the ML analyses is ultimately understandable because the patterns in this sensor parameter are relatively pronounced and thus dominant. Air pressure is always fairly constant, and even small variations or differences in pressure between individual data sequences are clearly visible to the algorithms. All other environmental parameters are noisy and the patterns in them are less clearly visible.

The importance of air pressure is evident in the results of the experiments conducted with and without the barometric air pressure data included in the analyses (see Table 7 and Table 8). The inclusion of the air pressure values irrelevant for the AM process (1st experiment) initially increases the calculation effort slightly in principle. However, the performance of the ML algorithms without the air pressure data (2nd experiment) is always worse and tends to overfitting. Thus, the barometric air pressure parameters basically have a stabilizing influence on the analyses and contribute to a better generalization of the studied ML architecture. This in turn ultimately has a positive effect on the classification of new, unknown data. Therefore, despite a somewhat higher resource consumption, it may make sense to collect as many process parameters as possible with little effort in order to first investigate their respective relevance for ML analyses and their influence on their generalization capability.

Furthermore, the investigations with the main dataset show that all algorithms classify similarly well (see Table 7), whereby simpler algorithms require significantly shorter computing times and are therefore more resource-efficient. However, considering the susceptibility to overfitting (see Figure 19), only two algorithms, the simpler RNN LSTM and the more complex XceptionTime, achieve really good results with effective classification. But, this effectiveness could only be confirmed for XceptionTime in the ablation study with the smaller ablation dataset (see Table 8). This modern algorithm copes with less and at the same time more differentiated data much better than the RNN LSTM, where no classification took place and already in the 1st experiment (with the stabilizing air pressure values) an overfitting of the training data occurred (see Figure 20). In accordance with this finding, the following further conclusions can be derived specifically from the ablation study performed:

- For effective classification of sensor parameter sequences, larger datasets with as many recorded sensor parameters as possible are useful.
- For small datasets, modern and more complex ML algorithms are more effective than simple algorithms in classifying sensor data sequences.
- With little data and no air pressure values, the XceptionTime algorithm classifies very effectively and is also robust against overfitting.
- XceptionTime also generalizes very well with more complex data and basically allows effective classification of 3D printing conditions with environmental sensor data.

Overall, the results of the ML analyses can make a productive contribution to QA in AM. The trained algorithms can, for example, analyze data in parallel with process monitoring and provide information relatively quickly about the current and further expected print quality. Furthermore, based on the presented ML analysis method, intelligent online services can be

developed in the future that interact with 3D printers connected via the Internet and continuously monitor the printing process as well as automatically optimize it. In addition, the generated ML results can also serve as a supplement to conventional QA or even replace established quality assurance procedures such as optical 3D scans. A 3D scan can usually only be used superficially and only after the part has been manufactured, and is also very poor at distinguishing between different printing conditions. ML, on the other hand, is much better suited to classify printing conditions with special algorithms. Corresponding ML analyses also enable QC for external as well as internal part structures and can be performed faster, more precisely, more simply and integrated into production. ML data analysis are also non-destructive, relatively inexpensive to implement, and enable process-integrated, 100% QC as well as documentation in near real-time.

However, for a corresponding industrial application of the presented methods, improved and increasingly automated data processing and data analysis procedures must first be developed. In addition, more and more diverse 3D printing data needs to be included in the algorithms' database to ensure a more robust classification. Finally, in view of the constantly growing volumes of data, aspects of data management must also be considered.

5.2 Development of digital quality management for additive manufacturing based on blockchain technology (from [III])

The management of manufacturing data was considered in the development of the digital quality assurance system in the publication [III]. In this context, the combination of AM and blockchain technology for quality improvement was also fundamentally investigated and a blockchain-based QM for digitally mapping the value chain of a metal FDM process was initially designed. In the course of this, all physical and digital data of the individual manufacturing process steps, in particular also image and sensor datasets for ML analyses, are also recorded. The digital quality assurance system was then implemented as a prototype in the form of an AM part record, based on the concept of a digital QM (see also section 3, Figure 13), and validated in a demonstration study on three concrete part examples. In this context, the AM part record represents the practically implemented and functional development status of the digital quality assurance system, which in principle enables cross-company digital QM of data along the entire AM value chain and also includes data from conventional and data-based QA methods. The definition and implementation of concrete goals, which are to be achieved with the new digital quality assurance system and have also been largely achieved so far, show that the quality of AM can already be fundamentally increased through the use of the AM part record.

Due to the unchangeable storage of all manufacturing-relevant events and protocols on-chain on the blockchain or traceable and tamper-proof off-chain in the IPFS, every transaction and documentation of the FDM value chain can be digitally tracked and traced. This enables, for example, detailed process reproducibility and repeatability, a high degree of certainty with regard to process conformity (to standards, guidelines, customer specifications, etc.) and increased confidence in manufacturing and supply chains (with regard to the raw materials used, qualification of the employees deployed, compliance with time specifications, etc.). In addition, the data is no longer managed centrally by one party, but decentrally by its respective originator. In this way, the originator can determine for himself with whom he shares which data, which ultimately makes data manipulation more difficult and also serves data security. Moreover, the risk of complete data loss is reduced because if one storage location fails, the data is still available elsewhere. However, the technological implementation is initially relatively demanding and even a good implementation of the solution then still depends on physically correct and conscientiously executed processes. Furthermore, the storage of erroneous information in the blockchain cannot be automatically prevented, so that these errors are subsequently documented in an immutable manner.

The cost analysis of the entire production documentation according to the functions defined in the smart contract shows the cost efficiency of the digital documentation process. The creation of a smart contract, the execution of a transaction, and the storage of data on the blockchain incur costs in this context. Here, the creation of the smart contract is the most expensive step, all other costs are comparatively low. The entire documentation of a metal FDM sample part according to the prototypically implemented digital quality assurance system generates an additional financial burden for QA processes in the amount of €17.66, which is distributed among all parties involved in the manufacturing process and the smart contract. For smaller, low-cost parts, this is a major cost point in conjunction with the normal manufacturing effort. For expensive parts with higher unit costs, however, this is less significant, so that the AM part record represents an economical solution for the digital management of quality data here in particular. In addition to the pure costs, there are also other aspects to be considered. For example, the use of the AM part record enables transparency and security between the individual parties, it reduces the coordination and discussion effort through automatically executed transactions, and it avoids miscommunication and unnecessary consumption of resources by being able to react to changing boundary conditions and errors at an early stage. Ultimately, the solution is only implemented as a prototype and still needs to be adapted for a performant function. The use of another blockchain network should also be provided for, as the Ropsten test network is only for

development purposes. Faster blockchain networks such as Hyperledger [173] or Polygon (MATIC) [174] are recommended as alternatives.

When a smart contract function is executed, the blockchain address of the function caller is always stored securely in the blockchain. The function caller can then be tracked at any time and is accountable for his actions [175]. This means that all those involved in the value chain already have detailed digital documentation of the transaction processes during the manufacturing process, which can be used to quickly identify the individual responsibilities in the event of irregularities. However, it should be noted that the developed AM part record currently works with the publicly available Ropsten Ethereum blockchain and, accordingly, privacy, confidentiality, and trade secret issues must be considered. This is because the information stored on the blockchain is cryptographically secured in principle, but in the current concept it can be decrypted by a specially programmed function in the smart contract. In this regard, the future use of a private blockchain such as Hyperledger or the use of a transparent zero-knowledge proof system such as ZK-STARK [176] could contribute to both better data protection and greater acceptance of the developed AM part record.

The transaction processes and all other on-chain data are stored decentrally on the network nodes involved in the network. This means that the information is redundantly backed up and is still accessible even if a node fails. With the blockchain explorer Etherscan, this data can be accessed at any time and from any location via the Internet. The fast update of the data depends on the execution of the functions in the smart contract. In principle, digital documentation can therefore take place immediately after the physical process has been carried out and can also be viewed via Etherscan within a few seconds. This is much more effective than conventional procedures, which require agreements to be made, data to be exchanged, partners to be informed and, if necessary, authorized to view the data. In addition to data protection aspects and the public accessibility of the data, however, it must also be considered that the blockchain network is generally not self-governing and that unwanted changes, e.g., through updates, can occur at any time.

Overall, the digital quality assurance system therefore currently covers only specific documentation and storage processes on-chain. However, the system can be extended. For example, regulatory stakeholder (authorities) or certification bodies can also be integrated into the digital quality assurance system. They will then also have transparent, traceable and secure access to manufacturing and quality information, on the basis of which part certificates or process qualifications can subsequently be issued more quickly and easily. In order to make this possible, the AM part record must find sufficient acceptance in the AM industry and be able to represent

as many AM processes and procedures as possible in a suitable manner. Furthermore, legal foundations for data protection must be clarified and solutions found for the lack of control over the blockchain network.

5.3 Digital quality assurance system consisting of data-based quality assurance and digitalized quality management (from [I] - [III])

In addition to general acceptance, the functionality and efficiency of the digital quality assurance system are very important to be considered as a serious alternative for industrial AM applications. Functionally, an attempt was already made during the development of the AM part record to enable a combination of blockchain-based QM and data-based QA through ML analyses, and at least to map the data into the AM part record as well. However, this has proven to be inadvisable in terms of efficiency, as the resulting data volumes are too large to store effectively and sustainably on- or off-chain. There are also still limitations in the real-time evaluation of the decentrally stored data, both in this respect and in general [177].

For this reason, a more efficient solution was designed in which data-based QA acts as a link between conventional QM or QA and AM part record (see section 3, Figure 13). Thus, in the future, an intelligent evaluation of manufacturing data is to be carried out by ML algorithms, as has already been demonstrated in principle for image and data analyses in the SLS and FDM process. The adaptation and optimization of the algorithms developed in [I] and [II] in combination with the building of a comprehensive AM training database can enable an intelligent and automated evaluation of large amounts of data, extracting from the data of a manufacturing process an overall result in terms of part and process quality, which is subsequently stored in the AM part record. This eliminates the need for decentralized storage of large amounts of manufacturing data, which would greatly improve the efficiency of the AM part record. Large amounts of manufacturing data can then be stored locally as part of a digital twin, and stored as before with a reference to the storage location in the part record. With powerful AI algorithms, automated real-time analysis of AM process data is then already possible during the manufacturing process to quickly detect the occurrence of quality defects and process irregularities and automatically correct them as part of closed-loop control by optimizing the process parameters. In the future, in order to make this local process secure and traceable, the datasets and data analytics must also be included in some form in the AM part record. Sensor data can be streamed to a cloud and monitored in near real-time via special, trusted sensors that are always connected to the internet. In the cloud, the data can then be evaluated directly by automated analysis scripts and pre-trained AI algorithms and the results visualized. The exceeding of threshold values, the detection of critical part defects or the failure of sensor signals can then

trigger an alarm message, which in turn is stored transparently in the AM part record. In principle, the large datasets and extensive analysis results remain locally in the cloud and only the extracted alarm messages with references to further information are stored on the blockchain in the event of irregularities. In this way, production data can be recorded immediately in the future based on the adapted digital quality assurance system, evaluated and displayed almost in real time based on data, and at the same time documented securely, transparently and digitally.

5.4 Summary and delimitation

In this cumulative work, a digital quality assurance system for AM was developed that extends existing QM and QA processes with digital solutions based on blockchain technology and ML methods. To this end, an overall concept was first developed that combines the general AM value chain and the current QM and QA structures with a complementary digital QM and data-based QA based on ML. The functionality of the digital quality assurance system was then demonstrated and evaluated in detail in individual scientific publications through the practical implementation of sample solutions. For this purpose, the digital QM was implemented in the form of an AM part record based on blockchain technology, which can be used to digitally map the AM value chain across company boundaries. In the context of data-based QA, two different implementation examples for selected AM processes were presented. Thus, an image-based defect detection for the SLS process and a completely different sensor-based print condition classification for the FDM process were developed and successfully implemented. The investigations show that the implemented solutions offer new possibilities for all quality-relevant AM aspects, both individually and in the context of the overall system, and contribute to a more predictable and reproducible 3D printing process.

However, the digital quality assurance system is currently limited to the ML solutions and AM processes under study. Extensive investigations on possibly more efficient ML approaches as well as the implementation on further AM processes are no longer part of this work. Nevertheless, the transferability of the digital quality assurance system to other AM procedures is possible with isolated adaptations. In the developed digital quality assurance system there are currently also further technological limits in the areas of data processing and data storage, the optimization of which outside the implementation examples is also no longer part of this work. But even these limits can be overcome in the future through conceptual adjustments.

6 Conclusions

Digital technologies such as blockchain or artificial intelligence (AI) systems have great disruptive potential to improve the quality of additive manufacturing (AM) and the repeatability and reproducibility of AM processes with new methods and procedures. Different machine learning (ML) algorithms have already been studied in the literature in this context, but could not show detailed implementations as quality assurance processes. A blockchain-based AM quality management that digitally maps the entire value chain of an AM process has not even been explored yet.

In this work, a digital quality assurance system for AM is developed based on blockchain-based quality management (QM) and data-based quality assurance (QA) through ML analyses. With the implementation of data-based QA methods, a blockchain-based QM and the conceptual linking of both aspects, three main areas of investigation were addressed in this context.

In this regard, different ML algorithms for data-based QA were first developed, implemented and evaluated with respect to their performance. The suitability of special convolutional neural networks (CNN) such as VGG16 for defect detection and image classification in powder bed images in selective laser sintering (SLS) has been demonstrated, as well as the effectiveness of state-of-the-art ML algorithms such as XceptionTime for the classification of sequenced environmental sensor data in fused deposition modeling (FDM). Effective implementations of these algorithms may ultimately provide complementary or alternative methods for nondestructive in-situ QA.

Based on this, a digital, cross-company and blockchain-based quality assurance system for AM was conceptualized and prototypically implemented as an AM part record for the value chain of a metal-based FDM process. For this purpose, a digital QM consisting of a web application for data collection, a decentralized data storage, a smart contract for automated processing of manufacturing events and an Ethereum Blockchain for data documentation was developed first. The solution, declared as an AM part record, thus enables digital QM with transparent, tamper-proof and traceable documentation of all quality information along the AM value chain based on cryptographic principles. The cost-effectiveness of the solution as well as its digital integrity, traceability, accessibility and extensibility could be proven in a demonstration study. All these aspects ultimately contribute to greater digitization and quality improvement in AM part production. Deficits were only identified with regard to the effectiveness of decentralized storage of large volumes of production data.

However, as part of the development and implementation of the AM part record, it has already been conceptually investigated how these deficits can be remedied by linking data-based QA

and blockchain-based QM to form an adapted digital quality assurance system, in order to enable real-time process data analyses and effective data storage and documentation processes in the future as well. Through the ML-supported analysis of large amounts of data stored locally in a digital twin extracts an overall result of the part and process quality from the data of a manufacturing process, which is then stored in the AM part record in a tamper-proof and traceable manner. The use of sensors connected to the internet also makes the adapted digital quality assurance system even safer and enables automated real-time analyses in principle.

This is where future research should start in order to implement, analyze and evaluate the designed expansion of the digital quality assurance system. In addition, certification functions should be implemented, authorities and certification bodies should be involved via the smart contract, and an extension of the AM part record to other AM process chains and process flows should be made. Especially in the ML context, the analysis efficiency and performance of further algorithms need to be investigated to possibly achieve even better classification and defect detection results. It should also be further investigated which data have which influence on the AM process in order to better understand the AM process on the one hand and to be able to evaluate the ML analysis results in a more differentiated way on the other hand. Moreover, further data should be collected and summarized in increasingly complex training datasets to continuously optimize the ML algorithms. Finally, the automation of the individual process steps such as data acquisition, preparation, analysis, evaluation and presentation are also an important research aspect in order to enable comparable and reproducible processes and results. In this context, the development and definition of new standardization procedures is particularly useful.

References

- [1] I. Gibson, D. Rosen, B. Stucker, M. Khorasani, *Additive Manufacturing Technologies*, Springer, New York, NY, 2021.
- [2] T. Wohlers, Wohlers Associates, I. Campbell, O. Diegel, R. Huff, J. Kowen, Wohlers Report 2020. 3D Printing and Additive Manufacturing State of the Industry, Wohlers Associates, 2020.
- [3] S.A. Tofail, E.P. Koumoulos, A. Bandyopadhyay, S. Bose, L. O'Donoghue, C. Charitidis, Additive manufacturing: scientific and technological challenges, market uptake and opportunities, *Materials Today* 21 (2018) 22–37. <https://doi.org/10.1016/j.mat-tod.2017.07.001>.
- [4] C. Ebert, C.H.C. Duarte, Digital Transformation, *IEEE Softw.* 35 (2018) 16–21. <https://doi.org/10.1109/MS.2018.2801537>.
- [5] F. Matos, R. Godina, Digital Transformation and Additive Manufacturing, in: F. Matos, V. Vairinhos, I. Salavisa, L. Edvinsson, M. Massaro (Eds.), *Knowledge, People, and Digital Transformation. Contributions to Management Science*, Springer, Cham, 2020, 275–291. https://doi.org/10.1007/978-3-030-40390-4_18.
- [6] P. Charalampous, I. Kostavelis, D. Tzovaras, Non-destructive quality control methods in additive manufacturing: a survey, *RPJ* 26 (2020) 777–790. <https://doi.org/10.1108/RPJ-08-2019-0224>.
- [7] G. Tapia, A. Elwany, A Review on Process Monitoring and Control in Metal-Based Additive Manufacturing, *J. Manuf. Sci. Eng.* 136 (060801) (2014) 1–10. <https://doi.org/10.1115/1.4028540>.
- [8] Y. Huang, M.C. Leu, J. Mazumder, A. Donmez, Additive Manufacturing: Current State, Future Potential, Gaps and Needs, and Recommendations, *J. Manuf. Sci. Eng. Trans. ASME* 137 (1) (014001) (2015) 1–10. <https://doi.org/10.1115/1.4028725>.
- [9] C.K. Chua, C.H. Wong, W.Y. Yeong, *Standards, quality control, and measurement sciences in 3D printing and additive manufacturing*, Elsevier Academic Press Inc., San Diego, CA, 2017.
- [10] J.M. Waller, B.H. Parker, K.L. Hodges, J.L. Walker, E.R. Burke, *Nondestructive evaluation of additive manufacturing state-of-the-discipline report*, NASA, Houston, TX, 2014.
- [11] H. Yang, P. Rao, T. Simpson, Y. Lu, P. Witherell, A.R. Nassar, E. Reutzel, S. Kumara, Six-Sigma Quality Management of Additive Manufacturing, *Proc. IEEE Inst. Electr. Electron. Eng.* 109 (2021). <https://doi.org/10.1109/JPROC.2020.3034519>.

- [12] S.K. Everton, M. Hirsch, P. Stravroulakis, R.K. Leach, A.T. Clare, Review of in-situ process monitoring and in-situ metrology for metal additive manufacturing, *Materials & Design* 95 (2016) 431–445. <https://doi.org/10.1016/j.matdes.2016.01.099>.
- [13] D. Mies, W. Marsden, S. Warde, Overview of Additive Manufacturing Informatics: “A Digital Thread”, *Integr Mater Manuf Innov* 5 (2016) 114–142. <https://doi.org/10.1186/s40192-016-0050-7>.
- [14] C.F. Durach, S. Kurpjuweit, S.M. Wagner, The impact of additive manufacturing on supply chains, *IJPDLM* 47 (2017) 954–971. <https://doi.org/10.1108/IJPDLM-11-2016-0332>.
- [15] K.V. Wong, A. Hernandez, A Review of Additive Manufacturing, *ISRN Mechanical Engineering* 2012 (2012) 1–10. <https://doi.org/10.5402/2012/208760>.
- [16] DIN EN ISO/ASTM 52900:2022-03: Additive Fertigung - Grundlagen - Terminologie (ISO/ASTM 52900:2021), Beuth, Berlin. <https://doi.org/10.31030/3290011>.
- [17] J.C. Najmon, S. Raeisi, A. Tovar, Review of additive manufacturing technologies and applications in the aerospace industry, in: *Addit. Manuf. Aerosp. Ind.* Elsevier (2019), 7–31. <https://doi.org/10.1016/B978-0-12-814062-8.00002-9>.
- [18] D.F. Braga, S. Tavares, L.F. Da Silva, P. Moreira, P.M. de Castro, Advanced design for lightweight structures: Review and prospects, *Prog. Aerosp. Sci* 69 (2014) 29–39. <https://doi.org/10.1016/j.paerosci.2014.03.003>.
- [19] M. Salmi, Additive Manufacturing Processes in Medical Applications, *Materials* 14 (2021) 1–16. <https://doi.org/10.3390/ma14010191>.
- [20] F. Rengier, A. Mehndiratta, H. von Tengg-Kobligk, C.M. Zechmann, R. Unterhinninghofen, H.-U. Kauczor, F.L. Giesel, 3D printing based on imaging data: review of medical applications, *Int. J. CARS* 5 (2010) 335–341. <https://doi.org/10.1007/s11548-010-0476-x>.
- [21] C.L. Ventola, Medical applications for 3D printing: current and projected uses, *Pharm. Ther.* 39 (2014) 704–711.
- [22] N. Guo, M.C. Leu, Additive manufacturing: technology, applications and research needs, *Front. Mech. Eng.* 8 (2013) 215–243. <https://doi.org/10.1007/s11465-013-0248-8>.
- [23] R. Leal, F.M. Barreiros, L. Alves, F. Romeiro, J.C. Vasco, M. Santos, C. Marto, Additive manufacturing tooling for the automotive industry, *Int J Adv Manuf Technol* 92 (2017) 1671–1676. <https://doi.org/10.1007/s00170-017-0239-8>.
- [24] F. Bos, R. Wolfs, Z. Ahmed, T. Salet, Additive manufacturing of concrete in construction: potentials and challenges of 3D concrete printing, *Virtual Phys. Prototyp.* 11 (2016) 209–225. <https://doi.org/10.1080/17452759.2016.1209867>.

- [25] S. Lim, R.A. Buswell, T.T. Le, S.A. Austin, A. Gibb, T. Thorpe, Developments in construction-scale additive manufacturing processes, *Autom. Constr.* 21 (2012) 262–268. <https://doi.org/10.1016/j.autcon.2011.06.010>.
- [26] A. Paolini, S. Kollmannsberger, E. Rank, Additive manufacturing in construction: A review on processes, applications, and digital planning methods, *Addit. Manuf.* 30 (2019) 100894. <https://doi.org/10.1016/j.addma.2019.100894>.
- [27] S. Ford, M. Despeisse, Additive manufacturing and sustainability: an exploratory study of the advantages and challenges, *J. Clean. Prod.* 137 (2016) 1573–1587. <https://doi.org/10.1016/j.jclepro.2016.04.150>.
- [28] S.H. Huang, P. Liu, A. Mokasdar, L. Hou, Additive manufacturing and its societal impact: a literature review, *Int J Adv Manuf Technol* 67 (2013) 1191–1203. <https://doi.org/10.1007/s00170-012-4558-5>.
- [29] U.M. Dilberoglu, B. Gharehpapagh, U. Yaman, M. Dolen, The Role of Additive Manufacturing in the Era of Industry 4.0, *Procedia Manuf.* 11 (2017) 545–554. <https://doi.org/10.1016/j.promfg.2017.07.148>.
- [30] W. Alkhader, N. Alkaabi, K. Salah, R. Jayaraman, J. Arshad, M. Omar, Blockchain-Based Traceability and Management for Additive Manufacturing, *IEEE Access* 8 (2020) 188363–188377. <https://doi.org/10.1109/ACCESS.2020.3031536>.
- [31] H.G. Lemu, On Opportunities and Limitations of Additive Manufacturing Technology for Industry 4.0 Era, in: *Advanced Manuf. and Autom.*, Springer, Singapore (2018), 106–113. https://doi.org/10.1007/978-981-13-2375-1_15.
- [32] K.-S. Wang, Z. Li, J. Braaten, Q. Yu, Interpretation and compensation of backlash error data in machine centers for intelligent predictive maintenance using ANNs, *Adv. Manuf.* 3 (2015) 97–104. <https://doi.org/10.1007/s40436-015-0107-4>.
- [33] J. Jiang, Y. Xiong, Z. Zhang, D.W. Rosen, Machine learning integrated design for additive manufacturing, *J Intell Manuf* (2020). <https://doi.org/10.1007/s10845-020-01715-6>.
- [34] Z.Y. Chua, I.H. Ahn, S.K. Moon, Process monitoring and inspection systems in metal additive manufacturing: Status and applications, *Int. J. of Precis. Eng. and Manuf.-Green Tech.* 4 (2017) 235–245. <https://doi.org/10.1007/s40684-017-0029-7>.
- [35] M. Klöckner, S. Kurpjuweit, C. Velu, S.M. Wagner, Does Blockchain for 3D Printing Offer Opportunities for Business Model Innovation?, *Res. Technol. Manag.* 63 (2020) 18–27. <https://doi.org/10.1080/08956308.2020.1762444>.

- [36] A. Realyvásquez-Vargas, K.C. Arredondo-Soto, J.L. García-Alcaraz, E.J. Macías, Improving a Manufacturing Process Using the 8Ds Method. A Case Study in a Manufacturing Company, *Applied Sciences* 10 (2020) 2433. <https://doi.org/10.3390/app10072433>.
- [37] M. Schmid, G. Levy, Quality management and estimation of quality costs for Additive Manufacturing with SLS, *Proceedings of the Fraunhofer Direct Digital Manufacturing Conference, Berlin, 2012*.
- [38] D. Olivier, S. Borros, G. Reyes, Application-driven methodology for new additive manufacturing materials development, *RPJ* 20 (2014) 50–58. <https://doi.org/10.1108/RPJ-01-2012-0002>.
- [39] L.F.C.S. Durão, R. Barkoczy, E. Zancul, L. Lee Ho, R. Bonnard, Optimizing additive manufacturing parameters for the fused deposition modeling technology using a design of experiments, *Prog Addit Manuf* 4 (2019) 291–313. <https://doi.org/10.1007/s40964-019-00075-9>.
- [40] Y. AbouelNour, N. Gupta, In-situ monitoring of sub-surface and internal defects in additive manufacturing: A review, *Materials & Design* 222 (2022) 111063. <https://doi.org/10.1016/j.matdes.2022.111063>.
- [41] Y. Wu, J. Fang, C. Wu, C. Li, G. Sun, Q. Li, Additively manufactured materials and structures: A state-of-the-art review on their mechanical characteristics and energy absorption, *Int. J. Mech. Sci.* (2023). <https://doi.org/10.1016/j.ijmecsci.2023.108102>.
- [42] T. DebRoy, H.L. Wei, J.S. Zuback, T. Mukherjee, J.W. Elmer, J.O. Milewski, A.M. Beese, A. Wilson-Heid, A. De, W. Zhang, Additive manufacturing of metallic components – Process, structure and properties, *Prog. Mat. Sci.* 92 (2018) 112–224. <https://doi.org/10.1016/j.pmatsci.2017.10.001>.
- [43] C.-J. Bae, A.B. Diggs, A. Ramachandran, Quantification and certification of additive manufacturing materials and processes, in: *Addit. Manuf. MPQA* (2018), 181–213. <https://doi.org/10.1016/B978-0-12-812155-9.00006-2>.
- [44] Z. Chen, C. Han, M. Gao, S.Y. Kandukuri, K. Zhou, A review on qualification and certification for metal additive manufacturing, *Virtual Phys. Prototyp.* 17 (2022) 382–405. <https://doi.org/10.1080/17452759.2021.2018938>.
- [45] DIN EN ISO/ASTM 52920:2021-08 - Entwurf: Additive Fertigung - Qualifikationsprinzipien - Anforderungen an Standorte für industrielle additive Fertigung (ISO/ASTM DIS 52920:2021), Beuth, Berlin. <https://dx.doi.org/10.31030/3276535>.

- [46] DIN SPEC 17071:2019-12: Additive Fertigung - Anforderungen an qualitätsgesicherte Prozesse für additive Fertigungszentren, Beuth, Berlin.
<https://dx.doi.org/10.31030/3119149>.
- [47] S. Kurpjuweit, C.G. Schmidt, M. Klöckner, S.M. Wagner, Blockchain in Additive Manufacturing and its Impact on Supply Chains, *J Bus Logist* 42 (2021) 46–70.
<https://doi.org/10.1111/jbl.12231>.
- [48] E. Benos, R. Garratt, P. Gurrola-Perez, The Economics of Distributed Ledger Technology for Securities Settlement, *ledger* 4 (2019). <https://doi.org/10.5195/ledger.2019.144>.
- [49] V. Buterin, A next generation smart contract & decentralized application platform, white paper, Ethereum (2014) Available: https://finpedia.vn/wp-content/uploads/2022/02/Ethereum_white_paper-a_next_generation_smart_contract_and_decentralized_application_platform-vitalik-buterin.pdf.
- [50] K. Christidis, M. Devetsikiotis, Blockchains and Smart Contracts for the Internet of Things, *IEEE Access* 4 (2016) 2292–2303. <https://doi.org/10.1109/ACCESS.2016.2566339>.
- [51] S. Nakamoto, Bitcoin A Peer-to-Peer Electronic Cash System (2008) Available: <https://bitcoin.org/bitcoin.pdf>.
- [52] G. Wood, Ethereum: a secure decentralized generalised transaction ledger, yellow paper, Ethereum (2014) Available: <https://gavwood.com/paper.pdf>.
- [53] D. Yaga, P. Mell, N. Roby, K. Scarfone, Blockchain technology overview, NIST Internal Report, Gaithersburg, MD, 2018.
- [54] P. Rogaway, T. Shrimpton, Cryptographic Hash-Function Basics: Definitions, Implications, and Separations for Preimage Resistance, Second-Preimage Resistance, and Collision Resistance, in: *Int. workshop on fast software*, Springer, Berlin, 371–388.
https://doi.org/10.1007/978-3-540-25937-4_24.
- [55] Z. Zheng, S. Xie, H. Dai, X. Chen, H. Wang, An Overview of Blockchain Technology: Architecture, Consensus, and Future Trends, in: *2017 IEEE International Congress on Big Data (BigData Congress)*, 557–564. <https://doi.org/10.1109/BigDataCongress.2017.85>.
- [56] A. Kaushik, A. Choudhary, C. Ektare, D. Thomas, S. Akram, Blockchain — Literature survey, in: *IEEE RTEICT 2017, Bangalore, India*, 2145–2148.
<https://doi.org/10.1109/RTEICT.2017.8256979>.

- [57] T.M. Fernandez-Carames, P. Fraga-Lamas, Towards Post-Quantum Blockchain: A Review on Blockchain Cryptography Resistant to Quantum Computing Attacks, *IEEE Access* 8 (2020) 21091–21116. <https://doi.org/10.1109/ACCESS.2020.2968985>.
- [58] N. Alzahrani, N. Bulusu, Towards True Decentralization: A Blockchain Consensus Protocol Based on Game Theory and Randomness, in: Bushnell, L., Poovendran, R., Başar, T. (eds) *Decision and Game Theory for Security. GameSec* (2018), 465–485. https://doi.org/10.1007/978-3-030-01554-1_27.
- [59] D.P. Oyinloye, J.S. Teh, N. Jamil, M. Alawida, Blockchain Consensus: An Overview of Alternative Protocols, *Symmetry* 13 (2021) 1363. <https://doi.org/10.3390/sym13081363>.
- [60] S. Gilbert, N. Lynch, Brewer's conjecture and the feasibility of consistent, available, partition-tolerant web services, *SIGACT News* 33 (2002) 51–59. <https://doi.org/10.1145/564585.564601>.
- [61] L. Lamport, R. Shostak, M. Pease, The Byzantine Generals Problem, *ACM Trans. Program. Lang. Syst.* 4 (1982) 382–401. <https://doi.org/10.1145/357172.357176>.
- [62] M. Nofer, P. Gomber, O. Hinz, D. Schiereck, Blockchain, *Bus Inf Syst Eng* 59 (2017) 183–187. <https://doi.org/10.1007/s12599-017-0467-3>.
- [63] N. Szabo, Formalizing and Securing Relationships on Public Networks, *First Monday* 2 (1997). <https://doi.org/10.5210/fm.v2i9.548>.
- [64] J. Fairfield, Smart Contracts, Bitcoin Bots, and Consumer Protection, *Washington and Lee Law Rev. Online* 71 (2) (2014) 35–49.
- [65] W. Cai, Z. Wang, J.B. Ernst, Z. Hong, C. Feng, V.C.M. Leung, Decentralized Applications: The Blockchain-Empowered Software System, *IEEE Access* 6 (2018) 53019–53033. <https://doi.org/10.1109/ACCESS.2018.2870644>.
- [66] Etherscan.io, Ethereum (ETH) Blockchain Explorer, 2023. <https://etherscan.io/> (accessed 16 January 2023).
- [67] Protocol Labs Inc., IPFS powers the Distributed Web, 2022. <https://ipfs.tech/> (accessed 8 December 2022).
- [68] M. Holland, J. Stjepandic, C. Nigischer, Intellectual Property Protection of 3D Print Supply Chain with Blockchain Technology, in: *Conference proceedings ICE/IEEE ITMC, Stuttgart, IEEE, Piscataway, NJ, 2018*, pp. 1–8.
- [69] A. Haridas, A.A. Samad, V. D, D.L. K, V. Pathari, A blockchain-based platform for smart contracts and intellectual property protection for the additive manufacturing industry, in: *IEEE SPICES 2022, India, IEEE, Piscataway, NJ, 2022*, pp. 223–230.

- [70] A. Bahga, V.K. Madiseti, Blockchain Platform for Industrial Internet of Things, *JSEA* 09 (2016) 533–546. <https://doi.org/10.4236/jsea.2016.910036>.
- [71] W. Baumung, V. Fomin, Framework for enabling order management process in a decentralized production network based on the blockchain-technology, *Procedia CIRP* 79 (2019) 456–460. <https://doi.org/10.1016/j.procir.2019.02.121>.
- [72] A. Vatankhah Barenji, Z. Li, W.M. Wang, G.Q. Huang, D.A. Guerra-Zubiaga, Blockchain-based ubiquitous manufacturing: a secure and reliable cyber-physical system, *Int. J. Prod. Res.* 58 (2020) 2200–2221. <https://doi.org/10.1080/00207543.2019.1680899>.
- [73] N. Papakostas, A. Newell, V. Hargaden, A novel paradigm for managing the product development process utilising blockchain technology principles, *CIRP Annals* 68 (2019) 137–140. <https://doi.org/10.1016/j.cirp.2019.04.039>.
- [74] S. Zhang, Z. Lin, H. Pan, Research on 3D printing platform of blockchain for digital spare parts management, *J. Phys.: Conf. Ser.* 1965 (2021) 12028. <https://doi.org/10.1088/1742-6596/1965/1/012028>.
- [75] RWTH Aachen, Add2Log – Dezentrale Produktion auf Basis von additiver Fertigung und agiler Logistik, 2023. <https://projekte.fir.de/add2log/> (accessed 11 January 2023).
- [76] Technische Universität Hamburg, SAMPL Secure Additive Manufacturing Platform, 2023. <https://sampl.fks.tuhh.de/en/home.html> (accessed 11 January 2023).
- [77] Bundesanstalt für Materialforschung und -prüfung, QI Digital - Additive Manufacturing for Small and Medium-sized Enterprises, 2023. <https://www.qi-digital.de/en/additive-manufacturing-for-smes> (accessed 11 January 2023).
- [78] P. Raj, Empowering digital twins with blockchain, in: *Adv. Computers* (2021), 267–283. <https://doi.org/10.1016/bs.adcom.2020.08.013>.
- [79] L. Zhang, X. Chen, W. Zhou, T. Cheng, L. Chen, Z. Guo, B. Han, L. Lu, Digital Twins for Additive Manufacturing: A State-of-the-Art Review, *Applied Sciences* 10 (2020) 8350. <https://doi.org/10.3390/app10238350>.
- [80] A. Gaikwad, R. Yavari, M. Montazeri, K. Cole, L. Bian, P. Rao, Toward the digital twin of additive manufacturing: Integrating thermal simulations, sensing, and analytics to detect process faults, *IISE Transactions* 52 (2020) 1204–1217. <https://doi.org/10.1080/24725854.2019.1701753>.
- [81] D. Guo, S. Ling, H. Li, D. Ao, T. Zhang, Y. Rong, G.Q. Huang, A framework for personalized production based on digital twin, blockchain and additive manufacturing in the context of Industry 4.0, in: *2020 IEEE 16th International Conference on Automation Science and Engineering (CASE)*, Hong Kong, Hong Kong, IEEE, 2020, pp. 1181–1186.

- [82] C. Mandolla, A.M. Petruzzelli, G. Percoco, A. Urbinati, Building a digital twin for additive manufacturing through the exploitation of blockchain: A case analysis of the aircraft industry, *Computers in Industry* 109 (2019) 134–152. <https://doi.org/10.1016/j.com-pind.2019.04.011>.
- [83] P. Witherell, Digital Twins for Part Acceptance in Advanced Manufacturing Applications with Regulatory Considerations, 46th MPA Seminar, Stuttgart (2021).
- [84] D. Mahmoud, M. Magolon, J. Boer, M.A. Elbestawi, M.G. Mohammadi, Applications of Machine Learning in Process Monitoring and Controls of L-PBF Additive Manufacturing: A Review, *Applied Sciences* 11 (2021) 11910. <https://doi.org/10.3390/app112411910>.
- [85] S.A. Shevchik, G. Masinelli, C. Kenel, C. Leinenbach, K. Wasmer, Deep Learning for In Situ and Real-Time Quality Monitoring in Additive Manufacturing Using Acoustic Emission, *IEEE Trans. Ind. Inf.* 15 (2019) 5194–5203. <https://doi.org/10.1109/TII.2019.2910524>.
- [86] S. Ho, W. Zhang, W. Young, M. Buchholz, S.A. Jufout, K. Dajani, L. Bian, M. Mozumdar, DLAM: Deep Learning Based Real-Time Porosity Prediction for Additive Manufacturing Using Thermal Images of the Melt Pool, *IEEE Access* 9 (2021) 115100–115114. <https://doi.org/10.1109/ACCESS.2021.3105362>.
- [87] A. Paul, M. Mozaffar, Z. Yang, W. Liao, A. Choudhary, J. Cao, A. Agrawal, A Real-Time Iterative Machine Learning Approach for Temperature Profile Prediction in Additive Manufacturing Processes, in: 2019 IEEE International Conference on Data Science and Advanced Analytics (DSAA), Washington, DC, USA, IEEE, 2019, pp. 541–550.
- [88] Z. Ghahramani, Probabilistic machine learning and artificial intelligence, *Nature* 521 (2015) 452–459. <https://doi.org/10.1038/nature14541>.
- [89] T.A. Runkler, *Data analytics: Models and algorithms for intelligent data analysis*, secondnd ed., Springer Vieweg, Wiesbaden, 2016.
- [90] C.-W. Tsai, C.-F. Lai, H.-C. Chao, A.V. Vasilakos, Big data analytics: a survey, *Journal of Big Data* 2 (2015). <https://doi.org/10.1186/s40537-015-0030-3>.
- [91] P. Russom, Big data analytics, TDWI Research Best Practice Report, 2011.
- [92] C. Ma, H.H. Zhang, X. Wang, Machine learning for Big Data analytics in plants, *Trends Plant Sci.* 19 (2014) 798–808. <https://doi.org/10.1016/j.tplants.2014.08.004>.
- [93] R. Soltanpoor, T. Sellis, Prescriptive Analytics for Big Data, in: M.A. Cheema, W. Zhang, L. Chang (Eds.), *Databases Theory and Applications: 27th Australasian Database*

- Conference, ADC 2016, Springer, Cham, 2016, 245–256. https://doi.org/10.1007/978-3-319-46922-5_19.
- [94] D. Delen, *Real-World Data Mining: Applied Business Analytics and Decision Making*, Pearson Education Lim., Sydney, 2014.
- [95] A. Banerjee, T. Bandyopadhyay, Prachi T. Acharya, Data Analytics: Hyped Up Aspirations or True Potential?, *J. Deci. Makers* 38 (4) (2013) 1–11.
- [96] M.G. Kibria, K. Nguyen, G.P. Villardi, O. Zhao, K. Ishizu, F. Kojima, Big Data Analytics, Machine Learning, and Artificial Intelligence in Next-Generation Wireless Networks, *IEEE Access* 6 (2018) 32328–32338. <https://doi.org/10.1109/ACCESS.2018.2837692>.
- [97] D. Delen, H. Demirkan, Data, information and analytics as services, *Decision Support Systems* 55 (2013) 359–363. <https://doi.org/10.1016/j.dss.2012.05.044>.
- [98] H. Baumgartl, J. Tomas, R. Buettner, M. Merkel, A deep learning-based model for defect detection in laser-powder bed fusion using in-situ thermographic monitoring, *Prog Addit Manuf* 5 (2020) 277–285. <https://doi.org/10.1007/s40964-019-00108-3>.
- [99] M.I. Jordan, T.M. Mitchell, Machine learning: Trends, perspectives, and prospects, *Science* 349 (2015) 255–260. <https://doi.org/10.1126/science.aaa8415>.
- [100] F. Chollet, *Deep learning with Python*, Manning Publications Co, Shelter Island, NY, 2018.
- [101] T. Mitchell, B. Buchanan, G. DeJong, T. Dietterich, P. Rosenbloom, A. Waibel, Machine Learning, *Annu. Rev. Comput. Sci.* 4 (1990) 417–433. <https://doi.org/10.1146/annurev.cs.04.060190.002221>.
- [102] J. Qiu, Q. Wu, G. Ding, Y. Xu, S. Feng, A survey of machine learning for big data processing, *EURASIP J. Adv. Signal Process.* 2016 (2016). <https://doi.org/10.1186/s13634-016-0355-x>.
- [103] L.P. Kaelbling, M.L. Littman, A.W. Moore, Reinforcement Learning: A Survey, *jair* 4 (1996) 237–285. <https://doi.org/10.1613/jair.301>.
- [104] C.J.C.H. Watkins, P. Dayan, Q-learning, *Mach Learn* 8 (1992) 279–292. <https://doi.org/10.1007/BF00992698>.
- [105] G. James, D. Witten, T. Hastie, R. Tibshirani, *An introduction to statistical learning: With applications in R*, Springer, New York, NY, 2017. <https://doi.org/1007/978-1-4614-7138-7>.

- [106] T.K. Das, A. Gosavi, S. Mahadevan, N. Marchallick, Solving Semi-Markov Decision Problems Using Average Reward Reinforcement Learning, *Management Science* 45 (1999) 560–574. <https://doi.org/10.1287/mnsc.45.4.560>.
- [107] R.S. Sutton, Learning to predict by the methods of temporal differences, *Mach Learn* 3 (1988) 9–44. <https://doi.org/10.1007/BF00115009>.
- [108] Y. Li, Deep Reinforcement Learning, eprint arXiv, 2018. <https://doi.org/10.48550/arXiv.1810.06339>.
- [109] J.M. Johnson, T.M. Khoshgoftaar, Survey on deep learning with class imbalance, *J Big Data* 6 (2019). <https://doi.org/10.1186/s40537-019-0192-5>.
- [110] M. Feurer, F. Hutter, Hyperparameter Optimization, in: F. Hutter, L. Kotthoff, J. Vanschoren (Eds.), *Automated Machine Learning*, Springer Nature, Cham, 2019, 3–33. https://doi.org/10.1007/978-3-030-05318-5_1.
- [111] N. Srivastava, G. Hinton, A. Krizhevsky, I. Sutskever, R. Salakhutdinov, Dropout: A Simple Way to Prevent Neural Networks from Overfitting, *J. Mach. Lern. Res.* 15 (2014) 1929–1958.
- [112] S.J. Pan, Q. Yang, A Survey on Transfer Learning, *IEEE Trans. Knowl. Data Eng.* 22 (2010) 1345–1359. <https://doi.org/10.1109/TKDE.2009.191>.
- [113] K. Weiss, T.M. Khoshgoftaar, D. Wang, A survey of transfer learning, *J Big Data* 3 (2016). <https://doi.org/10.1186/s40537-016-0043-6>.
- [114] A. Krizhevsky, I. Sutskever, G.E. Hinton, ImageNet classification with deep convolutional neural networks, *Commun. ACM* 60 (2017) 84–90. <https://doi.org/10.1145/3065386>.
- [115] N.S. Johnson, P.S. Vulimiri, A.C. To, X. Zhang, C.A. Brice, B.B. Kappes, A.P. Stebner, Invited review: Machine learning for materials developments in metals additive manufacturing, *Addit. Manuf.* 36 (2020) 101641. <https://doi.org/10.1016/j.addma.2020.101641>.
- [116] M.Z. Naser, A.H. Alavi, Error Metrics and Performance Fitness Indicators for Artificial Intelligence and Machine Learning in Engineering and Sciences, *Archit. Struct. Constr.* (2021). <https://doi.org/10.1007/s44150-021-00015-8>.
- [117] M. Hossin, M.N. Sulaiman, A Review on Evaluation Metrics for Data Classification Evaluations, *IJDKP* 5 (2015) 1–11. <https://doi.org/10.5121/ijdkp.2015.5201>.
- [118] M. Grandini, E. Bagli, G. Visani, Metrics for Multi-Class Classification: an Overview, eprint arXiv, 2020. <https://doi.org/10.48550/arXiv.2008.05756>.
- [119] T. Fawcett, An introduction to ROC analysis, *Pattern Recognition Letters* 27 (2006) 861–874. <https://doi.org/10.1016/j.patrec.2005.10.010>.

- [120] K. Woods, K.W. Bowyer, Generating ROC curves for artificial neural networks, *IEEE Trans. Med. Imaging* 16 (1997) 329–337. <https://doi.org/10.1109/42.585767>.
- [121] P. Branco, L. Torgo, R.P. Ribeiro, A Survey of Predictive Modeling on Imbalanced Domains, *ACM Comput. Surv.* 49 (2016). <https://doi.org/10.1145/2907070>.
- [122] R.R. Selvaraju, M. Cogswell, A. Das, R. Vedantam, D. Parikh, D. Batra, Grad-CAM: Visual Explanations from Deep Networks via Gradient-Based Localization, *Int J Comput Vis* 128 (2020) 336–359. <https://doi.org/10.1007/s11263-019-01228-7>.
- [123] S. Albawi, T.A. Mohammed, S. Al-Zawi, Understanding of a convolutional neural network, in: *International Conference on Engineering 2017*, <https://doi.org/10.1109/ICEng-Technol.2017.8308186>.
- [124] M.H. Hassoun, *Fundamentals of artificial neural networks*, MIT Press, Cambridge, Mass., 1995.
- [125] M.M. Waldrop, What are the limits of deep learning?, *Proc. Natl. Acad. Sci. U.S.A.* 116 (2019) 1074–1077. <https://doi.org/10.1073/pnas.1821594116>.
- [126] T. Rashid, *Make your own neural network*, CreateSpace Independent Publishing, North Charleston, SC, US, 2017.
- [127] Y. LeCun, Y. Bengio, G. Hinton, Deep learning, *Nature* 521 (2015) 436–444. <https://doi.org/10.1038/nature14539>.
- [128] S. Leijnen, F. van Veen, The Neural Network Zoo, *Proceedings* 47 (2020) 9. <https://doi.org/10.3390/proceedings2020047009>.
- [129] C. Janiesch, P. Zschech, K. Heinrich, Machine learning and deep learning, *Electron Markets* 31 (2021) 685–695. <https://doi.org/10.1007/s12525-021-00475-2>.
- [130] H.I. Fawaz, G. Forestier, J. Weber, L. Idoumghar, P.-A. Muller, Deep learning for time series classification: a review, *Data Min Knowl Disc* 33 (2019) 917–963. <https://doi.org/10.1007/s10618-019-00619-1>.
- [131] Y. LeCun, Y. Bengio, Convolutional Networks for Images, Speech, and Time Series, in: *The Handbook of Brain Theory and Neural Networks*, MIT Press, Cambridge, MA, USA, 1998, pp. 255–258.
- [132] Z.C. Lipton, J. Berkowitz, C. Elkan, A Critical Review of Recurrent Neural Networks for Sequence Learning, eprint arXiv, 2015. <https://arxiv.org/pdf/1506.00019>.
- [133] S. Dick, *Artificial Intelligence*, *Harvard Data Science Review* 1 (1) (2019). <https://doi.org/10.1162/99608f92.92fe150c>.

- [134] J. McCarthy, M.L. Minsky, N. Rochester, C.E. Shannon, A Proposal for the Dartmouth Summer Research Project on Artificial Intelligence, *AIMag* 27 (2006) 12.
<https://doi.org/10.1609/aimag.v27i4.1904>.
- [135] L. Floridi, *The fourth revolution: how the infosphere is reshaping human reality*, Oxford University Press, Oxford, 2014.
- [136] C. Wang, X.P. Tan, S.B. Tor, C.S. Lim, Machine learning in additive manufacturing: State-of-the-art and perspectives, *Addit. Manuf.* 36 (2020) 101538.
<https://doi.org/10.1016/j.addma.2020.101538>.
- [137] J. Qin, F. Hu, Y. Liu, P. Witherell, C.C. Wang, D.W. Rosen, T.W. Simpson, Y. Lu, Q. Tang, Research and application of machine learning for additive manufacturing, *Addit. Manuf.* 52 (2022) 102691. <https://doi.org/10.1016/j.addma.2022.102691>.
- [138] Z. Jin, Z. Zhang, K. Demir, G.X. Gu, Machine Learning for Advanced Additive Manufacturing, *Matter* 3 (2020) 1541–1556. <https://doi.org/10.1016/j.matt.2020.08.023>.
- [139] L. Meng, B. McWilliams, W. Jarosinski, H.-Y. Park, Y.-G. Jung, J. Lee, J. Zhang, Machine Learning in Additive Manufacturing: A Review, *JOM* 72 (2020) 2363–2377.
<https://doi.org/10.1007/s11837-020-04155-y>.
- [140] D. Grierson, A.E.W. Rennie, S.D. Quayle, Machine Learning for Additive Manufacturing, *Encyclopedia* 1 (2021) 576–588. <https://doi.org/10.3390/encyclopedia1030048>.
- [141] G.X. Gu, C.-T. Chen, D.J. Richmond, M.J. Buehler, Bioinspired hierarchical composite design using machine learning: simulation, additive manufacturing, and experiment, *Mater. Horiz.* 5 (2018) 939–945. <https://doi.org/10.1039/C8MH00653A>.
- [142] S. Guo, M. Agarwal, C. Cooper, Q. Tian, R.X. Gao, W. Guo, Y.B. Guo, Machine learning for metal additive manufacturing: Towards a physics-informed data-driven paradigm, *J. Manuf. Syst.* 62 (2022) 145–163. <https://doi.org/10.1016/j.jmsy.2021.11.003>.
- [143] N. Razaviarab, S. Sharifi, Y.M. Banadaki, Smart additive manufacturing empowered by a closed-loop machine learning algorithm, in: *Nano-, Bio-, Info-Tech Sensors, and 3D Systems III*. Society for Optics and Photonics, SPIE, Bellingham, WA, USA, 2019, 17.
<https://doi.org/10.1117/12.2513816>.
- [144] J. Schöning, A. Riechmann, H.-J. Pfisterer, AI for Closed-Loop Control Systems, in: *2022 14th International Conference on Machine Learning and Computing (ICMLC)*, ACM, New York, NY, USA, 2022, 318–323. <https://doi.org/10.1145/3529836.3529952>.
- [145] C. Gobert, E.W. Reutzler, J. Petrich, A.R. Nassar, S. Phoha, Application of supervised machine learning for defect detection during metallic powder bed fusion additive

- manufacturing using high resolution imaging, *Addit. Manuf.* 21 (2018) 517–528.
<https://doi.org/10.1016/j.addma.2018.04.005>.
- [146] A. Caggiano, J. Zhang, V. Alfieri, F. Caiazzo, R. Gao, R. Teti, Machine learning-based image processing for on-line defect recognition in additive manufacturing, *CIRP Annals* 68 (2019) 451–454. <https://doi.org/10.1016/j.cirp.2019.03.021>.
- [147] Y. Fu, A.R. Downey, L. Yuan, T. Zhang, A. Pratt, Y. Balogun, Machine learning algorithms for defect detection in metal laser-based additive manufacturing: A review, *J. Manuf. Proc.* 75 (2022) 693–710. <https://doi.org/10.1016/j.jmapro.2021.12.061>.
- [148] M. Ghayoomi Mohammadi, D. Mahmoud, M. Elbestawi, On the application of machine learning for defect detection in L-PBF additive manufacturing, *Optics & Laser Tech.* 143 (2021) 107338. <https://doi.org/10.1016/j.optlastec.2021.107338>.
- [149] R. Li, M. Jin, V.C. Paquit, Geometrical defect detection for additive manufacturing with machine learning models, *Materials & Design* 206 (2021) 109726.
<https://doi.org/10.1016/j.matdes.2021.109726>.
- [150] Z. Li, Z. Zhang, J. Shi, D. Wu, Prediction of surface roughness in extrusion-based additive manufacturing with machine learning, *Robotics and Comp-Integ. Manuf.* 57 (2019) 488–495. <https://doi.org/10.1016/j.rcim.2019.01.004>.
- [151] C. Xia, Z. Pan, J. Polden, H. Li, Y. Xu, S. Chen, Modelling and prediction of surface roughness in wire arc additive manufacturing using machine learning, *J Intell Manuf* 33 (2022) 1467–1482. <https://doi.org/10.1007/s10845-020-01725-4>.
- [152] V. Akhil, G. Raghav, N. Arunachalam, D.S. Srinivas, 2020. Image Data-Based Surface Texture Characterization and Prediction Using Machine Learning Approaches for Additive Manufacturing. *J Comput Inf Sci Eng* 20, 021010.
<https://doi.org/10.1115/1.4045719>.
- [153] L. Cao, J. Li, J. Hu, H. Liu, Y. Wu, Q. Zhou, Optimization of surface roughness and dimensional accuracy in LPBF additive manufacturing, *Optics & Laser Tech.* 142 (2021) 107246. <https://doi.org/10.1016/j.optlastec.2021.107246>.
- [154] D. Wu, Y. Wei, J. Terpenney, Surface Roughness Prediction in Additive Manufacturing Using Machine Learning, in: *ASME 2018 13th Int. Manuf. Sci. Eng. Conf. MSEC 2018, 2018*, 1–6. <https://doi.org/10.1115/MSEC2018-6501>.
- [155] J. Petrich, Z. Snow, D. Corbin, E.W. Reutzel, Multi-modal sensor fusion with machine learning for data-driven process monitoring for additive manufacturing, *Addit. Manuf.* 48 (2021) 102364. <https://doi.org/10.1016/j.addma.2021.102364>.

- [156] X. Xiao, C. Waddell, C. Hamilton, H. Xiao, Quality Prediction and Control in Wire Arc Additive Manufacturing via Novel Machine Learning Framework, *Micromachines* (Basel) 13 (2022). <https://doi.org/10.3390/mi13010137>.
- [157] S. Liu, A.P. Stebner, B.B. Kappes, X. Zhang, Machine learning for knowledge transfer across multiple metals additive manufacturing printers, *Addit. Manuf.* 39 (2021) 101877. <https://doi.org/10.1016/j.addma.2021.101877>.
- [158] C. Liu, L. Le Roux, Z. Ji, P. Kerfriden, F. Lacan, S. Bigot, Machine Learning-enabled feedback loops for metal powder bed fusion additive manufacturing, *Proc. Comp. Sci.* 176 (2020) 2586–2595. <https://doi.org/10.1016/j.procs.2020.09.314>.
- [159] V. Renken, L. Lübbert, H. Blom, A. von Freyberg, A. Fischer, Model assisted closed-loop control strategy for selective laser melting, *Procedia CIRP* 74 (2018) 659–663. <https://doi.org/10.1016/j.procir.2018.08.053>.
- [160] Y. Zhang, Y. Fiona Zhao, A Web-based automated manufacturability analyzer and recommender for additive manufacturing (MAR-AM) via a hybrid Machine learning model, *Expert Syst. Applic.* 199 (2022) 117189. <https://doi.org/10.1016/j.eswa.2022.117189>.
- [161] S.E. Ghiasian, K. Lewis, A Machine Learning-Based Design Recommender System for Additive Manufacturing, in: *Proceedings of the ASME 2020 International Design Engineering Technical Conferences and Computers and Information in Engineering Conference (IDETC-CIE2020)*, ASME, New York, NY, 2020.
- [162] X. Yao, S.K. Moon, G. Bi, A hybrid machine learning approach for additive manufacturing design feature recommendation, *RPJ* 23 (2017) 983–997. <https://doi.org/10.1108/RPJ-03-2016-0041>.
- [163] M. Khanzadeh, P. Rao, R. Jafari-Marandi, B.K. Smith, M.A. Tschopp, L. Bian, 2018. Quantifying Geometric Accuracy With Unsupervised Machine Learning: Using Self-Organizing Map on Fused Filament Fabrication Additive Manufacturing Parts. *J. Manuf. Sci. Eng.* 140, 031011. <https://doi.org/10.1115/1.4038598>.
- [164] K.L.S. Sharma, *Overview of industrial process automation*, Elsevier, Amsterdam, 2011. <https://doi.org/10.1016/C2015-0-01929-3>.
- [165] R. Khosravian, B.S. Aadnøy, Introduction to digital twin, automation and real-time centers, in: B.S. Aadnøy, R. Khosravian (Eds.), *Methods for Petroleum Well Optimization: Automation and Data Solutions*, Gulf Publishing, 2021, 1–30. <https://doi.org/10.1016/B978-0-323-90231-1.00006-6>.

- [166] G.P. Greeff, M. Schilling, Closed loop control of slippage during filament transport in molten material extrusion, *Addit. Manuf.* 14 (2017) 31–38. <https://doi.org/10.1016/j.addma.2016.12.005>.
- [167] F. Caltanissetta, M. Grasso, S. Petrò, B.M. Colosimo, Characterization of in-situ measurements based on layerwise imaging in laser powder bed fusion, *Addit. Manuf.* 24 (2018) 183–199. <https://doi.org/10.1016/j.addma.2018.09.017>.
- [168] M. Rahman, D. Brackett, K. Milne, A. Szymanski, A. Okioga, L. Huertas, S. Jadhav, An integrated process and data framework for the purpose of knowledge management and closed-loop quality feedback in additive manufacturing, *Prog Addit Manuf* 7 (2022) 551–564. <https://doi.org/10.1007/s40964-021-00246-7>.
- [169] Q. Fang, G. Xiong, M. Zhou, T.S. Tamir, C.-B. Yan, H. Wu, Z. Shen, F.-Y. Wang, Process Monitoring, Diagnosis and Control of Additive Manufacturing, *IEEE Trans. Automat. Sci. Eng.* (2022) 1–27. <https://doi.org/10.1109/TASE.2022.3215258>.
- [170] K. Simonyan, A. Zisserman, Very Deep Convolutional Networks for Large-Scale Image Recognition, arXiv preprint, arXiv:1409.1556, (2014).
- [171] F. Chollet, Xception: Deep Learning with Depthwise Separable Convolutions, in: 2017 IEEE Conference on Computer Vision and Pattern Recognition (CVPR), Honolulu, HI, USA, 2017, 1800–1807. arXiv preprint, arXiv:1610.02357.
- [172] C. Fawcett, H.H. Hoos, Analysing differences between algorithm configurations through ablation, *J Heuristics* 22 (2016) 431–458. <https://doi.org/10.1007/s10732-014-9275-9>.
- [173] C. Cachin, S. Schubert, M. Vukolić, Non-determinism in Byzantine Fault-Tolerant Replication, 2016. <http://arxiv.org/pdf/1603.07351v2>.
- [174] J. Kanani, S. Nailwal, A. Arjun, Matic whitepaper, 2018. <https://github.com/maticnetwork/whitepaper> (accessed 30 January 2023).
- [175] S. Wang, D. Li, Y. Zhang, J. Chen, Smart Contract-Based Product Traceability System in the Supply Chain Scenario, *IEEE Access* 7 (2019) 115122–115133. <https://doi.org/10.1109/ACCESS.2019.2935873>.
- [176] E. Ben-Sasson, I. Bentov, Y. Horesh, M. Riabzev, Scalable, transparent, and post-quantum secure computational integrity, *Cryptology ePrint Archive* (2018). <https://eprint.iacr.org/2018/046.pdf>.
- [177] B.-M. Roh, S.R.T. Kumara, H. Yang, T.W. Simpson, P. Witherell, Y. Lu, In-Situ Observation Selection for Quality Management in Metal Additive Manufacturing, in: 41st

- Computers and Information in Engineering Conference (CIE), ASME, 2021, <https://doi.org/10.1115/DETC2021-70035>.
- [178] D. Chauveau, Review of NDT and process monitoring techniques usable to produce high-quality parts by welding or additive manufacturing, *Weld World* 62 (2018) 1097–1118. <https://doi.org/10.1007/s40194-018-0609-3>.
- [179] Y. Chen, X. Peng, L. Kong, G. Dong, A. Remani, R. Leach, Defect inspection technologies for additive manufacturing, *Int. J. Extrem. Manuf.* 3 (2021) 22002. <https://doi.org/10.1088/2631-7990/abe0d0>.
- [180] J.L. Bartlett, F.M. Heim, Y.V. Murty, X. Li, In situ defect detection in selective laser melting via full-field infrared thermography, *Addit. Manuf.* 24 (2018) 595–605. <https://doi.org/10.1016/j.addma.2018.10.045>.
- [181] J. Schwerdtfeger, R.F. Singer, C. Körner, In situ flaw detection by IR-imaging during electron beam melting, *RPJ* 18 (2012) 259–263. <https://doi.org/10.1108/13552541211231572>.
- [182] S. Guo, G. Ren, B. Zhang, Subsurface Defect Evaluation of Selective-Laser-Melted Inconel 738LC Alloy Using Eddy Current Testing for Additive/Subtractive Hybrid Manufacturing, *Chin. J. Mech. Eng.* 34 (2021). <https://doi.org/10.1186/s10033-021-00633-9>.
- [183] C. Millon, A. Vanhoye, A.-F. Obaton, J.-D. Penot, Development of laser ultrasonics inspection for online monitoring of additive manufacturing, *Weld World* 62 (2018) 653–661. <https://doi.org/10.1007/s40194-018-0567-9>.
- [184] P.J. Withers, C. Bouman, S. Carmignato, V. Cnudde, D. Grimaldi, C.K. Hagen, E. Maire, M. Manley, A. Du Plessis, S.R. Stock, X-ray computed tomography, *Nat Rev Methods Primers* 1 (2021). <https://doi.org/10.1038/s43586-021-00015-4>.
- [185] A. Thompson, I. Maskery, R.K. Leach, X-ray computed tomography for additive manufacturing: a review, *Meas. Sci. Technol.* 27 (2016) 72001. <https://doi.org/10.1088/0957-0233/27/7/072001>.
- [186] H. Wu, Y. Wang, Z. Yu, In situ monitoring of FDM machine condition via acoustic emission, *Int J Adv Manuf Technol* (2015). <https://doi.org/10.1007/s00170-015-7809-4>.
- [187] K. Wasmer, T. Le-Quang, B. Meylan, S.A. Shevchik, In Situ Quality Monitoring in AM Using Acoustic Emission: A Reinforcement Learning Approach, *J. of Materi Eng and Perform* 28 (2019) 666–672. <https://doi.org/10.1007/s11665-018-3690-2>.
- [188] R. Wang, A.C. Law, D. Garcia, S. Yang, Z. Kong, Development of structured light 3D-scanner with high spatial resolution and its applications for additive manufacturing

- quality assurance, *Int J Adv Manuf Technol* 117 (2021) 845–862.
<https://doi.org/10.1007/s00170-021-07780-2>.
- [189] I. Garmendia, J. Leunda, J. Pujana, A. Lamikiz, In-process height control during laser metal deposition based on structured light 3D scanning, *Procedia CIRP* 68 (2018) 375–380. <https://doi.org/10.1016/j.procir.2017.12.098>.
- [190] X. Qi, G. Chen, Y. Li, X. Cheng, C. Li, Applying Neural-Network-Based Machine Learning to Additive Manufacturing: Current Applications, Challenges, and Future Perspectives, *Engineering* 5 (2019) 721–729. <https://doi.org/10.1016/j.eng.2019.04.012>.
- [191] H. Kim, Y. Lin, T.-L.B. Tseng, A review on quality control in additive manufacturing, *RPJ* 24 (2018) 645–669. <https://doi.org/10.1108/RPJ-03-2017-0048>.
- [192] A.B. Spierings, M. Schneider, R. Eggenberger, Comparison of density measurement techniques for additive manufactured metallic parts, *RPJ* 17 (2011) 380–386.
<https://doi.org/10.1108/13552541111156504>.
- [193] I. Akilan, C. Velmurugan, Mechanical Testing of Additive Manufacturing Materials, in: M.A. Khan, J.T.W. Jappes (Eds.), *Innovations in additive manufacturing*, Springer, Cham, 2022, 239–277. https://doi.org/10.1007/978-3-030-89401-6_11.

Annotations

Appendix A - Test methods in additive manufacturing

Table A-1 : Test methods of additive manufacturing processes and parts.

Method	Type	Description
Visual inspection	non-destructive, ex-situ	Visual inspection is usually carried out with the naked eye, if necessary supported by aids such as magnifying glasses or mirrors, in order to check surfaces, external structures and dimensions non-destructively and to draw conclusions about their origin [178].
Infrared thermal imaging test	non-destructive, in- and ex-situ	Infrared thermal imaging can be used to non-destructively detect differences in the thermal radiation intensity of shapes and contours in AM parts and clearly identify defects compared to the surrounding material [179–181].
Penetration test	non-destructive, ex-situ	A colored or fluorescent penetrant is applied to the surface of a non-porous AM part, penetrates surface defects by capillary action, and can then be non-destructively visualized by the addition of a developer [10,179].
Eddy current test	non-destructive, ex-situ	Electromagnetic induction on conductive AM parts induces eddy currents whose changes, e.g. due to surface defects, can be measured non-destructively [179,182].
Ultrasonic test	non-destructive, ex-situ	Ultrasonic waves are transmitted via a transmitter or a laser into a metallic AM part. Inside the part, the sound waves propagate and are reflected differently at interfaces (e.g. cracks, melt defects, pores), which in turn can be detected non-destructively [179,183].
Computed tomography (CT) scan	non-destructive, ex-situ	X-ray computed tomography (CT) can be used to create three-dimensional images of an AM part non-destructively by taking many X-ray images around a rotational axis and using them to reconstruct a 3D model, for example, to identify internal pores and structural irregularities [184,185].
Acoustic emission test	non-destructive, in- und ex-situ	Acoustic emission sensors can capture acoustic information of the AM process and infer different emission sources (such as cracks, pores, specific process parameters, etc.) using different frequency spectra [186,187].
3D imaging	non-destructive, in- und ex-situ	Using cameras and 3D scanners, the surface topography of AM parts can be digitally reconstructed with sometimes high precision and then analyzed on a computer to characterize defects, deviations and geometries relatively quickly [188]. Mostly cameras are used to observe the AM process [189]. Other 3D imaging techniques include interferometry, laser triangulation, structured light 3D scanners, laser line scanners, and photogrammetry [188,189].

Method	Type	Description
Data analytics and machine learning	non-destructive, in- und ex-situ	ML and data analysis algorithms are increasingly used for non-destructive defect detection and in-situ monitoring in AM [137]. Various 1D data (e.g. spectra), 2D data (e.g. images) and 3D data (e.g. tomography scans) are collected, analyzed and used to train ML algorithms, which subsequently lead to an artificial control system and improve the quality of the AM part or, in the case of closed-loop feedback to the AM machines, also minimize quality problems during the printing process [190,191].
Density and porosity measurements	non-destructive / destructive, ex-situ	Knowing the density and porosity of AM components is critical for quality assessment, but there is no preferred standard measurement method for this purpose [192]. Commonly used measurement principles include microscopic analysis, CT scans, gravimetric analysis, and gas pycnometry.
Mechanical tests	non-destructive / destructive, ex-situ	The analysis of the mechanical properties of AM parts forms the basis for comparison with conventionally manufactured parts in order to assess the suitability of AM for use [193]. Typical mechanical test methods include hardness testing, tensile and compressive strength testing, surface roughness measurement, fracture toughness and fatigue strength analysis.

Appendix B - Functionality of neural networks

Artificial neural networks are modeled on the signal transmission between biological neurons of the human and animal brain (see Figure B-1, left) [126]. To represent this natural model artificially, contiguous layers of artificial neurons are usually represented (Figure B-1, right).

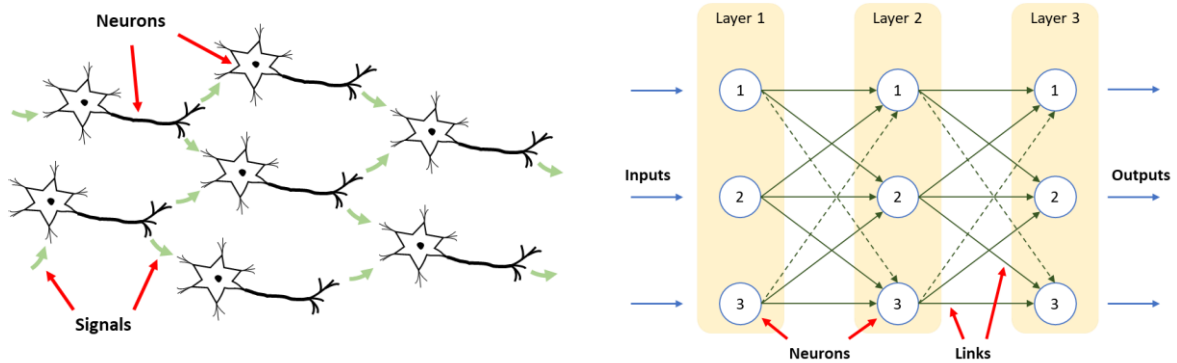


Figure B-1: Multiple interconnected neurons (left) and representation of an artificial neural network (right) according to [126].

The model shown in Figure B-1 consists of three layers, each with three artificial neurons or nodes. Each node here is connected to other nodes of the previous or following layer to form a network. In order to learn, the strength of the connections between the nodes must now be adjusted. For this purpose, each connection is first assigned a weighting (see Figure B-2). In this regard, a low weight weakens a signal and a high weight strengthens it [126]. It follows that not all nodes have to be connected to every other node of each layer, because some weights can also become almost zero as the network learns. In concrete terms, this means that these signals cannot pass at these points and the network has learned that these signals are not that important.

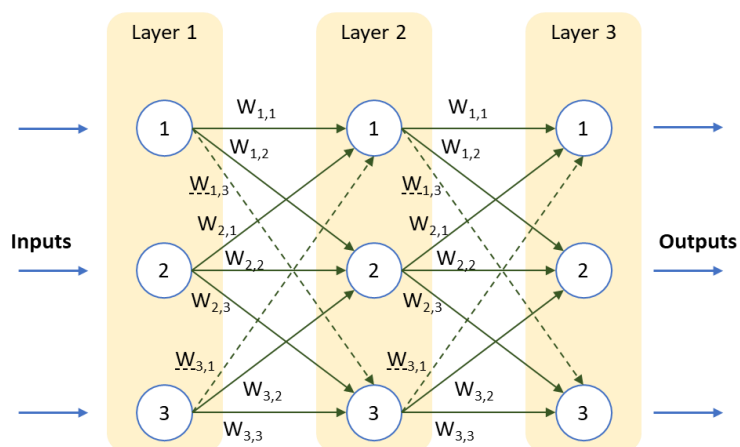


Figure B-2: Weighted neural network related to [126]. The small numbers illustrate the signal progression, e.g. $W_{2,3}$ means the signal goes from node two in one layer to node three in the next layer.

The learning process for a small neural network is shown in Figure B-3, left. The output values X of the next layer is calculated with randomly selected input values I and weights W of a layer using matrix multiplication and activation function:

$$X = W \times I \quad (1)$$

$$\begin{pmatrix} (input_1 \times w_{1,1}) + (input_2 \times w_{2,1}) \\ (input_1 \times w_{1,2}) + (input_2 \times w_{2,2}) \end{pmatrix} = \begin{pmatrix} w_{1,1} & w_{2,1} \\ w_{1,2} & w_{2,2} \end{pmatrix} \times \begin{pmatrix} input_1 \\ input_2 \end{pmatrix}. \quad (2)$$

The activation or step function accepts the summed input signals and finally controls the output of the output signal, taking a threshold value into account. If the combined input signal is not large enough, the threshold function suppresses the output signal from passing through. However, when the input signal is large enough and reaches the threshold, the artificial neuron fires and transmits the output signal [126]. A frequently used activation function is the sigmoid function, which does not have an abrupt jump but is smoother and thus appears more natural and realistic:

$$y = \frac{1}{(1 + e^{-x})}. \quad (3)$$

The result of the activation function then represents the output of the node. For the nodes of the second layer from Figure B-3, right it follows from equations (1) and (2):

$$X = \begin{pmatrix} (1.0 \times 0.7) + (0.5 \times 0.9) \\ (1.0 \times 0.3) + (0.5 \times 0.4) \end{pmatrix} = \begin{pmatrix} 1.15 \\ 0.5 \end{pmatrix}. \quad (4)$$

The output signals from each node are then determined from the combined inputs and using the sigmoid function of equation (3):

$$y = \begin{pmatrix} 0.7595 \\ 0.6225 \end{pmatrix}. \quad (5)$$

These relatively complex calculations can be performed quickly with computers, which means that much larger and more complex networks can also be used.

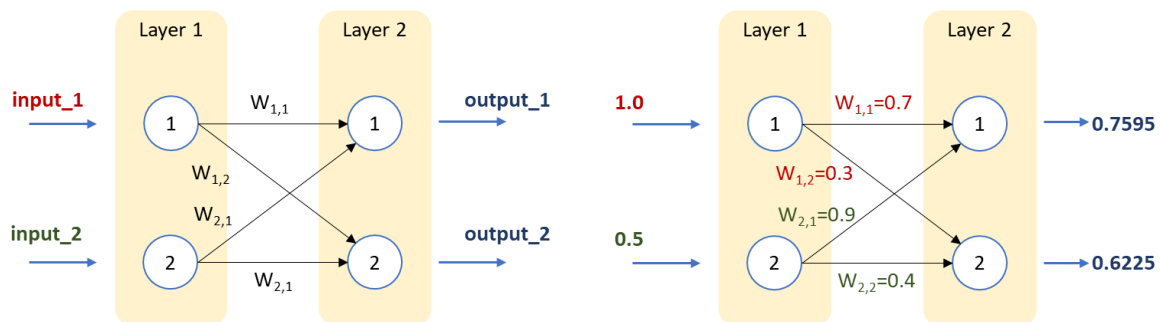


Figure B-3: Basic input, weight and output values of a neural network (left) and a calculation example with randomly selected input values, weights and the calculated outputs (right).

After the input signal has passed through the neural network, the resulting output signal is compared to a training sample to determine an error or difference e between the determined output value o and a known training value t :

$$e_n = t_n - o_n. \quad (6)$$

Based on the error, the neural network must be refined so that the output values obtained are closer to the true values, so the network must be constantly trained and optimized. The training is done by feeding the output errors back into the network according to the weighted node connections against the output signal calculation. This method is called backpropagation [126]. Figure B-4, left shows the backpropagation of the output errors using a simple neural network. In Figure B-4, right the previous calculation example is continued, where with known training data t , the output layer error e is calculated for each node according to equation (6).

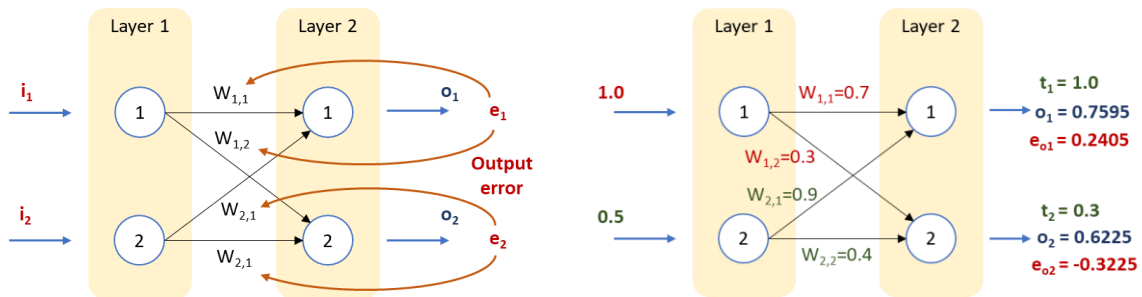


Figure B-4: Backpropagation with output error (left) and continuation of the calculation example with concrete calculation values (right).

Then, the backpropagation of the output error e_o back to the previous layer is performed. Here, the error of each node is first divided proportionally among the weighted connections w according to the following equation:

$$e_{L_n} = e_{o_n} \times \frac{W_{1,n}}{W_{1,n} + W_{2,n}}. \quad (7)$$

The error of the previous layer e_L is then given by the sum of the divided output errors of the connections e_o . For more complex neural networks, the error backpropagation can again be expressed as a matrix multiplication and computed more quickly via a computer code. In the following, Figure B-5 only continues the previously considered computational example with a simple neural network for a basic understanding.

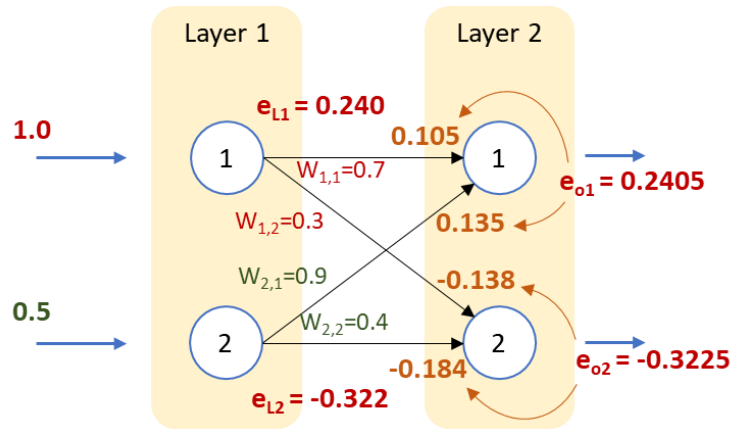


Figure B-5: Backpropagation with error calculation based on the calculation example.

The errors of node one of the first layer determined by backpropagation are calculated according to equation (7) and summarized as follows:

$$e_{L1} = \begin{pmatrix} 0.2405 \times \frac{0.7}{0.7 + 0.9} \\ -0.3225 \times \frac{0.9}{0.9 + 0.7} \end{pmatrix} = \begin{pmatrix} 0.105 \\ 0.135 \end{pmatrix}. \quad (8)$$

Subsequently, the sum of the weighted errors for each node and thus the summarized error of the respective node for the first layer is formed. For node one this results in:

$$\Sigma e_{L1} = 0.105 + 0.135 = 0.240. \quad (9)$$

For node two of the first layer, the calculation of e_{L2} is analogous to equations (8) and (9) with the values of e_{o2} and the weights associated with this node.

Once the errors have been attributed to each layer of the neural network, the weights of the network must be updated in order to optimize the output signal generated by the network. For this purpose, mathematically the method of gradient descent is used, with which the error of the network can be represented and minimized. A well understood explanation of the gradient descent method can be found in [126]. The derivation of a so-called error function for the adjustment of the weights is also described there. This is because in order to improve the neural network, the errors must be reduced by the network adjusting its weights. The calculation of the error increase results from the change of the error E depending on the change of the weight $w_{j,k}$ as follows (detailed derivation in [126]):

$$\frac{\partial E}{\partial w_{j,k}} = -(t_k - o_k) \times \text{sigmoid}(\Sigma_j w_{j,k} o_j) \left(1 - \text{sigmoid}(\Sigma_j w_{j,k} o_j)\right) \times o_j. \quad (10)$$

In Figure B-6, the known example is now supplemented by the weight adjustment. If the calculation from equation (10) for updating the weights $w_{1,1}$ of the first node of the first layer is carried out step by step, the following values result:

- The term $(t_k - o_k)$ is the error $e_{o1} = 0.2405$ (see already Figure B-4, right).

- The sum of the sigmoid function $\sum_j w_{j,k} o_j$ gives $(0.7 \times 1.0) + (0.9 \times 0.5) = 0.315$. Substituting into the sigmoid function $1/(1 + e^{-0.315})$ yields the intermediate result 0.578, which in turn is substituted into the mean expression: $0.578 \times (1 - 0.578) = 0.244$.
- The last element is the output of the node that is before the weighting, in this case the input signal $o_j = 1.0$, since the weighting w_{11} is considered (the error e_L is not yet considered in the input layer).

Multiplying all three terms results in an error increase of -0.059. In the neural network, the updates of the weights are usually multiplied by a so-called learning rate α to better represent certain problems and to avoid overshooting of the updates due to bad training examples [126]. This ultimately results in the following weight adjustment:

$$w_{j,k \text{ new}} = w_{j,k} - \alpha \times \frac{\partial E}{\partial w_{j,k}}. \quad (11)$$

Thus, for a learning rate of, for example, 0.1, adjusting the weighting $w_{1,1}$ according to equation (11) leads to:

$$w_{1,1 \text{ new}} = 0.7 - 0.1 \times (-0.059) = 0.7059. \quad (11)$$

The individual weight changes are relatively small, but over hundreds of iterations, stable weight configurations eventually result, producing a well-trained neural network that generates output signals that match the training examples and predict accordingly realistic outputs even for new data without available training examples.

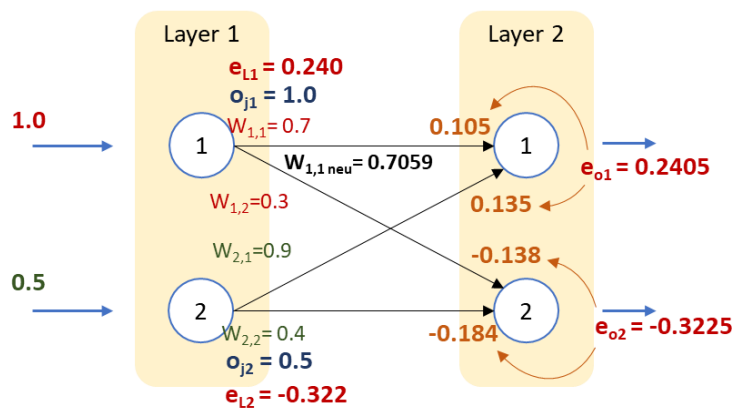


Figure B-6: Back propagation with calculation of error increase and weight adjustment based on the calculation example.

Statutory declaration

I declare that I have written this dissertation on my own and that I have not used any auxiliary materials other than those indicated. I have marked all passages taken over verbatim or in terms of content as such. I assure that the submitted dissertation has not been submitted to any other examination authority.

Waren (Müritz), 31 August 2023

Erik Westphal

Scientific publications

List of scientific publications

- 2023 **Westphal, Erik;** Leiding, Benjamin; Seitz, Hermann (2023):
Blockchain-based quality management for a digital additive
manufacturing part record. *Industrial Information Integration*
35.
DOI: 10.1016/j.jii.2023.100517 (IF 2023: 15,7)
- 2022 **Westphal, Erik & Seitz, Hermann** (2022):
Machine learning for the intelligent analysis of 3D printing
conditions using environmental sensor data to support quality
assurance. *Additive Manufacturing* 50.
DOI: 10.1016/j.addma.2021.102535 (IF 2022: 11,6)
- 2021 Krüsemann, Horst; Töllner, Philip; **Westphal, Erik;** Hofrich-
ter, Jaqueline; Seitz, Hermann (2021):
Design and 3D printing of miniaturized dialyzers for laboratory
use. *Trans. AMMM*, Vol 3, No 1, 2021.
DOI: 10.18416/AMMM.2021.2109545 (IF 2021: N/A)
- 2021 **Westphal, Erik & Seitz, Hermann** (2021):
Digital and Decentralized Management of Patient Data in
Healthcare Using Blockchain Implementations. *Frontiers in*
Blockchain 4.
DOI: 10.3389/fbloc.2021.732112 (IF 2021: 3,1)
- 2021 **Westphal, Erik & Seitz, Hermann** (2021):
A machine learning method for defect detection and visualiza-
tion in selective laser sintering based on convolutional neural
networks. *Additive Manufacturing* 41.
DOI: 10.1016/j.addma.2021.101965 (IF 2021: 10,9)
- 2020 **Westphal, Erik;** Mau, Robert; Dreier, Tim; Seitz, Hermann
(2020):
3D printing of frames for anti-coronavirus face shields using
different processes and materials. *Trans. AMMM*, Vol 2, No 1,
2020.
DOI: 10.18416/AMMM.2020.2009008 (IF 2020: N/A)

Conference contributions

- 2023 **Westphal, Erik;** Seitz, Hermann (2023):
Non-destructive defect detection in additive manufacturing using machine learning and image classification (Lecture).
1st Conference on Artificial Intelligence in Materials Science and Engineering (AI MSE), Saarbrücken, Germany.
- 2021 Krüsemann, Horst; Töllner, Philip; **Westphal, Erik;** Hofrichter, Jacqueline; Seitz, Hermann (2021):
Design and 3D printing of miniaturized dialyzers for laboratory use (Paper). *Additive Manufacturing Meets Medicine 3 (AMMM)*, Lubeck (virtual), Germany.
<https://doi.org/10.18416/AMMM.2021.2109545>
- 2020 **Westphal, Erik;** Mau, Robert; Dreier, Tim; Seitz, Hermann (2020):
3D printing of frames for anti-coronavirus face shields using different processes and materials (Lecture and Paper). *Additive Manufacturing Meets Medicine 2 (AMMM)*, Lubeck (virtual), Germany. <https://doi.org/10.18416/AMMM.2020.2009008>

List of Appended Publications

Publication [I]

E. Westphal & H. Seitz, A machine learning method for defect detection and visualization in selective laser sintering based on convolutional neural networks. In *Additive Manufacturing* 41 (2021), <https://doi.org/10.1016/j.addma.2021.101965>

E. Westphal & H. Seitz, Corrigendum to: “A machine learning method for defect detection and visualization in selective laser sintering based on convolutional neural networks. *Additive Manufacturing* 41 (2023), <https://doi.org/10.1016/j.addma.2023.103739>

Publication [II]

E. Westphal & H. Seitz, Machine learning for the intelligent analysis of 3D printing conditions using environmental sensor data to support quality assurance. In *Additive Manufacturing* 50 (2022), <https://doi.org/10.1016/j.addma.2021.102535>

Publication [III]

E. Westphal; B. Leiding; H. Seitz, Blockchain-based quality management for a digital additive manufacturing part record. In *Industrial Information Integration* 35 (2023), <https://doi.org/10.1016/j.jii.2023.100517>

Author's Contribution to the Publications

Publication [I]

The idea of the paper was developed and conceptualized by Westphal. Westphal also performed the data collection and data analysis as well as the methodology, programming and writing (Seitz supervised the process, assisted with the methodology, and contributed to the writing and review).

Publication [II]

The idea of the paper was developed and conceptualized by Westphal. Westphal also performed the data collection and data analysis as well as the methodology, programming and writing (Seitz supervised the process, assisted with the methodology, and contributed to the writing and review).

Publication [III]

The idea of the paper was developed and conceptualized by Westphal. Westphal also performed the data collection and data analysis as well as the methodology, programming and writing (Seitz supervised the process, assisted with the methodology, and contributed to the writing and review; Leiding also assisted with the methodology, and contributed to the writing and review).

Author's publications not appended to the thesis

E. Westphal & H. Seitz, Digital and Decentralized Management of Patient Data in Healthcare Using Blockchain Implementations. In *Frontiers in Blockchain 4 (2021)*, <https://doi.org/10.3389/fbloc.2021.732112>

H. Krüsemann; P. Töllner; **E. Westphal**; J. Hofrichter; H. Seitz, Design and 3D printing of miniaturized dialyzers for laboratory use. In *Trans. AMMM, Vol 3, No 1 (2021)*, <https://doi.org/10.18416/AMMM.2021.2109545>

E. Westphal; R. Mau; T. Dreier; H. Seitz, 3D printing of frames for anti-coronavirus face shields using different processes and materials. In *Trans. AMMM, Vol 2, No 1 (2020)*, <https://doi.org/10.18416/AMMM.2020.2009008>

Publications

Original work for the cumulative dissertation

Publication [I]

E. Westphal & H. Seitz, A machine learning method for defect detection and visualization in selective laser sintering based on convolutional neural networks

E. Westphal & H. Seitz, Corrigendum to: “A machine learning method for defect detection and visualization in selective laser sintering based on convolutional neural networks



Research Paper

A machine learning method for defect detection and visualization in selective laser sintering based on convolutional neural networks

Erik Westphal^{a,*}, Hermann Seitz^{a,b}

^a Chair of Microfluidics, University of Rostock, 18059 Rostock, Germany

^b Dept. Life, Light & Matter, University of Rostock, 18059 Rostock, Germany

ARTICLE INFO

Keywords:

Additive manufacturing
Selective laser sintering
Process monitoring
Machine learning
Convolutional neural network

ABSTRACT

Part defects and irregularities that influence the part quality is an especially large problem in additive manufacturing (AM) processes such as selective laser sintering (SLS). Destructive and non-destructive testing procedures are currently mostly used for quality control and defect detection of AM parts after production. In this context, machine learning (ML) algorithms are increasingly being used to enable computer-aided defect detection through automatic classification of manufacturing data. Convolutional neural networks (CNN) based on ML methods are widely used for this task. In this paper, complex transfer learning (TL) methods are presented, which enable the automatic classification of powder bed defects in the SLS process using very small datasets. The proposed methods use the VGG16 and the Xception CNN model with pretrained weights from the ImageNet dataset as initialization and an adapted classifier to classify good and defective image data recorded during part manufacturing. Known performance metrics were determined to evaluate and compare the performance of the models. The VGG16 model architecture achieved the best results for Accuracy (0.958), Precision (0.939), Recall (0.980), F1-Score (0.959) and AUC value (0.982). These results show the effectiveness of defect detection based on CNN and can offer an alternative method for non-destructive quality assurance and manufacturing documentation for additively manufactured parts.

1. Introduction

As one of the most popular additive manufacturing (AM) processes, selective laser sintering (SLS) is well suited for the production of individual, complex and topology-optimized parts for various industrial sectors. With the SLS process, powder particles are locally fused using a heat source (e. g. a laser). The laser sintering of a defined contour and the layer wise repetition of the sintering process then create a three-dimensional (3D) part.

The SLS process usually processes polyamides (PA) such as PA 11 and PA 12, polystyrene (PS), thermoplastic elastomers (TPE), polypropylene (PP) and certain polycarbonates (PC) or variations thereof [1]. The connection of the individual powder particles to one another takes place through thermal influence, fusion and subsequent solidification of the material. This process leads to high-quality part properties of the laser sintered structures that meet the requirements for functional components. According to Schmid [2], there are increased requirements inter alia for:

- a reproducible quality,
- process security and
- the automation of production processes.

In order to establish itself as a serious production process, quality controls and quality management must be developed, implemented and optimized for the entire SLS process chain in order to be able to compare the manufacturing process with other production techniques in terms of quality standards [2]. The quality of the parts manufactured by means of SLS is not only determined by the fusion of the powder particles of successive layers, but also by the integrity of the powder bed and the stability of the powder application [3]. A uniformly distributed powder bed, without irregularities, is desirable for a good part quality, see for example Fig. 1(a) and (c). However, various irregularities such as foreign bodies, part edges, powder accumulations and powder trenches, collectively referred to as powder bed defects, can occur in the powder bed, as shown in Fig. 1(b) and (d). These powder bed defects can lead to deficiencies in the part quality and the part properties up to quality-related rejects of the parts, which in turn results in considerable

* Corresponding author.

E-mail addresses: erik.westphal@uni-rostock.de (E. Westphal), hermann.seitz@uni-rostock.de (H. Seitz).

<https://doi.org/10.1016/j.addma.2021.101965>

Received 30 November 2020; Received in revised form 19 February 2021; Accepted 17 March 2021

Available online 22 March 2021

2214-8604/© 2021 The Author(s). Published by Elsevier B.V. This is an open access article under the CC BY license (<http://creativecommons.org/licenses/by/4.0/>).

additional costs, material waste and ties up machine capacity [3]. This affects according to Xiao et al. [3] the widespread application of SLS as a profitable production technique in which constant quality, reproducibility and cost as well as waste reduction are critical. By detecting powder bed defects as early as possible during the production process, corrective measures can be initiated immediately, thereby ensuring quality as well as the reduction of costs, waste and capacity utilization [3].

The approach of the work presented here is to monitor the SLS powder bed for signs of defects using machine learning (ML) methods. For these complex methods, the recording of large amounts of image data is necessary, since a ML algorithm is trained using this data instead of being explicitly programmed [4]. ML methods are then a possibility to evaluate this amount of data almost in real time and to identify complex non-linear relationships in the datasets [5]. Conventional ML techniques are, according to Baumgartl et al. [5], divided into the three categories of supervised, semi-supervised and unsupervised learning.

These conventional ML techniques are only able to process unstructured data in its raw form (for example images, natural language etc.) to a limited extent [6]. Using modern state-of-the-art ML algorithms based on deep learning (DL), such raw data can also be processed and features extracted from it automatically [6,7]. For this process, convolutional neural networks (CNN) are almost always used in DL, because they are very effective in discovering complex structures in large amounts of data and can process unstructured data such as color images [4,6]. However, the key aspect of DL is, according to LeCun et al. [6] that a functional extractor is not designed by human developers, but is learned from data using a general learning process.

In this work complex ML algorithms based on deep learning and CNN were implemented. Process images were recorded as raw data during selective laser sintering using an inexpensive camera setup and pre-processed in a defined manner. The image data were then used to train two different CNN architectures for the classification of powder bed defects and thus to develop an automatic method for process assessment and documentation. Established evaluation metrics such as accuracy, precision, sensitivity and F1-Score were used to assess the performance of the CNN models. In addition, metrics such as the receiver operator characteristic (ROC) curve as well as the area under the curve (AUC) and heat maps were used to evaluate and visualize the results of the ML models.

2. Related work

ML methods have already been used in various AM processes and different AM procedures for error detection. Xiao et al. [3] have developed a CNN for the detection of three different types of powder bed defects during selective laser sintering. For this purpose, images of the powder bed were recorded with a digital camera and analyzed using a two-stage CNN. In the first module of the CNN, the location of the defect

was identified and in the second module, error masks were generated for each specific location of the error. Compared to other methods, the accuracy of the error detection has been significantly improved by using the two-stage CNN model. However, the datasets have also been especially preconfigured to a considerable extent in order to simulate special error cases. Detailed statements on the accuracy of the two-stage CNN with real manufacturing datasets are not given.

Scime and Beuth [8] used grayscale areas from images of an integrated camera of a laser powder bed fusion (LPBF) machine to differentiate between metal-based powder bed irregularity classes. The classes were subsequently used to develop an ML algorithm for in-situ process monitoring and to analyze powder bed images. The algorithm described works in principle for the LPBF process, but has to be improved with regard to the classification accuracy.

Gobert et al. [9] used a high resolution digital single-lens reflex camera for layer-by-layer imaging in order to record images for a supervised learning of defects during a metal powder bed fusion (PBF) process. CT scans were then used to assess the results of ML detection. The resulting accuracies of the error detection algorithms during the manufacturing process reached values of up to 85%, but refer exclusively to the metal PBF process. In addition, a linear support vector machine (SVM) algorithm was used for error detection instead of a CNN.

Baumgartl et al. [5] used a combination of thermographic and off-axis in-situ imaging in a LPBF system. The images served as a data source for a DL-based CNN to identify printing errors. The model is well suited for thermographic in-situ defect detection in LPBF processes and achieves accuracies of over 96%. However, this CNN model can only detect spatter and delamination defects in metal LPBF. Other types of defects such as cracks, pores and unmelted powder, as well as additional processes such as SLS were not investigated.

In the review by Yadav et al. [10], further methods for automated in-situ process error monitoring and detection were listed and examined with regard to current progress in the field of process data analysis. Furthermore, the working principles of the most common in-situ sensor systems and commercially available in-situ monitoring solutions for metal LPBF systems were considered. The review article shows that the in-situ process recording is still at an early stage. Much of the research carried out actually focuses on the metal LPBF and the development of in-situ sensor systems to better understand this process. Detailed investigations into other PBF processes such as selective laser sintering with plastics as well as investigations for error detection in real time for both the SLS and the LPBF process still have to be investigated.

3. Materials and methods

In this section, the experimental setup used in this research is first described in detail. After that the dataset used in this paper is discussed. Thereby the generation, extraction and preprocessing of the data is described as well as some performance indicators used for the

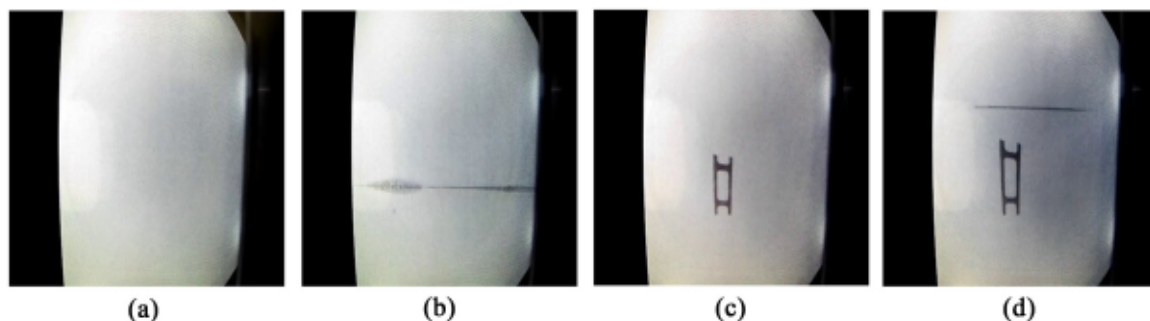


Fig. 1. Image examples from the dataset of a SLS print job with: (a) a powder bed without sintered elements and irregularities; (b) a powder bed without sintered elements with irregularities; (c) a powder bed with a sintered element without irregularities and (d) a powder bed with a sintered element and irregularities. Original images are available in a public repository (<https://doi.org/10.17632/2yzjmp52fw.1>). (The DOI of the dataset is reserved, but not active).

classification task plus evaluation and visualization techniques. Furthermore, CNN architectures are presented and the approaches and architectures used for this work are considered.

3.1. Experimental setup

The SLS process was monitored in real time with a high-resolution camera and recorded using a simple setup consisting of a high definition (HD) Universal Series Bus (USB) webcam and a single-board computer in order to obtain image data of the powder bed. An S2 laser sintering system (Sintratec AG, Brugg, Switzerland) was used for selective laser sintering. The laser sintering system has a 10 W diode laser with a laser wavelength of 1064 nm and a round powder bed shape with an effective printing area of 130 mm in circumference and a maximum build height of 360 mm. The build chamber can be heated up to 180 °C and does not require any operating gas during the entire printing process. The material used for printing is PA 12, which was printed with a layer thickness of 100 μm. The laser spot size was 145 μm and the scan speed 3 m/s.

The setup for recording the image data consisted of a simple Plusonic HD USB webcam (Allnet GmbH, Gemering, Germany) with a resolution of 3 megapixels and a 3.6 mm focal lens as well as a Raspberry Pi 3B (OKdo Technology Limited, London, UK). A 128 GB 3.0 Ultra USB stick (SanDisk Corp., Milpitas, US) was used to store the data and a 5.1 V with 2.5 A power adapter unit (TT Electronics IoT Solutions Ltd., Woking, UK) was used for the power supply. In addition, a 7-inch Raspberry Pi touchscreen (OKdo Technology Limited, London, UK) was used for operational control and a standard camera tripod for positioning of the webcam. The camera was then mounted on the tripod and positioned as well as focused in front of the machine display of the laser sintering system. The high-resolution camera built into the S2 system was used to monitor the powder bed directly from above in real time and a live stream was shown on the system display, which in turn was recorded via the webcam. The recordings were made with a resolution of 640 × 480 pixels (px), whereby the recorded build area had physical dimensions of approx. 250 × 150 mm. The recordings were processed with self-written python programs. The open source programming language python, version 3.7.9 (python software foundation, Fredericksburg, US) was used for programming.

3.2. SLS powder bed dataset

The dataset used in this work was extracted from video recordings of the powder bed surface, which were recorded on an SLS printing system with a frame rate of two frames per second during manufacturing. In order to obtain individual images of the powder bed surface, the recorded Matroska (MKV) video files were broken down into individual frames without video compression and with a resolution of 640 × 480 px. Every 20th frame has been saved as a JPEG image and compressed or cropped to a size of 300 × 300 px to remove unnecessary information and image areas such as time stamps and image resolution specifications.

The dataset generated in this way comprised 9426 powder bed images. Extraneous images were then initially removed from the dataset (e.g. images with recording anomalies, images where the powder distribution unit of the system was also recorded, images with unfavorable light reflections). The remaining images were then manually divided into two different classes, OK and DEF, using process knowledge and additive expertise. Both classes together result in the adapted dataset with 8514 images. All images that showed a uniform powder bed surface without defects were classified into the OK class. This class contained 7808 images. All images on which an uneven powder bed surface with defects (cracks, ditches, foreign bodies etc.) could be seen were classified into the DEF class. As a result, 706 images were divided into the DEF class.

The dataset can be downloaded from the following address under a

creative commons attribution 4.0 international license: <https://doi.org/10.17632/2yzjmp52fw.1>.

3.2.1. Class imbalance problem

In a binary classification problem with data from two classes, a class imbalance occurs when one class contains significantly fewer samples (minority class) than the other class (majority class) [11,12]. In the dataset used here, the two classes OK and DEF also have a different number of images. The imbalance ratio (IR) of the dataset can be calculated as follows:

$$\text{IR} = \frac{\text{Number of majority class samples}}{\text{Number of minority class samples}} \quad (1)$$

Liu et al. [13] examined various datasets related to the IR. The IR ranges from 1.7 to 24.3 and can, according to Wu et al. [14] also achieve values such as 10^6 . The IR of this SLS powder bed dataset is:

$$\text{IR} = \frac{\text{Number of OK class samples}}{\text{Number of DEF class samples}} \quad (2)$$

Compared to the considered datasets examined by Liu et al. [13], an IR of 11.06 is not uncommon, but it is already one of the more imbalanced datasets.

This data imbalance must always be considered in intelligent classification algorithms. When evaluating the classification results, standard metrics such as accuracy and error rate are used most often, but these are unsuitable for class imbalances since the result is dominated by the majority class [11,12]. In this way, a data distribution of 1% positive examples to 99% negative examples, the accuracy of a classification can be 99%, in that the classifier simply evaluates all examples as negative. Because of this, special metrics are required to evaluate imbalanced classification tasks. In addition, there are also various techniques that can be used to deal with imbalanced problems. These are described in detail in Section 3.2.2 below.

3.2.2. Techniques for class imbalanced data

The imbalance between two classes can be reduced by changing the data imbalance or by changing the underlying learning and decision-making process of the model to increase sensitivity to the minority class [11]. According to Johnson and Khoshgoftaar [11], the methods for dealing with class imbalances can accordingly be divided into techniques at the data level, methods at the algorithm level and hybrid approaches.

Data level techniques include oversampling, undersampling and modifying the data distributions to compensate for the level of imbalance [11]. The simplest forms of these methods are random undersampling (RUS), in which data is randomly removed from the majority class and random oversampling (ROS), in which data from the minority class is randomly duplicated [15]. In previous experiments it was found that RUS led to good results overall and often exceeded ROS [11]. Methods at the algorithm level do not change the data distribution. Instead, according to Johnson and Khoshgoftaar [11], either the learning process is adapted so that the importance of the minority class increases, or the decision threshold is shifted so that the tendency towards the majority class is reduced. Hybrid approaches combine data and algorithm methods in different ways. For example, one approach involves first data sampling to reduce the imbalance and then applying a shift in the decision threshold to reduce the influence of the majority class [11].

In this work a combination of RUS and ROS method was used. RUS was used to randomly remove data from the OK class and ROS to randomly duplicate data from the DEF class. As a result, 5808 images were removed from the OK class and 1294 images were added to the DEF class by duplicating the existing image data, thus balancing the OK and DEF classes. The dataset ultimately used for this work thus contains a total of 4000 images.

3.2.3. Image preprocessing and data structure

The images of the SLS powder bed dataset were created using a simple preprocessing procedure according to Pasa et al. [16] processed further, in order to obtain only the especially interesting image area with as much relevant information as possible. The preprocessing steps performed here are as follows:

- Remove any black stripes from the edges of the images.
- Resize the image so that the smaller edge (in this case) is 180 px long.
- Extraction of a centered square image area of 180×180 px.

These steps were carried out automatically by a simple, self-programmed python script. An example of the preprocessing procedure and a preprocessed image is shown in Fig. 2. With this procedure, an attempt was made to use only relevant information in the image and to only supply the CNN with pixels of interest (preferably no black borders, since no useful information for the intended classification task can be extracted from it and the calculation times take longer). It should be noted here that the square printing area (or the usable powder bed) of the laser sintering system is displayed vertically distorted as a result of the image recording (Fig. 2(a), red dashed border) and therefore could not be completely covered by a square image area (Fig. 2(a), blue border) without including undesired black border areas in the image recording. It is important to understand that square images are more beneficial for the ML model architectures. Fig. 2(b) thus shows an optimized square image of the powder bed printing area of the laser sintering system.

The dataset balanced with the RUS and ROS methods consists of 4000 images, which are automatically divided into 2000 different OK and 2000 partially different and partially duplicated DEF images using a simple, self-programmed python script. The data structure of this dataset was further subdivided according to [17] by creating three subgroups, each with separate directories for both classes: a training dataset with 1000 automatically selected images in each class, a validation dataset with 500 images in each class and a test dataset with also 500 images in each class. The 500 OK images each for the validation and test dataset were again randomly and automatically selected by a self-programmed python script from the 2000 OK images and moved to the appropriate directory. A slightly different method was used for the 500 DEF images of the validation and test dataset, as it must be ensured that no image appears twice in the individual subgroups and sub-directories, otherwise the results of the classification could be distorted. For this reason, the original 706 individual DEF images were randomly and automatically divided by a python script and accordingly 306

images were assigned to the DEF directory of the training dataset and 200 DEF images each to the DEF directories of the validation and test dataset. Another python script randomly selected DEF images in the respective DEF directories were then automatically copied until the directories contained the defined size of 1000 DEF training images and 500 DEF validation and test images each. Fig. 3 shows a general flow chart for creating the data structure described.

The preprocessed image data from the individual subgroups and directories of the dataset were then checked again manually for correct assignment. Incorrectly assigned images (which were overlooked during the initial assignment or for which a classification was unclear) were removed manually and replaced with other images that were randomly selected by an additional python script according to the respective directory.

3.2.4. Data augmentation and hyperparameter tuning

Data augmentation was carried out as a regulatory mechanism in order to avoid an immediate overfitting of the model to the training data. This would have a negative impact on the model performance on newly viewed data. With data augmentation, various operations are performed on the training dataset in real time. These operations are:

- Rescaling factor of $1/255$ for normalizing the image data
- Horizontal flip of the images
- Zoom range of image area 0.15
- Width shift 0.20
- Height shift 0.20
- Shear rate 0.15
- Fill mode "nearest"
- Random image rotation of ± 20 degrees

The principles and operations of data augmentation are described in detail by Shorten and Khoshgoftaar [18] and also in the Keras library [19]. In addition to the preprocessing of the image data and data augmentation, the settings of the hyperparameters were an essential part of training the CNN models. The best model for classification of the powder bed images was only achieved after various iterations and configurations of the hyperparameters. The hyperparameters of the CNN models used in this work are listed in Table 1 and are explained in detail by Hutter et al. [20].

3.3. Convolutional neural network

Classic ML approaches to image recognition consist of two separate

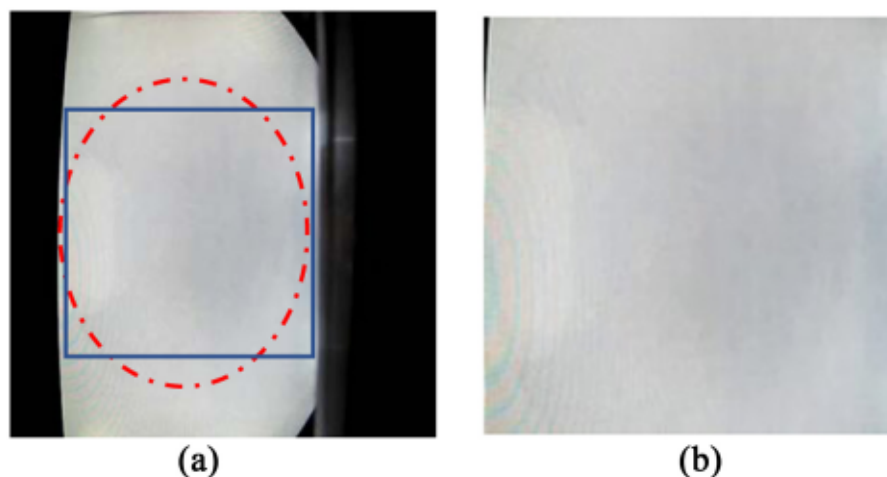


Fig. 2. Preprocessing steps that were applied to all images of the powder bed dataset. (a) The previously cropped powder bed image of the size 300×300 px with schematically shown printing area (red) and a maximum relevant square image area (blue); (b) the final image with the maximum square dimensions of 180×180 px. (For interpretation of the references to colour in this figure legend, the reader is referred to the web version of this article.)

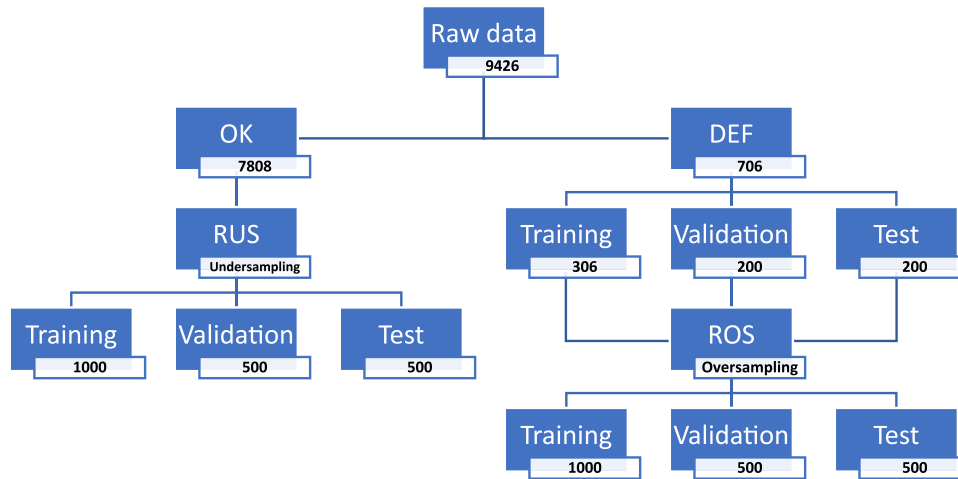


Fig. 3. General procedure for creating the data structure described from the powder bed dataset.

Table 1
CNN hyperparameters.

Cost function	Learning rate (Lr)	Optimizer	No. Epochs	Batch size	Lr decay	Early stopping
Binary cross entropy	1 10 ⁻³	Adam 1 0.9 2 0.999	30	64	patience 5	patience 20

steps [4,6]. In the first step, in what is known as feature engineering, an attempt is made to extract relevant data structures from the raw image data using various algorithms. In the second step, what is known as classification, an ML algorithm then attempts to learn a pattern that can map the data structures and a target variable. However, these patterns must have previously been extracted during feature engineering for learning. This approach often leads to unsatisfactory classification results [6].

For this reason, CNN have been widely used in recent years to solve various complex computer vision problems [16,21,22]. These modern ML architectures are also used specifically to monitor and classify certain additive manufacturing processes [3,5,8,9]. CNN are based on the complex structures of real human brain structures of the visual cortex and are one of the latest methods of DL in the field of image recognition [5,6,23]. According to Baumgartl et al. [5], the fundamental difference between a CNN and a classic ML approach lies in the combination of feature engineering and classification.

3.3.1. Transfer learning

The training of a CNN model from scratch requires a lot of data to get a good predictive model [21]. However, often insufficient data is available, which requires complex techniques that can produce acceptable prediction results with less data. Transfer learning (TF) offers such a technique. In the case of TF, the features of an already trained CNN model are used as initialization for training the CNN used for the actual classification. According to Tsiakmaki et al. [24], it is an effective ML method to use a CNN model that was previously trained on a very large dataset and the features generated in this way as an initialization for a new CNN model on a much smaller dataset and reuse it with a different purpose. This method is often informative, even if the new classification task is significantly different from the one for which the original model was trained.

There are two methods of using TL [4]. On the one hand, you can use a previously trained CNN model as a feature extractor for a completely different classifier. On the other hand, you can partially use the model again and carry out what is commonly known as a fine-tuning (FT). For this purpose, the top layers of the previously trained CNN model are trained again and optimized in order to better adapt the features generated there to the new dataset.

3.3.2. CNN architectures used in this work

As previously mentioned, a common and very effective approach for DL with small image datasets is to use a pretrained network. In this work two different CNN models are used for feature extraction and the results are compared. For this purpose, both networks are instantiated with pretrained weights and implemented with a new classifier. Before training the CNN models with the powder bed data, the individual layers of the models are frozen or defined as non-trainable so that the pretrained weights are not updated again during the new training cycle and thus destroy the previously learned features. With this setting, only the weights from the layers of the new classifier that were added to the CNN models are trained. After the training run, the networks are fine-tuned. For this purpose, individual layers of the respective network are again defined as trainable and used for feature extraction. These layers are then trained again together with the classifier. This re-uses the previously pretrained features of the CNN models to make them more relevant to the new problem. Thus, in such an approach, this investigation enables a better classification of SLS powder bed images. The CNN model architectures presented below enable a production-integrated method for the continuous detection of defects in recorded powder bed images during selective laser sintering and for classification into good and bad production images. The information generated in this way can then contribute to the assessment of the manufactured part quality. Both CNN models first analyse manually preselected image data using special computational operations and learn layer by layer possibly interesting image features. These learned features are then used to evaluate unknown images and thus enable automatic, intelligent image classification.

A CNN model that is used here for feature extraction is the VGG16 architecture, which was developed by Simonyan and Zisserman [25] in 2014. It is a simple and widespread CNN architecture, but which, in principle, no longer corresponds to the current state of the art. A more modern, state-of-the-art CNN architecture, which was also used here as a comparison, is the Xception model designed by Chollet in 2016 [25]. Some important details of the pretrained CNN models that are used with the additional classifier inserted over both architectures are explained below.

The VGG16 architecture is a pretrained CNN from the Visual Geometry Group (VGG) at Oxford University. The model was developed to

significantly increase the depth of the existing CNN architectures and uses 16 network layers for object recognition [25,26]. According to Simonyan and Zisserman [25], 224×224 px RGB images are provided as input, which are then passed through a block of convolution layers with a very small filter size (matrix) of 3×3 and a convolution step of 1 px. After the respective convolution layers, five Max-Pooling layers with a 2×2 px window and a convolution step of 2 px are embedded in order to compress the spatial representation of the input data [25]. The convolutional layer blocks are followed by three fully connected layers, of which the first two each have 4096 channels and the third is used for classification and has 1000 channels for 1000 different classes. A softmax layer followed as the last layer. Fig. 4 shows the structure of the VGG16 network architecture.

Based on the VGG16 architecture, the Xception CNN architecture was developed, which is schematically similar in some areas. Xception is based entirely on the approach of the depthwise separable convolution (DWSC) layers [23]. This is a more up-to-date approach than the previously frequently used separable convolutions, which were described by Mamalet and Garcia [27] in 2012. Sifre [28] developed depthwise separable convolutions in 2013 at Google Inc. and listed detailed experimental results in his doctoral thesis. The DWSC therefore not only deals with the spatial dimensions in neural networks, but also with the depth or the number of color channels of an input [28].

The Xception architecture consists of 36 convolution layers that enable feature extraction. These layers are structured in 14 modules (one module is repeated eight times), all of which, except for the first and the last module, have linear direct connections to one another. The DWSC is a spatial convolution that is executed independently of one another in parallel via each input channel and is followed by a point-by-point 1×1 convolution that projects the output of the channel onto a new channel [23]. According to Chollet [23], this results in deeper models that are extremely efficient. Another advantage of this network architecture is that fewer operations are performed, which means that the computational costs of the model is lower. The Xception model has many more parameters compared to the VGG16 network, but is usually more efficient and faster [23]. The general structure of the Xception CNN architecture is shown in Fig. 5.

Both the VGG16 and the Xception architectures are first instantiated with pretrained weights from the ImageNet dataset. This dataset is a very large benchmark dataset for the detection of objects [29,30]. The respective classification layers of the two models are not loaded in order to enable an efficient feature extraction. A new classifier is implemented for this purpose. Furthermore, the layers of the CNN models are frozen or made untrainable to prevent the pretrained weights from being updated. The new classifier is then trained with the powder bed image data. After this first training run, defined layers of the CNN models are made trainable again and used together with the classifier for fine-tuning and retraining. The classifier is identical for all investigations in this work and consists of a fully connected layer with 1000 channels, a dropout layer with a retention rate of 0.25 and a batch normalization operation. Finally, another fully connected layer with only one channel and a sigmoid activation function was provided to

predict the probability of the classes or to perform the binary classification between the OK and DEF classes. Fig. 6 shows a flow chart of the entire TL process.

All calculations were carried out on a local workstation computer, which provides a Windows environment with 32 GB RAM and a GPU Nvidia GeForce RTX 2080 Ti with 11 GDDR6 VRAM.

3.4. Experimental test execution

After video files of the SLS process were recorded, broken into individual frames and cropped, the resulting dataset was cleaned up and the imbalance problem between the two classes was fixed using different techniques. The processed images were then divided into a defined data structure and checked again with regard to their correct classification.

After these steps, the VGG16 and the Xception CNN model were implemented using the Python programming language in the deep learning framework TensorFlow [31], which provides an interface for programming ML algorithms and an implementation for executing them. TensorFlow also includes a data preprocessing tool that is applied to the training and validation groups. After preprocessing the data, the respective network and an additional classifier were trained on the data and then optimized by fine-tuning. These optimized model variants were in turn used to classify the test data and compared with suitable evaluation metrics and visualization methods. Lastly, heat maps were generated to locate the defects in the powder bed images using the Grad-CAM process. The experimental procedure and the proposed methodology can be summarized as follows:

1. Recording and preprocessing of SLS image data.
2. Implementation of the CNN models in TensorFlow.
3. Train the respective architecture with the training and validation data.
4. Fine-tuning of the top network layers to improve performance.
5. Enter test data into the trained network to obtain classification results.
6. Evaluation and comparison of the classification results of the networks.
7. Use Grad-CAM to create a heatmap to point to possible defect locations in the test image data.

3.5. Performance measures

At a classification task, the results can be presented and summarized in the form of a special matrix, the confusion matrix (CM) [11]. This CM is shown in Table 2 as an example. In the case of a binary classification, the CM contains the following information:

- Number of examples that are predicted to be recognized as true positive (TP)
- Number of examples that are predicted to be recognized as true negative (TN)

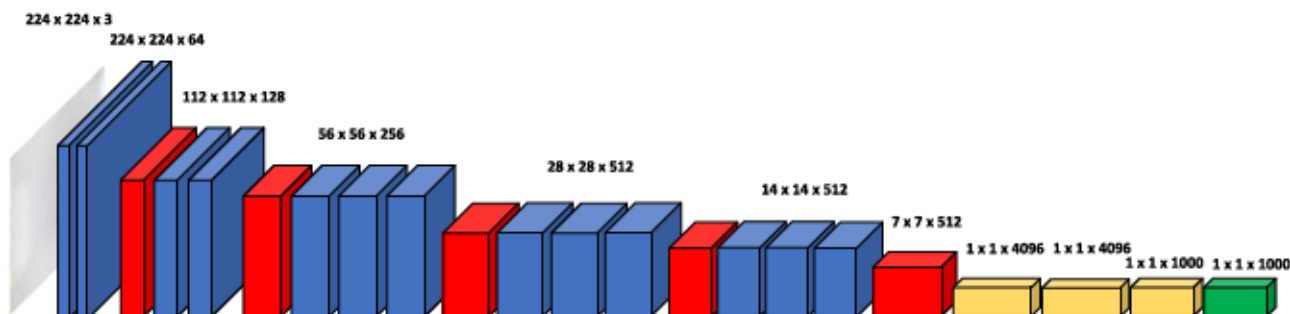


Fig. 4. VGG16 CNN model for the detection and classification of powder bed defects at the SLS.

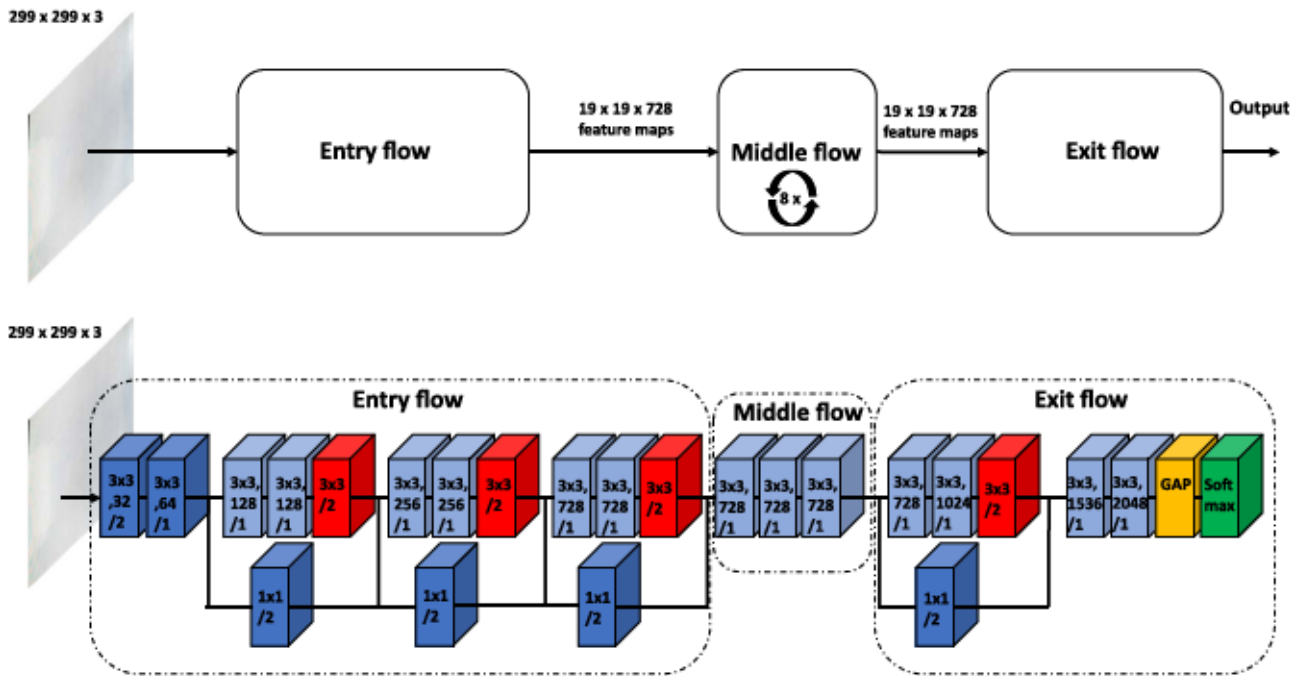


Fig. 5. Xception CNN architecture for the detection and classification of powder bed defects at the SLS. (a) Shows the general structure of the Xception model; (b) shows the detailed architecture of the original Xception model. A batch normalization operation is performed after each convolution and each spatial convolution block. Each block is numbered, the first being the kernel size, the second being the number of filters in the particular block, and the last being the size of the convolution step.

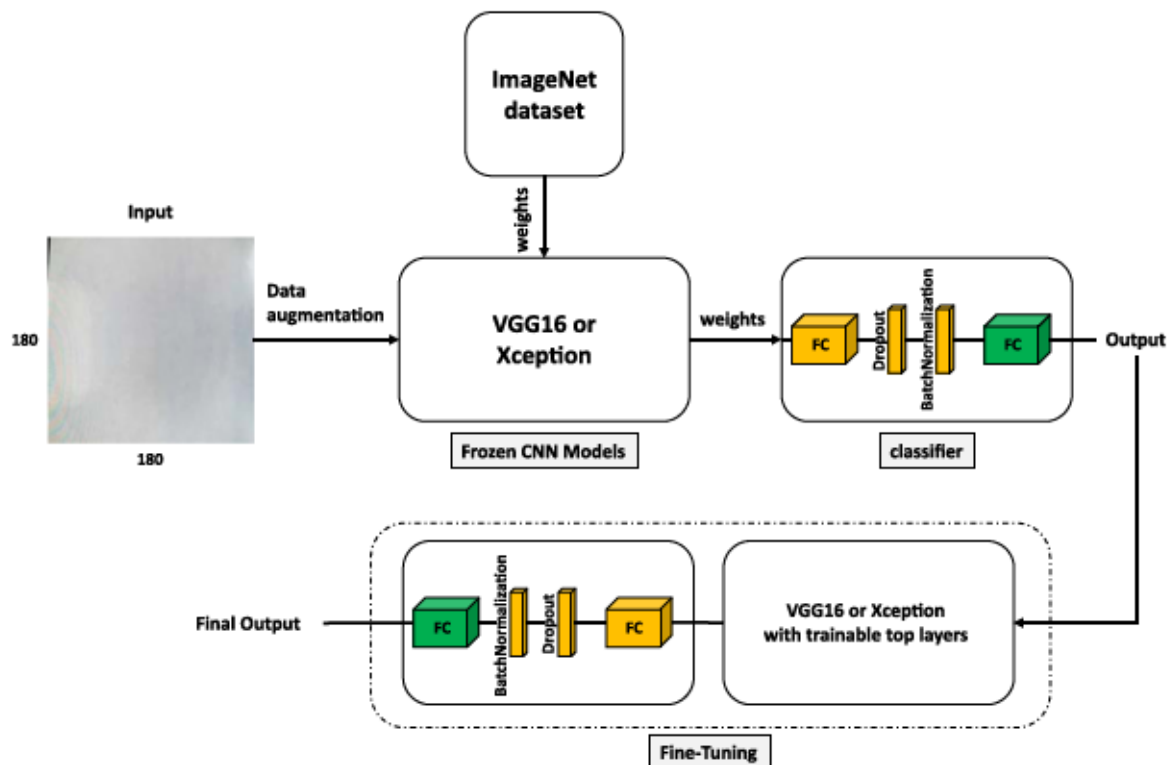


Fig. 6. Flow chart of the TF with the powder bed data.

- Number of examples that are predicted to be recognized as false positives (FP)
- Number of examples that are predicted to be recognized as false negative (FN)

Further metrics for evaluating the performance of a CNN model can then be derived from this CM. The accuracy is the most frequently used metric for binary classification and evaluates the overall effectiveness of a classifier or indicates the proportion of correct predictions. The accuracy is further explained and defined by Johnson and Khoshgoftaar

Table 2
Confusion matrix according to Johnson and Khoshgoftaar [11].

	Actual positive	Actual negative
Predicted positive	True positive (TP)	False positive (FP)
Predicted negative	False negative (FN)	True negative (TN)

[11] as well as by Branco et al. [32]. Especially when working with an imbalanced dataset (but also for balanced datasets), other metrics are often used to evaluate performance. The most frequently used are then precision, recall (formally also referred to as sensitivity) and the F1-Score [11,32].

A graph such as the ROC curve and the associated AUC measure are other useful metrics for evaluating and visualizing the performance of a CNN model in the case of imbalanced data [32,33]. The ROC curve is a graphic representation of the true positive rate (TPR) against the false positive rate (FPR) for all possible prediction thresholds. In other words, it visualizes the trade-off between correctly classified positive examples and misclassified negative examples. The terms used for the ROC curve and the AUC value are defined and further explained by Johnson and Khoshgoftaar and Branco et al. [11,32]. ROC curves, in and of themselves, do not offer a comparable performance indicator [32]. A corresponding value is determined by the AUC. The AUC value is a summarizing performance measure for all possible prediction threshold values and is, according to Branco et al. [32], often used to compare performance between different models.

In most cases, accuracy and loss or respectively cost functions are also recorded to evaluate the performance of the DL [19]. The accuracy graph shows the performance of a classification as a percentage. The loss graph considers the uncertainties of a forecast based on how much it deviates from the actual value. There are several loss functions, not expressed as a percentage, that represent the sum of the errors made for each data item in training or validation sets. This value should always be minimized during training. Both diagrams thus characterize the training process and provide initial information about the effectiveness of the selected hyperparameters and how they should be changed for more efficient training. A commonly used loss function is cross-entropy loss, and especially for binary classification tasks (such as the classification of OK and DEF SLS powder bed images), binary cross-entropy loss [34,35].

In this work, the performance of the CNN models was additionally assessed using the gradient-weighted class activation mapping (Grad-CAM) method according to Selvaraju et al. [36], which offers a heat map for localizing possible powder bed irregularities. Grad-CAM is a technique for the visual description of CNN models, that creates a rough localization map, which highlights the areas of interest in the image for the prediction.

4. Results

4.1. Validation results

Two experiments (the first with the data augmentation described under 3.2.4, the second without) were carried out using the proposed method with the pretrained VGG16 and Xception networks and the additional classifier. For this purpose, the resulting CNN architectures were first trained with the training data and then validated with the validation data. The experiments were also set up in two stages. In the first step, the pretrained network including the classifier was trained with the data and, in a second step, it was optimized through fine-tuning and renewed training.

A third experiment was performed with VGG16 and Xception networks as well as the additional classifier, which were not trained in advance (by ImageNet). For this purpose, the untrained networks including the classifier were trained with the balanced data and the proposed data augmentation and then optimized through fine-tuning and retraining to compare the results with the other experiments.

In this context, Fig. 7 shows the course of accuracy and loss of all three experiments for both the training and the validation data during fine-tuning.

The smoothed curves were presented in the graphs using the exponentially weighted moving average (EWMA). The EWMA course is a weighted representation of the data points of a time series. There the weights decrease exponentially, so that newer data points are weighted more heavily than those that are further back in time [37,38]. The weighting factor on which the EWMA representations are based is 0.75. The two CNN architectures were each trained over 30 epochs and then trained again over 30 epochs in the course of fine tuning.

For the first (1st) experiment with data augmentation, the training accuracy of the VGG16 model was then about 91%, that of the Xception model approx. 94% (see Fig. 7(a), upper graph). The training loss was around 0.24 for the VGG16 architecture and around 0.14 for the Xception architecture (Fig. 7(a), lower graph). In terms of validation accuracy, the VGG16 network architecture achieved with approx. 90% better results than the Xception architecture with approx. 80% (Fig. 7(b), upper graph). With the validation loss, the values of the VGG16 model with approx. 0.25 are ultimately also lower than with the Xception model with approx. 0.5 (see Fig. 7(b), lower graph).

For the second (2nd) experiment without data augmentation, the training accuracy of the VGG16 model was 100%, that of the Xception model was also 100%, but was stopped after 21 epochs due to the defined early stopping hyperparameter (see Fig. 7(a), upper graph). The training loss for the VGG16 model was almost 0.0 and for the Xception model architecture also around 0.0 with a stop in the calculation after 21 epochs (Fig. 7(a), lower graph). In the validation accuracy, the VGG16 network architecture without data augmentation achieved with approx. 98% much better results than the Xception architecture, which was stopped after 21 epochs with exactly 50% validation accuracy (Fig. 7(b), upper graph). At validation loss, the values of the VGG16 model with approx. 0.1 are very much lower than with the Xception model with approx. 0.464 after an early stop at 21 epochs (see Fig. 7(b), lower graph).

For the third (3rd) experiment with networks that were not previously trained, the training accuracy of the VGG16 model was then about 51%, that of the Xception model was about 77% (see Fig. 7(a), upper graph). The training loss was 0.7 for the VGG16 and about 0.5 for the Xception architecture (Fig. 7(a), lower graph). The validation accuracy of the VGG16 network architecture was slightly better with 51% than with the Xception architecture with approx. 50% (Fig. 7(b), upper graph). In the validation loss, the values of the VGG16 model with approx. 0.7 are significantly lower than with the Xception model with approx. 9.0 (see Fig. 7(b), lower graph).

4.2. Test results

As described above, the powder bed dataset contains preselected test data consisting of a predefined number of 500 OK and 500 DEF images, each selected at random from the total dataset. DEF images were also copied randomly during oversampling to achieve the predefined number of images. After the training, optimization and validation of the two CNN model variants with the training and validation data, the test image data were examined with the models. The same data was used for both models and all experiments. The results are displayed in Table 3 in the form of Confusion Matrix, Precision, Recall (TPR), FPR, F1 Score and AUC values. The best results for each parameter are printed in bold.

To enable a more precise comparison of the two CNN models, the respective ROC curves are, according to Johnson et al. [17], a mandatory part of ML and are also shown in Fig. 8.

First, the individual experiments are considered. It can be stated that the VGG16 model from the 2nd experiment, without data augmentation, initially delivers the best results. The accuracy (0.971) and the ROC-AUC value (0.993) are better than the accuracy (0.958) and the ROC-AUC value (0.982) for the second-best result, which was achieved in the 1st experiment using the VGG16 model architecture with data

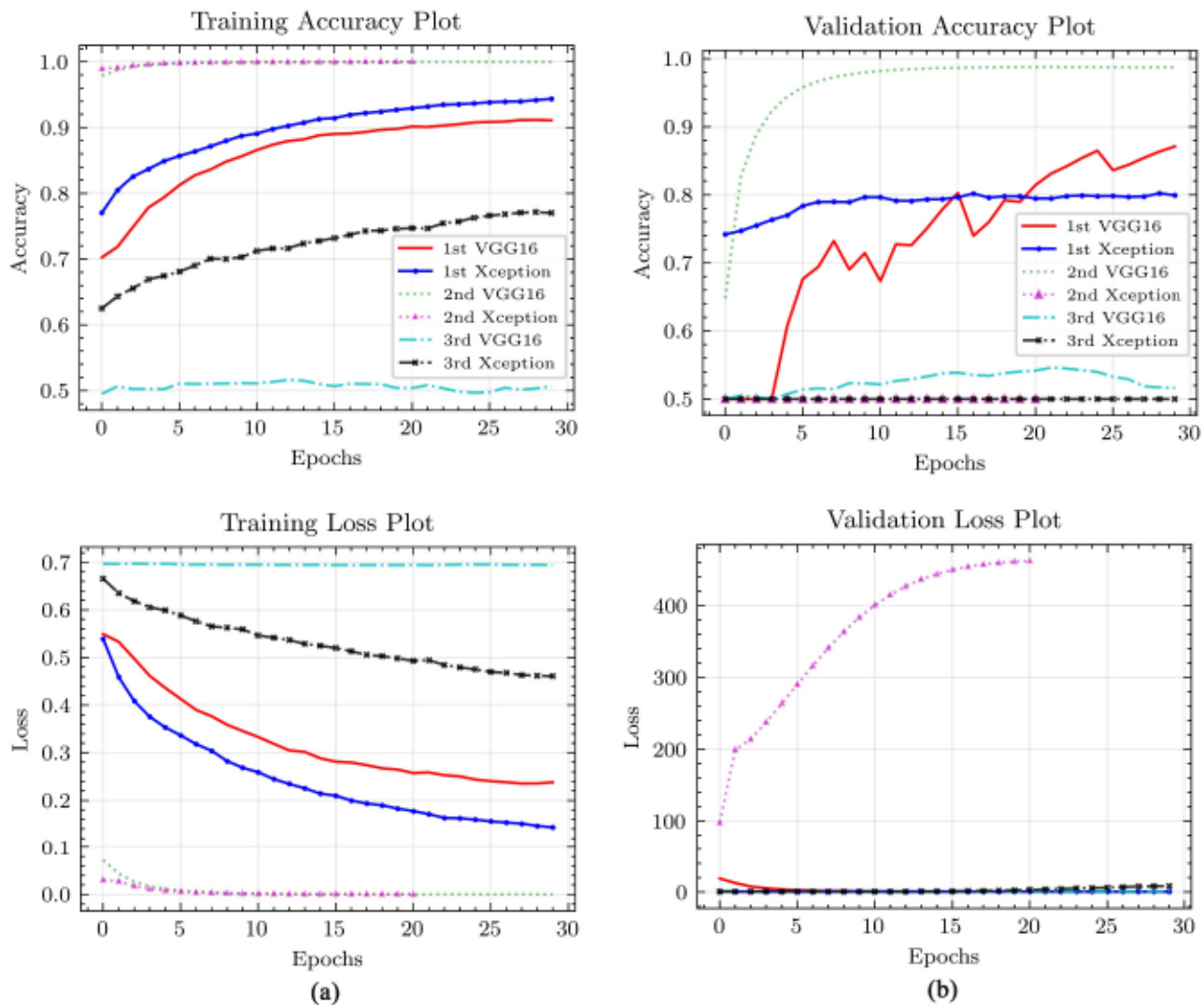


Fig. 7. Accuracy and loss of the used and optimized CNN model architectures and experiments in EWMA representations. (a) shows the course of accuracy (above) and loss (below) in the training data. (b) shows the course of accuracy (above) and loss (below) for the validation data.

Table 3

Confusion matrices and performance parameters for the examined CNN architectures for the classification of powder bed defects at the SLS process for all experiments carried out.

Experiment	Model	Confusion matrix		Accuracy	Precision	Recall (TPR)	FPR	F1-Score	ROC-AUC
1st	VGG16	490	10	0.958	0.939	0.980	0.064	0.959	0.982
	Xception	32	468	0.894	0.876	0.918	0.130	0.897	0.934
		65	435						
2nd	VGG16	496	19	0.971	0.968	0.980	0.038	0.972	0.998
	Xception	10	481	0.500	1.000	0.500	0.500	0.667	0.514
		500	0						
3rd	VGG16	180	320	0.515	0.360	0.522	0.489	0.426	0.525
	Xception	165	335	0.500	1.000	0.500	0.500	0.667	0.526
		500	0						
		500	0						

The best results for each parameter are printed in bold.

augmentation. The results of the 3rd experiment achieve accuracies of approx. 0.5 and ROC-AUC values of about 0.52 for both models considered. These results are therefore well below the values of the other two experiments. In the following, the results of the 1st experiment are discussed in more detail, as these values were obtained using the previously proposed method.

The test results of the 1st experiment show that the values of the CM and the performance metrics derived from it for the VGG16 model are higher than those of the Xception model and thus enable a better classification of the test data. Essentially, the accuracy allows a first direct comparison of the performance of the models, whereby the VGG16 accuracy of 0.958 is well above the Xception accuracy of 0.894. The

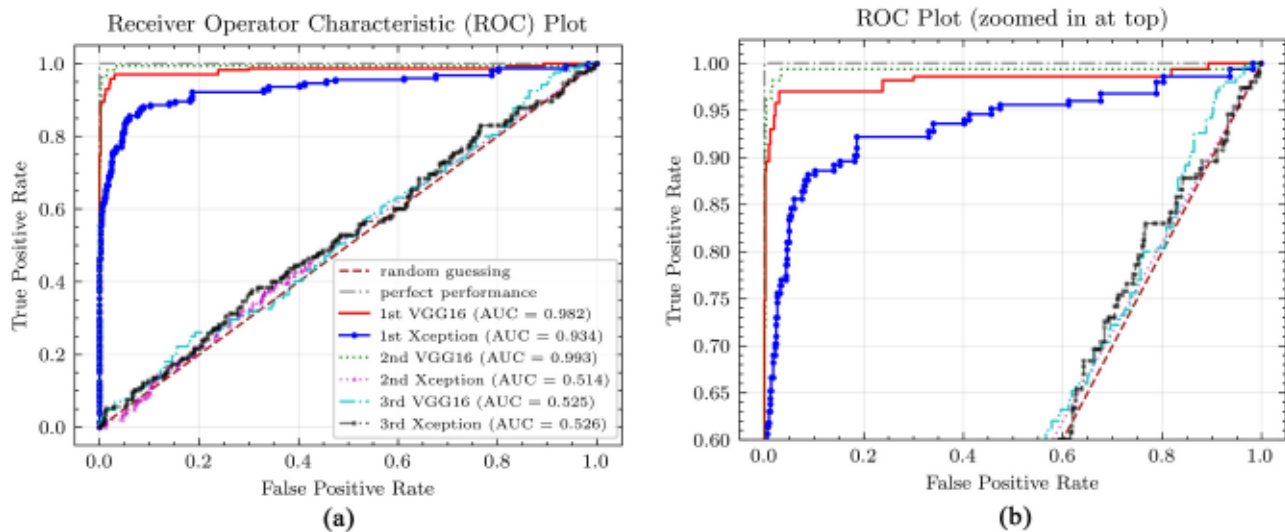


Fig. 8. ROC curves and AUC metrics of the implemented models for every three experiments. The linear dashed lines represent the ROC curve of a completely random classifier and that of a perfect classifier. (a) shows the plot of the ROC curves of the implemented models; (b) shows a zoomed in version of the top part plot.

precision shows the correspondence of the correct class with the correctly classified predictions of the model and shows a significantly better value for the VGG16 model with 0.939 than for the Xception model with 0.876. The recall indicates the efficiency of the model for the classification of the relevant class, here the DEF class and with the VGG16 model with 0.980 it is above the value of the Xception model with 0.918. In this examination with the powder bed image data, the most important thing is to correctly identify all images where defects appear (high recall values). In this way, good component quality can always be guaranteed. But, exclusive consideration of the recall without considering the precision is not recommended. For example, high precision with a low recall results in a very precise but incomplete classification. For this reason, the F1-Score was also calculated. It specifies a harmonic mean between precision and recall and defines how precisely and robustly the models perform on the test data. In principle, a higher F1-Score means a more powerful model. Accordingly, the VGG16 model with an F1-Score of 0.959 allows for a much better and more effective classification of powder bed images than the Xception model with a F1-Score of 0.897.

The ROC curves of the model architectures shown in Fig. 8 were created after fine-tuning the models of each experiment. For this purpose, the TPR was plotted over the FPR and an AUC value was determined. The maximum AUC value (0.982) was achieved by the VGG16 CNN architecture. The Xception architecture achieved a lower AUC value (0.934), which is reflected in a flatter ROC curve.

For better visualization and explanation of the test results, a gradient-weighted Class Activation Mapping was created for selected test images. The Grad-CAM technology is used to create "visual explanations" of the CNN models [36]. According to Selvaraju et al. [36] convolutional layers retain natural spatial information that is subsequently lost in fully connected layers. In this way, semantic, class-specific image information can be searched for in the convolution layers (e.g. for object components such as eyes, ears, cracks etc.). Grad-CAM then uses the gradient information flowing into the final convolution layer of the CNN to generate importance values for a particular property of interest.

In this work, the activation maps of the VGG16 and the Xception model were presented and highlighted using the gradients of the last convolution layer. This made it possible to locate areas of the image that are of most interest for the CNN networks to make decisions. The areas of the image that are most interesting to the CNN are highlighted in red and the less interesting image areas are highlighted in blue. In the case of a DEF powder bed image, the visible defects in the powder bed were

recognized by both model architectures and a correct prediction was then made (see Fig. 9).

In the OK powder bed images, the CNN models partially recognized different, invisible image anomalies, which then partially influenced the prediction accuracy of the models (see Fig. 10).

5. Discussion

As shown in the 1st experiment in Table 3, the method described here for detecting and classifying powder bed defects works very well with selective laser sintering and produces excellent results. From these results it can be deduced that the VGG16 model architecture provides the best results with an AUC value of 0.982, an F1-Score of 0.959 and a test accuracy of 0.958. As a result, the developed VGG16 CNN architecture was best able to make predictions about the quality of unseen powder bed images. Unfortunately, there are no comparative values in the current literature to relate the results obtained to further CNN analyzes of powder bed images during selective laser sintering. However, Gobert et al. [9] analyzed CT scans of powder bed images during the SLM process for powder bed defects using an SVM algorithm, with a maximum accuracy of 0.85 being achieved.

The 2nd experiment in Table 3 shows that with the method proposed here and the VGG16 model without data augmentation with an AUC value of 0.993, somewhat better results can be achieved at first glance. This is basically comprehensible, since the data augmentation extends the relatively small dataset through special operations (image rotation, image mirroring etc.) in order to obtain a larger training base. For that, the complexity of the dataset increases, the individual images are no longer as similar as before and classification is more difficult for the model. According to Chollet [4], this is a desired effect in order to enable a better generalization of the models and to avoid overfitting. Especially for the 2nd experiment in Table 3, it can be seen from the curves in Fig. 7 (a) for the VGG16 model that the maximum values for accuracy and loss were already reached after a few training periods. This means that the model has learned patterns that are specific to this training data and can classify them almost perfectly. Since the validation and test data are very similar, the model was also able to achieve very good values there. In contrast to this, in the first experiment with data augmentation, a larger and more complex database was used for training, which resulted in somewhat poorer results, but the models generalize better and are better suited for larger datasets with less similarity among the individual images. For the Xception model from the 2nd experiment, it is immediately apparent that no learning effect has taken place and that the model

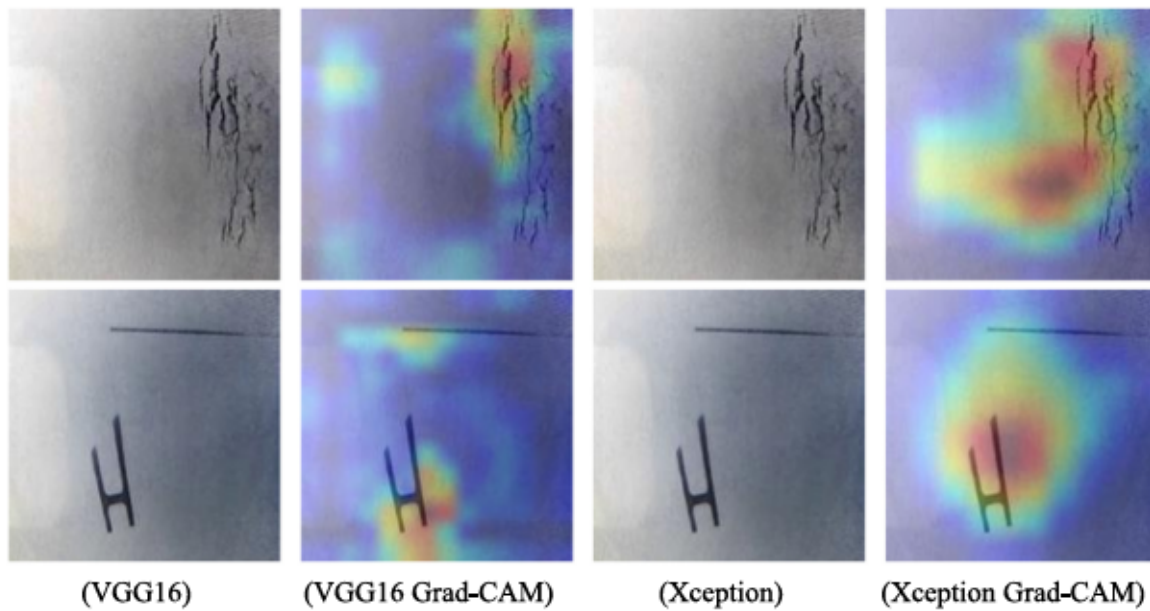


Fig. 9. Activation maps for powder bed recordings during the SLS process with visible powder bed defects. Defects were detected and localized by the CNN architectures. With the VGG16 model, a more precise localization of the effects could be achieved than with the Xception model. (For interpretation of the references to colour in this figure, the reader is referred to the web version of this article.)

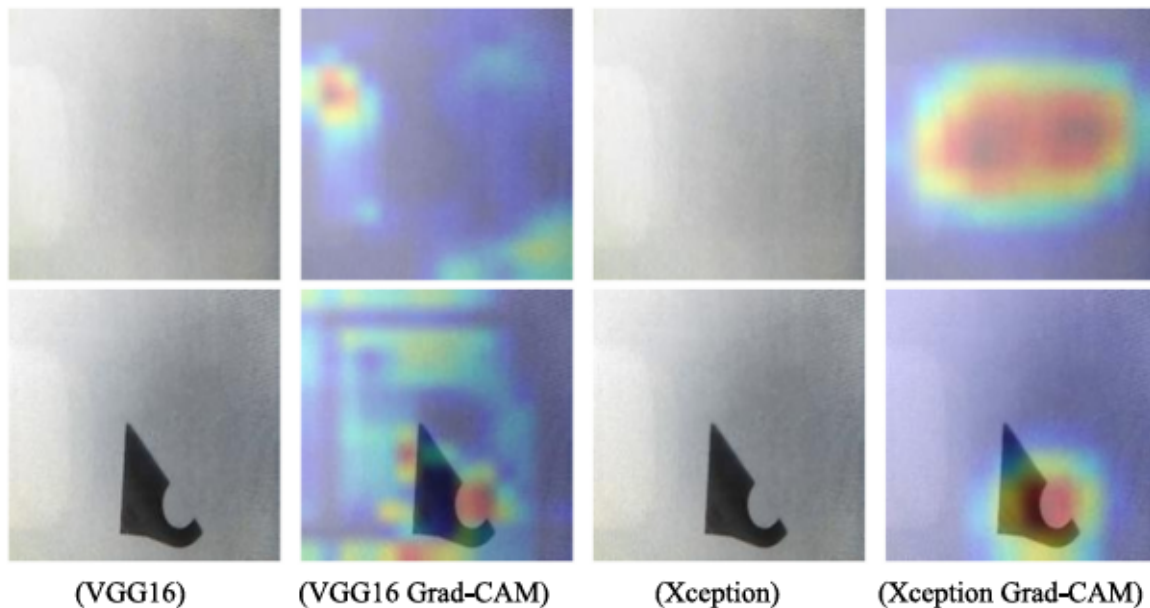


Fig. 10. Activation maps for powder bed recordings during the SLS process without visible powder bed defects. Image anomalies were detected and localized by the CNN architectures. Various anomalies were identified in the VGG16 model and localized relatively precisely. For the Xception model, larger image areas were identified as anomalies and the actual irregularities in the powder bed could therefore often be localized less precisely.

cannot classify the data without data augmentation. This means that the model behaves completely differently than the VGG16 model, but this is due to an overfitting after considering the curves from Fig. 7. The Xception model may have learned misleading or irrelevant information for classification during training. A similar behaviour can be observed for the Xception model from the 3rd experiment. Data augmentation was carried out there, but the models were not trained in advance with the ImageNet dataset. As a result, no learning successes could be determined in this experiment in the 30 observed epochs either. The same applies here to the VGG16 model. However, based on the curves of the validation accuracy and the validation loss in Fig. 7, an overfitting can also be concluded, which has a negative effect on the classification.

In summary, from the investigation of all three experiments it can be determined that the presented method with data augmentation and with pretraining with ImageNet is advantageous in order to achieve better results and to implement more robust model architectures. The data augmentation is particularly important for the generalization of the examined models and also avoids overfitting. A preliminary training with the weights from the ImageNet dataset saves a considerable amount of computational effort, since this has already been carried out there and the proposed models can be based on it. In addition, this also reduces the risk of overfitting, since a much larger database was considered when calculating the model weights.

This work also showed that both investigated CNN model

architectures could learn interesting features from the image data in order to be able to then automatically assess the quality of powder bed images. In the future, this can support the quality assurance of additively manufactured components, e.g. as a supplement to the downstream, non-destructive assessment of the part quality, but also for in-situ monitoring of the additive manufacturing process. Compared to the studies by Xiao et al. [3], real production datasets with real powder bed defects were used for this, while no powder bed irregularities were artificially introduced.

The activation maps generated in this work can specifically identify and localize powder bed defects. This was also shown in the work by Baumgartl et al. [5] for thermographic images during the SLM process, where possible delamination defects in the part layers were localized and detected through different temperature ranges. In this work, the VGG16 model architecture identified the defects more precisely than the more modern Xception architecture and is therefore better suited for image analysis for quality assurance in selective laser sintering. One reason for the better results of the VGG16 model may be that in this model a large number of model parameters (approx. 138 million) are distributed over relatively few model layers (23) and thus enable a more detailed analysis of the individual image data. In the Xception model, for example, there are far fewer parameters (about 23 million) that are distributed over a large number of layers (126). Another reason, however, is the relatively small amount of data, which can result in the Xception model not being able to learn sufficiently due to its complexity.

The lack of available data is a major problem in the basic classification of powder bed defects in selective laser sintering. Normally, DL models are trained over several thousand image data. Training CNN with only a small amount of data can easily lead to an inaccurate classification and can impair the generalization ability of the models. The adjusted powder bed dataset contained more than 8500 images, which were very unevenly distributed. It contained only 706 images with visible defects for the model to learn from. The lack of DEF data is therefore the main problem of the approach presented here. The performance of the models presented could increase as more DEF image data become available. This can first be evaluated with a so-called ablation analysis in a way that conserves resources [39]. According to Fawcett and Hoos [39], algorithms with many influencing parameters are examined with ablation studies to determine which parameters contribute most to changes in performance between two configurations of the algorithm and which changes in the standard configuration of the algorithm actually lead to better performance. For example, if an ablation study on a model architecture with less data achieves a performance comparable to that of a larger dataset (with the same parameter configuration), no significant increases in performance are expected from an even larger database.

Furthermore, the problem of image preprocessing must be considered. By cropping the images to a size of 180 × 180 pixels, it is not possible to capture the entire cylindrical build area of the SLS system without capturing undesired black border areas. This should be optimized through more suitable camera positioning and better camera focus.

Another difficulty in this investigation was the interpretation of the visualization results of the CNN models. A deeper understanding of the visual characteristics of a digital image and the individual convolutional operations within the neural networks is required in order to be able to explain the predictions and visualization results in detail. The resulting activation maps were recorded and fundamentally analyzed in this context, but further explanations are required in order to understand why the model particularly highlights specific areas of the image. These interpretation problems may be resolved in the future through larger datasets and more detailed research.

6. Conclusions

In this paper, we introduce different machine learning architectures

that can be used to automatically differentiate between good and bad powder bed images during selective laser sintering. There, good images without visible defects in the powder bed are marked as OK and images with visible defects and irregularities as DEF. The investigated methods used techniques of transfer learning with pretrained weights of the ImageNet dataset, which served as initialization for the VGG16 CNN model as well as for the Xception CNN model. Then a new classifier was provided consisting of a fully connected layer with 1000 channels, a dropout layer with a retention rate of 0.25, a batch normalization operation and another fully connected layer with only one channel and a sigmoid activation function. The images used were preprocessed in a defined manner, divided into classes and reproduced using established methods in order to generate a balanced dataset. With transfer learning it was then possible to work effectively with the small dataset. The VGG16 CNN architecture achieved the best results and clearly outperformed the results of the Xception architecture. With the VGG16 approach and a special data augmentation, a test accuracy of 0.958 was achieved, as well as a precision of 0.939, a recall of 0.980, an F1-Score of 0.959 and an AUC value of 0.982 for the VGG16 ROC curve. The results were visualized with the Grad-CAM method and compared for both methods. Both neural network architectures were able to recognize and localize powder bed irregularities.

As regards future work, so-called ablation studies should first be carried out in order to evaluate the CNN architectures presented and to examine the performance of the models with even smaller datasets. If performance results similar to those in this study are achieved, no significant increases in performance can be expected for these model architectures, even with larger amounts of data. Otherwise, investigations should be carried out on a larger dataset in future work. In particular, more DEF image data needs to be included in the examinations and the impact on the analyzed results considered. In addition, the effects of various data preprocessing steps and methods should be investigated and various hyper parameter configurations should be tested to further improve the performance of the models. Moreover, further CNN model variants and classifiers should be investigated with the powder bed data in order to generate even more powerful and faster transfer learning variants. Finally, according to the ImageNet dataset, a special dataset should be created with various classes and image examples on process irregularities and part defects in additive manufacturing, with which the respective model architectures can be trained in advance. This should significantly increase the effectiveness of CNN models in terms of error detection in various additive manufacturing processes.

Funding

This research was funded by the European Union, which was made available through the European Regional Development Fund (ERDF) and the Ministry for Economics, Employment and Health of Mecklenburg-Vorpommern, Germany, grant number TBI-V-1-345-VBW-118.

CRedit authorship contribution statement

Erik Westphal: Conceptualization, Data curation, Formal analysis, Funding acquisition, Investigation, Methodology, Resources, Software, Validation, Visualization, Writing - original draft. **Hermann Seitz:** Funding acquisition, Investigation, Supervision, Writing - review & editing.

Declaration of Competing Interest

The authors declare that they have no known competing financial interests or personal relationships that could have appeared to influence the work reported in this paper.

Acknowledgments

The authors gratefully acknowledge the project partner ESD Elektro-Systemtechnik GmbH Dargun for their technical support and the provision of the SLS printing system and SLS printing powder for the development of this work.

References

- [1] A. Mazzoli, Selective laser sintering in biomedical engineering, *Med. Biol. Eng. Comput.* 51 (2013) 245–256, <https://doi.org/10.1007/s11517-012-1001-x>.
- [2] M. Schmid, *Laser Sintering with Plastics: Technology, Processes, and Materials*, 2018, Hanser; Munich, GER, <https://doi.org/10.3139/9781569906842>.
- [3] L. Xiao, M. Lu, H. Huang, Detection of powder bed defects in selective laser sintering using convolutional neural network, *Int. J. Adv. Manuf. Technol.* 107 (2020) 2485–2496, <https://doi.org/10.1007/s00170-020-05205-0>.
- [4] F. Chollet, *Deep Learning with Python*, Manning, Shelter Island, NY, 2018.
- [5] H. Baumgartl, J. Tomas, R. Buettner, M. Merkel, A deep learning-based model for defect detection in laser-powder bed fusion using in-situ thermographic monitoring, *Prog. Addit. Manuf.* 5 (2020) 277–285, <https://doi.org/10.1007/s40964-019-00108-3>.
- [6] Y. LeCun, Y. Bengio, G. Hinton, Deep learning, *Nature* 521 (2015) 436–444, <https://doi.org/10.1038/nature14539>.
- [7] H. Shen, W. Du, W. Sun, Y. Xu, J. Fu, Visual detection of surface defects based on self-feature comparison in robot 3-D printing, *Appl. Sci.* 10 (2020) 235, <https://doi.org/10.3390/app10010235>.
- [8] L. Scime, J. Beuth, Anomaly detection and classification in a laser powder bed additive manufacturing process using a trained computer vision algorithm, *Addit. Manuf.* 19 (2018) 114–126, <https://doi.org/10.1016/j.addma.2017.11.009>.
- [9] C. Gobert, E.W. Reutzel, J. Petrich, A.R. Nassar, S. Phoha, Application of supervised machine learning for defect detection during metallic powder bed fusion additive manufacturing using high resolution imaging, *Addit. Manuf.* 21 (2018) 517–528, <https://doi.org/10.1016/j.addma.2018.04.005>.
- [10] P. Yadav, O. Rigo, C. Arvieu, E. Le Guen, E. Lacoste, In situ monitoring systems of the SLM process: on the need to develop machine learning models for data processing, *Crystals* 10 (2020) 524, <https://doi.org/10.3390/cryst10060524>.
- [11] J.M. Johnson, T.M. Khoshgoftaar, Survey on deep learning with class imbalance, *J. Big Data* 6 (2019) 27, <https://doi.org/10.1186/s40537-019-0192-5>.
- [12] M. Buda, A. Maki, M.A. Mazurowski, A systematic study of the class imbalance problem in convolutional neural networks, *Neural Netw.* 106 (2018) 249–259, <https://doi.org/10.1016/j.neunet.2018.07.011>.
- [13] X.-Y. Liu, J. Wu, Z.-H. Zhou, Exploratory undersampling for class-imbalance learning, *IEEE Trans. Syst. Man Cybern. B Cybern.* 39 (2009) 539–550, <https://doi.org/10.1109/TSMCB.2008.2007853>.
- [14] J. Wu, S.C. Brubaker, M.D. Mullin, J.M. Rehg, Fast asymmetric learning for cascade face detection, *IEEE Trans. Pattern Anal. Mach. Intell.* 30 (2008) 369–382, <https://doi.org/10.1109/TPAMI.2007.1181>.
- [15] J. van Hulse, T.M. Khoshgoftaar, A. Napolitano, Experimental perspectives on learning from imbalanced data, in: *ICML '07 & ILP '07: The 24th Annual International Conference on Machine Learning held in conjunction with the 2007 International Conference on Inductive Logic Programming*, Corvallis Oregon USA, Association for Computing Machinery New York NY United States, (2007), pp. 935–942.
- [16] F. Pasa, V. Golkov, F. Pfeiffer, D. Cremers, D. Pfeiffer, Efficient deep network architectures for fast chest X-ray tuberculosis screening and visualization, *Sci. Rep.* 9 (2019) 6268, <https://doi.org/10.1038/s41598-019-42557-4>.
- [17] N.S. Johnson, P.S. Vulimiri, A.C. To, X. Zhang, C.A. Brice, B.B. Kappes, A. P. Stebner, Invited review: machine learning for materials developments in metals additive manufacturing, *Addit. Manuf.* 36 (2020), 101641, <https://doi.org/10.1016/j.addma.2020.101641>.
- [18] C. Shorten, T.M. Khoshgoftaar, A survey on image data augmentation for deep learning, *J. Big Data* 6 (2019) 60, <https://doi.org/10.1186/s40537-019-0197-0>.
- [19] Chollet, F. (2015). Keras, <https://keras.io>.
- [20] F. Hutter, L. Kotthoff, J. Vanschoren, *Automated Machine Learning*, Springer International Publishing, Cham, 2019.
- [21] J. Lujan-García, C. Yanez-Marquez, Y. Villuendas-Rey, O. Camacho-Nieto, A transfer learning method for pneumonia classification and visualization, *Appl. Sci.* 10 (2020) 2908, <https://doi.org/10.3390/app10082908>.
- [22] M.F. Hashmi, S. Katiyar, A.G. Keskar, N.D. Bokde, Z.W. Geem, Efficient pneumonia detection in chest X-ray images using deep transfer learning, *Diagnostics* 10 (2020), <https://doi.org/10.3390/diagnostics10060417>.
- [23] F. Chollet, Xception: deep learning with depthwise separable convolutions, in: *Proceedings of the 2017 IEEE Conference on Computer Vision and Pattern Recognition (CVPR)*, Honolulu, HI, IEEE, 21.07.2017 - 26.07.2017, pp. 1800–1807.
- [24] M. Tsiakmaki, G. Kostopoulos, S. Kotsiantis, O. Ragos, Transfer learning from deep neural networks for predicting student performance, *Appl. Sci.* 10 (2020) 2145, <https://doi.org/10.3390/app10062145>.
- [25] S. Karen, and A. Zisserman. "Very deep convolutional networks for large-scale image recognition." arXiv preprint arXiv:1409.1556 (2014).
- [26] H. Shin et al., "Deep Convolutional Neural Networks for Computer-Aided Detection: CNN Architectures, Dataset Characteristics and Transfer Learning," in *IEEE Transactions on Medical Imaging*, vol. 35, no. 5, pp. 1285–1298, May 2016, doi: 10.1109/TMI.2016.2528162.
- [27] F. Mamalet, C. Garcia, *Simplifying ConvNets for fast learning. Artificial Neural Networks and Machine Learning ICANN 2012*, Springer-Verlag Berlin Heidelberg, Lausanne, Switzerland, 2012.
- [28] L. Sifre, *Rigid-Motion Scattering For Image Classification* (Ph.D. thesis), 2014, CiteSeerX: Paris, FR.
- [29] O. Russakovsky, J. Deng, H. Su, J. Krause, S. Satheesh, S. Ma, Z. Huang, A. Karpathy, A. Khosla, M. Bernstein, A.C. Berg, L. Fei-Fei, ImageNet large scale visual recognition challenge, *Int. J. Comput. Vis.* 115 (2015) 211–252, <https://doi.org/10.1007/s11263-015-0816-y>.
- [30] A. Krizhevsky, I. Sutskever, G.E. Hinton, ImageNet classification with deep convolutional neural networks, *Commun. ACM* 60 (2017) 84–90, <https://doi.org/10.1145/3065386>.
- [31] Abadi, Martín, et al. "Tensorflow: Large-scale machine learning on heterogeneous distributed systems." arXiv preprint arXiv:1603.04467 (2016).
- [32] B. Paula, L. Torgo, and R. Ribeiro. "A survey of predictive modelling under imbalanced distributions." arXiv preprint arXiv:1505.01658 (2015).
- [33] T. Fawcett, An introduction to ROC analysis, *Pattern Recognit. Lett.* 27 (2006) 861–874, <https://doi.org/10.1016/j.patrec.2005.10.010>.
- [34] Yaoshiang Ho and Samuel Wookey, The real-world-weight cross-entropy loss function: Modeling the costs of mislabeling, *IEEE Access*, 8:4806–4813, 2019.
- [35] U. Ruby, Binary cross entropy with deep learning technique for Image classification, *IJATCSE* 9 (2020) 5393–5397, <https://doi.org/10.30534/ijatcse/2020/175942020>.
- [36] R.R. Selvaraju, M. Cogswell, A. Das, R. Vedantam, D. Parikh, D. Batra, Grad-CAM: visual explanations from deep networks via gradient-based localization, *Int. J. Comput. Vis.* 128 (2020) 336–359, <https://doi.org/10.1007/s11263-019-01228-7>.
- [37] T. Fehlmann, E. Kranich, Exponentially Weighted Moving Average (EWMA) prediction in the software development process, in: *Proceedings of the 2014 Joint Conference of the International Workshop on Software Measurement and the International Conference on Software Process and Product Measurement*, Rotterdam, Netherlands, IEEE, 06.10.2014 - 08.10.2014, pp. 263–270.
- [38] D. Leung, J.A. Romagnoli, *Fault diagnosis methodologies for process operation, in: Software Architectures and Tools for Computer Aided Process Engineering*, Elsevier, 2002, pp. 535–556.
- [39] C. Fawcett, H.H. Hoos, Analysing differences between algorithm configurations through ablation, *J. Heuristics* 22 (2016) 431–458, <https://doi.org/10.1007/s10732-014-9275-9>.



Corrigendum

Corrigendum to: “A machine learning method for defect detection and visualization in selective laser sintering based on convolutional neural networks” [Addit. Manuf., 41 (2021), 101965]

Erik Westphal^{*}, Hermann Seitz

Chair of Microfluidics, University of Rostock, 18059, Rostock, Germany

The authors regret the typing error in section “4.2 Test results”, which slightly changes some values in Table 3 (page 9) and thus even slightly improves them in terms of accuracy and precision. The updated Table 3 with the correct values is shown below.

Due to the changes in some values in Table 3, some references in the manuscript also change. The old text references and the new, updated text passages are listed below.

List of text references that need to be updated due to the changed values in Table 3:

The authors regret the typing error in section:	Regarding the old references in the manuscript:	The new updated references are as follows:
“Abstract” (page 1)	The VGG16 model architecture achieved the best results for Accuracy (0.958), Precision (0.939), Recall (0.980), F1-Score (0.959) and AUC value (0.982).	The VGG16 model architecture achieved the best results for Accuracy (0.958), Precision (0.980), Recall (0.989), F1-Score (0.959) and AUC value (0.982).
“4.2 Test results” (page 8)	The accuracy (0.971) and the ROC-AUC value (0.993) are better than the accuracy (0.958) and the ROC-AUC value (0.982) for the second-best result, ...	The accuracy (0.977) and the ROC-AUC value (0.993) are better than the accuracy (0.958) and the ROC-AUC value (0.982) for the second-best result, ...
“4.2 Test results” (page 10)	The precision shows the correspondence of the	The precision shows the correspondence of the

(continued on next column)

(continued)

The authors regret the typing error in section:	Regarding the old references in the manuscript:	The new updated references are as follows:
“6. Conclusions” (page 12)	correct class with the correctly classified predictions of the model and shows a significantly better value for the VGG16 model with 0.939 than for the Xception model with 0.876. The recall indicates the efficiency of the model for the classification of the relevant class, here the DEF class and with the VGG16 model with 0.980 it is above the value of the Xception model with 0.918. With the VGG16 approach and a special data augmentation, a test accuracy of 0.958 was achieved, as well as a precision of 0.939, a recall of 0.980, an F1-Score of 0.959 and an AUC value of 0.982 for the VGG16 ROC curve.	correct class with the correctly classified predictions of the model and shows a significantly better value for the VGG16 model with 0.980 than for the Xception model with 0.918. The recall indicates the efficiency of the model for the classification of the relevant class, here the DEF class and with the VGG16 model with 0.989 it is above the value of the Xception model with 0.876. With the VGG16 approach and a special data augmentation, a test accuracy of 0.958 was achieved, as well as a precision of 0.980, a recall of 0.989, an F1-Score of 0.959 and an AUC value of 0.982 for the VGG16 ROC curve.

The authors would like to apologise for any inconvenience caused.

DOI of original article: <https://doi.org/10.1016/j.addma.2021.101965>.

^{*} Corresponding author.

E-mail address: erik.westphal@uni-rostock.de (E. Westphal).

<https://doi.org/10.1016/j.addma.2023.103739>

Available online 21 August 2023

2214-8604/© 2023 The Author(s). Published by Elsevier B.V. This is an open access article under the CC BY license (<http://creativecommons.org/licenses/by/4.0/>).

Table 3

Confusion matrices and performance parameters for the examined CNN architectures for the classification of powder bed defects at the SLS process for all experiments carried out.

Experi-ment	Model	Confusion Matrix		Accuracy	Precision	Recall (TPR)	FPR	F1-Score	ROC-AUC
1st	VGG16	490	10	0.958	0.980	0.939	0.021	0.959	0.982
		32	468						
	Xception	459	41	0.894	0.918	0.876	0.086	0.897	0.934
		65	435						
2nd	VGG16	496	4	0.977	0.992	0.963	0.008	0.977	0.993
		19	481						
	Xception	500	0	0.500	1.000	0.500	0.500	0.667	0.514
		500	0						
3rd	VGG16	180	320	0.515	0.360	0.522	0.489	0.426	0.525
		165	335						
	Xception	500	0	0.500	1.000	0.500	0.500	0.667	0.526
		500	0						

Publication [II]

E. Westphal & H. Seitz, Machine learning for the intelligent analysis of 3D printing conditions using environmental sensor data to support quality assurance



Machine learning for the intelligent analysis of 3D printing conditions using environmental sensor data to support quality assurance

Erik Westphal ^{a,*}, Hermann Seitz ^{a,b}

^a Chair of Microfluidics, University of Rostock, 18059 Rostock, Germany

^b Dept. Life, Light & Matter, University of Rostock, 18059 Rostock, Germany

ARTICLE INFO

Keywords:

Additive manufacturing
Fused deposition modeling
Machine learning
Quality assurance
Time series classification

ABSTRACT

Process and environmental parameters that influence manufacturing processes and results are of great importance in additive manufacturing processes such as Fused Deposition Modeling (FDM). The recording and analysis of these parameters is an important task of quality assurance (QA). For this purpose, sensors are increasingly used, which continuously record the environmental data during the printing process. Subsequently, algorithms for machine learning (ML) are suitable for the data analysis of data sequences as well as for the intelligent classification of the results in defined 3D printing condition classes. In this paper different state-of-the-art ML algorithms are presented, which enable a supervised learning classification approach of environmental sensor data (temperature, humidity, air pressure, gas particles) in the FDM process. For this purpose, a new data preparation method was developed which sequences different sensor time series data. FDM sensor parameters of various 3D printing conditions were recorded, preprocessed accordingly and saved in two differently sized datasets. Furthermore, a sensitivity analysis was carried out in order to examine the influence of the individual sensor parameters on the ML analyses. Interestingly, the air pressure values were characterized as being most relevant to the analyses. Better results were always achieved with the air pressure values than without. The air pressure values have a stabilizing effect on the analyses and reduce overfitting. In the further course of the investigations, tests were carried out on the two datasets of different sizes with all considered ML algorithms as well as tests with and without the air pressure values. There, the modern XceptionTime architecture has proven to be the most effective and robust against overfitting. XceptionTime can achieve excellent results with a minimum of 95% accuracy with both a small and a large database. The Macro F1-Scores are also always above 89% and indicate a good classification for all 3D printing conditions examined. The ML investigations were then compared in a proof of concept with 3D scan examinations established in quality assurance. The 3D scans of the printed FDM components could not provide any clear information about the different printing conditions and only the component surface could be analyzed. The ML analyses, especially with the XceptionTime architecture, enable an effective alternative to quickly and easily differentiate between different 3D printing conditions. The ML time series classification presented in this work is accordingly well suited for use in an industrial environment and, with special optimizations, can be effectively applied in practice to support quality assurance in additive manufacturing. This quality assurance approach is completely new and offers immense potential to increase trust in and acceptance of additive manufacturing processes.

1. Introduction

Additive manufacturing (AM) or 3D printing is a term for the layer-by-layer manufacturing process of components from three-dimensional computer-aided design (CAD) files [1]. In research and industry, as

well as to a large extent by non-industrial home users, the method of material extrusion defined in accordance with ISO/ASTM 52900, which is also known under the brand name Fused Deposition Modeling (FDM), is often used. In the FDM process, a filament material is melted and selectively applied to a print bed through a nozzle, creating the desired

* Corresponding author.

E-mail addresses: erik.westphal@uni-rostock.de (E. Westphal), hermann.seitz@uni-rostock.de (H. Seitz).

<https://doi.org/10.1016/j.addma.2021.102535>

Received 25 August 2021; Received in revised form 22 October 2021; Accepted 29 November 2021

Available online 2 December 2021

2214-8604/© 2021 Elsevier B.V. All rights reserved.

contour and the three-dimensional (3D) component in layers [2].

With the FDM process, various thermoplastics such as polylactide (PLA), acrylonitrile butadiene styrene (ABS) and polyamide (PA) can be used [2]. Moreover, high-performance plastics such as polyetherimide (PEI) and polyetheretherketone (PEEK) can be processed with special FDM systems [3]. This means that the process is also of interest for applications in the aerospace and medical technology sectors. However, in order to be perceived as a serious production process in these regulated industrial sectors, special quality assurance (QA) and quality management (QM) requirements must be met.

In AM processes in general and especially in FDM, there are a large number of process and environmental parameters that influence both the printing process and the printing result and have an impact, for example, on geometric, mechanical or surface properties as well as process stability [4]. Reliable detection and analysis systems have to be developed to characterize these parameters in order to ensure a stable AM process with optimal process specifications, process results with defined quality requirements as well as a certified QM [5].

Machine learning (ML) is increasingly being used to monitor the manufacturing process in order to analyze image and process data and to derive predictions about the expected component quality [6,7]. With the help of cameras and sensors, special process data can initially be recorded and monitored on site [8,9]. Using process analyses based on artificial intelligence (AI), computer-based learning processes can then be performed. These are then trained to evaluate the recorded data or to predict future data courses and can thus provide early conclusions about the printing process and the component quality. In addition, the manufacturing results can also be examined after the printing process by means of optical 3D scans and evaluated in terms of their component quality [4].

In this paper, a supervised learning strategy based on different intelligent ML algorithms are developed and compared with regard to their performance in order to detect irregularities in environmental sensor data in the FDM process. The overriding goal is then to use the analysis results to identify various 3D printing condition classes and process errors at an early stage and thereby achieve better process reliability, repeatability and QA in FDM. The findings are then correlated with the results of optical 3D scans of the printed components and the effectiveness evaluated with regard to the classification of different printing conditions.

2. Related work

In the field of AM, ML is already used in a variety of ways and in various sub-processes, for instance to monitor processes, evaluate process images or detect process errors. For example, a prediction method for warping in FDM was developed based on thermal time series data that was recorded from the print bed via thermocouples and evaluated using a K-nearest neighbors algorithm [10]. The prediction method works, but the classification accuracy still needs improvement. Furthermore, no comparisons with other algorithms were undertaken.

In another publication, a monitoring solution for the processing of ABS using the FDM method was developed, in which environmental parameters in the form of volatile organic compounds (VOCs) are recorded and analyzed by an intelligent Support Vector Machine (SVM) algorithm [11]. The results are then used to predict that a defined threshold value for the VOC concentration will be exceeded. However, the component quality achieved was not assessed in this way, but the exposure to potentially harmful environmental parameters during the

printing process was monitored.

An ML methodology based on regression algorithms was developed by Charalampous et al. [4] to investigate the dimensional deviations of CAD models and the manufactured physical components. For this purpose, a database with optical 3D scan data was created in which printed components with various printing parameters were stored as a data basis for regression analyses and thus different correlations between printing parameters and dimensional deviations can be shown. These investigations are limited to the regression algorithms and do not use manufacturing process data, but optical evaluations of the printing results after the manufacturing process. This means that internal part areas in particular cannot be mapped using this method.

Wu et al. [8] developed an in situ monitoring of FDM machine conditions using acoustic emission data in order to detect normal and abnormal system conditions using an SVM algorithm. In another publication, Wu et al. [12] also developed a principal component analysis (PCA) with the acoustic data, which significantly reduced the complexity of the computation. Acoustic signals have also already been examined in a metal-based powder bed fusion (PBF) process with complex, efficient and widespread neural network architectures in order to enable the printed structures to be classified [13]. All investigations recognized that the evaluation of acoustic process data is effective identifying different operating states of the systems used, but only one specific acoustic parameter was recorded in each case.

Another application of ML is to analyze process parameter sets of a metal PBF process via optical image data in order to find clusters that represent a high-quality print result [14]. Such a process was also developed for selective laser sintering (SLS) with plastics [7]. There, image data were analyzed with complex transfer learning methods so as to develop an automatic classification of powder bed defects during the SLS process. These ML applications are very complex and require more powerful computing hardware, which means that the computing costs are relatively high and the analysis times are relatively long. In addition, the return of the analysis results for the intelligent optimization of the production system is, in principle, more complex than with sensor-based approaches.

Image-based error detection systems based on convolutional neural networks (CNN) are already available especially for the FDM process, which can analyze the process in real time and detect incorrect printing conditions [15,16]. Both investigations are limited to clearly recognizable geometry defects that were analyzed using a CNN algorithm. Jin et al. [17] have linked a corresponding CNN architecture with a modern localization algorithm in order to enable the localization of printing defects in addition to the detection of unfavorable printing conditions. This optical analysis method is very effective, but does not allow direct analysis of the process parameters.

Further comprehensive studies on quality control and in situ process monitoring with one-, two- and three-dimensional data (e.g. sensor, image and tomography data) in AM can also be found in the literature, e.g. clearly in the publication by Kim et al. [5] and Qi et al. [9] collected as well as especially for FDM in the review of Fu et al. [18].

Overall, it can thus be stated that various ML methods are used in the literature to differentiate between machine and printing conditions in AM systems. Among other things, special sensor data are also used, which already enable very effective classifications between quality-related aspects. However, this work is about the development of a strategy and method for evaluating larger amounts of environmental sensor data and the efficient classification of this data as a coherent process. In addition, the findings are used to support quality assurance



Fig. 1. FDM nozzles with different degrees of wear and clogging (which, in principle, were also used for the investigations). Left: a completely new nozzle, right: a used nozzle with over 50 h of printing time.

and compared with an established optical scanning process. The joint ML analysis of several different environmental parameters in combination with different ML algorithms has not yet been carried out and, based on the previous literature results, represents a very interesting approach, e.g. for FDM. In the following, this study develops and describes an ML approach in which four environmental sensor parameters (temperature, humidity, air pressure, gas particles) are recorded together, evaluated using different ML algorithms and then compared to optical 3D scans.

3. Materials and methods

The experimental setup used in this study, the data acquisition and the generated datasets are described in detail below. In addition, the data preprocessing, the ML algorithms and finally the performance metrics that are used are explained.

3.1. Experimental structure and data acquisition

The FDM process was connected to a system consisting of an environmental sensor and a single-board computer and thus monitored inline. An i3 Mega S low-cost FDM printer (Anycubic Technology Co., Shenzhen, China) was used for production. A 0.4 mm nozzle and a

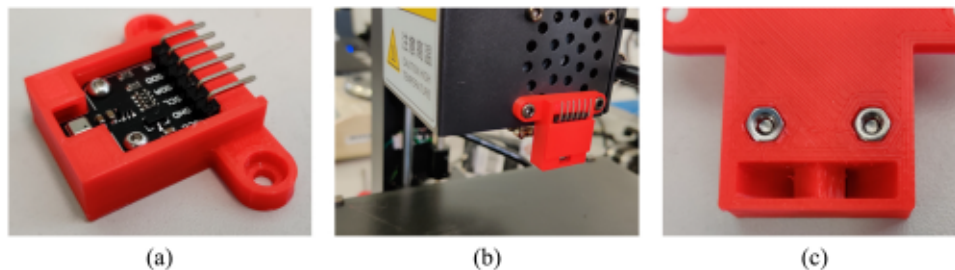


Fig. 2. Experimental setup of the sensor and preparation on the FDM printer. (a) shows the sensor board with the printed housing. (b) shows the mounting near the print nozzle. (c) visualizes the flow opening of the housing.

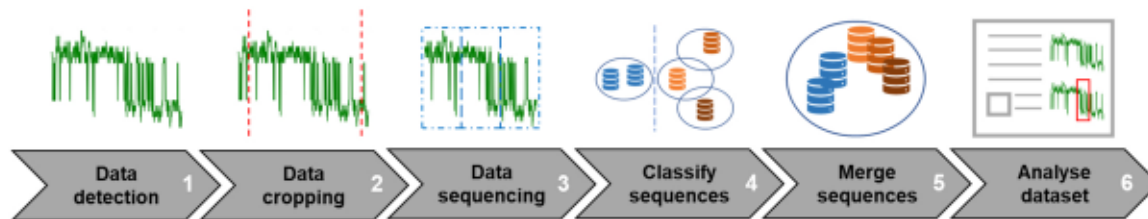


Fig. 3. Data preprocessing steps carried out for the ML investigations.

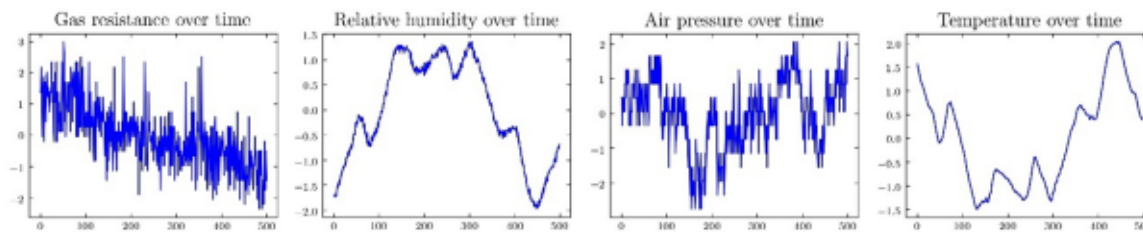


Fig. 4. Visualization of four different standardized environmental sensor parameter time series over the printing time for one normal FDM manufacturing process.

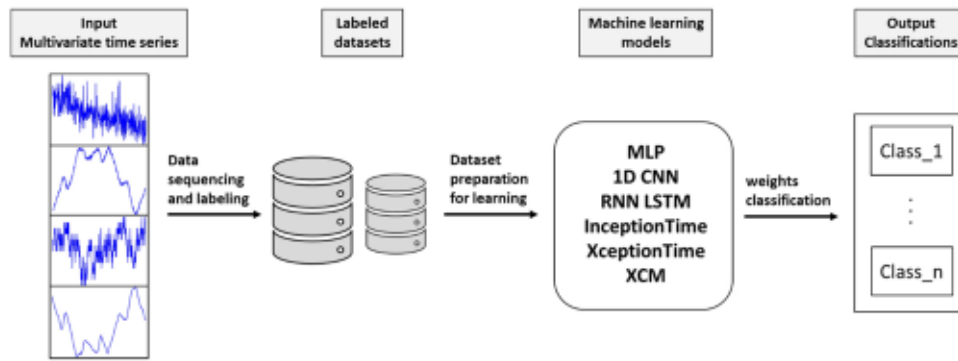


Fig. 5. Basic process flow of ML analyses with FDM environmental sensor data in this work.

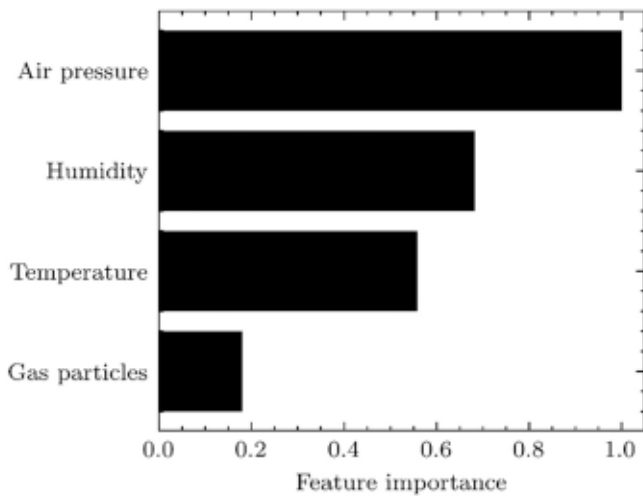


Fig. 6. Permutation feature importance analysis for the environmental sensor parameters based on the main dataset.

heatable glass plate print bed were used for printing. The printing material was PLA+ (Filamentworld, Neu-Ulm, Germany) with a filament diameter of 1.75 mm. A simple gearwheel with a base diameter of 35 mm and a height of 30 mm was constructed as the print object. The CAD program Autodesk Inventor Professional 2019 (Autodesk Inc., San Rafael, USA) was used for the design. The printed gear is shown in Section 4.2 in Fig. 9.

The necessary printing process parameters were set using the slicing software Ultimaker Cura version 4.8.0 (Ulimaker B.V., Utrecht, Netherlands) and adapted to different 3D printing conditions. The printing conditions result from the setting and variation of special print process parameters that are very relevant for the print quality in the FDM process (see Table 1). Basically, a distinction is made between one normal ("normal") and five different, deviating (here referred to as "defect") 3D printing conditions. The normal printing condition (normal_01) is the basic setting for the investigations and is made up of recommended process parameter settings for printing temperature and printing speed (recommended by material and system manufacturers) as well as filament and nozzle conditions usually present in production environments (we assume that due to continuous production and machine usage, there are always relatively new filament material and

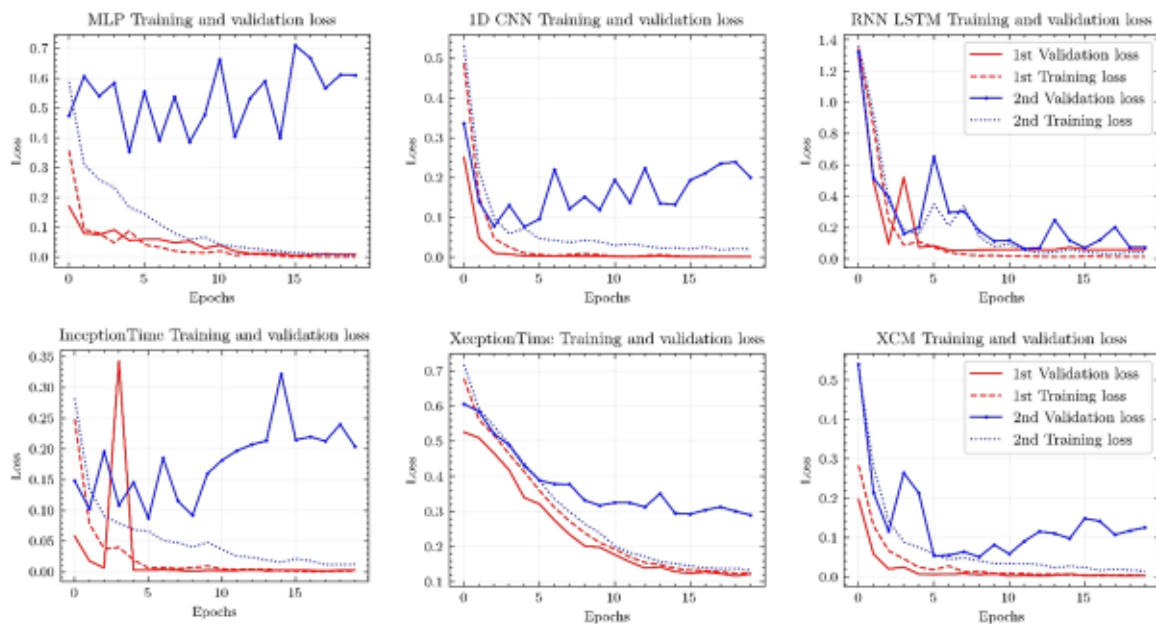


Fig. 7. Training and validation loss plots of the used ML algorithms with the main dataset.

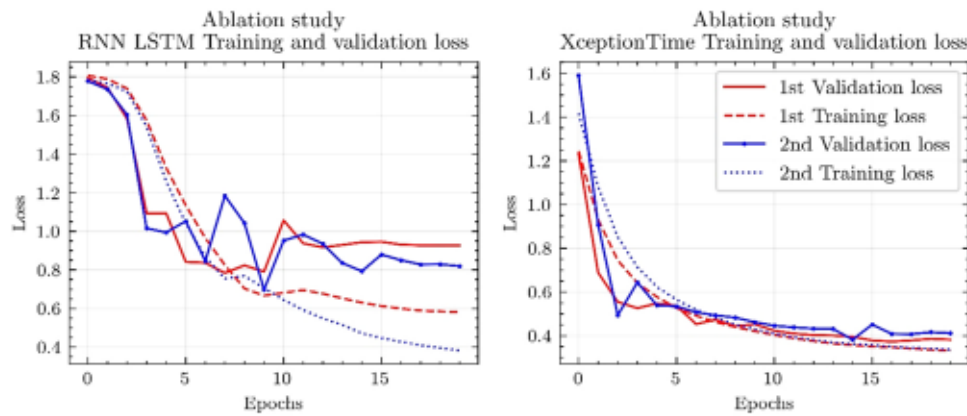


Fig. 8. Training and validation loss plots of the RNN LSTM (left) and XceptionTime (right) algorithms with the ablation dataset.

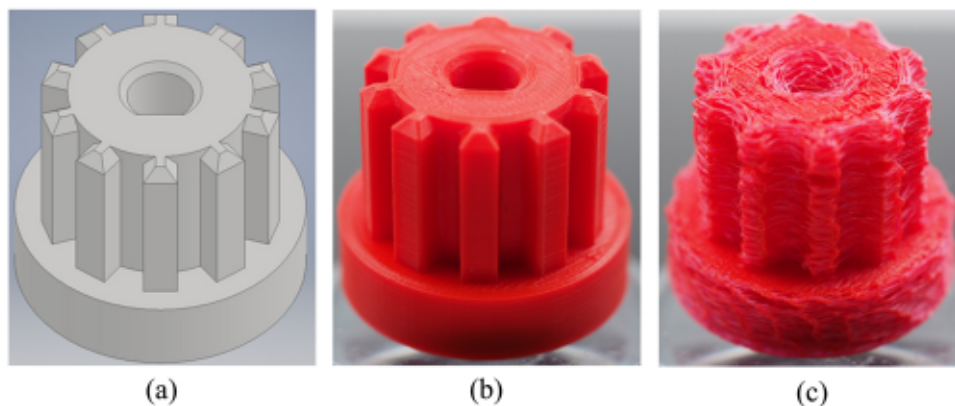


Fig. 9. Geometry spectrum of the designed and printed parts. (a) CAD design, (b) normal printed part, (c) printed part with clearly visible geometric defects.

retracted, used nozzles).

In terms of filament condition, a distinction is made between “new” (filament taken directly from an unopened original packaging, opened for a maximum of 7 days) and “old” (filament stored openly in a normal production environment for at least 12 months). The nozzle condition is divided between “new” (unused up to a maximum of 10 manufacturing hours of the nozzle used) and “used” (at least 15 manufacturing hours of the nozzle). The background to this is, on the one hand, that the nozzle wears out continuously in the course of its use [19]. On the other hand, we also suspect that it is simultaneously clogged with burnt filament particles (see also Fig. 1). It is therefore assumed that a used nozzle releases more gas particles, which affects the ML analyses. Thus, a new nozzle in FDM results in a different 3D printing condition. However, due to the assumption of continuous production, a new nozzle is a relatively rare and uncommon condition and is therefore considered below as a (defect) condition that deviates from the normal 3D printing condition.

The printing temperature is measured indirectly via the air temperature. It is assumed that, for example, the printing temperature ranges recommended by the filament manufacturers and temperature ranges that deviate from them can be recorded relatively easily. Knowledge of whether or not the recommended printing temperature ranges have been adhered to can then be used both to certify the printing process and, in combination with other sensor parameters, to characterize different 3D printing conditions.

The deviations from the normal state were set to simulate irregularities and printing errors or rather to enable different 3D printing conditions. To do this, the filament condition was first changed from “normal_01” by using an old filament. This 3D printing condition class is then referred to as “defect_01”. In addition, the condition of the nozzle was changed by using a new, unused nozzle for the printing tests. This printing condition class is characterized as “defect_02”. Another variation is “defect_03”, in which a new nozzle was used and a higher printing

Table 1
FDM process parameters for different 3D printing conditions.

Process parameter	Unit	normal_01 “optimal settings”	defect_01 “old filament”	defect_02 “new Nozzle”	defect_03 “higher temp”	defect_04 “higher speed”	defect_05 “blocked nozzle”
Nozzle	–	used	used	new	new	new	used
Filament	–	new	old	new	new	new	old
Print temperature	°C	210	210	210	240	210	240
Print speed	mm/sec	50	50	50	50	100	50
Constant parameters over all printing conditions							
Layer thickness	mm	0.2					
Infill	%	100					
Filament flow	%	100					
Initial layer speed	mm/sec	25					
Bed temperature	°C	60					

Table 2
Bosch BME680 environmental sensor parameter specifications [20].

Parameter	Temperature	Humidity	Air pressure	Gas particle resistance
Operation range	-40 85 C	0 100% r. H.	300 1100 hPa	50 300000
Accuracy	1 C	3% r.H.	0.6 hPa	2 5%
Resolution	0.01 C	0.008% r.H.	0.18 Pa	0.08%
Noise	0.005 C	0.01% r.H.	1.4 Pa	1.5%

temperature was set. A new nozzle was also installed for "defect_04" and the printing speed was increased. "defect_05" is a special condition class, as a regular printing error due to a partially blocked nozzle was recorded here during the production. All printing process parameters for the different printing condition classes are listed in Table 1. Only exemplary combinations of the printing process parameters considered were examined, as otherwise the production and time expenditure would have been too high. This work is also not a 3D printing study, but an ML study with special method development, in which the consideration of exemplary sample cases is sufficient.

The environmental sensor data was recorded using a Bosch BME680 environmental sensor (Bosch Sensortec GmbH, Reutlingen, Germany), which was already installed on a development board (SIMAC Electronics GmbH, Neukirchen.Vluyn, Germany) and a Raspberry Pi 3B (OKdo Technology Ltd., London, UK). A 128 GB USB stick (SanDisk Corp., Milpitas, US) was used for data storage. The technical data of the sensor with the specifications of the individual measured variables are defined in [20] and listed in Table 2. In addition, a self-developed and 3D-printed sensor housing made of PLA was designed to accommodate the sensor board and mount it on the printing extruder in such a way that all sensor parameters can be measured as close as possible to the filament extrusion (see Fig. 2). For this purpose, the sensor was placed next to the printer nozzle in the air flow of the component cooling. In order to protect the sensor from excessive high temperatures and soiling by plastic threads, it was installed facing away from the nozzle and provided with a flow opening.

The Raspberry Pi serves as a voltage source and for data transmission with the environmental sensor. The data transfer was provided via Inter-Integrated Circuit (I²C), with the Raspberry Pi acting as the master of the I²C communication. Concerning the hardware, the connection is implemented via copper cables with DuPont connectors, which are fixed with strain relief to ensure reliable communication.

For the interaction between the single board computer and the environmental sensor, a computer program was written with the programming language Python Version 2.7.16 (python software foundation, Fredericksburg, US). In addition, a special BME680 software library (Pimoroni Ltd., Sheffield, UK) was implemented in order to be able to use predefined functions for I²C communication, sensor configuration as well as measuring and reading out the data. This was then used to set oversampling values for the temperature, air pressure and humidity recording and to define the temperature and heating duration of the gas particle measurement. The basic values from the BME680 library were used as the starting point for the sensor configuration. The resulting python program saves the detected data during the measurements in a comma-separated values file (CSV file).

For further processing of the recorded environmental sensor data, a web server was installed on the Raspberry Pi which enables internet access to the CSV files via an internet protocol (IP) address and a web browser. Using the Secure File Transfer Protocol (SFTP) it is then possible to transfer encrypted data between the Raspberry Pi and an external computer. The open-source program FileZilla version 3.53 (FileZilla-Project.org, Cologne, Germany) was used to the securely transfer the CSV sensor files.

3.2. Environmental sensor datasets

In this work, two datasets are used for supervised learning. A larger dataset with labeled data and an unbalanced structure (approx. three times more data of the "normal" 3D printing condition class are recorded than for the other printing condition classes) for the main investigations (main dataset) and a smaller dataset with labeled data and a balanced structure (all printing condition classes have the same number of data) for a subsequent ablation study (ablation dataset). According to Biedenkapp et al. [21], the ablation study aims to examine the influence of certain parameter meanings or analysis conditions (in this case the size of the dataset and the distribution of the data) on the changes in performance of the ML algorithms.

The datasets used in this work are composed of the environmental sensor parameters recorded by the environmental sensor during the additive manufacturing process on an FDM printer. During the process, constant current time stamps of the environmental sensor values as well as the environmental sensor parameters temperature at the sensor, humidity, air pressure and resistance of the gas particles were detected with a recording rate of 2 Hz. We initially assume that each of the environmental sensor parameters recorded has sufficient influence on the printing process, which can then be recorded by the ML algorithms. Since we initially have no system knowledge about the influence of the respective parameters on the ML analyses, we do not categorically exclude any parameters from the investigations in advance. Moreover, the effort required to record all the environmental parameters examined here is low. However, as part of the scope of the investigations, a feature importance analysis was also carried out to determine the relevance of the individual sensor parameters for the ML analyses.

All data of a manufacturing process were then written to a CSV file. The main dataset generated in this way consists of 19 individual CSV files with the recorded environmental sensor data for each production process. This results in 19 physically printed components, with ten components being manufactured with the process parameter configuration "normal_01" and three components each with the configurations "defect_01", "defect_02" and "defect_03". The ablation dataset is smaller with a total of six CSV files and only contains one CSV file each for the process parameter configuration "normal_01", "defect_01", "defect_02", "defect_03", "defect_04" and "defect_05".

3.2.1. Data preprocessing and data structure

For the planned investigations in this paper, the data must be pre-processed. To do this, they are first detected during the manufacturing process and saved in a CSV file. The data files are then manually cropped to remove the start and end data values. Accordingly, the exact time of the start of printing of the first printing layer and the exact end time of the last printing layer were recorded for each production process. All values before and after were deleted from the CSV file. In addition, the first two minutes of the production process were also deleted, since, at this point, there was not yet a stable and consistent printing process in place. This results in CSV files with exactly 20000 value pairs for the main dataset, which represent a stable production process of approximately 2 h 48 min. For the ablation dataset, CSV files with 12000 value pairs were created, which represent a production process of approximately 1 h 40 min. Then, using a python script, the cropped data records are automatically divided into sequences with exactly 500 consecutive value pairs and a title line for the column names. This results in 40 sequences for the main dataset and 24 for the ablation dataset. The sequences are then manually divided into the respective 3D printing condition classes of "normal" and "defect" and assigned a corresponding binary identifier. The classified and marked data are then merged to form a new overall dataset. After this step, the main dataset comprises 380000 pairs of sensor values and the ablation dataset 72000, which are then analyzed by ML algorithms for special features. The individual preprocessing steps are listed in Fig. 3 below.

For the classification and training of the ML algorithms, this results

Table 3
Hyperparameter settings for all ML algorithms used in this work.

Cost Function	Learning rate (Lr)	Optimizer	No. Epochs	Batch size	Lr Decay
Categorical cross entropy	1 10^{-3}	Adam	20	64	patience 5

in a data structure based on individual manufacturing process data, each of which is subdivided into time-dependent sequences with always 500 successive pairs of sensor values and one line of text. The sequences are then marked and merged to form larger datasets. The manufacturing process data, the data structure of the resulting datasets and the individual sequences are accessible online in a data repository: <https://doi.org/10.17632/pprxj2yfyby.1>.

3.2.2. Data distribution and hyperparameter settings

The main dataset and the ablation dataset each have a different data distribution. The main dataset is created with a data imbalance and the ablation dataset with a data balance. A (binary) data imbalance occurs when one class contains significantly more values than another class [22]. Accordingly, a data balance characterizes a uniform data distribution over the classes to be classified. However, the main dataset generated here does not exhibit a binary imbalance problem because it contains more than two different classes. This problem is, according to Tanha et al. [23] described as a multi-class imbalance. In this case, the dataset is imbalanced if the number of values in a class is significantly above or below the number of the individual remaining classes [23,24]. In the main dataset, the class with the normal values is more than three times as extensive as the remaining defect classes. Within the ablation dataset, all classes are evenly distributed and have the same number of sensor values. The data distribution must therefore be taken into account when evaluating the investigations, as there are different techniques for balanced and imbalanced problems [24]. The evaluation techniques used in this work are described below in Section 3.5.1.

So-called hyperparameters are used to vary certain settings in ML algorithms. For the training of the ML algorithms investigated in this research, suitable hyperparameters were determined in preliminary tests and then held constant throughout all investigations. The hyperparameter settings used are listed below in Table 3 and are described by Hutter et al. [25] in detail.

3.3. Artificial intelligence and machine learning

AI is defined as the automation of intellectual tasks normally performed by humans [26]. ML takes a relatively new approach to AI development, in which computer algorithms perform analyses, which in turn enable computer programs to automatically improve themselves through experience [26,27]. Correspondingly, according to Chollet [26], a ML system is trained rather than explicitly programmed. A lot of data for a task to be examined is then considered by the ML system and analyzed in terms of a statistical structure, which then enables the system to develop rules for automating the task at hand. In the process, ML is used, for example, to identify objects in images, to convert speech into text or to make predictions from data. All these applications increasingly make use of a special class of techniques, which in turn are referred to as deep learning (DL) and are a sub-area of ML [28]. In this context, DL is a new way of looking at learning information from data, with a focus on learning from successive layers of increasingly important data representations [26]. Learning with these layer representations takes place using models that are referred to as artificial neural networks [26]. These neural networks are relatively easy to implement, computer-based computational models that were inspired by the neurosciences and are used for a variety of problems such as pattern classification and pattern recognition [29]. Artificial neural networks are one of the most powerful ML methods and are extremely suitable for processing large amounts of

data [30].

A multilayer perceptron (MLP) is the simplest and most original form for DL architectures and is also referred to as a fully-connected (FC) network which consists of a linear stack of completely connected network layers, since every neuron in one layer is connected to every neuron in a next layer [31]. Because of this property, the number of network parameters (such as neurons with their adapted weightings and the respective threshold value) can become very high and tend to have redundancies. Another disadvantage is that spatial information is not considered, e.g. each time stamp has its own weighting, whereby the time information is lost and the time series elements are treated independently of each other [31].

One of the most popular DL implementations for modeling spatial and temporal correlations is the convolutional neural network (CNN) [32]. CNN implementations are state-of-the-art in image and speech processing [33]. However, it is also possible to use it to evaluate time-correlated measured values of time series signals. [34]. In this context, a convolution can be viewed as a filter that is applied and shifted over the time series, whereby the filter has only one dimension (time) instead of two dimensions as with images (width and height) [31]. The classification of activities or peculiarities in the time series is then based on the extraction of special distinguishing features in the one-dimensional time series, which are recorded by sensors [35]. There, it is important, on the one hand to have strongly correlated, temporally close measured values [32] and, on the other hand, appropriately designed feature representations of sensor data and suitable classifiers [35].

Another frequently used DL implementation for the analysis of large amounts of data is recurrent neural networks (RNN), which are capable of learning long-term dependencies in sequential data [36]. A modern RNN architecture with very good performance, inter alia when evaluating raw time series data, is the long short-term memory (LSTM) architecture [37,38]. The LSTM architecture has a very good learning capability and corresponds to the state-of-the-art in several areas, both practically and theoretically [39].

Other modern DL implementations for time series analyses are partly based on known network architectures that are already successfully used in image analyses. These include, among others, InceptionTime [40] and XceptionTime [41]. New models for extracting information from time series based on compact convolutional neural network elements are also being developed. This includes in particular the eXplainable Convolutional neural network for Multivariate time series classification architecture (XCM) [42]. All of these modern networks have a very deep and complex structure, which enable high accuracy, good generalization and scalability, but also require more computing power and possibly computing time.

3.4. Machine learning structures used in these investigations

In this work, different ML models were used to detect specific activities in sequenced environmental sensor data. Fig. 4 shows excerpts of the recorded and standardized environmental sensor parameters of a normal FDM printing process, which are then analyzed by the architectures described below. In this process, all examinations were undertaken using a local workstation computer with a Windows 10 environment, a Nvidia GeForce RTX 2080 Ti GPU with 11 GDDR6 VRAM and an Intel Core i7 9700k CPU with 3.6 GHz, 8 cores and 32 GB RAM.

All ML algorithms used were implemented with the open-source DL package tsai [43] in python version 3.7.7. This means that current state-of-the-art time series classification models based on scientific publications are utilized, which can be applied in a comparable and reproducible manner. The basic process flow from the input of the sensor data to the output of the classification results is the same for all implemented algorithms and is shown in Fig. 5.

A simple MLP was used as the first ML architecture for the investigations. The basic structure of the MLP developed in this work is

based on the architecture developed and proposed by Wang et al. [44]. There, the network consists of three layers, all of which are completely interconnected. Then a relatively simple 1D CNN was used. The architecture was again developed by Wang et al. [44]. By that, the 1D CNN has a very compact structure with three convolution blocks consisting of a convolution, a batch normalization and a ReLU activation layer. The batch normalization accelerates the convergence speed and helps to improve the generalization of the network and to avoid overfitting. The features of each classification category extracted from the convolution blocks are then vectorized by a global average pooling operation (GAP) [45] and transferred to the output layer with a softmax classifier. With GAP, the classification of the network is easier to interpret and less prone to overfitting than the FC layers otherwise commonly used [45]. A third neural network architecture is based on an LSTM architecture in accordance with Hochreiter and Schmidhuber [37]. The model consists of three LSTM layers with an input unit, an output unit and a cell block, which can be thought of as a complex memory cell that regulates the flow of information and can run through several time steps without losing the information and weightings recorded in the process [36]. The LSTM generalizes well for many problems, which is good for avoiding overfitting and also results in more stable runs and faster learning times than other algorithms [37].

The InceptionTime, XceptionTime and XCM architectures were used to compare the models described before with these recent state-of-the-art DL implementations. InceptionTime generalizes well to real datasets, reduces the dimensionality of the time series as well as the model complexity, whereby overfitting can be reduced with a sufficiently large number of training data [40]. XceptionTime is very robust against temporal interruptions in the input and independent from the length of the input. In addition, the use of the depth wise separable convolutions makes it far less complex and less prone to overfitting [41]. The XCM architecture extracts information directly from the input data (with 1D and 2D filters) and thus enables good generalization to both small and large datasets with little susceptibility to overfitting [42].

3.5. Performance measures

Three aspects are analyzed in this study. One is the sensitivity of the environmental sensor parameters in the ML examinations. Another is the performance of the developed ML algorithms and the last is the comparison of the recording of the part quality with the printed test parts. In

order to examine the sensitivity of the sensor parameters, a permutation feature importance analysis is carried out. To evaluate the algorithms, specific performance metrics are used to present and summarize the results. To evaluate the part quality, an optical 3D measurement of the components is carried out with a 3D scanner to enable a quality comparison between the different 3D printing condition classes.

3.5.1. Neural network evaluation metrics

The selection of a suitable metric for examining and differentiating the performance of different classification algorithms is an important aspect in ML, because the correct selection of the metric ensures that the classification training of the algorithms is uniformly evaluated according to suitable criteria [46,47]. There are balanced and unbalanced records in the data on which the classification tasks are based. The main dataset results in an unbalanced dataset with a multi-class problem. For the investigations of the ablation dataset, a balanced dataset was created in which each class is equally likely. For classification tasks, the results can still be displayed in a specific confusion matrix (CM) [48]. The CM is a crosstab that records the number of specific cases between the present classes and between two criteria (predicted and actually occurred) [47]. A basic example for the CM of the investigations carried out in this work is given in Table 4. The most important are the True Positive (TP) values, which represent the correctly classified sequences. True Negative (TN) values are all other, incorrectly classified sequences. False Positive (FP) and False Negative (FN) values are the summed, misclassified elements in the columns and rows. They are also relevant for calculating the performance metrics.

It should be noted that there is a multi-class classification for both generated datasets and correspondingly adapted calculation bases are to be used. For this reason, Accuracy, Macro Average Precision, Macro Average Recall and Macro F1-Score were used for the investigations carried out in this work. These metrics are defined below and explained in detail by Sokolova and Lapalme [49] as well as Grandini et al. [47]:

$$Accuracy = \frac{TP + TN}{TP + TN + FP + FN} \tag{1}$$

$$Macro\ Average\ Precision = \frac{\sum_{k=1}^K \frac{TP_k}{FP_k}}{K} \tag{2}$$

$$Macro\ Average\ Recall = \frac{\sum_{k=1}^K \frac{TP_k}{FN_k}}{K} \tag{3}$$

$$Macro\ F1-Score = 2 * \left(\frac{Macro\ Average\ Precision * Macro\ Average\ Recall}{Macro\ Average\ Precision^{-1} + Macro\ Average\ Recall^{-1}} \right) \tag{4}$$

Table 4
Principal CM scheme for the examinations in this work. The red border characterizes the CM for examinations with the main dataset and the blue border characterizes the examinations with the ablation dataset.

		Predicted class					total	
		Classes	normal 01	defect 01	defect 02	defect 03		defect 04
True class	normal 01	TP	TN	TN	TN	TN	TN	FN
	defect 01	TN	TP	TN	TN	TN	TN	FN
	defect 02	TN	TN	TP	TN	TN	TN	FN
	defect 03	TN	TN	TN	TP	TN	TN	FN
	defect 04	TN	TN	TN	TN	TP	TN	FN
	defect 05	TN	TN	TN	TN	TN	TP	FN
total		FP	FP	FP	FP	FP	FP	

To find out more information about the sensitivity of the environmental sensor parameters to the ML algorithms, a permutation feature analysis is performed. This feature importance measurement was introduced by Breiman [50] especially for random forests. In principle, the increase in the prediction error of the respective model is determined after individual values of a feature have been swapped [50]. The importance of a feature is measured accordingly, with a feature being important when the model error increases (the characteristic is important for a good classification) and unimportant when it decreases (the characteristic leaves the model error unchanged and is of limited relevance for the classification). This is a common way of measuring the sensitivity of input characteristics in ML.

3.5.2. 3D Scan for part quality measurement

In order to enable an optical quality comparison between the different 3D printing condition classes, a dimensional check was carried out on the printed components with a 3D light scanner with ATOS Core Sensor (GOM GmbH, Braunschweig, Germany). This method has been used in previous publications to compare the impacts of printing

parameters on the respective dimensional deviations of the printed parts [4]. The optical scanning system used has a camera resolution of 2448 × 2050 pixels at a frame rate of 7 Hz and 5 million measuring points per scan. The system is therefore suitable for capturing details and even the smallest geometrical deviations in the printed components. For the overall result, several individual scans were performed to reproduce the surface topography of the components as completely as possible. GOMscan software (GOM GmbH, Braunschweig, Germany) was then used to convert the individual point clouds into complete scan views. Surface comparison measurements were made between the printed components and the designed CAD reference models to evaluate the effects of the various 3D printing condition classes and to make qualitative statements about the print quality. The surface comparisons then provide a colored representation of the inspected surface areas, which show their deviations from the CAD reference model.

4. Results

4.1. Permutation feature importance analysis

The sensitivity analysis of the sensor parameters was carried out with

Table 5

Performance metrics for ML algorithms for the classification of sensor data at the FDM process for all investigations with the main dataset.

Experiment	Model	Confusion Matrix				Accuracy	MacroAvg Precision	MacroAvg Recall	Macro F1-Score	Time [mm:ss]
1st	MLP	793	2	0	0	0.999	0.999	0.998	0.999	00:20
		0	236	0	0					
		0	0	240	0					
		0	0	0	239					
	1D CNN	795	0	0	0	0.999	0.999	0.999	0.999	
		0	235	1	0					
		0	0	240	0					
		0	0	0	239					
	RNN LSTM	795	0	0	0	0.991	0.986	0.989	0.988	
		0	231	5	0					
		0	0	236	4					
		4	0	0	235					
	Inception Time	795	0	0	0	0.999	0.999	0.999	0.999	
		0	235	1	0					
		0	0	240	0					
		0	0	0	239					
Xception Time	793	0	0	2	0.997	0.997	0.996	0.997		
	0	235	1	0						
	0	0	239	1						
	0	0	0	239						
XCM	795	0	0	0	0.999	0.999	0.999	0.999		
	0	236	0	0						
	0	0	240	0						
	0	0	1	238						
2nd	MLP	725	0	70	0	0.947	0.968	0.938	0.952	00:20
		2	234	0	0					
		4	0	235	1					
		0	0	3	236					
	1D CNN	724	0	71	0	0.952	0.976	0.941	0.958	
		0	235	1	0					
		0	0	239	1					
		0	0	0	239					
	RNN LSTM	793	2	0	0	0.989	0.985	0.987	0.986	
		1	231	4	0					
		0	0	235	5					
		4	0	0	235					
	Inception Time	726	0	69	0	0.953	0.976	0.942	0.959	
		0	235	1	0					
		0	0	239	1					
		0	0	0	239					
Xception Time	722	0	71	2	0.952	0.977	0.941	0.959		
	0	236	0	0						
	0	0	240	0						
	0	0	0	239						
XCM	724	0	71	0	0.951	0.975	0.941	0.957		
	1	235	0	0						
	1	0	238	1						
	0	0	0	239						

the larger main dataset. The four recorded values of temperature, humidity, air pressure and gas particles were declared as features. The result is a representation of the relative importance of the individual environmental sensor parameters for the analysis and is shown in Fig. 6.

The feature importance analysis shows a clear gradation of the relevance of the individual sensor parameters for the ML analyses. The air pressure has the greatest influence, followed by the humidity, the temperature and the gas particles, which are least relevant for the classifications. This order is unexpected and also illogical from the point of view of AM, since barometric air pressure is usually not a relevant influencing variable for the printing process. In the ML context, however, this feature is much more important, which in turn is understandable, since even minor changes in air pressure are clearly noticeable in the generally relatively constant air pressure curves and generate a fairly easy to analyze and quite meaningful pattern of the feature. This feature then superimposes all other features and is weighted more heavily by the algorithms.

Since the context of AM is of great interest in this work, experiments with and without air pressure are conducted as a result of the feature importance analysis. By that, this characterizes on the one hand the real influence of the air pressure on the ML analyses and, on the other hand, examines the performance of the algorithms without the air pressure parameters that are irrelevant for 3D printing.

4.2. Time series classification results

Using the described ML architectures and the recorded environmental sensor data, two examinations were carried out; a classification of data structures on the main dataset and a classification of the data on the ablation dataset as part of an ablation study and to validate the results. Two experiments were carried out again for each examination; one experiment with all recorded environmental sensor data (temperature, humidity, air pressure, gas particles) and a second experiment without the air pressure values.

In the process, all algorithms were first trained with 80% of the data from the datasets and then validated with the remaining 20%. This is an established method to, for example, detect overfitting. The results and relevant performance metrics of the examinations for the main dataset are listed in Table 5 below. In addition, Fig. 7 shows the accuracy and loss curve of the examinations for the training and validation data of all

ML architectures with the main dataset.

All ML algorithms perform very well with the main dataset, with efficient classification of the individual 3D printing condition classes (see Table 5). The accuracies of the 1st experiment are always over 99%. Only very few sequences are classified incorrectly by the algorithms, which means that all other metrics consistently achieve very good values of at least 98%. If one also considers the training and validation losses from Fig. 7, the results can at least be confirmed for the training data. In the 1st experiment, the training loss gradually decreases in all models and reaches very low values of almost 0. This suggests that all algorithms found a relatively good fit for the training data in the course of the training. The validation loss also gradually decreases to very low values for all models after four epochs at the latest and remains there. As a result, the ML architectures also perform very well on unknown data, which is ultimately also mapped in the CM (see Table 5). It is also noticeable that the algorithms have longer computing times with increasing complexity.

In the 2nd experiment, in which the air pressure values were not included in the analyses, the performance values were consistently lower. The accuracies here are only about 95%, only the RNN LSTM performs a little better with approximately 98%. However, the classification of the sequences is still very effective overall. With all algorithms, with the exception of the RNN, the greatest uncertainty is clearly in the distinction between the states "normal_01" and "defect_02", which can be seen in Table 5 about the CM values. Both states are actually comparable, but differ in the state of the nozzle. Since the air pressure is not considered in the 2nd experiment, the differences can in principle only be detected via the gas particles. Since this parameter is least relevant for the ML algorithms according to the feature importance analysis, it is likely that many sequences of both classes are the same for the algorithms and are classified incorrectly.

The loss plots from Fig. 7, however, provide somewhat more differentiated insights into the effectiveness of the individual algorithms. While the training loss of all models continue to run as expected and gradually decrease, the validation losses no longer behave as expected. For all algorithms, they do not achieve as low values as with the training data and, with the exception of XceptionTime, are relatively noisy. At the MLP, there is no decrease of the validation loss, and with the 1D CNN, InceptionTime and XCM, the values for the validation loss peak after just a few epochs and then begin to increase again. This is

Table 6

Performance metrics for the RNN LSTM and XceptionTime algorithm for the classification of sensor data at the FDM process for all investigations with the ablation dataset.

Experiment	Model	Confusion Matrix						Accuracy	MacroAvg Precision	MacroAvg Recall	Macro F1-Score	Time [mm:ss]
1st	RNN LSTM	45	0	0	0	0	0	0.741	0.750	0.632	0.686	03:41
		0	46	0	0	0	0					
		2	4	16	0	28	0					
		0	0	22	23	5	0					
		5	0	0	0	40	5					
	4	0	0	0	0	45						
	Xception Time	44	0	0	0	0	1	0.972	0.973	0.827	0.894	
		0	460	0	0	0	0					
		0	0	49	1	0	0					
		0	0	0	50	0	0					
6		0	0	0	44	0						
2nd	RNN LSTM	40	0	0	0	0	5	0.676	0.683	0.670	0.676	03:16
		0	41	5	0	0	0					
		0	0	19	0	31	0					
		0	0	0	7	43	0					
		8	0	0	0	40	2					
	0	0	0	0	0	49						
	Xception Time	45	0	0	0	0	0	0.969	0.970	0.830	0.895	
		0	46	0	0	0	0					
		0	0	49	1	0	0					
		0	0	0	50	0	0					
7		0	0	0	43	0						
1	0	0	0	0	48							

characteristic for overfitting and indicates that these algorithms adapt too much to the specific patterns of the training data. As a result, the algorithms initially do not generalize the information that has already been learned to the new, as yet unknown validation data. The nevertheless quite good performance values are probably due to the strong similarity of the training and validation data. The validation loss courses from the RNN and the XceptionTime algorithm shows no obvious overfitting. The computing times also increase with the increasing complexity of the algorithms in this experiment, but are in principle somewhat shorter than in the 1st experiment, which can be attributed to the lack of air pressure data.

The examinations with the ablation dataset are based on a much smaller database than with the main dataset. This fundamentally increases the risk of overfitting. For this reason, only the RNN LSTM and the XceptionTime algorithm are used for further investigations, as they proved to be the most resistant to overfitting in the first experiment with the main dataset. The results of the examinations with the ablation dataset are listed for the performance metrics in Table 6 and for the courses of training and validation loss in Fig. 8.

For the ablation dataset, the performance between the two algorithms used is very different. In the 1st experiment with the air pressure data, the RNN LSTM architecture only has an accuracy of approximately 74% and in the 2nd experiment without the air pressure values, it is even a slightly lower value of approximately 68%. But in view of the CM values, there is still a basically functioning classification, at least between special classes. If the Macro F1 score is also included, which only achieved values of just under 68–69% for both experiments, it can ultimately be concluded that the RNN LSTM algorithm predicts some classes poorly with little data and therefore does not work reliably overall. Looking at the loss profiles from Fig. 8, one explanation for the

poor performance, among other things, is overfitting. While the training loss in the 1st experiment gradually decrease and thus shows a good fit for the training data, a peak is reached in the validation data after nine epochs, after which the loss values rise again and before stagnating. Overfitting occurs. In the 2nd experiment, the loss courses for both the training and the validation data are similar. In addition, they do not reach as low values as in the 1st experiment and already indicate overfitting in the training data.

The XceptionTime algorithm shows good to very good values in all areas in both the 1st and 2nd experiments. The accuracies here are around 97% and the Macro F1 scores of around 90% indicate a good classification for all classes. Even more remarkable, however, are the loss courses from Fig. 8. Training and validation loss courses decrease successively in both experiments, reach approximately the same minimum values, are not very noisy and show no overfitting. This is optimal behavior and interesting in that it was not previously achieved with such clarity by any algorithm in the large main dataset.

4.3. Part quality results

In addition to the manufacturing parameter data and the ML algorithms, the manufacturing results were also examined in more detail. For this purpose, the geometric spectrum of the printed parts is first analyzed, from the CAD reference geometry used (Fig. 9, left) to a relatively precisely printed part (Fig. 9, middle) to a generated part with clearly recognizable geometric defects (Fig. 9, right).

This is followed by a quality comparison with an optical 3D scan for three components of every 3D printing condition class. The results of one analyzed component of each of the different 3D printing conditions are shown in Fig. 10. This should represent a first proof of concept, with

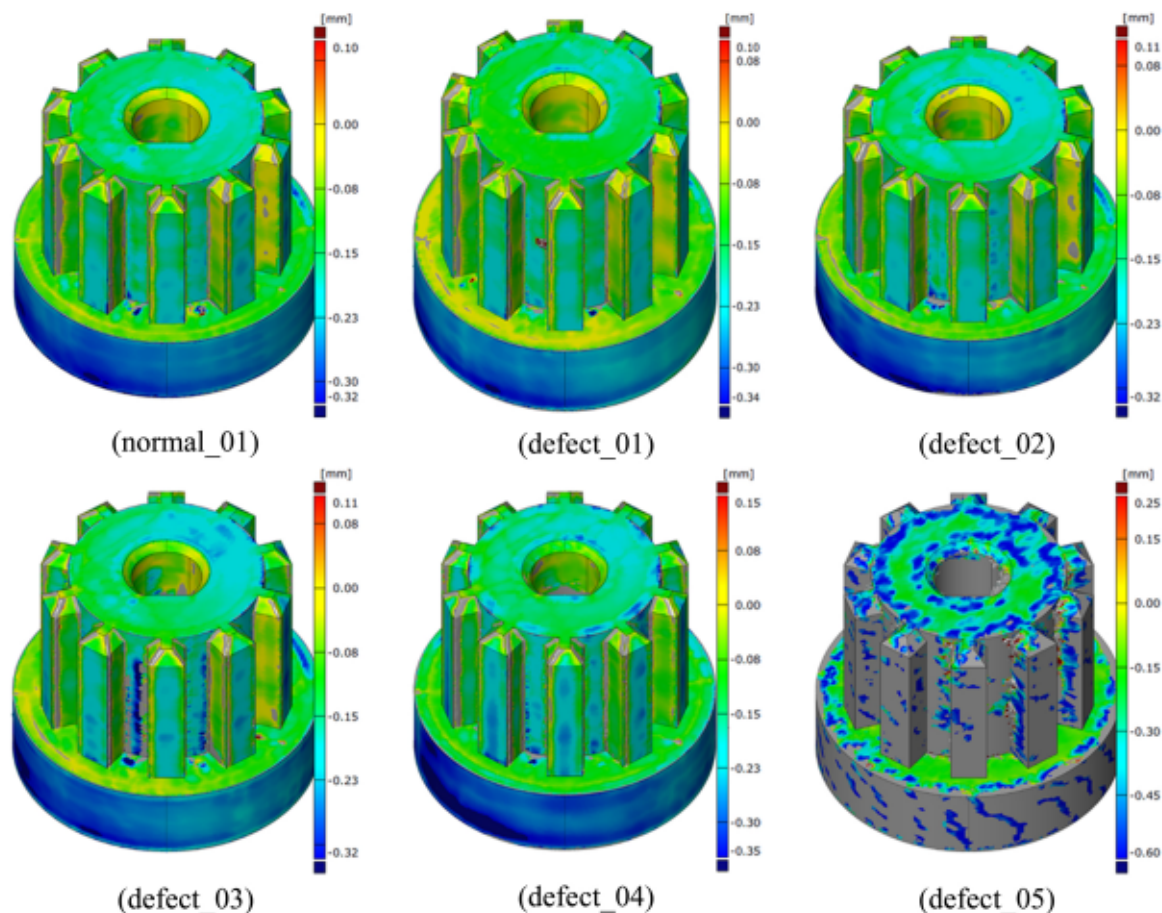


Fig. 10. Dimensional control with an optical 3D light scanner to compare the quality of the printed parts with the different printing conditions.

which it is shown that ML analyses enable an effective alternative to optical 3D scan examinations.

In the quality comparison generated in this work, the dimensional deviations between the specified CAD reference data and the generated part geometries are shown in color. The color representation is also associated with a numerical indication of the dimensional deviations in mm. Yellow and green areas correspond to very small to smaller deviations between the examined areas, blue areas visualize larger negative differences and red areas characterize maximum positive area differences. The quality comparisons between the 3D scans of the components printed with the individual 3D printing condition classes are all quite similar except for defect_05. At first, there is no clearly visible difference that can be seen. However, on taking a closer look at the legends of the 3D scan images, smaller gradations can be seen. The printing condition "normal_01" forms the reference with the optimal print settings and maximum deviations of 0.10 mm to 0.32 mm. In comparison, the printing condition "defect_01" shows slightly higher negative deviations of 0.34 mm. The 3D printing conditions defect_02 and defect_03 again show slightly higher positive deviations of 0.11 mm to normal_01, but are visually indistinguishable from one another. The condition "defect_04" deviates a little more from the optimal conditions, both positive with 0.15 mm and negative with 0.35 mm. Overall, however, the differentiation of the 3D printing conditions based on the optical 3D scans remains difficult. Only the condition "defect_05" can already be clearly recognized optically, since on the one hand the maximum deviations of 0.25 mm and 0.60 mm are clearly above the optimal conditions and on the other hand a large part of the component area was not captured by the 3D scan and is therefore shown in gray in the quality comparison images.

Overall, however, the differentiation of the 3D printing conditions based on the optical 3D scans remains difficult. Only the condition "defect_05" can already be clearly recognized optically, since on the one hand the maximum deviations of 0.25 mm and 0.60 mm are clearly above the optimal conditions and on the other hand a large part of the component area was not captured by the 3D scan and is therefore shown in gray in the quality comparison images.

5. Discussion

A large number of findings relating to various aspects of the investigation were generated from the research work previously carried out.

5.1. Findings related to additive manufacturing

With the proposed test setup, different environmental sensor data can be recorded and further processed in a simple manner during the AM process. The analysis of the detected and preprocessed data with state-of-the-art ML algorithms is then possible with a supervised learning approach. In this way, different 3D printing conditions that occur in reality can be labeled and used for effective algorithm training, which ultimately also enables automatic and intelligent classification of 3D printing condition classes by the ML algorithms. Not all recorded environmental sensor parameters are equally important for the ML analyses. The sensitivity analysis carried out showed that AM-relevant process parameters can have different relevance in the ML context. The barometric air pressure in particular is usually not of great importance for the printing process, but it is for the ML analyses. It is most relevant to the investigations carried out, followed by humidity, temperature and gas particles. It should be noted, however, that by using an open 3D printing system, the external environmental influence on the data turned out to be stronger and so changes in the environment of the printer might be included in the ML analyses to a greater extent than with a closed system. However, it can already be clearly seen here that differences in the printing temperature result in very well differentiable data (see CM in Table 5 and Table 6). The print status "defect_03" (higher temperature) was almost always detected without any doubt.

5.2. Findings related to machine learning

The strong relevance of the air pressure for the ML analyses is understandable, since the patterns present in this sensor parameter are relatively clearly recognizable and thus dominant. The air pressure is always fairly constant and even small fluctuations or pressure

differences between different data sequences are clearly visible. The other environmental parameters are noisy and patterns are less clearly recognizable. The importance of the air pressure becomes clear in the experiments carried out with and without air pressure data from Table 5 and Fig. 7 included in the analyses. The inclusion of the air pressure values, which are irrelevant for the AM process, initially increases the computational costs slightly. However, the performance of the ML algorithms is always worse without the air pressure data and tends more to overfitting. The air pressure parameters therefore basically have a stabilizing influence on the analyses and contribute to a better generalization of the examined ML architectures, which in turn is positive for the classification of new, unknown data. It can therefore make sense to record as many process parameters as possible, despite a slightly higher resource consumption, provided that the effort involved is low, in order to first examine their respective relevance for ML analyses and their effects on the generalization. Furthermore, it can be seen that older and at the same time simpler algorithms perform similarly to modern, more complex algorithms. However, the simpler algorithms require significantly shorter computing times and are therefore more resource-efficient. If the susceptibility to overfitting is considered, both the simpler RNN LSTM and the more complex XceptionTime architecture achieve the best results with an effective classification for the larger main dataset.

This effectiveness could only be confirmed for XceptionTime in the ablation study with the smaller ablation dataset (see Table 6). This modern algorithm copes much better with less and at the same time more differentiated data than the RNN LSTM, where no effective classification has taken place and overfitting has already occurred in the 1st experiment and there already in the training data (see Fig. 8). The following findings can thus be drawn specifically from the ablation study:

More data is better for an effective time series classification. Modern and more complex ML algorithms for time series classification perform better than simpler ones with smaller databases. With little data and even without the air pressure values, XceptionTime is very effective and robust against overfitting. XceptionTime generalizes better with more differentiated data and basically enables an effective classification of 3D printing conditions with environmental sensor data.

5.3. Findings related to quality assurance

The results of the ML analyses can make a productive contribution to quality assurance in AM. The trained algorithms can, for example, analyze data in the respective printer software in parallel with process monitoring and provide information on the current print quality relatively quickly. Furthermore, based on the presented ML analyses, intelligent online services could be developed which interact with 3D printers connected via the internet and continuously monitor the printing process. In addition, the generated results can serve as a supplement to conventional quality assurance or replace established quality assurance procedures such as optical 3D scans. The 3D scan can only be used superficially and after the component has been manufactured and is only very poorly suited to differentiating between different printing conditions. ML, on the other hand, is much better suited to differentiating the printing conditions with effective algorithms, as it can perform quality control for all external and internal component structures faster, more precisely, more easily and, above all, production-integrated. It is also non-destructive, can be implemented relatively cheaply and can also enable process-integrated, one hundred percent quality control and documentation in almost real time. For a corresponding industrial application of the presented methods, however, improved, increasingly automated processes must be developed. In addition, more and more diverse data must be added to the database of the algorithms to ensure even more robust classification.

6. Conclusions

In this work we present different simple and more complex state-of-the-art machine learning (ML) algorithms for an intelligent classification of manufacturing data, which was recorded during the Fused Deposition Modeling (FDM) process. For this purpose, the environmental process parameters temperature, humidity, air pressure and gas particles are recorded by an environmental sensor, sequenced and pre-classified for training the intelligent algorithms. A sensitivity analysis regarding the relevance of the parameters was also carried out. The air pressure is the most important parameter in the ML context and has the greatest influence on the analyses. The sequenced data were then stored into a larger unbalanced and a smaller balanced dataset. The datasets then served as the basis for data analyses using the deep learning techniques as well as for two experiments with and without the weighty air pressure parameters. The RNN LSTM and XceptionTime architecture obtained the most effective results overall, achieving high performance metrics and good robustness against overfitting with the large, unbalanced dataset. The results were then validated in an ablation study using the smaller, balanced dataset. The XceptionTime model performed best, with Accuracy (0.969) and Macro F1-Score (0.895) as well as good robustness against overfitting even on the 2nd experiment without the important air pressure values. In this way, an effective classification of 3D printing condition classes could be achieved. In a first proof of concept, the results of the data analyses were also compared with optical 3D scan component quality investigations. For this purpose, the printed FDM component samples were optically scanned and compared with a reference geometry in order to determine the dimensional deviations. However, the dimensional deviations for the various 3D printing condition classes examined in this work are usually very small and difficult to determine optically. The ML data analysis of the environmental parameter data of the FDM process has proven to be more effective, faster and more cost-effective in order to identify differences between the various 3D printing conditions. Based on all results, the modern XceptionTime architecture is the most effective and at the same time most suitable for a future real-time evaluation of FDM manufacturing data. It also enables an effective, inexpensive alternative to non-destructive quality assurance with optical 3D scans and can also enable process-integrated one hundred percent quality control.

In the future, the data analyses should be extended to include additional process parameters (e.g. acceleration and sound parameters) in order to achieve even more precise and stable analysis results. Another future task is to be able to perform data detection, preprocessing and analysis even more automatically and inline during the production process and to feed the results back to the production system in real time. A semi supervised learning approach with pretrained ML algorithms could be suitable for achieving automated, intelligent and self-optimizing quality assurance with ML. This approach could automatically divide new data into the trained classes and provide quality assurance with a continuously growing database for decision-making. This is of particular interest for the industrial use of ML algorithms, as this could implement an artificial intelligence for quality assurance of the printing process that does not need to be explicitly programmed or regularly optimized. The structure of the data preprocessing should also be optimized, e.g. improved data sequencing can contribute to simplified analyses and better results. Additional investigations with a larger database can also contribute to better classification results and new dropout and weight regularization operations can reduce overfitting. The inclusion of different manufacturing data in the database is also important in the future. A combination of the knowledge of the 3D printing conditions and the actual resulting component quality could also be beneficial for optimizing the classification results. For this purpose, the training database would have to be continuously adapted after the printing processes. Especially when comparing the ML analyses with the optical 3D scans, the proof of concept presented here must additionally be validated and the results evaluated in the future. For this

purpose, for example, a freeform part can be used, other manufacturing parameters can be selected or a completely different additive manufacturing process can be utilized.

Funding

This research was funded by the European Union, which was made available through the European Regional Development Fund (ERDF) and the Ministry for Economics, Employment and Health of Mecklenburg-Vorpommern, Germany, grant number TBI-V-1-345-VBW-118.

CRedit authorship contribution statement

Erik Westphal: Conceptualization, Data curation, Formal analysis, Funding acquisition, Investigation, Methodology, Resources, Software, Validation, Visualization, Writing original draft. **Hermann Seitz:** Funding acquisition, Investigation, Supervision, Writing reviewing & editing.

Declaration of Competing Interest

The authors declare that they have no known competing financial interests or personal relationships that could have appeared to influence the work reported in this paper.

References

- [1] I. Gibson, D. Rosen, B. Stucker, *Additive Manufacturing Technologies*, Springer, New York, New York, NY, 2015.
- [2] K.V. Wong, A. Hernandez, A review of additive manufacturing, *ISRN Mech. Eng.* 2012 (2012) 1–10, <https://doi.org/10.5402/2012/208760>.
- [3] M. Picard, A.K. Mohanty, M. Misra, Recent advances in additive manufacturing of engineering thermoplastics: challenges and opportunities, *RSC Adv.* 10 (2020) 36058–36089, <https://doi.org/10.1039/D0RA04857G>.
- [4] P. Charalampous, I. Kostavelis, T. Kontodina, D. Tzovaras, Learning-based error modeling in FDM 3D printing process, *RPJ* 27 (2021) 507–517, <https://doi.org/10.1108/RPJ-03-2020-0046>.
- [5] H. Kim, Y. Lin, T.-L.B. Tseng, A review on quality control in additive manufacturing, *RPJ* 24 (2018) 645–669, <https://doi.org/10.1108/RPJ-03-2017-0048>.
- [6] A. Dey, N. Yodo, A systematic survey of fdm process parameter optimization and their influence on part characteristics, *JMMP* 3 (2019) 64, <https://doi.org/10.3390/jmmp3030064>.
- [7] E. Westphal, H. Seitz, A machine learning method for defect detection and visualization in selective laser sintering based on convolutional neural networks, *Addit. Manuf.* 41 (2021), 101965, <https://doi.org/10.1016/j.addma.2021.101965>.
- [8] H. Wu, Y. Wang, Z. Yu, In situ monitoring of FDM machine condition via acoustic emission, *Int J. Adv. Manuf. Technol.* (2015), <https://doi.org/10.1007/s00170-015-7809-4>.
- [9] X. Qi, G. Chen, Y. Li, X. Cheng, C. Li, Applying neural-network-based machine learning to additive manufacturing: current applications, challenges, and future perspectives, *Engineering* 5 (2019) 721–729, <https://doi.org/10.1016/j.eng.2019.04.012>.
- [10] D. Song, A.M. Chung Baek, J. Koo, M. Busogi, N. Kim, Forecasting warping deformation using multivariate thermal time series and k-nearest neighbors in fused deposition modeling, *Appl. Sci.* 10 (2020) 8951, <https://doi.org/10.3390/app10248951>.
- [11] W. Wojnowski, K. Kalinowska, J. Gębicki, B. Zabiega a, Monitoring the BTEX volatiles during 3D printing with acrylonitrile butadiene styrene (ABS) using electronic nose and proton transfer reaction mass spectrometry, *Sensors* 20 (2020), <https://doi.org/10.3390/s20195531>.
- [12] H. Wu, Z. Yu, Y. Wang, Real-time FDM machine condition monitoring and diagnosis based on acoustic emission and hidden semi-Markov model, *Int J. Adv. Manuf. Technol.* 90 (2017) 2027–2036, <https://doi.org/10.1007/s00170-016-9548-6>.
- [13] K. Wasmer, T. Le-Quang, B. Meylan, S.A. Shevchik, In situ quality monitoring in AM using acoustic emission: a reinforcement learning approach, *J. Mater. Eng. Perform.* 28 (2019) 666–672, <https://doi.org/10.1007/s11665-018-3690-2>.
- [14] C. Silbernegel, A. Aremu, I. Ashcroft, Using machine learning to aid in the parameter optimisation process for metal-based additive manufacturing, *RPJ* 26 (2019) 625–637, <https://doi.org/10.1108/RPJ-08-2019-0213>.
- [15] H. Kim, H. Lee, J.-S. Kim, S.-H. Ahn, Image-based failure detection for material extrusion process using a convolutional neural network, *Int J. Adv. Manuf. Technol.* 111 (2020) 1291–1302, <https://doi.org/10.1007/s00170-020-06201-0>.

- [16] K. Paraskevoudis, P. Karayannis, E.P. Koumoulos, Real-time 3D printing remote defect detection (stringing) with computer vision and artificial intelligence, *Processes* 8 (2020) 1464, <https://doi.org/10.3390/pr8111464>.
- [17] Z. Jin, Z. Zhang, J. Ott, G.X. Gu, Precise localization and semantic segmentation detection of printing conditions in fused filament fabrication technologies using machine learning, *Addit. Manuf.* 37 (2021), 101696, <https://doi.org/10.1016/j.addma.2020.101696>.
- [18] Y. Fu, A. Downey, L. Yuan, A. Pratt, Y. Balogun, In situ monitoring for fused filament fabrication process: a review, *Addit. Manuf.* 38 (2021), 101749, <https://doi.org/10.1016/j.addma.2020.101749>.
- [19] P. Pitayachaval, K. Masnok, Feed rate and volume of material effects in fused deposition modeling nozzle wear, in: 2017 4th International Conference on industrial engineering and applications (ICIEA), 21.04, Nagoya, Jpn., IEEE (2017) 39–44.
- [20] Bosch Sensortec GmbH, BME680 - Datasheet: Low power gas, pressure, temperature & humidity sensor BST-BME680-HS000 06, 1.6 (2020).
- [21] A. Biedenkapp, M. Lindauer, K. Eggenesperger, C. Fawcett, H. Hoos, F. Hutter, Efficient Parameter Importance Analysis via Ablation with Surrogates, *Proceedings of the AAAI Conference on Artificial Intelligence*, 31(1) (2017).
- [22] A. Ali, S. Shamsuddin, A. Ralescu, Classification with class imbalance problem: a review, *Int. J. Adv. Soft Comput. Appl.* (2013).
- [23] J. Tanha, Y. Abdi, N. Samadi, N. Razzaghi, M. Asadpour, Boosting methods for multi-class imbalanced data classification: an experimental review, *J. Big Data* 7 (2020), <https://doi.org/10.1186/s40537-020-00349-y>.
- [24] W. Shuo, Y. Xin, Multiclass imbalance problems: analysis and potential solutions, *IEEE Trans. Syst. Man Cybern. B Cybern.* 42 (2012) 1119–1130, <https://doi.org/10.1109/TSMCB.2012.2187280>.
- [25] F. Hutter, L. Kotthoff, J. Vanschoren, *Automated Machine Learning*, Springer International Publishing, Cham, 2019.
- [26] F. Chollet, *Deep learning with Python*, Manning Publications Co, Shelter Island New York, 2018.
- [27] T.M. Mitchell, *Machine learning*, WCB/McGraw-Hill, Boston, Mass. [u.a.], 1997.
- [28] Y. LeCun, Y. Bengio, G. Hinton, Deep learning, *Nature* 521 (2015) 436–444, <https://doi.org/10.1038/nature14539>.
- [29] M.H. Hassoun, *Fundamentals of Artificial. Neural Networks*, firstst, MIT Press, Cambridge, MA, USA, 1995.
- [30] S. Albawi, T.A. Mohammed, S. Al-Zawi, Understanding of a convolutional neural network, in: 2017 International Conference on Engineering and Technology (ICET), 21.08, Antalya, IEEE (2017) 1–6.
- [31] H. Ismail Fawaz, G. Forestier, J. Weber, L. Idoumghar, P.-A. Muller, Deep learning for time series classification: a review, *Data Min. Knowl. Disc* 33 (2019) 917–963, <https://doi.org/10.1007/s10618-019-00619-1>.
- [32] Y. LeCun, Y. Bengio, *Convolutional Networks for Images, Speech, and Time Series*, in: *The Handbook of Brain Theory and Neural Networks*, MIT Press, Cambridge, MA, USA, 1998, pp. 255–258.
- [33] A. Krizhevsky, I. Sutskever, G.E. Hinton, ImageNet classification with deep convolutional neural networks, *Commun. ACM* 60 (2017) 84–90, <https://doi.org/10.1145/3065386>.
- [34] C.A. Ronao, S.-B. Cho, Human activity recognition with smartphone sensors using deep learning neural networks, *Expert Syst. Appl.* 59 (2016) 235–244, <https://doi.org/10.1016/j.eswa.2016.04.032>.
- [35] T. Plotz, N.Y. Hammerla, P. Olivier, Feature Learning for Activity Recognition in Ubiquitous Computing, in: *Proceedings of the Twenty-Second International Joint Conference on Artificial Intelligence - Volume Volume Two*, AAAI Press, 2011, pp. 1729–1734.
- [36] Z.C. Lipton, J. Berkowitz, C. Elkan, *A Crit. Rev. Recurr. Neural Netw. Seq. Learn.* (2015).
- [37] S. Hochreiter, J. Schmidhuber, Long short-term memory, *Neural Comput.* 9 (1997) 1735–1780, <https://doi.org/10.1162/neco.1997.9.8.1735>.
- [38] Chao Liu, Jinhao Lei, Dongxiang Jiang, Fault diagnosis of wind turbine based on Long Short-term memory networks, *Renew. Energy* 133 (2019) 422–432, <https://doi.org/10.1016/j.renene.2018.10.031>.
- [39] G. van Houdt, C. Mosquera, G. Napoles, A review on the long short-term memory model, *Artif. Intell. Rev.* 53 (2020) 5929–5955, <https://doi.org/10.1007/s10462-020-09838-1>.
- [40] H. Ismail Fawaz, B. Lucas, G. Forestier, C. Pelletier, D.F. Schmidt, J. Weber, G. I. Webb, L. Idoumghar, P.-A. Muller, F. Petitjean, InceptionTime: Finding AlexNet for time series classification, *Data Min. Knowl. Disc* 34 (2020) 1936–1962, <https://doi.org/10.1007/s10618-020-00710-y>.
- [41] E. Rahimian, S. Zabihi, S.F. Atashzar, A. Asif, A. Mohammadi, XceptionTime: A Nov. Deep Archit. Based Depthwise Separable Convolutions Hand Gesture Classif. (2019).
- [42] K. Fauvel, T. Lin, V. Masson, E. Fromont, A. Termier, X.C.M. An, Explain. Convolutional Neural Netw. Multivar. Time Ser. Classif. (2020).
- [43] Ignacio Oguiza, tsai - A State—Art. Deep Learn. Libr. Time Ser. Seq. data (2020). <https://github.com/timeseriesAI/tsai>.
- [44] Z. Wang, W. Yan, T. Oates, Time series classification from scratch with deep, *Neural Netw.: A Strong Baseline* (2016).
- [45] M. Lin, Q. Chen, S. Yan, *Network Network* (2013).
- [46] M. Hossin, M.N. Sulaiman, A review on evaluation metrics for data classification evaluations, *IJDKP* 5 (2015) 1–11, <https://doi.org/10.5121/ijdkp.2015.5201>.
- [47] M. Grandini, E. Bagli, G. Visani, Metrics for Multi-Class Classification: an Overview, 2020.
- [48] K.M. Ting, *Confusion Matrix*, in: C. Sammut, G.I. Webb (Eds.), *Encyclopedia of Machine Learning*, Springer, US, Boston, MA, 2010, p. 209.
- [49] M. Sokolova, G. Lapalme, A systematic analysis of performance measures for classification tasks, *Inf. Process. Manag.* 45 (2009) 427–437, <https://doi.org/10.1016/j.ipm.2009.03.002>.
- [50] L. Breiman, Random forests, *Mach. Learn.* 45 (2001) 5–32, <https://doi.org/10.1023/A:1010933404324>.

Publication [III]

E. Westphal; B. Leiding; H. Seitz, Blockchain-based quality management for a digital additive manufacturing part record



Blockchain-based quality management for a digital additive manufacturing part record

Erik Westphal^{a,*}, Benjamin Leiding^b, Hermann Seitz^{a,c}

^a Chair of Microfluidics, University of Rostock, 18059, Rostock, Germany

^b Chair of Software Services for the Circular Economy, Clausthal University of Technology, 38678, Clausthal-Zellerfeld, Germany

^c Dept. Life, Light & Matter, University of Rostock, 18059, Rostock, Germany

ARTICLE INFO

Keywords:

Additive manufacturing
Quality management
Blockchain
Smart contract
Digital part record
Material extrusion

ABSTRACT

Quality management (QM) of additive manufacturing (AM) processes is currently immature in terms of transparency, traceability and security. In particular, quality-relevant documents are not documented and communicated in a traceable and transparent manner, which often leads to quality deficiencies. However, combining AM with blockchain technology can enable a solution that maps the AM value chain digitally, transparently, traceably and securely in a part record. In this work, a quality assurance (QA) concept for the metal-based material extrusion (MEX) process is developed that enables a digital representation of the value chain in the form of an AM part record. The decentralized solution presented in this work uses an architecture consisting of a web application for data acquisition, a decentralized storage solution for storing larger amounts of data, a smart contract for capturing manufacturing events and the Ethereum blockchain for transparent, secure and traceable storage of blockchain data. The AM part record enables traceable and constantly available digital documentation of quality information. The cost-effectiveness of the solution is also shown in a demonstration study. The research results highlight the benefits of a blockchain-based AM part record for digital manufacturing documentation and represent an efficient alternative or extension to existing QM and QA solutions in AM.

1. Introduction

Additive manufacturing (AM), often also referred to as 3D printing, is the generic term for various manufacturing processes that build up layer by layer for the production of geometrically complex parts from digital, three-dimensional files [1]. The technology is becoming increasingly important for both scientists and users in the industrial environment and is changing from a rapid prototyping tool to an established manufacturing process in industrial production [2]. In the course of Industry 4.0, the digitization of the manufacturing industry is progressing rapidly, with AM in particular offering interesting digital transformation opportunities [3]. According to Alkhader et al. [3], the reduction in delivery times, the development of a decentralized and more sustainable production through AM can be cited in particular. At the same time, modern digital technologies of additive manufacturing also open up new possibilities for solving special process-specific problems. In particular, quality assurance (QA) and quality management (QM) still have great optimization potential in AM [4]. According to Yang et al. [4], the existing status quo of AM QM in particular should be

improved towards a philosophy that consists of emphasizing quality, involving every stakeholder in the QM process, communicating quality problems transparently and effectively documenting all quality-related aspects. Moreover, consensus on quality is difficult to achieve in a system of mutual distrust among stakeholders. Especially for decentralized collaboration, where no actor owns all the data centrally. This is exactly where blockchain technology can generate added value. According to Christidis and Devetsikiotis [5], a blockchain is essentially a distributed database architecture based on cryptographically linked blocks of information containing consensus-checked datasets. It is also the most well-known form of Distributed Ledger Technologies (DLT) and promises to ensure the authenticity of digital information and manage data ownership [6]. Thus, according to Kurpjuweit et al. [7], the combination of blockchain and AM can be particularly promising because:

- 1 The already highly digitized AM process chain can potentially be transferred directly to a digital infrastructure such as a blockchain.

* Corresponding author.

E-mail address: erik.westphal@uni-rostock.de (E. Westphal).

- 2 Data security risks in the digital process chain are minimized by enabling data immutability and protecting sensitive manufacturing information from manipulation.
- 3 Intellectual property risks and constraints can be managed.
- 4 Transparency in the AM supply chain is increased and more trusting relationships are created between the individual transaction partners.

If these aspects are specially adapted to the QM of AM processes, digital, secure, unchangeable and transparent part documentation can be made possible, for example. Klockner et al. [8] have already developed the basic idea of mapping the life cycle of a printed part on a blockchain, including all relevant actors and work processes. In the concept developed for this purpose, in addition to the actors involved in the physical flow of parts (OEMs, material suppliers, printing and logistics service providers, customers), the actors involved in the flow of information (external data generators, certification and regulatory authorities, financial service providers) are also considered in a 3D printing value chain.

This work builds on the previously mentioned, so far rather theoretical considerations about the combination of AM and blockchain technology for quality improvement. The main focus is on the development of a blockchain-based quality assurance concept for mapping an AM value chain in the form of a digital part record. Specifically, a concept solution consisting of a web application and a smart contract is being developed, which includes relevant aspects of AM QM as well as documentation of manufacturing and QA data of the AM printing process for subsequent machine learning (ML) analyses. A corresponding integration of ML analyses in real time is then analyzed within the concept and discussed as a necessary extension. The specific goal of this work lies in the elaboration of the QA concept as well as in the implementation and evaluation of a corresponding prototypical solution using an AM example process. Furthermore, the research question was pursued, which advantages the prototypical solution enables compared to current systems and processes. Metal-based material extrusion (MEX) is defined in ISO/ASTM 52,900 and also known under the brand name Fused Deposition Modeling (FDM). MEX was chosen as an example process, since additional post-processing steps (e.g. debinding, sintering) in this AM process result in traceable production and part documentation as well as QA across various stakeholders. For this reason, the use of a blockchain-based QM solution seems particularly useful, especially in a production network of several production companies that are connected via a supply chain.

2. Related work

Various research work on the use of blockchain in additive manufacturing has already been carried out and some of the first blockchain solutions have also been implemented. Klockner et al. [8] conducted an investigation on the use of blockchain in AM to evaluate the possibilities for business model innovations. Among other things, they have developed and described a detailed concept of a blockchain platform for the AM value chain. However, this concept was not implemented for the application and examined for practical feasibility.

Alkhader et al. [3] designed a blockchain-based solution for the traceability of additively manufactured products based on Ethereum smart contracts and demonstrated the implementation in a simple form. The solution guarantees secure and trustworthy supply chain management between the network participants involved and automated execution of transactions via smart contracts. Furthermore, the decentralized storage solution InterPlanetary File System (IPFS) is integrated to store and distribute design files, device data and product specifications [3]. However, the solution was not tested in a specific application in practical use and does not have a functional interface for interaction between the users of the solution and the Ethereum blockchain in the background. The digital mapping of the value chain of a specific AM

process to support QM was not considered in this work either.

A 3D printing platform for spare parts management based on blockchain technology was developed by Zhang et al. [9]. The prototypical system developed in the process enables the coordination of spare parts suppliers and the identification of their production standards in order to be able to quickly qualify suitable suppliers. Furthermore, on-chain and off-chain storage solutions have been implemented to ensure data sharing while respecting property rights, and a product traceability solution has been developed to ensure the safety and transparency of spare parts. However, there is no comprehensive documentation along the AM process and a digital QM based on the prototype system has also not been implemented.

Mandolla et al. [10] have examined an additive metal manufacturing process of a component using the example of the aircraft industry and designed a digital twin for manufacturing using a blockchain solution. A simplified blockchain model was developed to show how a digital twin of the AM manufacturing chain can be technically implemented in the aviation industry. However, the entire blockchain concept developed in the work was not put into practice, only the area of part design was considered in more detail.

A conceptual application of blockchain technology to manage product information in the AM development process was presented by Papakostas et al. [11]. In the concept study, a network is designed in which network participants interact with a blockchain agent via transactions. This demonstrates product lifecycle management that enables data exchange between network participants through a low-cost mechanism, creates greater transparency of all transactions, enables better traceability of operations and greater traceability of decisions. The concept is evaluated based on a general AM application scenario and implemented in a dedicated development environment. However, the paper by Papakostas et al. [11] only conceptualizes the implementation and does not describe it in detail. In addition, the presented use case is not very detailed, thus, for example process-specific pre- and post-processing steps were not sufficiently considered. Furthermore, blockchain functionalities were implemented separately in the form of an unspecified private blockchain.

Bonnard et al. [12] proposed and elaborated an object-oriented model for developing a digital AM process chain. Thereby, process parameters from product development to post-processing and validation are recorded and modelled in an object-oriented manner. Data stored in this way is useful for combining application and database development and enables a unified data model. In addition, the abstraction, inheritance and encapsulation of quality-relevant process data is supported. However, it is not a blockchain-based solution, which means that certain security and trust aspects, among others, have not been considered.

Guo et al. [13] designed a framework that includes personalized part production using AM techniques based on digital twins and blockchain. Product lifecycle information such as design, manufacturing and service data is stored as digital twin data in a blockchain. The blockchain then enables the authentic transfer of the digital twin data between customers and part manufacturers. However, the paper does not present an exemplary solution based on practical implementations, and the traceability and accessibility of the digital twin data between different process stakeholders remains unclear.

Zhang et al. [14] have written a review of digital twins in AM. Accordingly, digital twins are very helpful to better understand, analyze and improve a product, service or manufacturing process. In AM, digital twins are used primarily to collect data for process simulation, monitoring, and control, and to present this data in a form suitable for information retrieval. This is also used in the work of Witherell [15] to better understand the AM process and, for example, to derive acceptance criteria for AM components from digital twins. For the efficient use of a digital twin, there is still a considerable need for research on suitable hardware, databases, machine learning, data analysis and the interaction of all components with each other [14]. In addition, the integration of sensors for real-time data acquisition will also be required in the

future [15]. In both studies, however, the focus is currently increasingly on quality analyses that take place within a company and are summarized, visualized and evaluated in a digital twin. The traceability and accessibility of the digital twin data or the exchange of data across company boundaries, for example to track supply chains, remains open. Here, blockchain can be a useful addition to the concept of the digital twin.

Further studies specifically on QM in AM have been conducted by Yi et al. [16] and Schmid and Levy [17]. Both publications examine various aspects of QM as well as QA in additive manufacturing and also consider the costs incurred by these processes. General strategic approaches and concepts for specific AM QM are also developed. However, these also focus more on the AM production process within a company and address less the necessary exchange of QM data between different companies. Accordingly, the developed QM concepts are rather unsuitable for cross-company QM, which is, however, necessary e.g. for the tracking of supply chains. Here, blockchain can be a suitable solution to specifically enable a secure, transparent and traceable data exchange between different companies.

A comprehensive review on qualification and certification for metal-based AM has been prepared by Chen et al. [18]. There will be a summary of the current state of standardization and challenges in qualification and certification of metal AM components, as well as an outlook on future research topics such as establishing trust and security in AM using blockchain technology.

Another review on the general use of blockchain in supply chain management was done by Chang et al. [19]. By analyzing various recent publications, product traceability was cited as the most important criterion for using blockchain in supply chain management. In addition, there is a general steadily growing interest in blockchain technology, especially in healthcare and government, but also specifically for supply chain management. In these areas, there are also strong links between Internet-of-Things (IoT) data and blockchain technology. According to Chang et al. [19], future research activities should also focus more on this area.

Specific studies on the use of blockchain in supply chain management have been conducted by Gürpınar et al. [20] and Dietrich et al. [21]. The studies show that blockchain projects in agriculture and food supply chains are most commonly implemented in industry, followed by production, pharmaceuticals, and healthcare [20,21]. The most common use cases are tracking and tracing, open information access and fraud prevention [20]. With regard to supply chain management, a trustworthy supplier relationship is an important goal here, as is order fulfillment that is as automated as possible and transparent customer service management. In this regard, a holistic architecture based on smart contracts could be an important milestone in making the properties of blockchain technology accessible to complex production networks and supply chains [21].

3. Materials and methods

This research paper describes the design and development of a digital part record for mapping the value chain of a concrete AM process. This solution is intended to effectively support QM and QA to produce better AM parts. To this end, the following section first describes the metal-based FDM process used, defines quality-related AM processes, and determines the Ethereum blockchain and the necessary evaluation criteria for the solution. The envisaged boundary conditions, solution strategies and development tools are also considered in more detail.

3.1. Metal-based fused deposition modeling process chain

This work utilizes an FDM process that uses a metal-filled polymer filament in combination with special debinding and sintering steps to create an all-metal part. The processing of metal filaments in the FDM process is becoming increasingly important and enables cost-effective

additive manufacturing of functional parts with simple desktop FDM printers [22–24].

Accordingly, for the research conducted in this paper, a Makerbot Method X (Makerbot Industries, Brooklyn, USA) desktop 3D printer is used for fabrication. The material used was Ultrafuse 316l stainless steel composite metal filament (BASF, Heidelberg, Germany) with a metal particle content of 80 wt% and a filament diameter of 1.75 mm. In addition, a special experimental extruder (LABS Gen2, Makerbot Industries) with a 0.4 mm nozzle was used for printing.

Various AM print objects were designed using the computer aided design (CAD) program Autodesk Inventor Professional 2019 (Autodesk Inc., San Rafael, USA) and prepared for the printing process using the slicing software Makerbot Print version 4.10.1.2056 (Makerbot Industries). The manufacturing process steps for metal FDM printing are clearly shown below in Fig. 1. All QM-relevant data on the print jobs performed as part of this work are stored in detail in a public data repository [25].

The manufacturing process begins with the creation of a CAD design of the part to be printed. This design is then transferred in what is known as the Standard Tessellation Language (STL) file format to the slicing software, where special process-relevant settings for the printing parameters, material and part positioning are made and the file is divided into layers. A machine-readable print file is then created and transferred to the 3D printer. The printer then creates the 3D part layer by layer, which is initially called 'green part'. When the green part is printed, the filament consisting of metal particles and polymer material partially melts, with the polymer portion serving as a binder to bring the solid metal particles into a defined shape. The green parts are then subjected to a debinding process externally at a service provider, which removes most of the polymer binder. The resulting parts are subsequently very porous and are referred to as 'brown parts'. The brown parts are then sintered in the final step under vacuum or hydrogen to burn out the remaining binder content as well as to fuse the metal particles into a dense form. After this step, dense metallic parts result, which can be subjected to a final quality control.

3.2. AM quality-related processes

In the context of this work, various systems and processes for ensuring and improving part and process quality in AM are considered. First, a quality management system based on DIN EN ISO 9001 is considered, in which requirements and measures for improving process, product and work quality are defined. In the following, this is understood to mean all quality-relevant processes before, during and after component production. Part of these measures recorded in the QM system is referred to specifically as quality assurance in the further course and represents a further process for quality improvement. In this context, QA primarily contributes to ensuring and controlling defined quality requirements within a single company. This mainly involves processes for improving part quality during the printing process, e.g. through innovative data and ML analyses, but also conventional statistical process controls or six sigma methods to ensure product or process quality. Furthermore, according to Chen et al. [18], the terms qualification and certification are relevant to quality. The aspects defined as particularly critical - design, material, printing process, post-processing and inspection - are recorded in great detail so that processes and parts can be qualified and certified if necessary. For this, cross-company QM is important, where quality-relevant data of the entire supply chain can be efficiently tracked between different companies, e.g. via an 8D report to ensure the product quality of a filament supplier or to accurately document delivery processes. However, a correspondingly necessary data transfer between the companies is complex. Since initially unknown companies do not trust each other without further ado, secure, transparent and traceable documentation of the QM data is necessary. Here, blockchain can deliver significant added value for both QM and certification processes. For QM within a single company, these

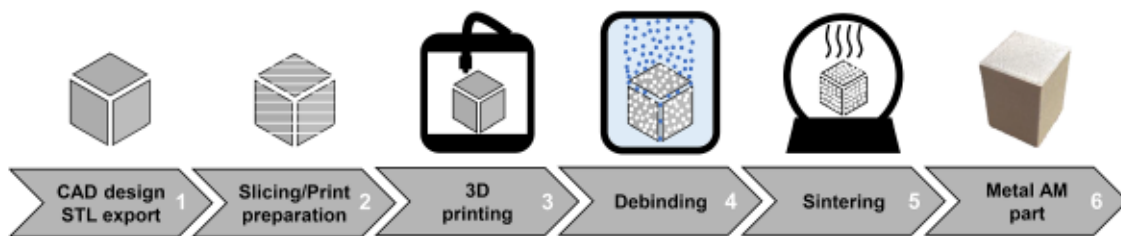


Fig. 1. Metal-based FDM processing steps.

requirements are not as complex and data transfer is usually simpler. For this reason, the use of blockchain-based QM is of limited benefit there and is not the main focus of this work.

In Section 4, a QA concept for the metal FDM process is designed that effectively combines QM and QA and digitally maps them into an AM part record. The new AM part record is intended to fundamentally increase quality in AM. The implementation of concrete goals to be achieved with the new QA concept enables an evaluation of the quality improvement compared to conventional solutions. The goals to be achieved are defined below both on the basis of general evaluation criteria found in other scientific publications [3,26] and on the basis of specifically self-defined aspects:

- **Digital integrity:** Digitized documentation and decentralized storage of conventional quality documentation processes of the FDM process, such as paper-based preparation protocols, material certificates, operator records, etc. across several companies.
- **Costs:** An economical alternative to current solutions.
- **Efficiency:** Compact documentation of large amounts of data, such as the manufacturing data of a print job, or efficient documentation of ML-based evaluation results of printing data.
- **Accountability:** Holistic, detailed, traceable and tamper-proof documentation of the entire value chain and information flow.
- **Availability:** A solution for constant, location-independent availability and timely updating of manufacturing and quality information for all parties involved.
- **Expandability:** A way to simplify and speed up the certification of AM parts.

3.3. Distributed ledgers, blockchain and Ethereum

This section defines and explains important terms related to DLT, blockchain, and Ethereum that contribute to a better understanding of this work. Table 1 provides an overview of the terms relevant in this context.

Distributed ledgers are essentially identical copies of files that record transactions, are stored in multiple locations, and are verified by a consensus algorithm [30]. A popular DLT is blockchain, where the distributed ledger is organized as a chain of information blocks and each block is linked to the previous block via a cryptographic reference (hash). Thereby, each hash is unique and can be checked automatically, which means that all recorded blocks can no longer be changed or manipulated unnoticed [33]. If the content of a block were to be changed, the hash would also change and no longer match the linked hash of the previous block. This makes it possible to quickly detect manipulations and changes to the blockchain information.

The first known blockchain was released in 2008 as the Bitcoin blockchain [31]. However, this work is built on the decentralized Ethereum blockchain, which was conceived in 2014 by Buterin [30] and Wood [34]. Ethereum is based on the concept of the Bitcoin blockchain and can be seen as an extension that primarily enables the creation of digital contracts with the help of cryptography [30,35]. Through appropriate consensus-enabled applications known as smart contracts, custom rules for ownership, transactions, and state transitions can be

Table 1
Blockchain-related terms relevant to this paper.

Term	Explanation
Distributed ledger technology (DLT)	System for digitally storing and synchronising multiple identical copies of data in different locations.
Blockchain	Implementation of a DLT in the form of a cryptographically linked chain of information blocks.
Hash	Cryptographic representation of data originally intended to be stored on a blockchain.
Ethereum	Blockchain with integrated programming language that allows for smart contracts and decentralized applications.
Ethereum Ropoten Testnet	Proof-of-Work based Ethereum Blockchain for testing to simulate own applications without using real cryptocurrency [27].
Consensus	Status in distributed data processing in which all participants in a network have agreed on the same data values [28].
Smart contract	Computer programs that digitally execute and secure processes and user inputs in an automated manner over computer networks [29].
Solidity	Object-oriented, Turing-complete programming language for implementing Ethereum smart contracts.
Cryptocurrency	Digital currency based on a distributed ledger to record and prove ownership relations. Cryptocurrencies are stored in crypto wallets such as Metamask.
Ether (ETH)	Intrinsic currency of the Ethereum blockchain, used to purchase computing power on the network.
Gas	Fee to be paid for performing calculation steps of a smart contract to avoid errors and infinite loops [30].
dApp	A decentralized application with code and data stored on a distributed ledger.
Peer-to-Peer (P2P) network	Network in which nodes can exchange data directly with other nodes without having to involve a third party [31].
IPFS	A decentralized system for tamper-proof storing and transparent access to large amounts of data such as files, images and videos.
On-chain storage	Storage of information on the blockchain itself with accessibility for all network participants [32].
Off-chain storage	Storage of large amounts of data outside of the blockchain without immediate accessibility for other participants in a blockchain network [32].

defined to transform the entire transaction process through automated contract execution in a cost-effective, transparent, and secure manner [36]. The Ethereum blockchain was chosen for this work based on these characteristics, among others. In addition, Ethereum is a fully decentralized, public permissionless blockchain in which a very large number of participants can read, write and validate information [37]. This has the advantage that Ethereum-based solutions can be used by smaller companies with only few potential network participants. Moreover, in addition to the Ethereum mainnet, there are also several test networks that can be used to experiment initially and simulate well the real deployment of solutions and smart contracts [27]. However, it should be noted that transaction costs are incurred when using the Ethereum mainnet and the performance of the framework is limited by these sometimes high costs and long transaction times due to high network load [38]. However, according to Almeshal et al. [37], these costs are not critical factors for companies, as well as for this work, when

choosing the Ethereum blockchain.

To execute a smart contract, so-called 'gas' is consumed, which is required in the Ethereum network to execute computational steps in the contract code and to keep the network functional against programming errors and hacker attacks [39]. Ethereum smart contracts are written in a programming language such as Solidity and compiled into readable machine code using a compiler. In this work, Solidity and the open source program Remix IDE version 0.22.2 (remix-project.org) were used to program the smart contract. Remix is a web application that helps write smart contracts and verify their functionality. To interact with the Ropsten Ethereum network via the smart contract and to manage the individual user accounts, Metamask version 9.3.0 (ConsenSys Software Inc., New York City, USA) is also used in this work. Metamask is an open-source crypto wallet that also enables convenient connection of smart contracts, crypto accounts and blockchain networks. Metamask also provides users with a secure interface to perform blockchain-based transactions.

The best-known application of a blockchain is currently digital currencies, otherwise known as cryptocurrencies [40]. In addition, the development of decentralized applications (dApps) is growing strongly as another use case of DLT [41]. dApps are software applications whose data and processes are stored in a blockchain. Decentralized storage systems represent another application. These are the counterpart to a centralized data storage server and consist of a peer-to-peer (P2P) network of users, each storing only a portion of the total data, creating a robust data storage and sharing system for larger datasets [42]. An appropriate decentralized, low-cost off-chain storage solution for larger data volumes is, for example, the InterPlanetary File System [43]. Other possible uses of blockchains are listed in the work of Nuttah et al. [44]. There, various technologies are explained that can be combined with blockchain technology, such as edge computing, cloud manufacturing and supply chain management. According to Almesal et al. [37], blockchain will thus also disrupt entire industries such as healthcare, insurance as well as logistics. Especially in logistics in supply chain management, tracking systems can be developed in combination with blockchain technology to enable real-time traceability of products and secure information storage and distribution, which is already used in the food industry [45] and medical technology [46], for example. However, according to Nuttah et al. [44], in terms of solution implementation, blockchain technology is still in the introductory phase of its development and is currently being fundamentally discussed mainly in the academic literature, while purely blockchain-based solutions are still limited at the industrial level. Instead, hybrid solution approaches that combine distributed storage services and blockchain-based technologies are increasingly emerging in the industrial sector [47].

The same approach is also followed in this work. For this purpose, a combined application of blockchain, smart contract and decentralized storage solution in the form of a dApp is shown in Fig. 2. In the first step, data is transferred to the decentralized data storage system IPFS version 0.12.1 (Protocol Labs, San Francisco, US) via a web interface programmed with the open source programming language Python version 3.7.9 (python software foundation, Fredericksburg, US). The web application data is entered by users via a frontend interface and stored in a central MySQL database, which serves as a backend solution for the web interface application. From the MySQL database, all entered data and information of a part is exported together via the web application in the form of a JSON file and stored tamper-proof in a part folder in a decentralized storage network. Other relevant data can then be stored both in the central database as well as in the decentralized storage space, e.g. design files, slicer data and quality documents. Both the centralized and decentralized storage solutions are necessary, on the one hand to be able to quickly view all part data within a company via the central MySQL storage, and on the other hand to be able to exchange part data between different companies in the supply chain in a trustworthy and secure decentralized manner [44]. In the second step, interactions with a smart contract are performed by storing references to the location of the

dApp architecture

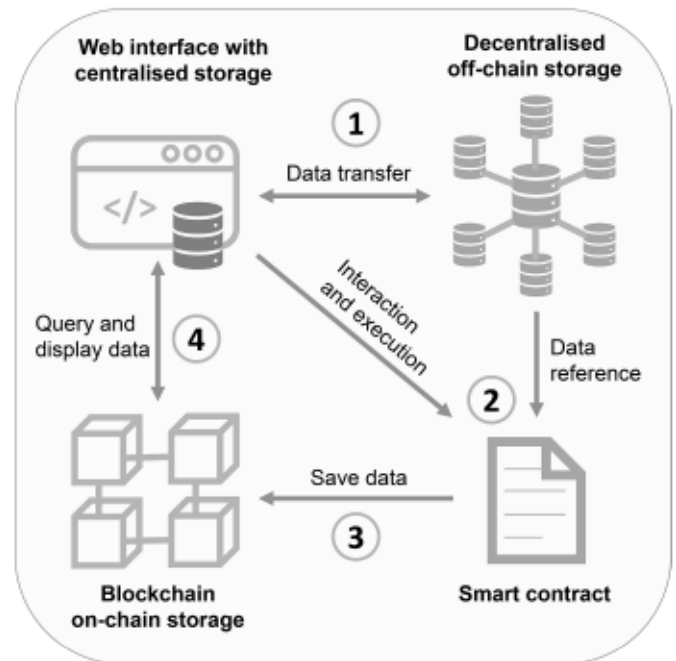


Fig. 2. Blockchain application in the form of a dApp.

decentrally stored data and other information in the smart contract via the web interface. The references are based on the cryptographic hash of the stored content. This ensures that any subsequent change to the stored content results in a new hash, making changes transparent and transactions more secure. The smart contract is then executed. The third step involves automated storage of the event and transaction data (generally the storage of the hash values) on the blockchain, before the fourth step enables the query of this data from the blockchain and visualization of the stored data via a web-based blockchain explorer.

4. Quality assurance concept development

In the following, a blockchain-based QM in the form of a digital AM part record for the metal FDM process is developed. For this purpose, the generalized architecture of the concept is first presented, the implementation of the solution in the form of a demonstration study is described and the validation is shown.

4.1. Generalised architecture for a digital, secure and trustworthy AM part record

The generalized architecture presented here considers the value chain of the metal-based FDM process in combination with a dApp based on a smart contract and blockchain-based as well as decentralized data processing and data storage solutions. The aim of the architecture developed is to digitally record the data of all physical and digital manufacturing process steps as part of a comprehensive QA concept, to map data inputs web-based in the AM part record, to store them securely and to make the results transparently accessible. Attention is always paid to the immutability and accountability of the published information, so that after the implementation of this architecture, the AM value chain is available in the form of a trustworthy, digital part record for each manufactured part. Fig. 3 provides an overview of the manufacturing processes documented in the QA concept, referred to below as the digital AM part record.

The manufacturing documentation of the digital AM part record for a metallic FDM part is composed of four processes and the associated data

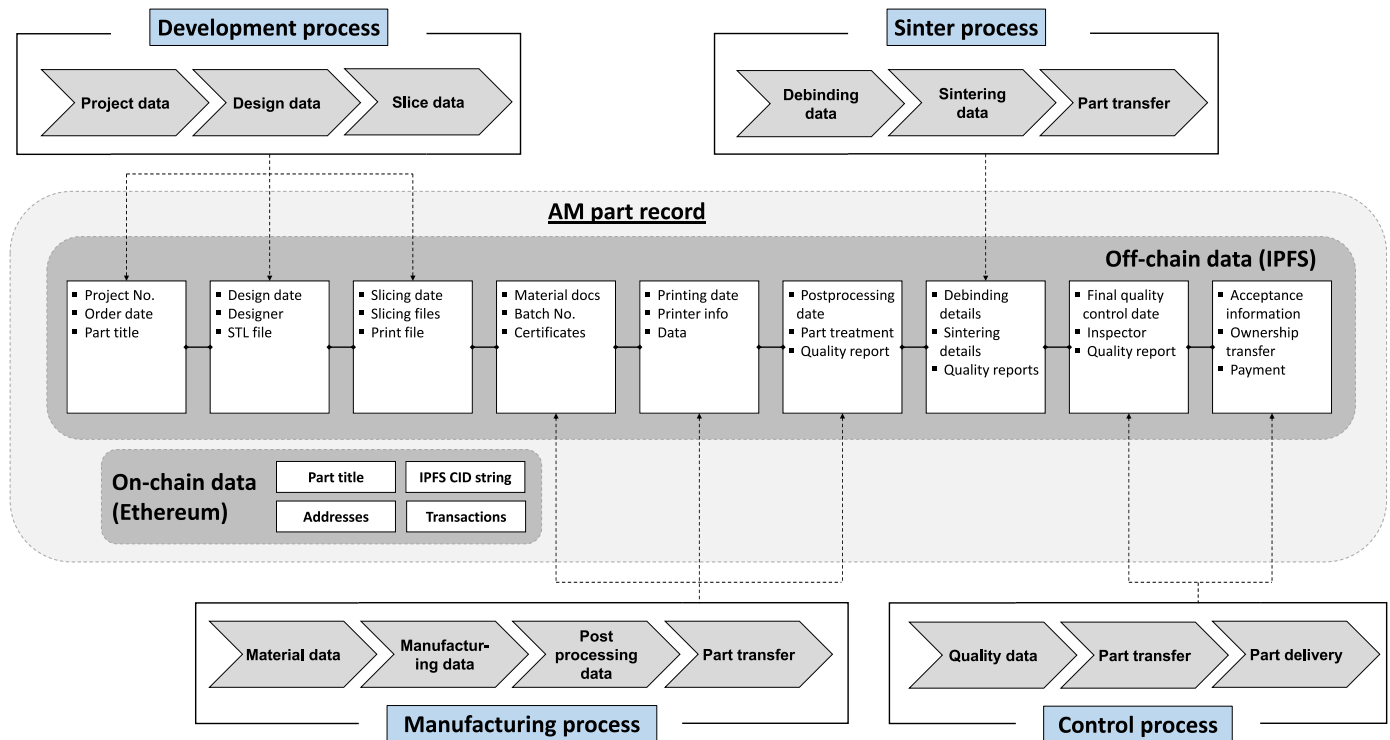


Fig. 3. Manufacturing processes of a digital, secure and trustworthy AM part record with important parameters to be stored in a blockchain.

entries, which are subsequently stored in the part record in the form of exported MySQL database entries as JSON files or documented reports, sensor data and CAD files:

4.1.1. Development process

In this process, project-related data, construction-, design- and slicing files are captured and stored in the central MySQL database as well as tamper-proof off-chain via the IPFS decentralized storage system. The printing material with the corresponding manufacturing process and e.g. the production of the printer, which are also part of the value chain, are not considered here to simplify the concept. The part name and the reference to the location of the files in the IPFS (known as a CID string, which is composed of the cryptographic hash of the files stored in the IPFS) are then stored in a smart contract and saved on-chain on the blockchain. In this architecture, the public Ropsten Ethereum testnet blockchain is specifically used.

4.1.2. Manufacturing process

Takes place physically after the development process, but the process data is stored together with the data from the development process. Here, relevant data on the material used, the machine, the QA of the manufacturing process and the post-processing are documented centrally in the MySQL database and decentrally off-chain in the IPFS. Moreover, the data for shipping to any service provider or subcontractor as well as the Ethereum addresses of the respective participants are tracked directly via a smart contract and stored as transactions on-chain in the Ethereum testnet.

4.1.3. Sinter process

In this work, sintering is carried out externally by a specialized service provider. Following the development and manufacturing documentation, the debinding and sintering process data is recorded off-chain in the IPFS and a CID string is stored on-chain in the smart contract. Prior to this, the arrival and acceptance of the parts delivered to the sintering service provider and, following the sintering process documentation, the return shipment to the part manufacturer are also

recorded via the smart contract on-chain.

4.1.4. Control process

After the parts have been returned by the sintering service provider, a final inspection is carried out by the part manufacturer. For this purpose, quality-relevant data is documented off-chain and the resulting CID string is stored on-chain for localization of the data. Shipping data, as well as data on the delivery of parts and the customer's acceptance or rejection of the entire order, are also tracked via the smart contract on-chain.

According to this concept architecture, information as well as files related to the manufacturing process are thus continuously stored off-chain and at the same time references to the files, transactions, and parties involved are transparently documented on-chain via the Ethereum Ropsten testnet. The data from off-chain and on-chain storage together then result in the AM part record. To represent such basic system architectures in a simplified way, the Unified Modeling Language (UML) is often used [48]. There, according to Gorski [48], special attention must be paid to the exchange of information between different systems, since business processes (such as supply chain processes in this case) often cross company boundaries and still require cooperation between companies (or stakeholders). A very popular and recognized model for software architectures is the "4-1 architectural view model by Kruchten [49], which includes a logical, a process, a physical as well as a development view of the software architecture. In recent years, however, Internet technologies have evolved rapidly, and increasingly decentralized (blockchain) solutions have emerged [50]. For this reason, the more sophisticated "1-5 model of architectural views was designed by Gorski [48], which considers the design of an IT system taking into account the collaboration with distributed systems. The model includes six different views of the software architecture, which also describe the exchange of information between the individual systems. Furthermore, the "1-5 model introduces additional UML language semantics to visualize the architecture of an IT system in terms of business processes [48,50]. In the following, the development view according to Kruchten [49] with certain extensions in a UML component

diagram as well as the logical view according to Gorski [48] are considered in more detail, in which the functions of the software system specified in the applications are represented and explained via a UML communication and sequence diagram in addition to the component diagram. Moreover, the consideration also takes into account new results on the development of distributed information systems defined by Aviv et al. [51] in terms of 16 architectural properties (AP).

The basic component architecture and process flow for implementing digital manufacturing documentation are shown in the UML component diagram in Fig. 4. The diagram shows the main components of the AM part record and their relationships or interfaces to each other.

The presented architecture includes all involved stakeholders, IT applications and processes of the conceptualized digital AM part record as well as their interactions with each other. In a distributed environment, a manufacturer interacts with a shipper, a sintering service provider, and a customer. In this process, physically manufactured parts are exchanged and, in parallel, digital manufacturing documentation is carried out, which has two main tasks: on the one hand, the digital recording of quality data and documents and, on the other hand, the transparent, tamper-proof and traceable storage of these assets. To realize this, a digital part record was designed, consisting of the following subsystems: Web application to collect and process quality data, centralized MySQL database for in-house storage and provision of data, decentralized IPFS storage for distributed storage and publication of data, smart contract and Ropsten Ethereum Blockchain for automated distribution of data references, and a Blockchain explorer for tracking and visualisation of data references. The resulting system architecture includes some basic blockchain APs such as P2P connectivity, ledger infrastructure, consensus algorithm, smart contracts, and the Ethereum Virtual Machine as a state machine.

When a new part is produced at the manufacturer, all quality-relevant data and documents are digitally recorded in parallel. The manufacturer logs into a web application and can enter data during production through the application's user interface (UI) and store it in a central MySQL database. Finally, via the UI and the MySQL database, the complete manufacturing documentation can be collected and

exported with storage references. This export data consists of JSON, image and document files and is then uploaded to the IPFS decentralized storage system via a special IPFS client application as off-chain data. There, the data or the part folder with all part-specific data receives a unique and cryptographically secured reference in the decentralized network, the CID string. The manufacturer then connects to the Ropsten Ethereum blockchain and its crypto wallet via a browser as well as Metamask. The Remix IDE is then used to invoke the smart contract, which queries data to be stored via programmed transactions, triggers events, and automatically stores the data and execution logs on the blockchain. The data, now referred to as on-chain data, is then broadcasted across the blockchain network according to the underlying APs and can be read via the blockchain explorer Etherscan. The Etherscan website can also be accessed via a browser. With a verified and published smart contract on Etherscan, all transactions as well as the on-chain data are then readable. The CIDs stored as on-chain data can ultimately also be used to retrieve the off-chain data stored in the IPFS. To better illustrate the communication between and the flow within the described system components of the AM part record architecture, a UML communication diagram is given in Fig. 5.

4.2. Demonstration study of the proposed digital AM part record architecture

This section describes how the previously designed AM part record is implemented in the form of a demonstration study. Fig. 6 illustrates the interaction of the individual participants in the production process within the smart contract in great detail in a UML sequence diagram. The smart contract process can be roughly divided into seven phases:

4.2.1. Manufacturing sequence

The manufacturing sequence includes both the development and the manufacturing process, since in this concept both processes are carried out by the manufacturer. However, the QM documentation with the AM part record only starts after the part production with the common storage of all relevant quality data in the IPFS. The IPFS CID, which is the

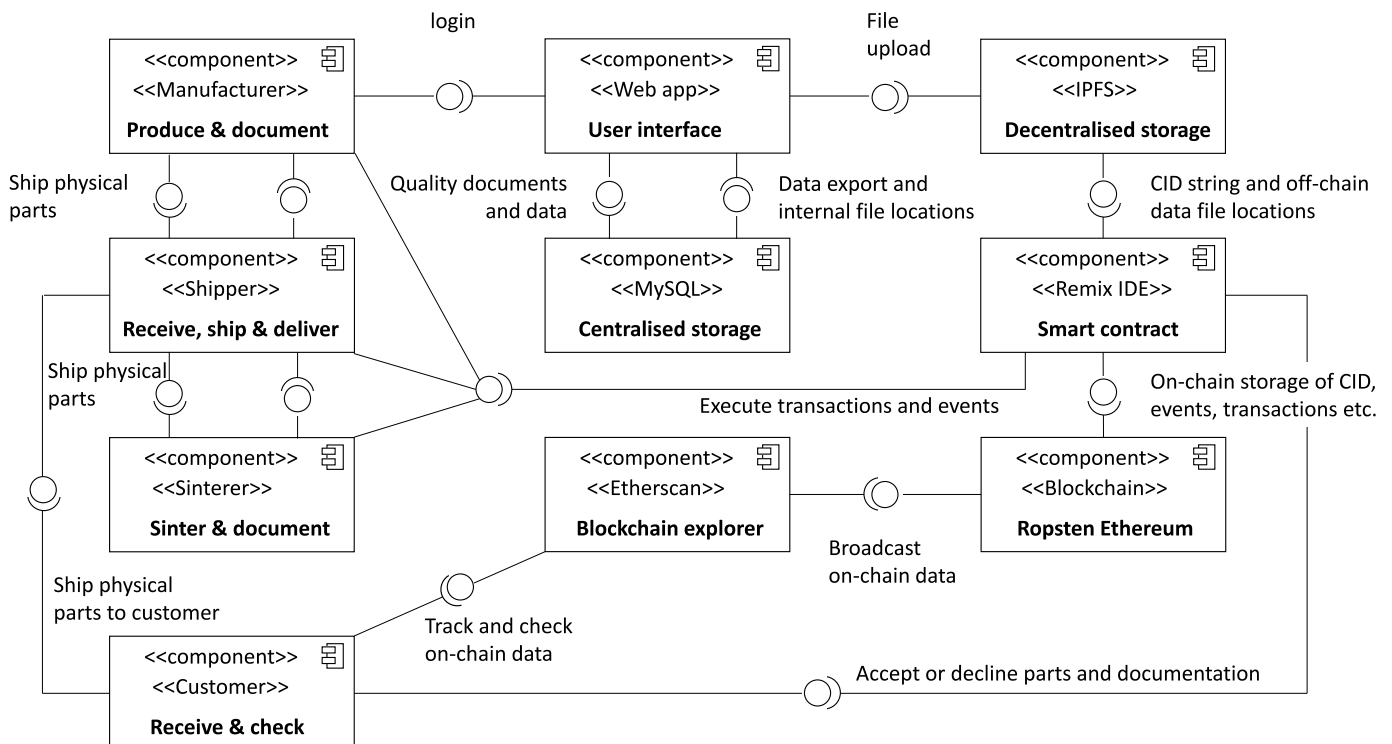


Fig. 4. UML component diagram for the proposed blockchain-based digital AM part record.

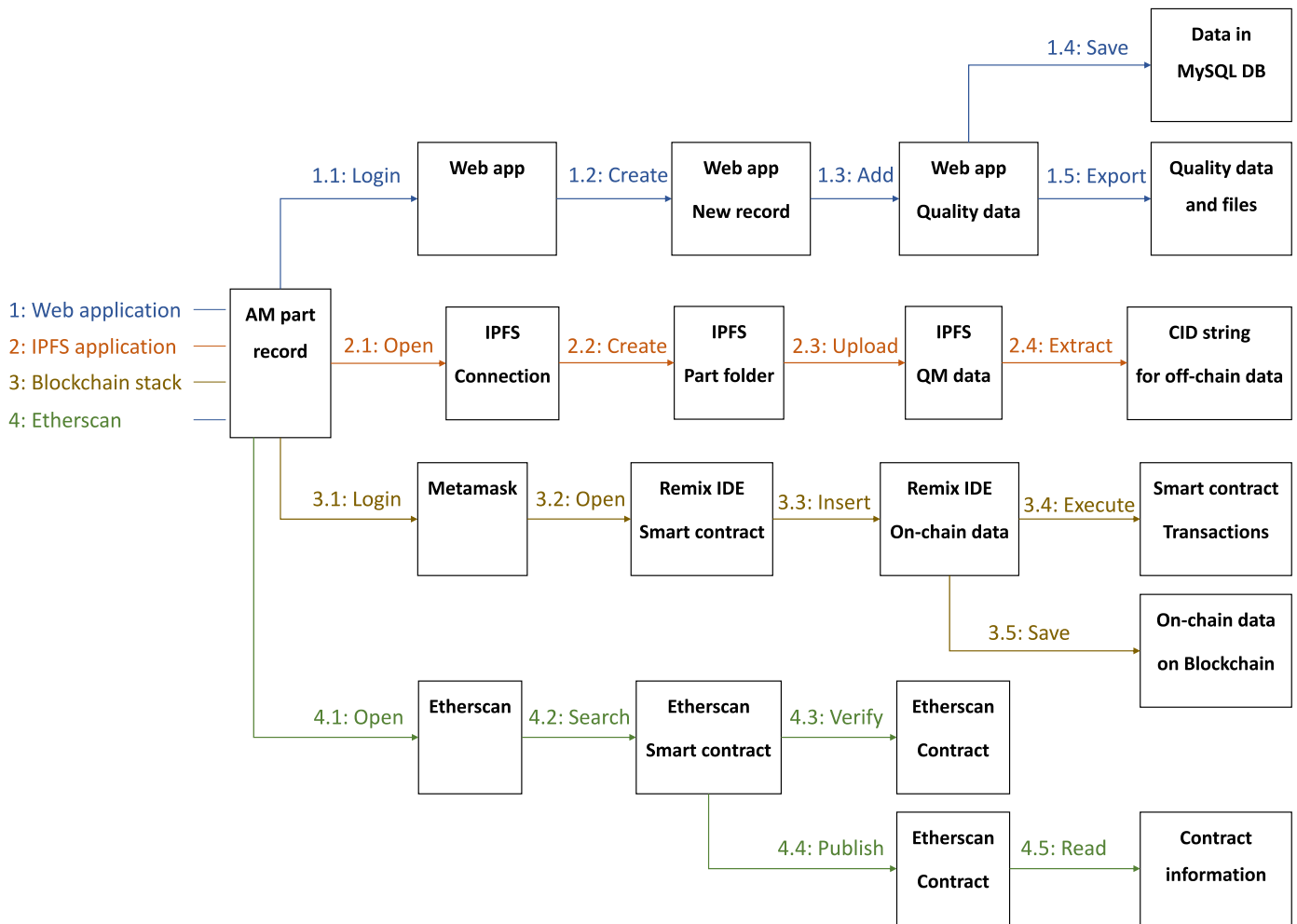


Fig. 5. UML communication diagram for the digital AM part record components.

hashed reference to the quality data, is then stored on the blockchain along with other development and manufacturing information about the smart contract. Finally, a request to ship the parts to the sintering service provider is stored via the smart contract.

4.2.2. Shipment to sinterer sequence

The submitted shipping request is accepted by a shipping service provider. The shipper then takes over the parts and transports them to the sintering service provider. Once the shipment has been handed over, the shipper stores corresponding information in the smart contract. After receiving the parts, the sintering service provider also stores the information about the receipt of the shipment in the smart contract.

4.2.3. Sintering sequence

After debinding and sintering of the parts, the sinterer stores all quality-relevant data (e.g. date, sintering parameters, quality reports) back in the IPFS. For this purpose, the folder already created by the manufacturer is reused in IPFS. The reference of the folder is transparently accessible to the sintering service provider. If data in the IPFS is changed, the CID also changes. Accordingly, an updated CID of the originally created folder is documented by the sinterer in the smart contract. This allowed change of the CID can be transparently tracked via the Etherscan history. Furthermore, the sinterer also stores a new request to send the parts back to the manufacturer.

4.2.4. Shipment back to manufacturer sequence

The shipping request is in turn accepted and executed by the shipper.

After the shipment is handed over to the manufacturer, the shipper again stores information in the smart contract, and the same applies to the receipt of the shipment from the manufacturer.

4.2.5. Quality control sequence

The manufacturer then performs a final quality control and checks all quality documents. A quality report is then created and saved in the IPFS folder that has already been created. The CID, which is updated again, is stored via the smart contract and a delivery request for the parts to the customer is stored.

4.2.6. Delivery to customer sequence

The delivery order is accepted by the shipper, the parts are taken over and delivered. The delivery is documented in the smart contract. The customer also documents the receipt of the order via the smart contract.

4.2.7. Customer decision sequence

The customer checks the parts as well as the quality documentation of the AM part record and decides on their acceptance or rejection. Access to the information and data of the AM part record takes place via Etherscan and can in principle already be tracked from part production onwards, provided that the customer is notified of the address of the smart contract at an early stage.

Finally, this process ensures that all transactions are stored and can be viewed and verified by all parties involved. This ultimately leads to better quality and more confidence in the parts, as well as the supply

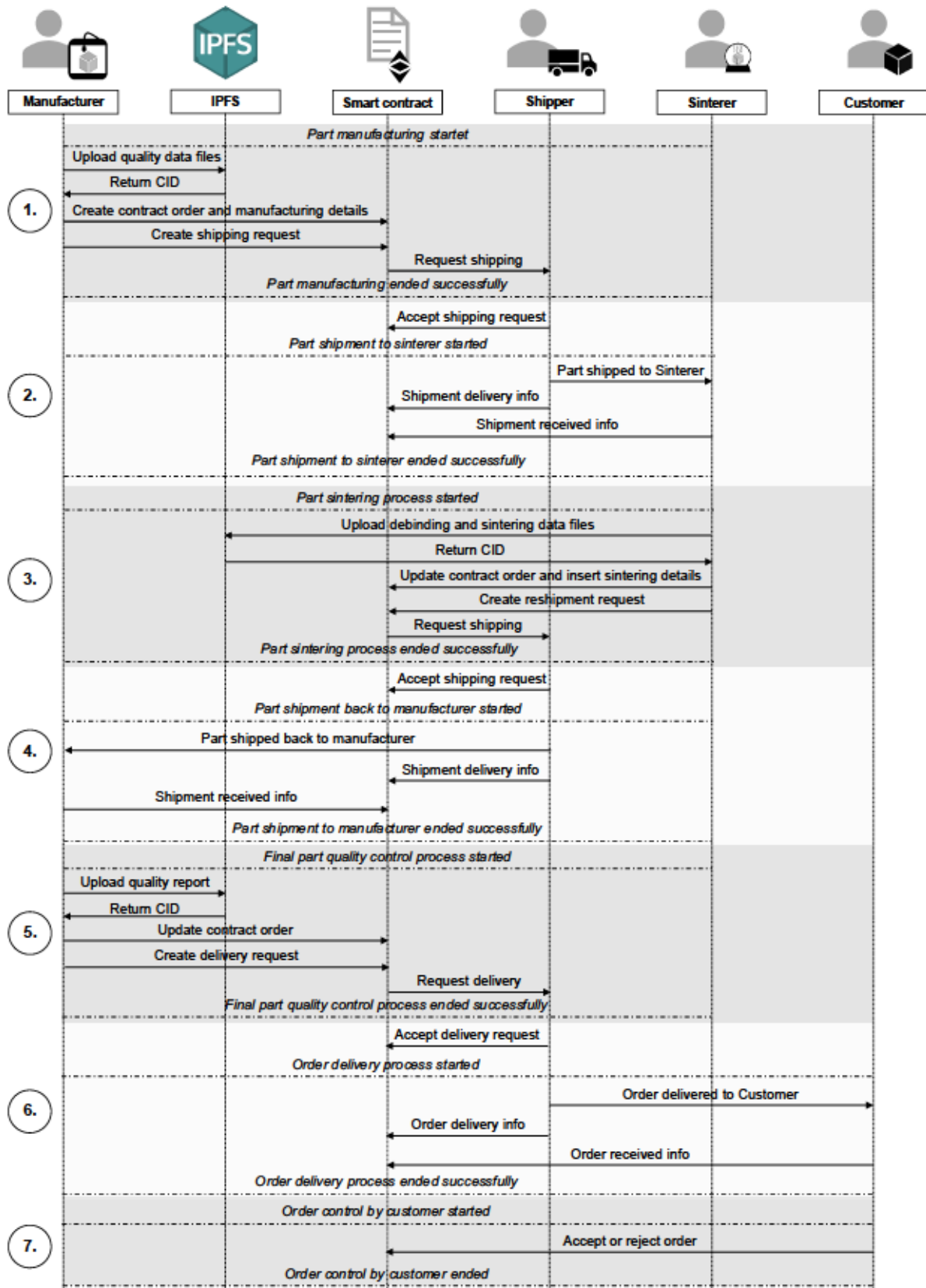


Fig. 6. UML sequence diagram for the interactions of the smart contract participants. Representation of the individual manufacturing sequences (numbered circles on the left) with the smart contract function calls (arrow lines) and the start and end of the respective function blocks (dashed lines).

chain and the supply chain participants. The smart contract is necessary to define clear actions and events to be fulfilled without discussions and room for interpretation. It reacts flexibly and immediately to inputs, without manual intervention, and thus enables an automated execution process, e.g. for the acquisition of data inputs, their storage in the network and their distribution to all participants. This avoids disconnected data silos and the parties involved still retain their data sovereignty due to access rights programmed in the smart contract. This reduces the coordination effort and saves a lot of time. The smart contract is also necessary to determine who can read what information under what conditions after decentralized storage on the blockchain.

4.3. Testing and validation of the implemented AM part record

To evaluate the functionalities of the developed QA system, real manufacturing processes are run through in the demonstration study and the data and transactions are recorded via the AM part record. All developed applications and processes (web application, decentralized storage, smart contract, data access via Etherscan) were tested and validated in the process. The parties involved in the production scenarios and their Ethereum addresses as well as the address of the smart contract are listed in Table 2. The most important tests are explained below.

More detailed documentation of the AM part record as well as the developed program codes, the additively manufactured parts and the performed functional tests are provided in a public data repository [25].

First, the part manufacturer logs into the developed web application and creates a part record for a new part (see Fig. 7). All relevant quality information is stored digitally. In addition, quality documents are created during production and the corresponding file and document names are inserted into the web application as a reference. Finally, a summary of all information is extracted via the web application in the form of a JSON file. All documents and descriptions relevant to this sub-process are available in detail and digitally in the public repository.

All created documents as well as the JSON file with the collected information about the part production are then uploaded to a part folder in the decentralized storage system IPFS (see Fig. 8). Each part folder is linked to its own CID string, which is used to access the folder in the IPFS and to access the data stored off-chain.

Subsequently, CID and further manufacturing information are stored on-chain via the Remix IDE and the developed smart contract. For this purpose, the different accounts of the process participants are simulated via Metamask. Each participant account is created in Metamask and the respective generated Ropsten Ethereum address is written to the smart contract. Using the order creation function programmed with Solidity, the part name, CID, and participant accounts are stored via the smart contract on-chain in the Ropsten Ethereum blockchain. Fig. 9 shows an example of the successful execution of the 'createOrder' function and the creation and storage of the transaction on the blockchain.

The 'createOrder' function is executed by the manufacturer who creates a new part record with the input of the partID and the IPFS_CID in the smart contract. The transaction takes place from the Ethereum address of the manufacturer to the address of the smart contract. In addition, the logs show that an event was successfully executed (green icon in the upper left corner of Fig. 9) and the job creation as well as indexing of a new part was completed. According to the sequence

Table 2
Ropsten Ethereum addresses of the participants of the AM part record.

Participant	Ropsten ethereum address
AMChain smart contract	0x34A253F8E74460F264A902E305990Df65FA6C5Ce
Manufacturer	0xebdc7eAdBc95aa5911A571cC589B0A42119D5dD
Shipper	0xA4084Fc2FeCBC4E20BaA2b5FA9Af3f5C72906536
Sinterer	0xadbe1C35f796C709A800DeF7A2e08ec34A2C139E
Customer	0x5c67433508a15829E7bcb0484AFefB07f88BA6Ce5

diagram presented earlier, all other functions of the smart contract can also be successfully invoked, the required information inserted, and the data stored on the blockchain.

In parallel to the production documentation, the data stored on-chain can be continuously viewed via the blockchain explorer Ropsten Etherscan. To access the documentation, the first step is to paste the address of the smart contract into the blockchain explorer. After the smart contract is invoked, the program code must be verified and published in Etherscan, whereupon a data query to the corresponding indexed parts is possible and the associated information stored on-chain can be read (Fig. 10).

4.4. Testing the download functionality of the decentrally stored quality files

After the on-chain data has been read out via Etherscan using the smart contract, the part quality data can be retrieved online via a browser using the CIDs. Table 3 below lists the CIDs that lead to three part records with their corresponding documentation files.

To access the contents of the IPFS, the following web address must be entered in the address bar of the browser: <https://ipfs.io/ipfs/CID>.

The part record with all the folders and files it contains is then visible via the browser (see Fig. 11). The files in the folders can be downloaded individually with a right mouse click and "Save link as" and saved locally (see Fig. 12). Entire folders are currently not downloadable at once.

5. Discussion and evaluation of the implemented AM part record

The following section examines whether the objectives listed in Section 3.2 (digital integrity, costs, efficiency, accountability, availability, expandability) can be achieved with the new QA concept or whether they have already been achieved with the prototype implementation of the AM part record. Furthermore, any particular disadvantages or aspects that require special attention during implementation are also discussed.

5.1. Digital integrity

One goal of the proposed blockchain-based QA architecture is to digitally track and document all transactions and conventional quality documentation processes of the FDM process. The traceability of the value chain as well as the ownership of the produced parts during manufacturing is also striven for. This is ensured by the AM blockchain solution, as all events and protocols are stored immutably on-chain on the blockchain or traceably and tamper-proof off-chain in the IPFS. Thus, every transaction and documentation within the FDM value chain is digitally traceable and can also be traced. Moreover, the proposed AM blockchain architecture, with its applications, processes, and participants, in principle forms a decentralized distributed system that offers several key advantages over the current mostly centralized solutions for digital data transfer between companies. While centralized QM data belongs only to the party that also operates the central storage, the data of a decentralized distributed system belongs to the respective originators of the data. They can always access their data and manage the authorizations for access and use of the data themselves. Using the AM Blockchain, each participant can make its QM data accessible to the other parties via IPFS, smart contract and Etherscan in a tamper-proof, transparent as well as traceable manner, which ultimately increases trust among each other. QM data is also stored more securely in principle in the decentralized distributed system than in centralized systems. A central server can fail or be attacked, resulting in downtime or data loss. The data distributed in a decentralized manner via IPFS and Ethereum is stored in multiple locations as a copy and is also efficiently protected against manipulation via the blockchain network by special consensus mechanisms. If a network participant fails, the data in the

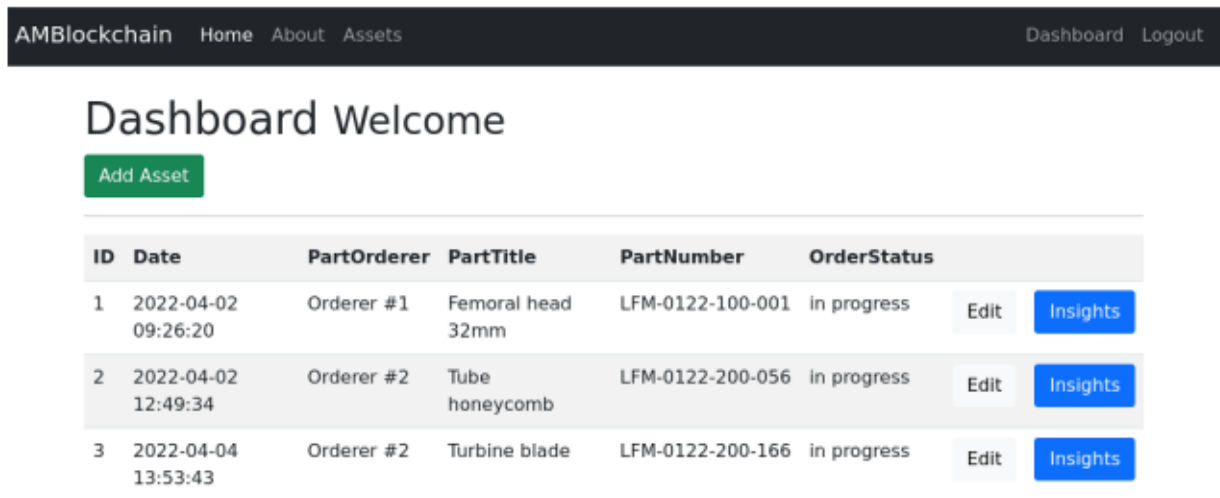


Fig. 7. User interface of the developed web application for creating new part records.

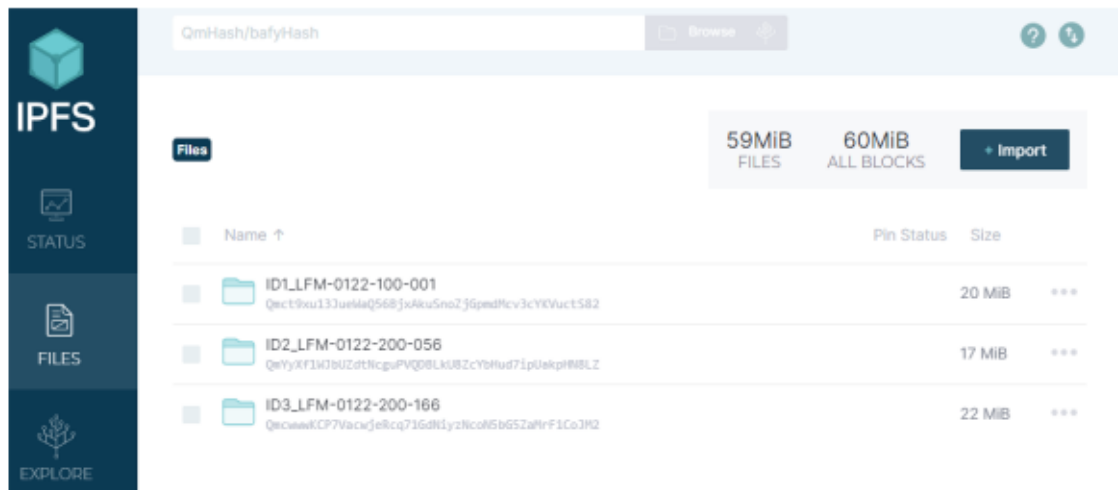


Fig. 8. IPFS user interface for decentralized storage of all manufacturing data in part-related folders.

network is still available and possible data manipulation by a network participant is also quickly detected and isolated by other participants.

It should be mentioned that the technological implementation is, however, initially demanding and requires good implementation in order to run efficiently digitally. The developed solution depends to some extent on a conscientious and correct execution. Only when quality is properly documented physically can it also be properly mapped digitally. In addition, the storage of incorrect information on the blockchain cannot be automatically prevented, so that errors can be documented immutably [52].

5.2. Cost analysis

Another goal of the AM blockchain architecture is to enable an economical alternative to currently used solutions and processes. For this purpose, a cost analysis of the smart contract code and the individual function calls is first performed. Every creation of a smart contract, every execution of a transaction, and every data storage in Ethereum incurs a cost [53].

Table 4 shows the transaction costs of the individual functions of the developed smart contract in the context of the demonstration study in ETH on the Ropsten testnet as well as the potential costs converted into a fiat currency (€). A gas price between 2.5 and 2.9 GWEI (based on Etherscan) resulted and the conversion rate from ETH to € as of

06.05.2022 (Google finance) was used. The gas price is very volatile and can more than double within a very short period of time, which in turn has a strong impact on the cost of digital documentation. Therefore, the cost analysis performed is only a snapshot.

The function to create the contract on the blockchain has the highest cost, which can be justified with the standard creation costs in Ethereum [34]. All other functions cause significantly lower costs, since only events are transmitted or only a few bytes of memory are required. The complete quality documentation of an FDM-printed metal part at an external sintering service provider via the AM part record accordingly costs approximately €17.66, depending on the current ETH price. These costs would be additional for each component as part of the QA process (each party involved bears a certain share of the costs). For smaller, low-cost parts, this amount is very high in addition to the normal manufacturing costs, but for more expensive parts with higher unit costs, it is not as significant.

In addition to the financial aspect, however, other topics such as process-related savings potential must also be included in a profitability analysis. Here, the AM part record can provide more trust between the individual parties, primarily due to automation, transparency, security and traceability, and thus, for example, reduce the need for coordination and discussion, avoid miscommunication and undesirable developments at an early stage, and react quickly to changing boundary conditions. The resulting cost savings must be set against the additional

```

[block:12242421 txIndex:33] from: 0xebd...905d0 to: AMChain_I1_createOrder(string,string,address,address,address) 0x34A...
status true Transaction mined and execution succeed
transaction hash 0x039aaaf20d7792575b5b5c9604389f3fce92de1a6c2b0e182d57806442f0d4
from 0xebdc7eAdBcC95aa5911A571c58980A4211905d0
to AMChain_I1_createOrder(string,string,address,address,address) 0x34A253F8E74468F264A902E305990Df65FA6C5c...

decoded input
{
  "string_partID": "I01",
  "string_IPFS_CID": "Qmct9xu13JuehQ568jxkuSnoZjGpndHcv3cYKvuct582",
  "address_shipper": "0xA4884Fc2FecBC4E280a2b5FA0Af3F5C72906536",
  "address_sinterer": "0xadbe1c35f796c709A880d6f7A2a08ec3AA2C139E",
  "address_customer": "0x5c6743588a15829E7bc0484AFEfB07F888A6c5"
}

decoded output
-

logs
[
  {
    "from": "0x34A253F8E74468F264A902E305990Df65FA6C5c",
    "topic": "0x2a3cd13b8797ba6cfff0d979f8ca085c61b638d739bd1911fd23e255398cc436",
    "event": "OrderCreated",
    "args": {
      "0": "0",
      "1": "0xebdc7eAdBcC95aa5911A571c58980A4211905d0",
      "2": "0xA4884Fc2FecBC4E280a2b5FA0Af3F5C72906536",
      "3": "0xadbe1c35f796c709A880d6f7A2a08ec3AA2C139E",
      "4": "0x5c6743588a15829E7bc0484AFEfB07F888A6c5",
      "Index": "0",
      "manufacturer": "0xebdc7eAdBcC95aa5911A571c58980A4211905d0",
      "shipper": "0xA4884Fc2FecBC4E280a2b5FA0Af3F5C72906536",
      "sinterer": "0xadbe1c35f796c709A880d6f7A2a08ec3AA2C139E",
      "customer": "0x5c6743588a15829E7bc0484AFEfB07F888A6c5"
    }
  }
]

```

Fig. 9. Log details of the successful execution of "createOrder" smart contract function.

documentation costs, and it must be determined in advance for each part as to whether correspondingly elaborate digital documentation is necessary. In general, it can thus be stated that the QA concept developed is fundamentally economical (with a relatively low gas price of about 2.5 GWEI) and, with increasing part requirements and costs, is also becoming increasingly economical despite the resulting transaction costs. This only applies to the Ropsten testnet studied in this work; significantly higher and real costs would currently occur on the Ethereum Mainnet (Ropsten ETH has no real monetary value, it exists only for testing purposes) [38]. Higher utilization of the Ropsten test network and different days of the week and times of day can also lead to significantly higher costs. However, the use of the Ethereum Mainnet is not even necessary for the current solution, as no direct payment transactions (with real money) are processed between the parties involved. Should this functionality be implemented in the future, the use of a more economical and faster solution like Hyperledger [54] or an Ethereum sidechain such as Polygon (MATIC) [55] would be recommended.

5.3. Efficiency

The compact and efficient documentation of manufacturing data is also being investigated as part of the QA concept. First of all, it should be noted that the accumulating production data, consisting of sensor values for process parameters and images of the print result, can be extensive (several gigabytes) and thus on-chain storage on the blockchain is not suitable or not possible, since on the one hand there are fundamental storage limits and on the other hand the storage costs are very high [34, 38,56]. For this reason, the storage of large amounts of data off-chain in the IPFS was considered. This procedure is possible in principle, but it is not very efficient, since such large amounts of data are frequently transmitted and stored several times in a decentralized manner. Under the AM blockchain architecture developed, the FDM manufacturing data was instead stored only locally on a central server and the location was noted in the part record.

A more efficient solution, but not yet implemented in the current concept, is the intelligent evaluation of manufacturing data using ML algorithms. In previous publications, corresponding solutions have already been demonstrated in principle for image [57–59] and sensor data analyses [60–62]. Adapting the algorithms developed there, as well

as building a dedicated metal FDM database, can enable intelligent evaluation of large amounts of data and extract an overall part quality result, which is then stored on- or off-chain. This eliminates the need for decentralized storage of large amounts of manufacturing data, which would greatly improve the efficiency of the AM part record. In addition, powerful AI algorithms can also enable automated real-time analysis of AM process data so that, for example, quality defects and process irregularities can be quickly identified and immediately corrected. To enable this securely and efficiently, datasets and data analytics will also be considered in the AM Blockchain concept in the future. For example, one could use special, trusted sensors that are constantly connected to the Internet and thus stream sensor data to a cloud-based database in near real time. In the cloud, the data can then be directly analyzed by automated analysis scripts and pre-trained AI algorithms, and the results visualized live. The exceeding of threshold values or the failure of sensor signals can then also be stored directly and transparently via alarm messages on the blockchain. However, the large datasets and analysis results remain stored locally in the cloud in principle, but can also be stored decentrally in the IPFS depending on the security standard. Only the reference to the storage location is stored on the blockchain. In this way, future production data can be recorded, evaluated and displayed immediately, and at the same time documented securely and transparently. Nevertheless, real-time evaluation of manufacturing data and decentralized storage of large volumes of sensor data are currently still a limitation [63]. This is also not implemented in the current QA concept, but the generalized architecture of the AM part record can still be extended in this respect.

5.4. Accountability

By executing a function in the smart contract, the Ethereum address of the executor is always stored securely on the blockchain. Thus, the function caller can be traced at any time and is accountable for his actions [64]. For example, in the FDM metal value chain, the manufacturer is accountable for each part he produces or documentation he creates, and the shipper is accountable for each delivery operation he performs. In the end, all parties involved in the part record have a detailed digital documentation available, which can be used to quickly identify accountability obligations in the event of any irregularities.

Etherscan

Ropsten Testnet Network

Contract `0x34A253F8E74460F264A902E305990Df65FA6C5Ce`

Contract Overview

Balance: 0 Ether

Transactions **Contract** Events

Code **Read Contract** Write Contract

Read Contract Information

1. `_00_getOrder`

`_index (uint256)`

0

Query

`↳ string, string, address, address, address, address, uint8`

```
[ _00_getOrder(uint256) method Response ]
>> string: ID1
>> string: Qmct9xu13JueWaQ56BjxAkuSnoZjGpmdMcv3cYKVuctS82
>> address: 0xebdc7eAdBCc95aa5911A571cC589B0A42119D5dD
>> address: 0xA4084Fc2FeCBC4E20BaA2b5FA9Af3f5C72906536
>> address: 0xadbe1C35f796C709A800DeF7A2e08ec34A2C139E
>> address: 0x5c6743508a15829E7bcb0484AFefB07f88BA6Ce5
>> uint8: 0
```

Fig. 10. Query of the part information stored on-chain via a smart contract published in Etherscan.

Table 3
Via Ropsten Ethereum and IPFS published AM part records and associated CIDs.

Part record	CID
ID1_LFM-0122-100-001	QmdFzUDmRsMNMZRjAmrDWXctiSHriCbYAapN9gU41hhrot
ID2_LFM-0122-200-056	QmYyXf1WJbUZdeNcguPVQDBlkU8ZcYbHud7ipUakpHN8LZ
ID3_LFM-0122-200-166	QmcwwwKCP7VacwjeRcq71GdNiyzNcoNSbG5ZaMrF1CoJM2

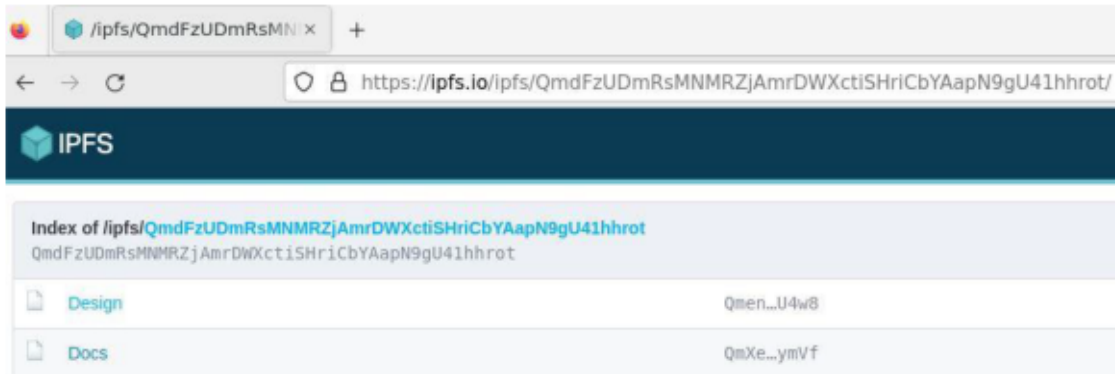


Fig. 11. Retrieval of the data stored decentrally in the IPFS via a web browser.

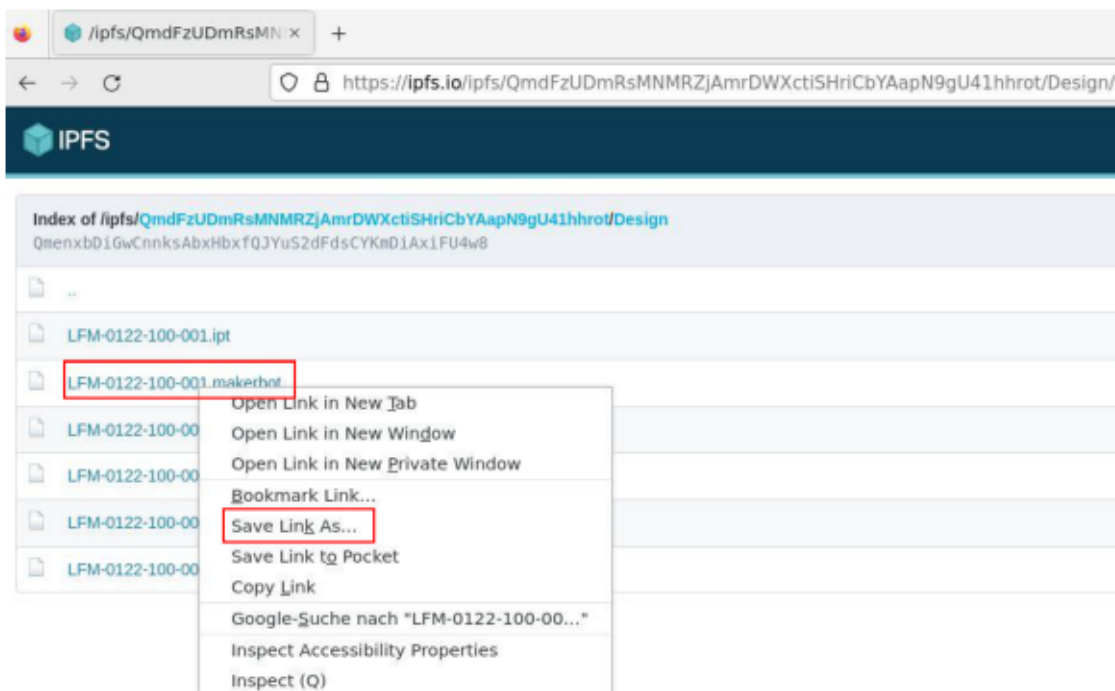


Fig. 12. Retrieval and local storage of individual files via the web browser.

However, since the developed AM blockchain architecture worked with the publicly available Ropsten Ethereum blockchain, there are privacy, confidentiality and trade secrets issues to consider here. The information stored on-chain is cryptographically secured in principle, but in the current concept it can be read out in decrypted form via a verified and published smart contract code using a specially programmed function. For this reason, the development of a solution based on a private blockchain such as Hyperledger [54] or the use of a transparent zero-knowledge proof system like ZK-STARK [65] could contribute to greater adoption and even better data protection in the future.

5.5. Availability

A blockchain stores all information decentrally on the participating network nodes. This means that all information is still accessible to all participants even if a node fails. Via the blockchain explorer Etherscan, current data can be accessed publicly at any time and from any location with an existing internet connection. Rapid updating of the information depends on the execution of the functions in the smart contract. In principle, the digital documentation can also be executed immediately after execution of the physical process and, moreover, the execution can be viewed within a few seconds via Etherscan. This is much more effective than conventional procedures, where agreements first have to

Table 4

Transaction costs of the smart contract functions in the demonstration study for the Ropsten Ethereum network (1 Eth equals 2.555 according to Google finance, as of 06.05.2022).

Function name	Function caller	Transaction costs [ETH]	Gas price [GWEI]	Costs []
DeployContract	Manufacturer	0.004734	2.879	11.95
CreateOrder	Manufacturer	0.000669	2.933	1.69
RequestShippingSintererOrder	Manufacturer	0.000109	2.808	0.28
AcceptShippingSintererOrder	Shipper	0.000107	2.746	0.27
CompleteShippingSintererOrder	Shipper	0.000105	2.699	0.27
ReceivedShippingSintererOrder	Sinterer	0.000106	2.723	0.27
SintererOrder	Sinterer	0.000144	2.713	0.36
RequestReshippingManufacturerOrder	Sinterer	0.000101	2.595	0.26
AcceptReshippingManufacturerOrder	Shipper	0.000099	2.551	0.25
CompleteReshippingManufacturerOrder	Shipper	0.000098	2.527	0.25
ReceivedReshippingManufacturerOrder	Manufacturer	0.000097	2.510	0.24
CheckOrder	Manufacturer	0.000133	2.508	0.34
RequestDeliveryCustomerOrder	Manufacturer	0.000098	2.504	0.25
AcceptDeliveryCustomerOrder	Shipper	0.000097	2.504	0.24
CompleteDeliveryCustomerOrder	Shipper	0.000097	2.502	0.24
ReceivedDeliveryCustomerOrder	Customer	0.000098	2.502	0.25
AcceptOrder	Customer	0.000098	2.501	0.25
DeclineOrder	Customer			
Total		0.00699		17.66

be made, data exchanged, partners informed and, if necessary, authorized to inspect the data.

It should be noted, however, that the network is not managed independently and that technology and program code can change at any time (e.g. through updates), so that accessibility is no longer given for solutions that have already been implemented.

5.6. Expandability

The QA concept presented currently only covers special documentation and storage processes. The concept is also suitable for certain extensions to implement further features to support quality processes or to enable procedures based on them. Regulatory stakeholders (authorities) or certification bodies, for example, can also be integrated into the QA concept and can also be given access to the part record. In this way, these stakeholders also gain transparent, traceable and secure access to manufacturing and quality information, on the basis of which part certificates and process qualifications can subsequently be issued more quickly and easily.

However, for this to happen, the AM Blockchain architecture must find sufficient acceptance in the AM industry and, if possible, be able to map all AM processes in a suitable manner. Furthermore, the legal basis for data protection must be clarified and solutions or regulations for the lack of control over the blockchain network used must be developed.

5.6.1. Expandability to other AM process flows

In this work, only 1 AM process with a specific process flow was considered. However, it is relatively easy to adapt the concept and programming to changing process flows. For example, a process without an external sintering service provider or the processing of other materials with different pre- and postprocessing steps can also be mapped.

5.6.2. Expandability to other AM process chains

Furthermore, the AM part record in the presented form is in principle also suitable for other AM processes with differently complex process chains. For example, to map a powder bed fusion-based AM process, the basic architecture of the AM part record can be retained, only additional parameters would need to be stored in the web application and adjustments made to the smart contract.

5.7. General impact of the AM part record solution on stakeholders

The use of the digital AM part record has different effects on the individual participants. From service provider to end customer, a

complex QM is created across the entire value chain of an AM part and beyond company boundaries, to which everyone involved has access or the opportunity to participate in a targeted manner.

Manufacturer: Manufacturers can map each product digitally and document it decentrally. All QM documents are transparently accessible to business partners at all times and stored in a virtually tamper-proof manner. In particular, this will simplify communication, avoid legal disputes, and enable the traceability of quality expenditures. However, this results in additional effort and costs for the documentation as well as for the implementation of the solution, which is still technically quite demanding. There are currently no regulatory requirements for such additional effort.

Shipper: The shipper can provide traceable and tamper-proof digital documentation of its activities. The data is stored decentrally, making it virtually impossible to change the information at a later date. In addition, the qualitative condition of the goods before and after delivery is precisely documented, which leads to greater trust between the parties involved. The actual shipping process flows can be adopted for the most part, only an additional financial outlay has to be considered. Especially for delivery service providers, the presented solution can therefore offer improved and easy-to-integrate documentation processes.

Sinterer: For the sintering service provider, the situation is comparable to that of the manufacturer. The sinterer can document his services digitally and thus reliably show what was done when and how. In addition, the transparent flow of information provides him with precise data about the processing status of the parts. This allows him to clock in and prepare his process steps at an early stage. Overall, this also results in increased effort for the sintering service provider in terms of documentation, correct implementation of the part record solution and additional documentation costs.

Customer: The customer has the greatest advantages from using the AM part record. Thanks to the transparent and tamper-proof documentation of the entire manufacturing and delivery process, he can track the processing status of his part, which materials, settings and processes were used and how the quality turned out in each case. Thus, the customer can obtain information about his part at any time and can react immediately in the event of errors or defects (e.g. by making a complaint or remanufacturing). There are no direct costs for the customer, but the additional effort for quality documentation can be reflected in higher quotation prices.

5.8. Comparison of the AM part record with other solutions for quality documentation in additive manufacturing

In the following, the AM part record is compared with other solutions already used for manufacturing and quality documentation of additively manufactured parts. Table 5 provides an overview of the results of the analysis. The analysis criteria are based on the evaluation criteria from Section 3.2 as well as on the investigations to this conducted previously.

In terms of digital integrity, only the AM part record presented here can be rated as good, as it is the only one capable of enabling digital and decentralized storage of data compared to the other solutions. ERP and DMS are also digital solutions, but do not allow decentralized storage without special extensions. Paper-based documentation is not digital, as the quality documents there are usually only physically available in file folders. Also from a cost perspective, the AM part record in its current form represents an economical alternative with relatively low costs to the other solutions. Documentation in paper form, on the other hand, is associated with a high level of manual and personnel effort as well as storage costs. An ERP system is relatively cost-intensive to purchase and support. Only in the case of the DMS are the costs moderate, since a simple DMS is not very expensive to purchase and the support effort is normally also relatively low. However, the DMS is only used to manage documents and not large datasets or ML analyses, so the efficiency of this solution can be classified as rather bad. The situation is similar with paper documentation. There, too, large amounts of data or analyses cannot be documented efficiently. But, this can be done very well using the AM part record architecture, possibly in combination with ML analyses. Only an ERP system can keep up with this, as these systems can also record and process all the data that arises. The disadvantage here is that these systems are usually used within a company and therefore there are no interfaces to the outside world and access from outside is not possible, which leads to poor accountability and availability. A DMS system usually behaves very similarly in these aspects and is therefore also to be evaluated like the ERP. In the case of paper documents, the situation is also considered bad because access to the physical documents is only possible in the place where they are stored, and therefore the documents can only be exchanged physically. In terms of expandability, both the AM part record and the ERP system offer good opportunities to help simplify and accelerate certification processes, for example. Paper documentation is the current standard, which is relatively time consuming and slow. A DMS is also to be rated as bad in this context, as not all necessary information such as datasets and analyses can be provided via it.

6. Conclusions

This work investigates the combination of AM and blockchain technology to improve quality assurance. In this context, a blockchain-based QM for the digital mapping of the value chain in the metal-based MEX process was designed and prototypically implemented as

Table 5
Comparison between AM part record and other solutions for quality documentation of AM parts.

Criteria	Paper-based documentation	Enterprise resource planning (ERP) software	Document management software (DMS)	AM part record architecture
Digital integrity	bad	bad	bad	good
Costs	high	high	moderate	low
Efficiency	bad	good	bad	good
Accountability	bad	bad	bad	good
Availability	bad	bad	bad	good
Expandability	bad	good	bad	good

AM part record. Individual manufacturing processes within the FDM value chain were analysed with regard to quality-relevant process parameters and documented in the context of real manufacturing jobs. Furthermore, a dApp was developed that stores all quality-relevant manufacturing events and protocols in an unalterable and tamper-proof manner according to cryptographic principles via a specially programmed web application, the decentralized storage solution IPFS and a special smart contract in the Ropsten ethereum blockchain. Via the blockchain explorer Ropsten Etherscan, the recorded events and the references of the stored data are subsequently accessible to all parties involved.

Moreover, this paper shows in a demonstration study that the presented QA concept in the form of a digital part record can be usefully applied to additively manufactured parts and thus lead to an improvement in quality. In particular, the digital documentation and traceability of transactions and documents within the value chain can be ensured. In this way, events and protocols in the AM part record are stored immutably on-chain on the blockchain and traceably as well as tamper-proof off-chain in the IPFS. In addition, the AM part record architecture was shown to be cost-effective both in terms of transaction costs for executing the various functions of the smart contract and in terms of the overall solution. Moreover, further analyses have shown that the developed architecture offers great advantages and potentials in terms of accountability, availability and expandability. Only in terms of effectiveness do the studies identify deficits in the decentralized storage of large amounts of manufacturing data. To solve this problem, ML-based manufacturing data analytics were considered, which in the future will perform an evaluation of the data during manufacturing and eventually extract an overall result on part quality, which will then be securely documented on the blockchain. Overall, the proposed architecture results in an additional documentation effort during the additive manufacturing process. But this additional effort is relatively low because the documentation processes and documents are usually already available and thus only need to be digitized and stored via the AM part record. In this context, the effects of the AM part record on the individual stakeholders were also evaluated. According to this, delivery service providers and end customers in particular can increasingly benefit from transparent and tamper-proof documentation processes. Furthermore, manufacturers and their suppliers will also benefit from a correspondingly traceable and secure mapping of the value chain, even if the additional efforts associated with additional costs are not yet required by the regulatory authorities.

In the future, the QA concept and the prototypical AM part record can be expanded to include special functionalities such as ML data analyses and certification solutions. Special concept supplements must be developed and software extensions programmed for this purpose. Extensibility to other AM process flows and AM process chains should also be the focus of future developments to enable broad acceptance of the concept. In addition, other participants such as authorities and certification bodies should be integrated into the smart contract as part of a part certification solution. Also, an automatic control should be provided that checks when the CID changes and shows exactly what has been changed. Furthermore, it will also be necessary to implement abort criteria in the event of faulty or defective parts in the manufacturing process in order to map physical processes more accurately in the AM part record and, if necessary, save resources by making decisions at an early stage (e.g. if a part is rejected due to a faulty printing or sintering process). Fundamental scientific research must also be conducted on the availability of blockchain networks and on data protection regulations in order to improve the acceptance and security of corresponding digitally documented part records. In a practical context, further technological developments related to software functionality, design and user experience also need to be targeted.

Funding

This research was funded by the European Union, which was made available through the European Regional Development Fund (ERDF) and the Ministry for Economics, Employment and Health of Mecklenburg-Vorpommern, Germany, grant number TBI-V-1 345-VBW-118.

CRediT authorship contribution statement

Erik Westphal: Conceptualization, Data curation, Formal analysis, Funding acquisition, Investigation, Methodology, Resources, Software, Validation, Visualization, Writing original draft. **Benjamin Leiding:** Investigation, Methodology, Writing review & editing. **Hermann Seitz:** Funding acquisition, Investigation, Supervision, Writing review & editing.

Declaration of Competing Interest

The authors declare that they have no known competing financial interests or personal relationships that could have appeared to influence the work reported in this paper.

Data availability

Data will be made available on request.

Acknowledgments

The authors gratefully acknowledge the project partner ESD Elektro-Systemtechnik GmbH Dargun for their technical support for the development of this work.

References

- [1] I. Gibson, D. Rosen, B. Stucker, *Additive Manufacturing Technologies*, Springer, New York, New York, NY, 2015.
- [2] C.F. Durach, S. Kurpjuweit, S.M. Wagner, The impact of additive manufacturing on supply chains, *IJPDLM* 47 (2017) 954–971, <https://doi.org/10.1108/IJPDLM-11-2016-0332>.
- [3] W. Alkhalder, N. Alkaabi, K. Salah, R. Jayaraman, J. Arshad, M. Omar, Blockchain-based traceability and management for additive manufacturing, *IEEE Access* 8 (2020) 188363–188377, <https://doi.org/10.1109/ACCESS.2020.3031536>.
- [4] H. Yang, P. Rao, T. Simpson, Y. Lu, P. Witherell, A.R. Nassar, E. Reutzel, S. Kumara, Six-sigma quality management of additive manufacturing, *Proc. IEEE Inst. Electr. Electron. Eng.* 109 (2021), <https://doi.org/10.1109/JPROC.2020.3034519>.
- [5] K. Christidis, M. Devetsikiotis, Blockchains and smart contracts for the internet of things, *IEEE Access* 4 (2016) 2292–2303, <https://doi.org/10.1109/ACCESS.2016.2566339>.
- [6] E. Benos, R. Garratt, P. Gurrola-Perez, The economics of distributed ledger technology for securities settlement, *Ledger* 4 (2019), <https://doi.org/10.5195/ledger.2019.144>.
- [7] S. Kurpjuweit, C.G. Schmidt, M. Klockner, S.M. Wagner, Blockchain in additive manufacturing and its impact on supply chains, *J. Bus. Logist.* 42 (2021) 46–70, <https://doi.org/10.1111/jbl.12231>.
- [8] M. Klockner, S. Kurpjuweit, C. Velu, S.M. Wagner, Does blockchain for 3D printing offer opportunities for business model innovation? *Res. Technol. Manag.* 63 (2020) 18–27, <https://doi.org/10.1080/08956308.2020.1762444>.
- [9] S. Zhang, Z. Lin, H. Pan, Research on 3D printing platform of blockchain for digital spare parts management, *J. Phys.: Conf. Ser.* 1965 (2021) 12028, <https://doi.org/10.1088/1742-6596/1965/1/012028>.
- [10] C. Mandolla, A.M. Petruzzelli, G. Percoco, A. Urbinati, Building a digital twin for additive manufacturing through the exploitation of blockchain: a case analysis of the aircraft industry, *Comput. Ind.* 109 (2019) 134–152, <https://doi.org/10.1016/j.compind.2019.04.011>.
- [11] N. Papakostas, A. Newell, V. Hargaden, A novel paradigm for managing the product development process utilising blockchain technology principles, *CIRP Ann.* 68 (2019) 137–140, <https://doi.org/10.1016/j.cirp.2019.04.039>.
- [12] R. Bonnard, J.Y. Hascoet, P. Mognot, E. Zancul, A.J. Alvares, Hierarchical object-oriented model (HOOM) for additive manufacturing digital thread, *J. Manuf. Syst.* 50 (2019) 36–52, <https://doi.org/10.1016/j.jmsy.2018.11.003>.
- [13] D. Guo, S. Ling, H. Li, A. Di, T. Zhang, Y. Rong, G.Q. Huang, A framework for personalized production based on digital twin, blockchain and additive manufacturing in the context of Industry 4.0, *IEEE 16th International Conference on Automation Science and Engineering (CASE)*, Piscataway, NJ, 2020.
- [14] L. Zhang, X. Chen, W. Zhou, T. Cheng, L. Chen, Z. Guo, B. Han, L. Lu, Digital twins for additive manufacturing: a state-of-the-art review, *Appl. Sci.* 10 (2020) 8350, <https://doi.org/10.3390/app10238350>.
- [15] P. Witherell, Digital twins for part acceptance in advanced manufacturing applications with regulatory considerations (2021).
- [16] L. Yi, C. Glaerner, J.C. Aurich, How to integrate additive manufacturing technologies into manufacturing systems successfully: a perspective from the commercial vehicle industry, *J. Manuf. Syst.* 53 (2019) 195–211, <https://doi.org/10.1016/j.jmsy.2019.09.007>.
- [17] M. Schmid, G. Levy, Quality management and estimation of quality costs for additive manufacturing with SLS, *10.3929/ethz-a-010335931*.
- [18] Z. Chen, C. Han, M. Gao, S.Y. Kandukuri, K. Zhou, A review on qualification and certification for metal additive manufacturing, *Virtual and Phys. Prototyping* (2021) 1–24, <https://doi.org/10.1080/17452759.2021.2018938>.
- [19] A. Chang, N. El-Rayes, J. Shi, Blockchain Technology for supply chain management: a comprehensive review, *FinTech* 1 (2022) 191–205, <https://doi.org/10.3390/fintech1020015>.
- [20] T. Guerpinar, G. Guadiana, P. Asterios Ioannidis, N. Straub, M. Henke, The current state of blockchain applications in supply chain management, in: *The 3rd International Conference on Blockchain Technology*, Shanghai China, ACM, New York, NY, USA, 2021, pp. 168–175, 03262021.
- [21] F. Dietrich, Y. Ge, A. Turgut, L. Louw, D. Palm, Review and analysis of blockchain projects in supply chain management, *Procedia Comput. Sci.* 180 (2021) 724–733, <https://doi.org/10.1016/j.procs.2021.01.295>.
- [22] Y. Thompson, J. Gonzalez-Gutierrez, C. Kukla, P. Felfer, Fused filament fabrication, debinding and sintering as a low cost additive manufacturing method of 316L stainless steel, *Additive Manuf.* 30 (2019), 100861, <https://doi.org/10.1016/j.addma.2019.100861>.
- [23] B. Liu, Y. Wang, Z. Lin, T. Zhang, Creating metal parts by fused deposition modeling and sintering, *Materials Letters* 263 (2020), 127252, <https://doi.org/10.1016/j.matlet.2019.127252>.
- [24] M. Vaezi, P. Drescher, H. Seitz, Beamless metal additive manufacturing, *Materials (Basel)* 13 (2020), <https://doi.org/10.3390/ma13040922>.
- [25] Github repository for the AMBlockchain. <https://github.com/eedinson/AM-Blockchain> (accessed 20 April 2023).
- [26] A. Musamih, K. Salah, R. Jayaraman, J. Arshad, M. Debe, Y. Al-Hammadi, S. Ellahham, A blockchain-based approach for drug traceability in healthcare supply chain, *IEEE Access* 9 (2021) 9728–9743, <https://doi.org/10.1109/ACCESS.2021.3049920>.
- [27] Y.C. Hu, T.T. Lee, D. Chatzopoulos, P. Hui, Hierarchical interactions between Ethereum smart contracts across Testnets, in: *Proceedings of the 1st Workshop on Cryptocurrencies and Blockchains for Distributed Systems*, Munich Germany, ACM, New York, NY, USA, 2018, pp. 7–12.
- [28] Y. Xiao, N. Zhang, W. Lou, Y.T. Hou, A survey of distributed consensus protocols for blockchain networks, *IEEE Commun. Surv. Tutorials* 22 (2020) 1432–1465, <https://doi.org/10.1109/COMST.2020.2969706>.
- [29] N. Szabo, Formalizing and securing relationships on public networks, *First Monday* 2 (1997), <https://doi.org/10.5210/fm.v2i9.548>.
- [30] V. Buterin, A next-generation smart contract and decentralized application platform, 2015.
- [31] S. Nakamoto, Bitcoin a peer-to-peer electronic cash system (2008).
- [32] T. Hepp, M. Sharinghausen, P. Ehret, A. Schoenhals, B. Gipp, On-chain vs. off-chain storage for supply- and blockchain integration, *Inf. Technol.* 60 (2018) 283–291, <https://doi.org/10.1515/itit-2018-0019>.
- [33] M. Di Piero, What is the blockchain? *Comput. Sci. Eng.* 19 (2017) 92–95, <https://doi.org/10.1109/MCSE.2017.3421554>.
- [34] Gavin Wood, Ethereum: a secure decentralized generalised transaction ledger, 2014.
- [35] M. Nofer, P. Gomber, O. Hinz, D. Schiereck, Blockchain, *Bus. Inf. Syst. Eng.* 59 (2017) 183–187, <https://doi.org/10.1007/s12599-017-0467-3>.
- [36] Joshua A.T. Fairfield, Smart contracts, Bitcoin bots, and consumer protection, *Wash Lee L Rev Online* 71 (2014) 35–299.
- [37] T.A. Almeshal, A.A. Alhagail, Blockchain for businesses: a scoping review of suitability evaluations frameworks, *IEEE Access* 9 (2021) 155425–155442, <https://doi.org/10.1109/ACCESS.2021.3128608>.
- [38] Y. Kurt Peker, X. Rodriguez, J. Ericsson, S.J. Lee, A.J. Perez, A cost analysis of internet of things sensor data storage on blockchain via smart contracts, *Electronics* 9 (2020) 244, <https://doi.org/10.3390/electronics9020244>.
- [39] H. Diedrich, *Ethereum: Blockchains, Digital Assets, Smart Contracts, Decentralized Autonomous Organizations*, Wildfire Publishing, 2016.
- [40] F. Casino, T.K. Dasaklis, C. Patsakis, A systematic literature review of blockchain-based applications: current status, classification and open issues, *Telematics and Inf.* 36 (2019) 55–81, <https://doi.org/10.1016/j.tele.2018.11.006>.
- [41] W. Cai, Z. Wang, J.B. Ernst, Z. Hong, C. Feng, V.C.M. Leung, Decentralized applications: the blockchain-empowered software system, *IEEE Access* 6 (2018) 53019–53033, <https://doi.org/10.1109/ACCESS.2018.2870644>.
- [42] Ethereum Foundation, Decentralized storage, 2022. <https://ethereum.org/en/developers/docs/storage/> (accessed 2 March 2022).
- [43] Protocol Labs Inc., IPFS powers the Distributed Web, 2022. <https://ipfs.io/> (accessed 2 March 2022).
- [44] M.M. Nuttah, P. Roma, G. Lo Nigro, G. Perrone, Understanding blockchain applications in Industry 4.0: from information technology to manufacturing and operations management, *J. Ind. Inf. Integration* 33 (2023), 100456, <https://doi.org/10.1016/j.jii.2023.100456>.

- [45] M.E. Latino, M. Menegoli, M. Lazoi, A. Corallo, Voluntary traceability in food supply chain: a framework leading its implementation in Agriculture 4.0, *Technol. Forecast. Soc. Change* 178 (2022), 121564, <https://doi.org/10.1016/j.techfore.2022.121564>.
- [46] J. Qu, Blockchain in medical informatics, *J. Ind. Inf. Integration* 25 (2022), 100258, <https://doi.org/10.1016/j.jii.2021.100258>.
- [47] N. Kawaguchi, Application of blockchain to supply chain: flexible blockchain technology, *Procedia Comput. Sci.* 164 (2019) 143–148, <https://doi.org/10.1016/j.procs.2019.12.166>.
- [48] T. Gorski, The 1–5 architectural views model in designing blockchain and IT system integration solutions, *Symmetry* 13 (2021) 2000, <https://doi.org/10.3390/sym13112000>.
- [49] P.B. Kruchten, The 4–1 view model of architecture, *IEEE Softw.* 12 (1995) 42–50, <https://doi.org/10.1109/52.469759>.
- [50] I.K. Kirpitsas, T.P. Pachidis, Evolution towards hybrid software development methods and information systems audit challenges, *Software* 1 (2022) 316–363, <https://doi.org/10.3390/software1030015>.
- [51] I. Aviv, A. Barger, A. Kofman, R. Weisfeld, Reference architecture for blockchain-native distributed information system, *IEEE Access* 11 (2023) 4838–4851, <https://doi.org/10.1109/ACCESS.2023.3235838>.
- [52] H. Al-Breiki, M.H.U. Rehman, K. Salah, D. Svetinovic, Trustworthy blockchain oracles: review, comparison, and open research challenges, *IEEE Access* 8 (2020) 85675–85685, <https://doi.org/10.1109/ACCESS.2020.2992698>.
- [53] Ethereum Foundation, Gas and fees, 2022. <https://ethereum.org/en/developers/docs/gas/> (accessed 27 April 2022).
- [54] C. Cachin, S. Schubert, M. Vukolic, *Architecture of the hyperledger blockchain fabric*, Zurich, 2016.
- [55] J. Kanani, S. Nailwal, A. Arjun, Matic whitepaper, 2018. <https://github.com/maticnetwork/whitepaper> (accessed 17 August 2022).
- [56] A. Bochém, B. Leiding, Reclaimed: sybil-resistant distributed identities for the internet of things and mobile Ad Hoc networks, *Sensors (Basel)* 21 (2021), <https://doi.org/10.3390/s21093257>.
- [57] L. Scime, J. Beuth, Anomaly detection and classification in a laser powder bed additive manufacturing process using a trained computer vision algorithm, *Additive Manuf.* 19 (2018) 114–126, <https://doi.org/10.1016/j.addma.2017.11.009>.
- [58] H. Kim, H. Lee, J.S. Kim, S.H. Ahn, Image-based failure detection for material extrusion process using a convolutional neural network, *Int. J. Adv. Manuf. Technol.* 111 (2020) 1291–1302, <https://doi.org/10.1007/s00170-020-06201-0>.
- [59] E. Westphal, H. Seitz, A machine learning method for defect detection and visualization in selective laser sintering based on convolutional neural networks, *Additive Manuf.* 41 (2021), 101965, <https://doi.org/10.1016/j.addma.2021.101965>.
- [60] H. Wu, Z. Yu, Y. Wang, Real-time FDM machine condition monitoring and diagnosis based on acoustic emission and hidden semi-Markov model, *Int. J. Adv. Manuf. Technol.* 90 (2017) 2027–2036, <https://doi.org/10.1007/s00170-016-9548-6>.
- [61] R. Drissi-Daoudi, V. Pandiyan, R. Loge, S. Shevchik, G. Masinelli, H. Ghasemi-Tabasi, A. Parrilli, K. Wasmer, Differentiation of materials and laser powder bed fusion processing regimes from airborne acoustic emission combined with machine learning, *Virtual and Phys. Prototyping* 17 (2022) 181–204, <https://doi.org/10.1080/17452759.2022.2028380>.
- [62] E. Westphal, H. Seitz, Machine learning for the intelligent analysis of 3D printing conditions using environmental sensor data to support quality assurance, *Additive Manuf.* 50 (2022), 102535, <https://doi.org/10.1016/j.addma.2021.102535>.
- [63] Byeong-Min Roh, Soundar R.T. Kumara, Hui Yang, Timothy W. Simpson, Paul Witherell, Yan Lu, In-situ observation selection for quality management in metal additive manufacturing. [10.1115/DETC2021-70035](https://doi.org/10.1115/DETC2021-70035).
- [64] S. Wang, D. Li, Y. Zhang, J. Chen, Smart contract-based product traceability system in the supply chain scenario, *IEEE Access* 7 (2019) 115122–115133, <https://doi.org/10.1109/ACCESS.2019.2935873>.
- [65] E. Ben-Sasson, I. Bentov, Y. Horesh, M. Riabzev, Scalable, transparent, and post-quantum secure computational integrity, *Cryptol. ePrint Archive* (2018). Report 2018/046.